Distribution Agreement

In presenting this thesis or dissertation as a partial fulfillment of the requirements for an advanced degree from Emory University, I hereby grant to Emory University and its agents the non-exclusive license to archive, make accessible, and display my thesis or dissertation in whole or in part in all forms of media, now or hereafter known, including display on the world wide web. I understand that I may select some access restrictions as part of the online submission of this thesis or dissertation. I retain all ownership rights to the copyright of the thesis or dissertation. I also retain the right to use in future works (such as articles or books) all or part of this thesis or dissertation.

Signature:

_____ _____

Alice Cho Date

Human memory B cells during development and after treatment of pemphigus vulgaris autoimmunity

By

Alice Hong Cho
Doctor of Philosophy

Graduate Division of Biological and Biomedical Science
Immunology and Molecular Pathogenesis

_____ [Advisor's signature]
Jens Wrammert, Ph.D.
Advisor

_____ [Member's signature]
Ron Feldman, M.D./Ph.D.
Committee Member

_____ [Member's signature]
Mandy Ford, Ph.D.
Committee Member

_____ [Member's signature]
Joshy Jacobs, Ph.D.
Committee Member

_____ [Member's signature]
Ignacio Sanz, M.D.
Committee Member

Accepted:

_____
Lisa A. Tedesco, Ph.D.
Dean of the James T. Laney School of Graduate Studies

_____
Date

Human memory B cells during development and after treatment of pemphigus vulgaris autoimmunity

By

Alice Hong Cho
B.S., B.A., Emory University, 2010

Advisor: Jens Wrammert, Ph.D.

An abstract of
a dissertation submitted to the Faculty of the
James T. Laney School of Graduate Studies of Emory University
in partial fulfillment of the requirements for the degree of
Doctor of Philosophy
in Graduate Division of Biological and Biomedical Science,
Immunology and Molecular Pathogenesis
2019

Abstract

Human memory B cells during development and after treatment of pemphigus vulgaris autoimmunity

By Alice Hong Cho

B cells are important immune effector cells, contributing to long-term protection from pathogens through antibody secretion or differentiation into long-lived memory B cells (MBCs). Developing MBCs must be diverse in order to bind all possible pathogens, but exclude self-reactive B cells, such as those causing pemphigus vulgaris (PV). PV is an human autoimmune blistering skin disease, driven by autoantibodies primarily targeting the well-characterized antigen Desmoglein-3 (Dsg3). Consequently, PV is a powerful model to study B cell-mediated autoimmunity in an antigen-specific fashion. In order to better understand human MBCs during autoimmunity, we studied their development during PV pathogenesis, and functionality after recovery from treatment with the B cell-depletive therapy, Rituximab.

First, we addressed how MBCs contribute to PV pathogenesis. We found that the emergence of activated Dsg3-specific MBCs correlates with disease presentation. Thus, we pursued an in-depth, single-cell analysis of Dsg3-specific MBCs by generating and characterizing a large panel of monoclonal antibodies from two recently diagnosed PV patients. Additionally, a unique, paired sample collected from one of the donors 15 months *prior* to symptom onset allowed us to determine how autoimmunity develops. Overall, our data suggests that Dsg3-specific B cells are generated from activation of low-affinity or non-autoreactive B cell precursors, possibly via bystander activation, which undergo extensive affinity maturation to select for high affinity, pathogenic B cells. The accumulation of these selected cells appears to drive initial disease presentation.

Next, we examined the quality of B cell responses to influenza vaccination in pemphigus patients previously treated with Rituximab. We found that despite numerical recovery of total peripheral B cells, patients lacked detectable influenza-specific MBCs. However, Rituximab-treated patients still mounted robust recall responses to influenza vaccination. This suggests that MBCs likely survive Rituximab treatment, possibly by residing in tissues, and can provide potent recall responses.

Overall, this dissertation provides novel insight into how autoimmune MBCs develop and contribute to PV pathogenesis, and how MBCs may recirculate through the periphery after Rituximab treatment. We believe that these results have implications for improving clinical care of PV patients, and raise important questions regarding the antibody-mediated mechanisms underlying how Dsg3-binding antibodies cause PV symptoms.

Human memory B cells during development and after treatment of pemphigus vulgaris autoimmunity

By

Alice Hong Cho
B.S., B.A., Emory University, 2010

Advisor: Jens Wrammert, Ph.D.

A dissertation submitted to the Faculty of the
James T. Laney School of Graduate Studies of Emory University
in partial fulfillment of the requirements for the degree of
Doctor of Philosophy
in Graduate Division of Biological and Biomedical Science,
Immunology and Molecular Pathogenesis
2019

Acknowledgements

First and foremost, I'd like to thank my mentor, Dr. Jens Wrammert. Not only did he teach me new techniques and how to plan better experiments, but he also challenged me every day to think more critically and voice my opinions. He encouraged me to always have an inquisitive mind and to hold myself to the highest standard of scientific reasoning. This really pushed me to grow as a scientist and become more independent, passionate, and confident in my work. Thanks, Jens, for your patience and for being a great mentor.

Thanks, also, to my fellow lab members, the "Wram Jams." Without their support intellectually, emotionally, and physically, being in lab would've been a daily struggle. You guys made me a better scientist, teammate, teacher, and student. Thank you for always being there when I needed help, and making even the late nights and long weekends in lab bearable. You guys are truly the best science family a PhD student could ask for.

I need to also thank my friends throughout graduate school. You guys were there for every celebration and failure, through laughter and tears. I wouldn't have made it through graduate school without the support and love of each and every one of you. From Colorado to Scotland, from eating Taco Bell to binge watching bad movies, thanks for all of the great memories. And of course, thank you to the lovely ladies of 94 Lucy – my roommates and best friends. It was incredible to have a real home, not just a house, during my 6 years in graduate school. You guys always reminded me to "Never don't mind about a thing" and

to not be discouraged just because of a bad day (or several bad months!) in lab. Thanks for keeping me grounded throughout this crazy process.

Lastly, I want to thank my family. To my sister, Jennifer, who remains my best friend and closest confidante. Thank you for being my favorite unnie and remaining my number one travel companion. Here's to many more years of precious times ahead. And of course, my amazing parents. Every day, I become more and more appreciative of their sacrifices that have lead me to accomplish everything I am. Thank you for your unwavering faith in me, and constantly pushing me to be a better version of myself. I hope I have made you proud. Saranghaeyo.

TABLE OF CONTENTS

Chapter 1: Introduction

B CELL IMMUNE RESPONSES

B cell development

Long-term protection against pathogens is provided by the adaptive immune system, which is derived from two distinct lymphoid lineages that are designated as humoral immunity, mediated by B cells (1), and cellular immunity, mediated by T cells (2, 3). B cells were first discovered in the 1960s via experiments using chickens in order to study the avian immune system. The thymus, bursa, or both were removed from newly born chicks which were then irradiated. Upon recovery, it was clear that removal of the thymus caused a reduction in lymphocytes, although plasma cells and serum antibodies persisted. Inversely, removal of the bursa was paired with a noted decrease in antibody responses with normal numbers of lymphocytes elsewhere in the body (4). Soon after, the bursa-equivalent in mammals was discovered via adoptive transfer of bone marrow lymphocytes and DNA labeling experiments, implicating the bone marrow as a major site of B cell differentiation (5, 6).

In the bone marrow, hematopoietic stem cells begin their commitment to B cell development. One crucial step in B cell development involves a complicated process of expressing a B-cell receptor (BCR) on the cell surface (7). The BCR, which resembles a membrane-bound antibody, involves a recombination of variable (V), diversity (D), and joining (J) genes to make up a heavy chain, pairing randomly with a recombination of V and J genes that make up a light chain (8). This rearrangement process is mediated by the enzyme called recombination activating gene (RAG)-1 (9). This recombination process allows for the finite number of V(D)J genes to come together to make up an almost unlimited number of diverse BCRs. Maintenance of this diverse pool of naïve B cells is

controlled by central (occurring in bone marrow) and peripheral (occurring outside the bone marrow) tolerance mechanisms, which allow for the persistence of B cells with the potential to bind to all possible pathogens while deleting any B cells with reactivity towards self-antigen (10).

B Cell Activation

Once a successful BCR has been expressed on the cell surface, the newly made naïve B cell is transported out of the bone marrow into the periphery, where it circulates through peripheral blood between secondary lymphoid tissues until it is activated. B cells can be activated via two different pathways: T cell-independent or T cell-dependent activation.

Some B cells can be activated through T cell-independent antigens, meaning a response to an antigen in the absence of any major histocompatibility complex (MHC) class II-dependent T cell help (11). The existence of these types of antigens were discovered when robust B cell responses were induced in both wildtype mice and athymic mice, which lack T cells (12). T cell-independent antigens is subset into two categories. First, there are TI-1 antigens, which are primarily B cell mitogens that can stimulate responses independently of signaling via Bruton's tyrosine kinase (13). Second is the TI-2 antigens, which primarily includes repetitive structures such as polysaccharides. Although immediate B cell responses to these antigens appear to be robust, there exists some controversy as to whether B cell responses towards TI antigens elicit fully mature effector B cells in terms of class-switched responses (12, 14) or even longevity (15-17).

Other B cells are activated through the more canonical response to T cell-dependent antigens. These responses begin in secondary lymphoid organs, such as lymph nodes, which have distinct regions which house germinal center reactions. When B cell encounters an antigen, it quickly processes the antigen and non-specifically re-expresses peptides on an MHC Class II molecule. When this peptide is recognized by a cognate T cell, the T cell is able to provide the correct signals needed to allow for the B cell to enter a germinal center reaction (18-20).

Germinal Center Reactions

Germinal centers are important for the proliferation and maturation of B cell responses (21). It is thought to be made of two distinct regions: the dark zone and light zone (19, 22). The dark zone is primarily made up of rapidly proliferating B cells that are undergoing somatic hypermutation (SHM), which introduce random mutations into the immunoglobulin gene of B cells (23). This mutation process is mediated primarily by the enzyme activation-induced cytidine deaminase (AID), which causes rapid mutations of the immunoglobulin gene in B cells (24). This mutation process can result in a BCR that no longer functions, causing the B cell to apoptose (25), or result in B cells which can migrate to the light zone and begin their selection process to see if the mutated BCR has gone through affinity maturation and now has improved binding in response to the antigen, or if it has lost the ability to bind to the antigen (26).

Antigen selection in the light zone is mediated primarily by two effector cells: the follicular dendritic cells (FDCs) and the follicular helper T (Tfh) cells. FDCs present antigen on its surface in an immune-complex mediated manner (27), where the newly

somatically hypermutated B cells are able to sample the antigen and go through a selection process for B cells that have the best affinity for the antigen (28). High-affinity B cells bind to the antigen of interest and present the antigen through an MHC Class II complex to a cognate Tfh cell (22). The dynamic interaction of B cells with Tfh cells in the light zone suggest that selection may be mediated by competition of GC B cells for binding to a limited number of available Tfh cells (29). Cognate Tfh cells are able to provide crucial cytokine signals that mediate expansion, survival and class-switching of B cells (30, 31). Class-switching is an additional B cell maturation process which diversifies the functionality of antibodies (32), and is a process also mediated by the same enzyme that controls somatic hypermutation, AID (33). A B cell may go through several cycles through the light and dark zone (34) before finally differentiating into an effector cells and leaving the germinal center to exit back into the periphery (35).

Differentiation into effector B cells

After a B cell has gone through the germinal center reaction, it becomes one of two major effector cell subsets: memory B cells and antibody secreting cells, with the latter sub-setting into short-lived, circulating plasmablasts and long-lived plasma cells. Although the exact signals necessary for the differentiation into a certain subset remains unknown (36, 37), the function of each effector cell subset has been well characterized.

Memory B cells are quiescent, long-lived B cells that are not secreting antibody, but do have a BCR that allows these memory B cells to rapidly engage an antigen upon a secondary exposure (38). Memory B cells can re-enter the germinal center and go through a second round of somatic hypermutation (SHM) and affinity maturation, allowing these

cells to provide a very rapid and highly-efficient secondary response (39-41). Additionally, some memory B cells are thought to immediately differentiate into plasma cells without re-entry into the germinal center (42). Because memory B cells represent all antigens encountered throughout a lifetime, frequencies of antigen-specific memory B cells found in the periphery are typically very low, at around 0.1-1% of total memory B cells (43). While memory B cells can be detected in peripheral blood, they can also be found in secondary lymphoid tissues such as the spleen and lymph nodes (44, 45). Although it is possible that MBCs found in these tissues are merely circulating through, recent reports suggest that tissue-resident MBCs in the lung can be induced in mice after influenza infection. These MBCs appear to have distinct characteristics compared to those found in circulation (46, 47), revealing a novel role of tissue-resident MBCs in contributing to long-term protection against pathogens. Future studies on tissue-resident memory B cells in response to other infection models, as well as their presence in humans, will have major implications in understanding how memory B cells circulate between the periphery and tissues, and may guide future efforts in designing vaccines that are able to effectively elicit long-lived, protective memory B cell responses.

Short-lived antibody secreting cells, called plasmablasts, are found in circulation that are rapidly produced into response a recent antigenic challenge. As such, a large frequency of the plasmablast response antigen-specific when analyzed during peak responses (48, 49). Their role has been described in response to an influenza vaccination, where antigen-specific plasmablasts were seen to quickly expand merely seven days post-vaccination. The response largely disappears by day 14, presumably because most of the cells die, although it is possible that some plasmablasts may home to the bone marrow and

become long-lived plasma cells (50). The quality of the plasmablast response correlates with influenza vaccine efficacy (51, 52), suggesting that efficient induction of these cells and the antibodies they secrete are an important aspect of B-cell mediated immune protection. Plasmablasts have since been described in the context of many other vaccinations (53, 54), infections (48, 55-57), and autoimmune diseases (58). Plasmablasts can differentiate in response to either a primary exposure, with the activation of a naïve B cell, or a secondary exposure through the activation of a memory B cell. The differences between these responses can be observed by the level of somatic hypermutation and isotype usage of the responses, with primary responses typically dominated by IgM-positive plasmablasts with low levels of mutations, and secondary response typically consisting of class-switched IgG and IgA responses with more mutations. Additionally, it is thought that naïve B cells take about 10 days to generate a plasmablast response, while secondary responses borne from memory B cells occur more rapidly and peak at day 7 post-exposure (59).

Long-lived antibody secreting cells, called plasma cells, are terminally differentiated antibody-secreting cells and survive primarily in the bone marrow, although some plasma cells are thought to reside also in the spleen (60) as well as the gut (61). Mouse studies revealed that the plasma cells that primarily survive in the bone marrow are able to independently persist for the entire lifespan of a mouse (62). The longevity of human plasma cell responses was also determined by secondary measures of calculating the half-life of serum antibody titers that plasma cells produce in response to childhood vaccinations. In these studies, the half-life of serum titers against measles were calculated to persist well-beyond a human life time, at up to 3,000 years (63). Considering that the

half-life of the IgG protein is on the span of 3-4 weeks (64) it is assumed that the longevity of measles serum titers is a testament to the long-lived nature of plasma cells. Serum titers had no correlation with the number of antigen-specific memory B cells, which further implicates long-lived plasma cells as the primary effector cell subset for producing these long-lasting serum antibody responses without additional input of the memory B cell pool (63). A recent study on human plasma cells was able to identify a distinct subset of plasma cells in the bone marrow that were thought to specifically represent the long-lived plasma cell compartment. By sub-setting plasma cells from bone marrow aspirates based on CD19, CD38, and CD138 expression, long-lived antibody responses to the MMR vaccine were found to originate from the CD19(-)CD38(hi)CD138(+) subset. Paired analysis of sequences from this cell subset with sequences of serum antibodies confirmed that the serum antibodies did originate from the CD19(-)CD38(hi)CD138(+) plasma cell subset (65). While it is unclear what exact signals are necessary for a plasma cell to persist, evidence suggests that there are defined bone marrow niches that provide the ideal environment to allow plasma cells to survive (60, 66).

Tolerance

B cell responses must strike a fine balance between developing a diverse repertoire that provides sufficient protection against a wide array of potential pathogens, while simultaneously preventing reactivity against self-antigens, which would result in autoimmune disorders. These mechanisms are incredibly important considering the high frequency of autoreactive naïve (67) and memory B cells (68) observed even in healthy humans, suggesting that multiple checkpoints successfully control tolerance of B cells.

Three major mechanisms for maintaining B cell tolerance which operate both centrally (within the bone marrow) and in the periphery have been identified: clonal deletion, receptor editing, and anergy (69).

Clonal deletion was the first method of tolerance observed in mice. In 1989, Nemazee et. al. very elegantly demonstrated clonal deletion with the use of transgenic mice expressing B cells specific for H-2K MHC class I allele. Mice were engineered to express both the transgene as well as wildtype immunoglobulin genes. Ultimately, only the transgenic B cells that expressed specificity against the H-2K MHC class I molecule, the self-antigen tested in this model, were completely excluded from populating the periphery, suggesting that these self-reactive B cells were clonally deleted from the antibody repertoire (70). These findings were confirmed in a bone marrow chimera model where transgenic B cells expressing antibodies against H-2K MHC class I molecules were transferred into either H-2K expressing or non-expressing mice. These B cells were excluded from the periphery of H-2K MHC class I expressing mice, whereas they were found at normal numbers in mice that did not express the H-2K MHC class I molecules (71). Autoreactive B cells that migrate outside of the bone marrow are able to go through clonal deletion in the periphery (72), or even later during germinal center reactions (73). Clonal deletion represents the mechanism underlying negative selection, also known as central tolerance.

Receptor editing usually occurs as an alternative for clonal deletion, where some self-reactive B cells in the bone marrow are able to undergo receptor editing to escape clonal deletion. In this process, the light chain gene can undergo a second rearrangement and re-pair with the expressed heavy chain to create a combination that is no longer self-

reactive. This was clearly observed in a transgenic mouse model where B cells were made to express a heavy chain associated with self-reactive anti-DNA antibodies. B cells from these transgenic adult mice had heavy/light chain pairings in which the light chain V gene usage was highly restricted, which suggested that light chains must compete for selection in order to create a non-autoreactive receptor (74).

Anergy is an alternate method of maintaining B cell tolerance and occurs after self-reactive B cells have escaped both clonal deletion and receptor editing, and reached circulation through the periphery. While clonally deleted B cells react to self-antigen via cell death, anergic B cells respond to self-antigen by downregulating membrane IgM. This requires these B cells to meet a higher antigenic threshold before being activated by self-antigen. Thus, in a normal setting where self-antigen is found at low levels, these cells are silenced and unable to be activated (75). The deciding factor between going through clonal deletion or anergy seems to lie in the nature of the antigen. Typically, soluble antigens that are unable to effectively crosslink the BCR tend to cause anergy in B cells (76, 77), whereas antigens that induce potent cell signaling appear to induce clonal deletion. Thus, most models studying anergy tend to use soluble hen egg lysozyme antigen, compared to studies of responses to potently multivalent membrane-bound antigen like MHC class I molecules that induce clonal deletion, as mentioned earlier in this section. A population of anergic B cells was identified from human cells, using single-cell methods to produce a panel of antibodies from mature human B cells. These antibodies were predominantly autoreactive/polyreactive, with anergic B cells showing an impaired ability to respond to receptor cross-linkage. However, increasing the intensity of the stimulation pushed these anergic B cells into responding, revealing *in vivo* relevance of anergy in humans (78).

The cytokine milieu is also known to have an impact on tolerance of B cells. Primarily, B cell Activating Factor (BAFF), a member of the TNF-family of cytokines and a critical signal needed for B cell survival, has been implicated in the selection of tolerant B cells. BAFF has an important role in the homeostasis of B cells. It has multiple receptors including TACI, BAFFR, and BCMA, with BAFF binding primarily to TACI and BAFFR (79). Expression of these receptors on specific B cell subsets appears to mediate how BAFF is able to impact certain B cells. Previous studies have shown that the survival for autoreactive B cells is dependent on BAFF signaling, with increased BAFF promoting the survival of autoantigen-specific B cells in a transgenic mouse model (80). BAFF dependency was specific for B cells in the late transitional stage (B cells that recently migrated from the bone marrow), as opposed to B cells during early differentiation in the bone marrow or early peripheral development (81). Thus, recent studies on B cell-mediated autoimmune diseases have also investigated a potential role for BAFF in the pathogenesis of autoimmunity in humans, leading to the hypothesis that BAFF-neutralizing therapies may also improve treatment of autoimmune diseases (82-84).

A new role for B cells in tolerance has been recently described by the ability of B cells to secrete regulatory cytokines such as IL10. These B cells, called Bregs, were first described in *in vivo* murine models (85). Bregs appear to be important in mitigating autoimmunity, as shown by the role of IL10-secreting plasmablasts in controlling autoimmune encephalomyelitis, the murine model of multiple sclerosis (86). It remains unclear if Bregs have any relevance in human immune responses, primarily due to the inability to detect a specific population of B cells that naturally produce IL10, although *in vitro* stimulation of plasmablasts (85) and transitional B cells (87) could cause these cells

to secrete IL10. In fact, transitional B cells were shown to be likely candidates as a Breg populations, as seen by their ability to maintain regulatory T cell populations in *in vitro* cultures via an IL10-dependent manner. Interestingly, transitional B cells isolated from patients diagnosed with the autoimmune disorder rheumatoid arthritis lost the ability to regulate T cell function (88). This further highlights the potential importance of Bregs in the maintenance of tolerance, and suggests that ongoing studies of this novel B cell population will provide greater insight into our understanding of how tolerance is maintained.

In general, polyreactive B cells can be detected at high levels even in healthy humans exhibiting no autoimmune disease. In the early immature B cell compartment, which contains B cells that have not undergone selection or affinity maturation via germinal center reactions, around 55-75% of these B cells were found to be polyreactive, binding to a panel of self-antigens including nuclear protein, dsDNA, ssDNA, insulin, and LPS (89). Similar autoreactive B cells were found in the IgM+ memory B cell compartment (68), IgG+ memory B cell compartment (90), and plasmablast compartment (91). However, the frequency of autoreactivity in these subsets was lower at an average of 20%, likely due to the fact that these are developed B cells which have undergone more rounds of selection and tolerance than the immature B cell compartment. Additional studies have observed even higher frequencies of autoreactive naïve B cells in patients with autoimmune disorders compared to healthy controls, suggesting systemic breakdown in tolerance may underlie the development of autoimmune disease (67, 92).

Overall, multiple checkpoints of tolerance mechanisms appear sufficient to protect the humans from developing autoimmune disorders. However, there are many B cell-

mediated autoimmune disease that can arise when tolerance fails, including rheumatoid arthritis (RA), systemic lupus erythematosus (80), Type I diabetes, immune thrombocytopenia, and autoimmune blistering skin diseases such a pemphigus vulgaris (93). Ongoing questions about how these autoimmune B cells break tolerance and ultimately cause disease will not only address interesting aspects of basic B cell biology, but provide important developments in the clinical care and treatment of patients with autoimmune disorders.

PEMPHIGUS VULGARIS

Autoimmune Blistering Skin Diseases

Autoimmune blistering skin diseases (AIBD) are a group of B cell-mediated autoimmune disorders affecting skin and/or mucous membranes, including pemphigoid and pemphigus (94-96). Pemphigoid is a blistering skin disease mediated by autoantibodies binding proteins in the hemidesmosome, a structure which allows skin cells in the basal layer of the epidermis to adhere with the dermal layer of the skin (Figure 1A). Common proteins targeted in pemphigoid include collagen XVII (also known as BP180) (97).

Pemphigus results in severe erosions caused by autoantibodies directed against intercellular adhesion proteins in the epidermis which contribute to the formation of the desmosome (Figure 1B) (98, 99). Subtypes of pemphigus include pemphigus foliaceous, a disease mediated by autoantibodies primarily targeting the desmoglein (Dsg)-1 protein (100). This is a protein typically found on the superficial layer of the epidermis (Figure 1A), and mucosal lesions are rarely observed in these patients (101). There is also an endemic form of pemphigus foliaceus found in a Brazil, called *fogo selvagem* (translated to "wildfire"). Its unique presentation in children and young adults, and prominence in the jungles of rural South America has made *fogo selvagem* distinct from pemphigus foliaceus, despite the description of similar autoantigenic targets (100). Currently, no etiology has been identified as to what makes *fogo selvagem* endemic in Brazil (101). Paraneoplastic pemphigus is another form of pemphigus, found to target the Dsg3 protein, with symptoms presented solely on mucous membranes. This disease is associated with the development of benign or malignant tumors occurring before, during, or after diagnosis of paraneoplastic pemphigus (102). Other rare forms of pemphigus have been described, with IgA antibodies

targeting desmocollin proteins, and a large presence of neutrophils found in skin pustules caused by the disease (103). Of all these subtypes of AIBDs, the most prevalent is the disease pemphigus vulgaris (102).

Desmoglein-3 as the major target in Pemphigus Vulgaris

Pemphigus vulgaris (PV) is an autoimmune disorder characterized by the presence of blisters and sores on skin and mucosal membranes (96, 104). These symptoms are a result of autoantibodies targeting adhesion proteins in the skin, called desmoglein (Dsg)-3 (105). It is a rare disease affecting about 1 in 100,000 people yearly, with higher rates of disease found within populations of Ashkenazi Jews (106). Unlike other B-cell mediated autoimmune disorders like rheumatoid arthritis (75) and systemic lupus erythematosus (76), which are systemic diseases with hundreds of autoantigenic targets described, PV is a unique autoimmune disorder in which a single autoantigen is primarily targeted (105). This makes PV stand out as a unique human B cell-mediated autoimmune disease to study at an antigen-specific level. Thus, studies of PV have not only provided insight into this understudied disease, but may also contribute to our broader understanding of the immunopathology of other B cell-mediated autoimmune disorders.

The autoantigenic target for PV was discovered by Masayuki Amagai and John Stanley, when they determined that serum antibodies from PV patients bind to a 130-kDa autoantigenic target isolated from epidermal extracts (98, 99, 107, 108). Cloning the cDNA of this unknown autoantigen revealed that it was homologous to cadherins, a family of calcium-dependent cellular adhesion proteins (109). The autoantigen was present only in stratified squamous epithelial cells, and was involved in cell adhesion (108, 110). The

protein was described to be Dsg3, a transmembrane protein component of the desmosome (Figure 1B), which is an important structure necessary for epidermal keratinocytes to adhere together (111, 112).

Further experiments using indirect immunofluorescence to probe serum from PV patients onto human epidermis showed that most patients exhibit autoreactivity to the Dsg3 protein, although some patients also had some reactivity towards the related protein Dsg1 (98). It is thought that while PV patients with disease localized to the mucosa have antibodies strictly against Dsg3, patients presenting with symptoms in both the mucosa and skin (mucocutaneous PV) will have antibodies directed towards both Dsg3 and Dsg1 (113). Nuanced differences in the presentation of disease symptoms likely rely on the predominance of Dsg3 in the mucosal and basal layers of the skin (114), while Dsg1 is primarily found in the superficial layer of the epidermis (Figure 1A) (98). Adsorption of patient serum with recombinant Dsg3 protein decreased binding of the serum to *ex vivo* human epidermis, further confirming Dsg3 as the likely target in PV pathogenesis (105). The synthesis of recombinant desmoglein proteins allowed for analysis of serum antibodies using ELISA assays, and showed that PV patients primarily had anti-Dsg3 antibodies in the serum, with some anti-Dsg1 reactivity. This was distinct from the related disease pemphigus foliaceus (115), where autoantibodies exclusively targeting Dsg1 were detected (100). The dependence of PV disease symptoms on the activity of a single antigen, Dsg3, was supported by the development of Dsg3-knockout mice, which exhibited similar disease symptoms to PV patients, including oral lesions, separated desmosomes, and acantholysis (116).

Although it is generally accepted that Dsg3 and Dsg1 are the major targets of PV, there exists some controversy as to the relevance of desmoglein as the sole target in PV (monopathogenic) versus a multi-coordinated attack of autoantibodies targeting both desmoglein as well as proteins involved in pro-apoptotic signals or cell-cell detachment signals (multipathogenic) (117, 118). The presence of additional autoantigenic targets in PV patients was described using a massive proteomic effort, in which PV patient serum was screened for reactivity against 500 different proteins. Targets including mitochondrial proteins and calcium pump-associated proteins were described to be higher in PV patients than healthy controls, in addition to the expected binding against desmosomal proteins (118). These findings support the observation of epitope spreading found in a small subset of PV patients who have reactivity to desmocollin-3 (Figure 1B), another major protein component of the desmosome (119), suggesting that autoantigenic targets other than Dsg3 may contribute to overall PV pathogenesis.

The multipathogenic hypothesis supports the observation that while serum antibody titers against Dsg3 generally correlate with disease progression and remission, there is a subset of patients who maintain anti-Dsg3 and anti-Dsg1 serum titers despite reaching remission (120), as well as the persistence of epidermis-binding antibodies after removal of Dsg3-reactivity from PV patients serum via adsorption with recombinant Dsg3 (105). However, it is possible that the recombinant Dsg3 proteins used in these assays does not express the relevant post-translational modifications necessary to express the epitopes necessary to really probe for Dsg3-specific autoantibodies that cause pathogenicity (121). Thus, the anti-Dsg3 serum antibody response persisting in remission patients may be representative of non-pathogenic B cell responses in PV patients. Additionally, it remains

unclear if the autoreactive antibodies that do not bind Dsg3 that are in PV patients actually contribute to disease pathogenesis, or if they are merely irrelevant, non-pathogenic autoantibodies that arise from a general lack of B cell tolerance mechanisms. Future studies detailing the mechanism underlying how antibodies cause pathogenicity will be important in answering these questions.

B cells mediate PV disease

Not only are autoantibodies targeting Dsg3 present in PV patients (105, 107, 108), but it is also clear that these autoantibodies and B cells are implicated in functionally causing PV disease symptoms. *In vivo* murine models showed that passive transfer of serum from PV patients into neonatal mice was sufficient in causing blistering in mice (107, 122). Conversely, the adsorption of Dsg3-specific autoantibodies from patient serum prevented the pathogenicity of the serum when passively transferred into mice, further implicating Dsg3-reactive autoantibodies in driving PV disease pathogenesis (105). Additionally, serum titers against Dsg3 and Dsg1 have been loosely correlated with severity of disease symptoms in mice models (120, 122).

An mouse model was developed to highlight the role of B cell in PV pathogenesis, in which Dsg3-knockout mice were immunized with recombinant Dsg3 protein to drive the development of autoreactive B cell responses towards the protein. PV-like disease symptoms were then observed with the splenocytes of the immunized Dsg3-knockout mice were transferred into Rag2-knockout mice, which were clearly driven by the transferred Dsg3-autoreactive B cells reacting with the normal expression of Dsg3 in the skin of the Rag2-knockout mice (123). This model allows not only for Dsg3 to be identified as the

major target of disease, but also implicated B cell-mediated mechanisms to underlie the manifestation of PV disease. A relevant *in vivo* PV disease model can also be induced in mice by immunizing Balb/c mice with rDsg3 to elicit a pathogenic anti-Dsg3 antibody response (124). While little is known about B cell subsets that are directly responsible for secreting pathogenic Dsg3-specific antibodies and causing disease, the Balb/c model suggested that antibody secreting cells specific for rDsg3 can be found primarily in the spleen and BM, although smaller numbers were also present in the LN and peripheral blood (125).

The role of autoantibodies in PV can also be seen in unique human case studies. Clinical studies have shown reports of newly born babies from mothers diagnosed with pemphigus, in which the newborns show pemphigus symptoms but only within the first 6 months of life, with symptoms waning after this time. It has been suggested that this may be due to the transfer of maternal antibodies that have been shown to provide protection in newborns for the first 6 months of their lifespan, during which time newborns are generating their own humoral immune responses (126). However, clinical studies on adults have shown that while Dsg3-specific antibodies are largely present in symptomatic PV patients, the correlation between Dsg3-specific titers and disease severity in humans is unclear, with some patients exhibiting high titers despite clinical improvement of disease symptoms (127). This clinical observation may be due to the impact of systemic therapies routinely given to pemphigus patients, which allow these patients to improve rapidly, prior to a decrease in serum antibody titers.

Similar to mice models, it remains unclear what B cell subset is important for driving pathogenesis in humans. Almost all PV patients have no Dsg3-specific antibody

secreting cells in the peripheral blood, with only those with severe activity showing very low frequencies of plasmablasts. However, a low-frequency of Dsg3-specific memory B cells could be detected in patients regardless of disease severity (125). Sequencing studies showed that these circulating memory B cells appear to be partially responsible for the serum antibodies detected in patients, although much more diversity was observed in the repertoire of serum antibodies than the circulating B cells, suggesting that non-circulating B cells may also be contributing to overall anti-Dsg3 serum antibody responses (128). A recent report suggests that it is possible that tissue-resident Dsg3-specific memory B cells and plasma cells to be found at the site of disease presentation in the skin and mucosal membranes (129). These skin-resident cells may explain the absence of Dsg3-specific antibody secreting cells in the periphery, and may provide novel insight into how B cells cause PV disease.

Contribution of other immune cells to PV pathogenesis

Although B cells are the major driver of PV disease pathogenesis, there is some evidence of the involvement of other immune cells in PV. Primarily, the role of T cells in PV has been fairly well characterized. Genome wide association studies (GWAS) showed that PV patients have a bias towards expressing HLA-DRB1*0402 and HLADQB1*0503 MHC class II allele usage (130). The prominence of these alleles was paired with the detection of Th1 and Th2 cells reactivity towards Dsg3, both in PV patients as well as in a few healthy controls who carried these specific HLA alleles (131). Although both Th1 and Th2 responses are observed in patients, it is thought that Th2 responses may be higher in pemphigus patients with active disease compared to those in remission (132), an

observation also seen in mice models of PV disease (133, 134). MBC cultures with targeted inhibition of T cell help using an anti-DR or anti-DQ antibodies decreased the detection of Dsg3+ MBCs, while an anti-DP control antibody had no effect, suggesting an important role of specific T cells in the activation of memory B cells (131). Further, humanized HLA-DRB1*0402 expressing mice showed larger, more robust responses when immunized with rDsg3 compared to transgenic mice with non-HLADRB1*0402 expression (130). Additionally, blocking T cell responses, either through T cell depletion or the use of anti-CD40L antibody, was shown to greatly decrease Dsg3-specific B cell responses (131). The prevalence of reactivity towards this MHC Class II allele in human pemphigus patients was confirmed with the ability to detect Dsg3-reactive T cells in humans using HLA-DRB1*0402 tetramers (135). Recently, circulating Tfhs were also found at higher frequencies in PV patients than healthy controls, with Tfh-associated cytokines like IL27 correlating with levels of serum antibodies against Dsg3 (136), suggesting that this subset of T cells may also be important in driving PV autoantibody development. Future experiments characterizing the Dsg3 peptides that bind to these HLA types would further enhance our understanding of the role of T cells in PV pathogenesis.

The development of autoreactive T cells specific for Dsg3 seems to mediated by AIRE expression in the thymus, which would allow for the expression of Dsg3 in mTECs, resulting in negative selection of T cells against this autoantigen. CD4 T cells from AIRE knock-out mice, which would not have had the opportunity for negative selection against Dsg, were able to induce detection of Dsg3-specific serum antibodies in mice when transferred with splenic B cells from Dsg3-knockout mice. However, no autoantibodies were detected in mice that received autoreactive splenic B cells with T cells from AIRE-

competent mice (137). This provides a potential model for the development of autoreactive T cells, which can in turn provide help for the development of autoreactive B cells.

There is also some indication that innate immunity and granulocytes may have a role in PV disease pathogenesis. One interesting characterization of pemphigus patients is the deposits of complement proteins in skin lesions of PV patients (138). Additionally, patient serum is able to fix complement to skin biopsies (138). However, it is unclear what this means for disease pathogenesis. Passive transfer of fAbs are able to cause disease in mice (139), suggesting that the Fc portion of antibodies, which would be necessary to fix complement via antibody-mediated mechanisms, is not necessarily important in causing disease. Additionally, mice depleted of C3 as well as C5-deficient mice, both which would lack complement activity, are still susceptible to PV disease, again further suggesting that complement is not sufficient in causing disease (140). However, other forms of autoimmune blistering skin diseases are definitively impacted by granulocyte activity (115), indicating that we cannot out rule the role of granulocytes in PV. Overall, it appears that while complement may exacerbate symptoms, it is not necessary to initiate PV pathogenesis.

Characterization of Dsg3-specific monoclonal antibodies

The identification of a single autoantigenic target in disease pathogenesis has made it possible to study monoclonal autoantibodies in order to better understand both B cell tolerance and PV disease pathogenesis. Antibodies specific for both Dsg3 and Dsg1 have been made from PV patients using antibody phage display (APD) (141) as well as generation of hybridomas from memory B cells (142, 143). Additionally, Dsg-specific

antibodies have also been generated and studied from mouse models of PV disease (144). Generally, antibodies showed specificity for either Dsg3 or Dsg1, with few antibodies exhibiting cross-reactivity to both Dsg3 and Dsg1 proteins (141, 142, 144). This matches with what has been observed in human serum from PV patients, where PV patents can have serum autoantibody reactivity solely against Dsg3 without any presence of serum antibodies specific for Dsg1 (145). The majority of clones from EBV-transformed memory B cells were of IgG1 isotype, although 40% of the antibodies were IgG4 isotype (142). This, again, matches with observations made on PV patient serum, where IgG4 and IgG1 antibodies seem to be predominantly found in PV patients exhibiting disease (145). Additionally, some evidence suggests that Dsg3-specific IgA antibodies may also present in PV patients (146-148), although their function in driving disease pathogenesis remains unclear. Another study using EBV transformation to isolate Dsg3-specific antibodies saw a large frequnecy of IgM isotype Dsg3-specific antibodies, in addition to IgG1 isotype. Large clonal expansions were also observed in this data set (143). Generally, large clonal expansions of Dsg3-specific monoclonal antibodies have not been observed (141, 142), although this may be due to the small numbers of antibodies derived from patients, which can make it difficult to fully analyze the repertoire of B cells. It is unclear why these studies differ so drastically from each other, highlighting the need to continue studying Dsg3-specific monoclonal antibodies derived from PV patients in order to better improve our understanding of how autoantibodies may develop and contribute to disease pathogenesis.

It is currently unknown what is the origin of these autoreactive monoclonal antibodies. Reversion of several antibodies into their germline sequence caused a loss of specificity towards Dsg3, suggesting that these antibodies are derived from non-reactive or

low-affinity naïve B cells, and that affinity maturation and SHM is necessary for the development of pathogenic Dsg3-specific B cells (142). However, a recent study showed that the reversion of autoantibodies that specifically use the V_H1-46 gene to their germline sequences are able to retain specificity for Dsg3, indicating that it there may be genetic hallmarks of the humoral immune response that underlie PV pathogenesis (149). These V_H1-46 antibodies have also been shown to be cross-reactive with rotavirus antigen (150), suggesting that molecular mimicry may play a role in driving the initial development of Dsg3-specific antibodies. Thus, autoantibodies are likely derived from non-autoreactive precursors activated by molecular mimicry, or very low affinity interactions with Dsg3.

Overall, both APD and EBV transformation methods of generating monoclonal antibodies have their strengths and weaknesses. While antibody phage display is a valuable tool to screen a large number of potential antibodies, it synthetically pairs heavy and light chains that may have been selected out endogenously by tolerance mechanisms, making its *in vivo* significance unclear, as well as making it difficult to analyze the repertoire of these autoreactive B cells (151). Inversely, EBV transformation of memory B cells does retain natural heavy and light chain pairings, but at the cost of efficiency that may result in neglecting potential clones from analysis (152). Thus, continued research to confirm these findings using different approaches may help us with a more complete picture of characterizing these antibodies.

Mechanism of action for pathogenic Dsg3-specific mAbs

It remains unclear how Dsg3-specific antibodies may ultimately cause acantholysis (the de-adhesion of skin cells), resulting in the blisters and sores symptomatically observed

in PV patients. Studies of Dsg3-specific monoclonal antibodies derived from patient PBMCs showed that these antibodies were a mix of both pathogenic and non-pathogenic antibodies when tested in both *in vitro* keratinocyte dissociation assays, as well as *in vivo* mouse models (141, 142). The observation that both pathogenic and non-pathogenic autoantibodies are commonly found in PV patients has led to active research in better understanding the differences between these antibodies in order to provide better treatment options for PV patients.

Epitope mapping of pathogenic antibodies showed that pathogenic antibodies were specific for the NH2 terminal end of the extracellular portion of Dsg3, closer to the EC1 and EC2 subdomains (142, 144), leading to the hypothesis that pathogenic Dsg3-specific antibodies likely target these domains because they are crucial for providing the heterophilic adhesion necessary for skin cells to adhere together. This suggests that the primary mechanism underlying the pathogenicity of Dsg3-reactive antibodies is by sterically hindering the formation of the desmosomal structure by binding epitopes important for heterophilic adhesion (142, 144, 153, 154). These finding were complemented by the observation that the pathogenic AK23 antibody lost activity when changed from an IgG antibody into a bulky, pentameric IgM (155), which suggests that steric access to Dsg3 found within the desmosomal core is crucial for the pathogenicity of this antibody. The importance of epitope specificity of pathogenic antibodies was also confirmed by the observation that non-pathogenic antibodies primarily bind either irrelevant epitopes, including non-conformational epitopes found on linearized recombinant Dsg3 protein, or Dsg3 pro-protein. Thus, binding of these types of epitopes

likely have no impact on the ability of in forming the desmosome and allowing skin cells to adhere together (121).

Another hypothesis of what may characterize pathogenic antibodies is that IgG4 antibodies are pathogenic while IgG1 antibodies are non-pathogenic. This idea is based on the observation that a higher frequency of IgG4 Dsg3-specific serum antibodies are present in PV patients with active disease compared to remission patients (145). However, mapping whole serum onto peptide fragments of Dsg3 show no different in epitope preference of IgG4 versus IgG1 serum antibodies (95). Additionally, switching the Fc domain of Dsg3-specific antibodies from IgG1 to IgG4 isotypes had no impact on the specificity, affinity, and *in vitro* pathogenicity of pathogenic antibodies, suggesting that the Fc domain and isotype usage has no impact on antibody binding properties (156). However, these studies are limited in scope and it remains unclear if IgG4 isotype usage could somehow result in an advantage for pathogenic antibodies. Future experiments probing the relevance of IgG4 in a humanized mouse model expressing relevant Fc receptors will provide information on the activity of IgG4 isotype in PV pathogenesis.

In depth characterization of the impact of pemphigus autoantibodies on the desmosomal structure is also currently being studied to better understand additional mechanisms underlying pathogenicity. Initial studies performed *in vivo* characterization of what happens to desmosomes after IgG binds Dsg3 in active PV models using immunoelectron microscopy. Non-acantholytic areas have IgG bound strictly to the extracellular part of desmosomes. However, in affected acantholytic areas, desmosomes were split and desmoplakin was observed to be internalized into the cytoplasm of skin cells (157). Imaging methods have since improved with recent technology, providing more

accurate pictures of what is occurring to desmosomes during pemphigus. Newer techniques showed that in *in vitro* models of pemphigus, using patient serum IgG and primary cell lines of human keratinocytes, the disruption of desmosomes was paired with a rapid internalization of Dsg3 from the cell surface. Since this endocytosis was colocalized with lysosomes, it is thought that Dsg3 is targeted for degradation (158, 159). Using high resolution structure illumination microscopy, studies were able to observe localization of patient IgG with lipid raft and endosomal markers. This was paired with decrease in size of desmosomes at the site of the split, which suggests that this clustering and endocytosis must be an underlying mechanism for the characteristic acantholysis observed in patients (160, 161). Other mechanisms suggest that pathogenic antibodies also engage in signaling pathways involving the p38 MAP-kinase, which may mediate the endocytosis and degradation of Dsg3 proteins (162, 163). Interestingly, the level of desmosomal disruption varies when comparing the addition of monoclonal antibodies to polyclonal antibodies (whole serum) (163), and mixtures of monoclonal antibodies can act synergistically to enhance overall pathogenic potential (164), emphasizing the importance of understanding how the mechanisms of pathogenicity may be different or similar when studying either monoclonal or polyclonal antibodies.

Overall, there appears to be multiple mechanisms underlying how a Dsg3-specific antibody may cause pathogenicity in PV patients. Both steric hindrance as well as signaling pathways likely contribute the pathogenicity of autoantibodies. Ongoing studies in better understanding these pathways will allow us to specifically target pathogenic antibodies and improve the treatment and clinical care of PV patients.

RITUXIMAB THERAPY

Treatment of PV disease with Rituximab

Treatment of PV has primarily involved the use of steroids and immunosuppressants, although prolonged usage of these therapies may lead to many severe side effects including death (165-167). Recently, use of the B cell ablative therapy Rituximab has found widespread use to treat PV (168, 169). Rituximab has great efficacy, as shown by improvement in symptoms in almost all patients treated. Additionally, side effects are infrequent and milder compared to those seen in patients treated with immunosuppressants (106, 165, 170).

Rituximab is a chimeric monoclonal anti-CD20 monoclonal antibody that is able to deplete all CD20 expressing cells. It works in a complement and monocyte-dependent manner (171, 172). Rituximab is currently FDA-approved to treat lymphoma, RA, and antineutrophil cytoplasmic antibody-associated vasculitis, (173), and its use for treating pemphigus was approved as of March of 2017 (174). Additionally, there is increasing off-label use to treat B-cell mediated autoimmune disorders including SLE and Type I diabetes (175), making Rituximab an important clinical drug to study in order to better understand how it effects autoimmune responses, as well as understanding if there are any long-term impacts on normal protective B cell responses which may be detrimental to patients.

Rituximab is often given either through the RA protocol, involving 4 doses of 375 mg/m^2 given weekly over the course of 4 weeks (176), or the lymphoma protocol given as two bullous doses of 1 g every two weeks (177). Rituximab effectively depletes all peripheral B cells, although plasma cells, which lack expression of CD20, are retained (65, 178). This means that even during potential immunosuppressive states where patients lack

B cells, total serum IgG and protective serum antibodies specific for childhood vaccine antigens like tetanus-toxoid and pneumocystis pneumonia are unchanged by Rituximab treatment. However, total IgM does decrease, reflecting the depletion of the B cell compartment despite retention of long-lived CD20-negative plasma cells. (179). While protective antibody titers remain elevated, autoantibody titers against Dsg3 and Dsg1 generally decrease in PV patients after Rituximab therapy (179). This suggests that disease-causing B cells are sensitive to Rituximab and are a result of ongoing immune responses to autoantigens. Additionally, there must be tolerance mechanisms in place that preclude these cells from becoming long-lived plasma cells.

Although peripheral B cells are completely depleted by Rituximab, they do eventually start to return to the periphery 6-9 months post-treatment with Rituximab (180). *In vitro* models show that 5 μg/mL of Rituximab is sufficient in preventing the proliferation of B cells, suggesting that even low levels or Rituximab are able to keep B cells depleted and may account for why it takes so long for B cells to being peripheral recovery after treatment (181). Despite recovery of total B cell numbers, most of these reconstituted B cells tend to be naïve cells, specifically translational B cells, which are newly immigrated B cells from the bone marrow (182). Additionally, there appears to be a long-term impact on peripheral memory B cell compartment, with CD27+ memory B cells remaining depleted in patients even 5 years post-treatment (183). It remains unclear if recovered memory B cells represent newly generated memory cells, on memory B cells that were refractory to Rituximab-mediated B cells depletion.

Rituximab therapy seems to have no impact on T cells, with total number for both CD4+ and CD8+ T cells unchanging after Rituximab treatment (184), although there

appears to be an impact on autoantigen-specific T cells, where Dsg3-specific T cells in PV patients decrease after treatment. However, normal protective Th1 responses towards tetanus toxoid appear unaffected by Rtx (184). It is unclear why Rituximab would have differing impact on pathogenic autoimmune versus normal protective T cell responses. Because total T cells appear to be unaffected by Rituximab, future studies on determining if distinct T cell subsets are effected by Rituximab, and determining their relationship with the B cell response will provide a deeper understanding as to why Rituximab may impact T cell responses, and if there are any long-term impacts of this treatment on T cells.

While the impact of Rituximab on peripheral B cells in humans is easily studied, there is still some debate on the efficacy of Rituximab-mediated depletion of B cells in tissues. Several human and monkey studies have suggested that a small number of B cells can survive depletion by homing to tissues, secondary lymphoid organs, and even the skin (44, 185-187). However, it is often difficult to interpret data from these studies due to low sample numbers and patient-to-patient variability. It has become increasingly important to determine whether Rituximab sufficiently depletes tissue-resident B cells, which may contribute to the repopulation of the B cell compartment after recovery from Rituximab treatment, or if all B cells are sufficiently depleted and reconstituted B cells represent newly generated cells.

Rituximab has been shown to be safe and efficacious in the treatment of pemphigus patients (106, 170). Although most patients respond to Rituximab therapy, about 40% of patients are prone to relapse within two years after treatment (169). Relapse in disease is also commonly observed in other B-cell mediated autoimmune disorders treated with Rituximab (169, 188). Some studies have suggested that a relapse in disease like RA can

be predicted by repopulation with higher number of memory B cells, establishing a vital role for memory B cells in disease pathogenesis (189). Interestingly, a lower frequency of CD4 T cells appears to be a biomarker PV for patients prone to relapse in disease (190), although the mechanism behind this finding remains unclear. The random nature of relapse in disease suggests a lack of understanding of the impact of Rituximab on the homeostatic return and quality of antigen-specific B cells. Thus, it has become increasingly important to study the impact of Rituximab on immune responses, observing both the protective and pathogenic autoimmune responses.

Relapse in PV disease after Rituximab treatment

Although Rituximab is efficacious in treating symptoms in patients, roughly 40% of Rituximab-treated patients will experience an unpredictable and random relapse in disease after reconstitution of the peripheral B cell compartment (169). While relapses generally correlate with repopulation of the B cell compartment (190) and an increasing rise in serum anti-Dsg3 titers (184), there are instances where this is not true. Thus, we need better biomarkers to be able to better predict which patients will eventually relapse in order to better guide the treatment of PV patients (191).

It is currently unclear what mechanism underlies PV relapse. It is possible that pathogenic B cells are continuously generated from naïve responses, suggesting that ongoing autoimmune dysfunction causes relapse in PV patients and can never be fully cured. However, it is also possible that Dsg3-specific responses are a result of a single break in tolerance, and that relapse is caused by repopulation of memory responses, suggesting that complete ablation of a reservoir of pathogenic clones will allow for patients

to be fully cured of symptoms. By using immunoscope to profile the CDR3 length of B cell in the periphery in order to identify abnormal clonal expansions, previous studies have shown that the B cell repertoire in PV patients is highly clonal. These clonal expansions are then abrogated after treatment with Rituximab, specifically within remission patients who have a normal distribution of CDR3 length after treatment. However, relapse patients re-express highly clonal B cell repertoires (179, 182). This suggests that relapse is caused by the presence of pre-existing pathogenic B cell clones that persist after Rituximab-mediated depletion. Interestingly, clonal expansions were identified in B cells expressing both IgG as well as IgM isotypes. Because Dsg3-specific antibodies in the serum are rarely IgM (145), it remains unclear if these clonal expansions represent antibodies that cause disease. However, since IgM usage is associated with naïve responses (192), it is also possible that the expansion of IgM clones may be representative of newly generated B cell responses towards Dsg3. Because immunoscope only sequences the CDR3 region of the antibody, it is not possible to check antigen-specificity of antibodies from the clonal expansion Additionally, immunoscope assays were done on total PBMCs, making it impossible to identify which B cell subset contains the clonal expansion. Because immunoscope asses total PBMCs and not specific B cell subsets, it is also possible that the large clonal expansion may have been caused by PCR amplification bias of the plasmablast compartment, which is clonal by nature and contains considerably larger amounts of mRNA that other B cell subsets. This could potentially lead to an exaggerated over-representation of clonal expansions in peripheral B cells.

A recent paper utilized both APD and targeted PCR to track Dsg3+ B cells in two patients over the course of 14 years of disease after Rituximab treatment. One patient

achieved long-term remission after Rituximab treatment, and had no Dsg3-specific clones that were identified at time of diagnosis could be detected during remission. However, the other patient relapsed and had detectable Dsg3+ clones that were present at the time of diagnosis, suggesting that remission can only be achieved by the complete elimination of pathogenic clones (193). Of course, we cannot out rule the possibility that Dsg3+ antibodies were not completely eliminated in the remission patient, but rather that they are present at such low numbers that they failed to be amplified via PCR. Overall, data suggests that relapse in disease is likely derived from the reoccurrence of pre-existing Dsg3-specific B cells rather than the generation of new autoreactive clones. However, future studies using more sensitive and extensive sequencing techniques, as well as analysis of additional PV patients, will confirm these findings.

Other B cells subsets have also been implicated in the relapse of PV patients. A subset of regulatory B cells, or IL10-secreting B cells, is also thought to drive relapse in PV disease. A long-term follow-up of a cohort of PV patients suggests that relapsing patients had lower frequencies of IL10-secreting transitional B cells compared to patients who remained in remission after Rituximab treatment (179). This suggests that ongoing immune dysfunction in patients, specifically in the ability to mediate tolerance through regulatory cytokine functions, may contribute to the development of PV disease. Another factor mediating relapse may be the increased presence of BAFF found in the serum after Rituximab treatment. BAFF is an important cytokine mediating cell survival and B cell tolerance (81). High levels of BAFF after Rituximab treatment directly correlated with an increase in protective antibody titers against pathogens such as VZV and EBV, while low levels of BAFF inversely correlated with high serum titers against Dsg3. This suggests that

BAFF may have differential effects on the maintenance of autoreactive Dsg3-specific B cells and protective pathogen-specific plasma cells (194). Because BAFF has an impact on tolerance and the selectivity of autoreactive B cells, this could be a potentially relevant finding that would guide the discovery of novel treatment options for Rituximab-treated patients. Further studies on the level of serum BAFF in relapse versus remission patients may further elucidate the role of this cytokine in the maintenance of Dsg3-specific B cells.

Mechanism of relapse in other B cell-mediated autoimmune diseases

Studies of other B cell mediated autoimmune disorders may help guide the identification of the underlying mechanism driving disease pathogenesis and relapse in PV patients. While general poly-autoreactive B cells can be commonly found in healthy controls when assessing both the naïve (46) and memory B cell compartments (89, 90), SLE patient tend to have even more autoreactive naïve B cells than healthy controls (67). When treated with Rituximab, SLE patients in remission will have a decrease in polyreactive mature naïve B cells, although these cells are still more common in the SLE remission patients compared to healthy controls (92). Next generation sequencing methods also identified autoreactive plasmablasts in SLE patients, with repertoire connectivity to the naïve B cell population. This is different from protective vaccine-related plasmablasts, which are typically more connected to the repertoire of MBC populations, and not naïve B cells (58). This suggests that relapse in SLE patients may be driven by ongoing break in tolerance resulting in the generation of autoreactive naïve B cells that eventually differentiate into pathogenic plasmablast expansions that drive SLE pathogenesis.

The impact of Rituximab on overall tolerance of B cells was also described in a cohort of patients with Type I Diabetes. In these patients, a panel of monoclonal antibodies was generated from the naïve B cell compartment. As expected, a large proportion of these antibodies were polyreactive with a panel of autoantigens. The frequency of these polyreactive antibodies did not change in reconstituted naive B cells collected 1 year post-Rituximab treatment, suggesting that tolerance checkpoints were not restored after Rituximab and that pre-existing defects in the tolerance pathway in patients with autoimmune disorders is not reset after Rituximab treatment (195). This model confirms the aforementioned studies of SLE patients, and suggest that autoreactivity is a result of ongoing failure in tolerance mechanisms, and that autoimmune B cells originate from naïve responses.

Studies of other diseases also suggest that memory B cells may be important in driving relapse in autoimmune disease. In rheumatoid arthritis patients, a higher frequency of memory B cells after treatment with Rituximab was identified as a biomarker for predicting relapse in patients (196), suggesting that a faster repopulation of persisting memory B cells may underlie the mechanism causing relapse in these patients. Memory B cells were also implicated in another B cell-mediated autoimmune disorder called anti-myelin-associated glycoprotein (anti-MAG) neuropathy. Single-cell analyses of memory B cells from these patients showed massive clonal expansions, and antibodies cloned from these expanded memory B cells were specific for MAG. These clones were ablated after Rituximab therapy, with non-responding patients who remained symptomatic showing persisting expansions in the MBC compartment (197). Overall, these data support the

hypothesis that memory B cells are driving autoimmunity, and targeting this subset of B cells will be important in treating patients.

Because serum antibodies appear to be important in driving PV disease, it remains important to understand how Rituximab may impact antibody secreting cells in general. Mouse models have suggested that Rituximab treatment targets short-lived autoreactive plasma cells that primarily reside in the spleen and lymph nodes. This is distinct from long-lived plasma cells that reside in the bone marrow, which remain unaffected by Rituximab therapy. This mouse study provides a mechanism of how Rituximab treatment ameliorates autoimmune diseases, and also suggests that those autoimmune-specific antibody secreting cells are inherently different from long-lived protective plasma cells (198). Additionally, this study highlights the fact that protective immune titers towards childhood vaccines are able to persist in Rituximab-treated patients, but that autoimmune titers rapidly drop (182), suggesting that tolerance mechanisms are in place to preclude autoimmune cells from becoming long-lived plasma cells. Otherwise, patients with autoimmune diseases would not respond positively towards Rituximab therapy.

Impact of Rituximab on B cell responses to influenza vaccination

Generally, long-lived serum antibody titers are unaffected by Rituximab treatment, with titers against tetanus and meningitis unchanging after treatment despite complete depletion of peripheral B cells (179, 182, 199). However, the long-term decrease of memory B cells (87) and delayed acquistiion of somatic hypermutation in the unswitched memory B cell compartment after B cell reconstitution (200) suggests that there may be some sort of lasting impact of Rituximab on normal B cell responses after reconstitution.

As there is a clear difference of the impact of Rituximab on pathogenic autoimmune responses compared to protective immune responses, is it important to better understand what impact Rituximab has on overall humoral immune responses in order to understand if there are any negative side effects that may be a result of Rituximab-induced dysfunction on the B cell compartment.

Because the seasonal influenza vaccine is given on a yearly basis to healthy controls, and immune-compromised, Rituximab-treated patients are clinically recommended to receive the vaccination, influenza is both a clinically relevant and accessible human model to study normal protective recall responses. Influenza is a major cause of morbidity and mortality worldwide. In the United States alone, influenza can cause more than 200,000 hospitalizations and 36,000 deaths per year (201, 202). Occasionally, a novel influenza strain can be introduced into the population. If little or no pre-existing immunity exists towards these new strains, a pandemic can occur, increasing both the healthcare and economic burden induced by influenza, as was recently observed during the 2009 H1N1 pandemic (203). These strains are typically a consequence of antigenic shift, in which two different strains of influenza virus exchange components of their segmented RNA genome to create a novel viral pathogen against which humans may have little to no pre-existing immunity (204, 205). While generally ineffective against these pandemic strains, the seasonal influenza vaccine has proven to be an effective preventative measure against commonly circulating influenza viruses. However, making the seasonal influenza vaccine is a complex and challenging process (206). A new vaccine is administered every season because protection is short-lived (207, 208), and the influenza virus can undergo antigenic drift, in which the virus mutates very rapidly, allowing it to produce escape

mutants that can evade immune recognition by the host. Antigenic drift can occasionally prevent the vaccine from targeting the circulating virus strain, which lowers the efficacy of the seasonal influenza vaccine. This scenario occurred most recently during the 2014/2015 flu season with a drifted H3 virus strain (209).

The vaccine works primarily by eliciting antibodies that target the hemagglutinin protein, which consists of two domains: HA1 and HA2. HA1, the head domain, allows the virus to attach to sialic acid receptors on host cells, allowing for endocytosis and entry of the virus into the target cell. HA2, the stem domain, controls the membrane fusion process. Of the two, HA1 is the immunodominant epitope, with a large majority of antibodies targeting this domain. Unfortunately, HA1 is highly variable between influenza strains, and is also the major site for mutations leading to antigenic drift (210). In contrast, the HA2 domain is much more conserved between virus strains and is relatively infrequently mutated (210). Based on a large body of evidence from the last several years (211-214), it is thought that preferentially targeting the antibody response against the HA2 domain will result in broadly neutralizing antibodies capable of protection against a wide spectrum of influenza viruses, including both pandemic and drifted strains of influenza. Intense efforts directed towards developing this type of "universal" vaccine are ongoing, as well as efforts to develop broadly neutralizing antibodies for use as therapeutic agents, particularly in vulnerable populations that normally do not respond well to vaccination.

Memory B cells are an important aspect of protection generated in response to vaccination, and is responsible for potent, rapid anamnestic responses upon re-exposure to influenza (215). Additionally, memory B cells with broad reactivity towards influenza were found to target both the HA head (216) and stem (217, 218) regions of influenza, suggesting

that induction of these cells may lead to long-lived protection against a broad spectrum of strains of influenza virus. While stem reactive memory B cells are a part of the normal human B cell repertoire, they normally exist at very low frequencies, and are only boosted in the context of exposure to a very different HA protein. Presumably, robust responses would be required for sufficient protection, and thus, many studies are currently focused on understanding how to target and boost B cells that secrete these broadly neutralizing antibodies. The current theory is that stem-reactive memory B cells exist in small numbers, whereas those specific for the head domain are more abundant. When encountering a new strain of influenza which lacks the immunodominant epitopes recognized by head-reactive memory B cells, the stem-reactive memory B cells can be preferentially boosted by subdominant conserved epitopes, as these cells respond much quicker than naïve B cells that must be primed by novel epitopes. This theory has been supported through observations that broadly neutralizing antibodies seem to be boosted in individuals responding to the novel 2009 pandemic H1N1 strain (219, 220). In addition, prior vaccination and infection history seems to impact the antibody response (221). People who have a more diverse history of influenza infection have much higher titers of antibodies specific for the HA stem domain, suggesting that prior encounters with diverse influenza virus strains greatly impact the number of protective broadly neutralizing antibodies that can be generated (222). Another study suggests that while diverse influenza strains may boost stem-reactive antibodies, repeat exposure to common influenza strains primarily boost head-reactive responses and limit the expansion of broadly neutralizing antibodies (215). A recent study was able to detect stem-reactive memory B cells in healthy controls prior to a recent infection or vaccination. However, these stem-reactive memory B cells

were found in much lower numbers than head-reactive memory B cells. Stem-reactive memory B cells could be boosted by an immunization with a novel H5N1 strain, whereas vaccination with the normal seasonal vaccine boosted head-reactive memory B cells with no effect on the number of stem-reactive memory B cells (217).

Targeting specific anatomical niches to boost broadly neutralizing antibody responses may also be important. A recent mouse study suggests that memory B cells specific for broadly neutralizing epitopes may reside primarily in the lungs instead of in circulation or in secondary lymphoid organs. These lung-resident memory B cells were highly mutated, and were generated as a result of local persistent germinal centers that are responding to prolonged viral antigens found in the lung. These tissue-resident memory B cells provided robust protection against a drifted virus in a secondary challenge model, confirming the importance of these memory B cells in generating a cross-reactive, broadly neutralizing antibody response against influenza (223). Although these findings have not yet been confirmed in humans, it does suggest a role for tissue-resident memory B cells in providing broadly neutralizing responses. Because most studies of human broadly neutralizing monoclonal antibodies have focused primarily on B cells isolated from blood samples, a focus on lung-resident memory B cells may provide greater insight in how to generate broadly neutralizing antibodies. Current vaccination delivery strategies may want to consider how to best boost lung-resident memory B cells to elicit potent broadly protective responses.

The importance of memory B cells in providing protective responses against influenza vaccination, especially these tissue-resident memory B cells with broadly neutralizing function, has made it clinically relevant to study if Rituximab-treated patients,

who lack peripheral memory B cells, can respond to vaccination. Several studies have described impaired responses to the influenza vaccination, primarily in the context of Rituximab-treated RA and lymphoma patients. Modest responses were observed in patients who were vaccinated after 6 months post-Rituximab treatment, although these responses were still significantly lower than those observed in vaccinated healthy controls. Additionally, studies have observed impaired humoral immune responses in Rituximab-treated rheumatoid arthritis patients and Type-I diabetes patients during recall responses to repeat vaccination with tetanus toxoid, as well as impaired naïve responses to immunizations with novel antigens such as bacteriophage phiX174 (199, 224). However, these autoimmune patients are often prescribed other immunosuppressive medications or chemotherapy simultaneously with Rituximab therapy (225-230). Thus, it is possible that impaired vaccine responses may not be truly representative of the impact of Rituximab on reconstituted B cell responses, but rather a secondary impact of immunosuppressive medications on the overall humoral immune response. Additionally, these patients are vaccinated prior to full return of the B cell compartment, during which time there may still be Rituximab in the system, which may also dampen the overall response to vaccination independent on the functionality of the B cells.

It is a well-accepted fact that total T cell numbers remain unaffected by B cell ablative therapy (231). While several studies using mice models have suggested impaired ability to generate memory T cells to viral infection after B cell depletion therapy (232, 233), little is known about T cell responses in humans after B cell ablative therapy. One study suggest that T cell responses to the influenza are unaffected by Rituximab, where T cells from Rituximab-treated patients stimulated with influenza peptides showing

productive cytokine secretion comparable to that observed in healthy controls (234). However, this does not out rule the possibility that distinct T cell subsets may be impact by Rituximab. Recent reports have described an important role for circulating T follicular helper cells in generating antibody responses to influenza vaccination (235, 236). Because Tfh development is thought to be dependent on the presence of B cells (35), it is unsurprising that studies have also found lower numbers of circulating Tfh cells in Rituximab-treated patients compared to healthy controls (237). Continued analysis of T cell responses in Rituximab-treated patients, with a focus on subsets of Tfh cells, may provide greater insight onto the impact of Rituximab on protective T cell immune responses.

SUMMARY

B cells are important immune effector cells. Their complicated development allows them to express a very diverse immunoglobulin repertoire that has the potential to target a wide array of pathogens. Additionally, multiple effector B cells subsets can develop in response to an antigenic challenge, including antibody secreting cells which contribute to the overall serum antibody response, as well as development of long-term memory B cells which can provide rapid and robust protection against secondary exposure to an antigen. Essential questions about the development of memory B cells and the selection process determining which cells are destined to become long-lived plasma cells are still an active area of research.

One of the biggest challenges of the developing immune system is to find a way to maintain a diverse repertoire of B cells that will provide protection against all possible pathogens, but somehow limiting diversity to specifically exclude B cells that may bind to self-antigen and cause autoimmunity. Various tolerance mechanisms are in place that prevent the activation of B cells that have the potential to react with self-antigen, while focusing maturation and antigen selection processes primarily on protective B cells that are specific to foreign pathogens. Despite these well-placed checkpoints, tolerance can be broken, causing human B cell-mediated autoimmune disorders such as rheumatoid arthritis, systemic lupus erythematosus, type I diabetes, as well as the rare, understudied autoimmune disease pemphigus vulgaris.

Pemphigus vulgaris is a disease in which patients present blistering sores on skin and mucosal membranes. Although pemphigus vulgaris is a rare disease, its well-characterized autoantigen and topical localization of symptoms present on the skin has

made pemphigus vulgaris a compelling human disease to study as a model to better understand the development of B cell-mediated autoimmune disorders. Pemphigus is often treated with Rituximab, a B cell depletive agent. However, patients are prone to relapse in disease after reconstitution of the B cell compartment. Additionally, people have observed long-term impacts of Rituximab on the immune system, as illustrated by the slow reconstitution of peripheral memory B cells. Thus, studies of PV patients have focused not only on characterizing disease pathogenesis and the mechanisms underlying Dsg3-specific antibody-mediated pathogenesis, but also understanding the impact of Rituximab on reconstituted B cell responses in terms of both autoimmune and protective immune responses (Figure 2).

There are many questions still left to answer concerning PV. What B cell subset is the origin of the antibody response? How do these autoimmune B cells develop? Are specific B cell clones responsible for disease, and is the persistence of these distinct clones the cause for relapse in disease after Rituximab treatment? Is there a way to predict which patients are prone to flare in disease? And lastly, does Rituximab have any impact on normal protective immune responses that allow B cells to prevent infection by foreign pathogens? These are important questions that will not only reveal aspects of basic B cell biology, but also guide the clinical care of both pemphigus patients and other patients with autoimmune diseases who receive Rituximab as a therapeutic. This dissertation aims to address essential questions about the development of memory B cells during pemphigus vulgaris pathogenesis, and the impact of the B cell ablative therapy Rituximab on protective memory B cell responses in these patients.

To better understand how memory B cells may drive B cell mediated autoimmune diseases, we studied their role in PV pathogenesis by generating and characterizing monoclonal antibodies derived from single Dsg3-specific memory B cells isolated from PV patients. In this study, we provide novel insight into the development of autoantigen-specific B cells, as well as the role of Dsg3-specific antibodies in driving pathogenic PV-causing responses (Chapter 2). Because the persistence of these memory B cells may provide a mechanism through which PV patients relapse after treatment with the B cell ablative therapy Rituximab, we next described the impact of previous Rituximab treatment on normal, protective memory B cells. Using influenza vaccine responses as a model of a protective B cell responses, we provide evidence that while Rituximab sufficiently depletes memory B cells from the periphery, a subset of memory B cells likely survive the depletion outside of peripheral blood and are able to provide rapid and robust recall responses to antigenic challenge (Chapter 3). The findings described in this dissertation will have implications in the understanding of the development of the B cell-mediated autoimmune disorder pemphigus vulgaris, and also contribute to our understanding of how Rituximab therapy may impact both autoreactive and protective immune responses in patients.

FIGURES AND LEGENDS

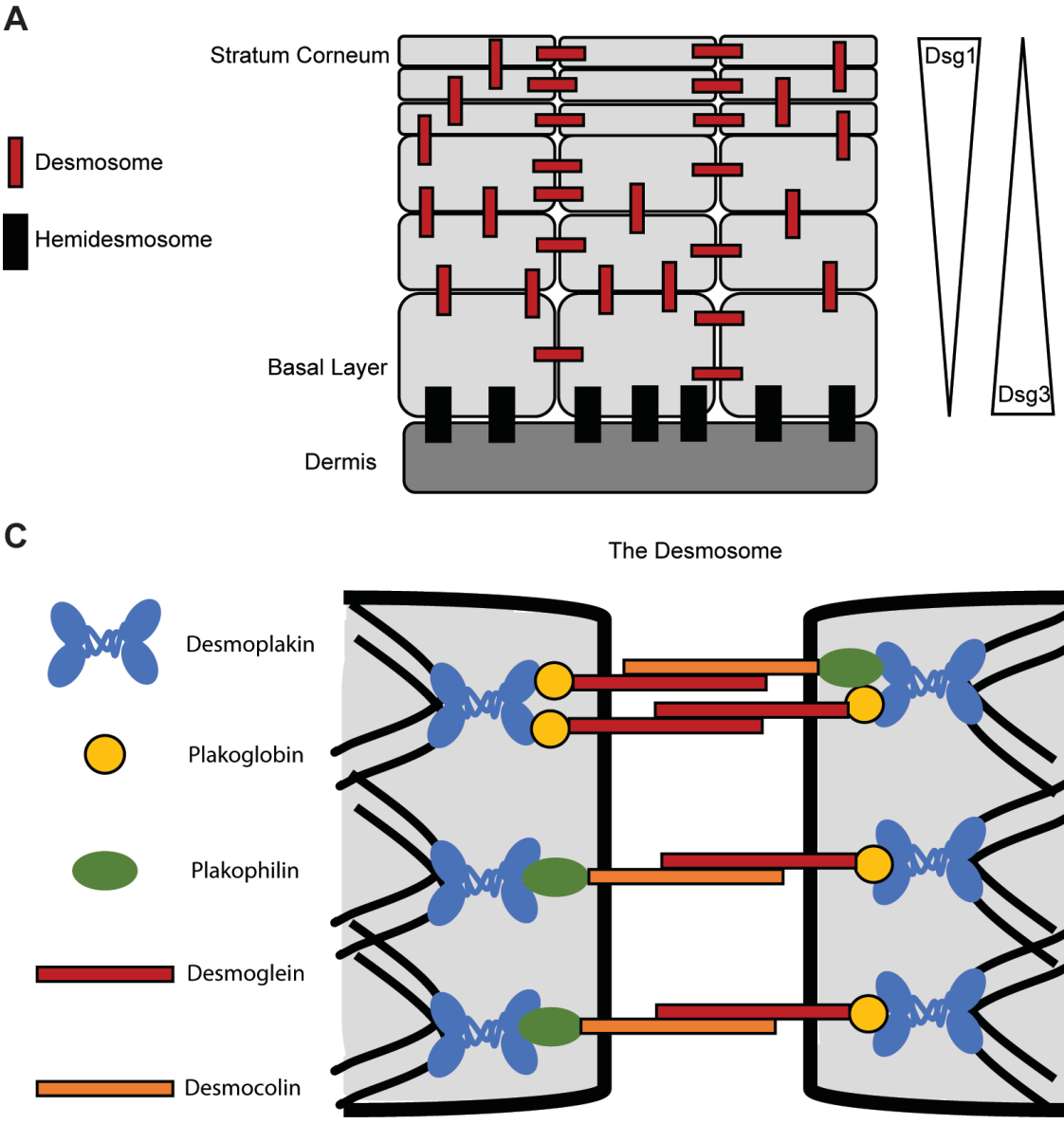

FIGURE 1. Structure of skin and desmosomes.

(A) The epidermis is the outermost component of the skin, and is composed of several layers. The stratum corneum is the outermost layer of the epidermis, and consists of fully differentiated keratinocytes, whereas the basal layer is at the bottom layer of the epidermis in which actively proliferating keratinocytes reside. The epidermal cells are able to adhere with each other via desmosomes, in which the extracellular protein desmoglein-1 mediates interactions at the top layer of the skin, while desmoglein-3 is found in the basal layer. The epidermis is connected to the dermal layer of the skin through an adhesive structure called the hemidesmosome. (B) The desmosome allows actin containing cells to adhere together, and is made of several protein components. The intracellular proteins include desmoplakin, as well as the armadillo family of proteins called plakoglobin and plakophilin. These proteins serve as a connection between the intracellular actin filaments, also called keratin in skin cells, and the extracellular proteins desmoglein and desmocollin, which provide the intercellular heterophilic adhesion necessary for the desmosome to form.

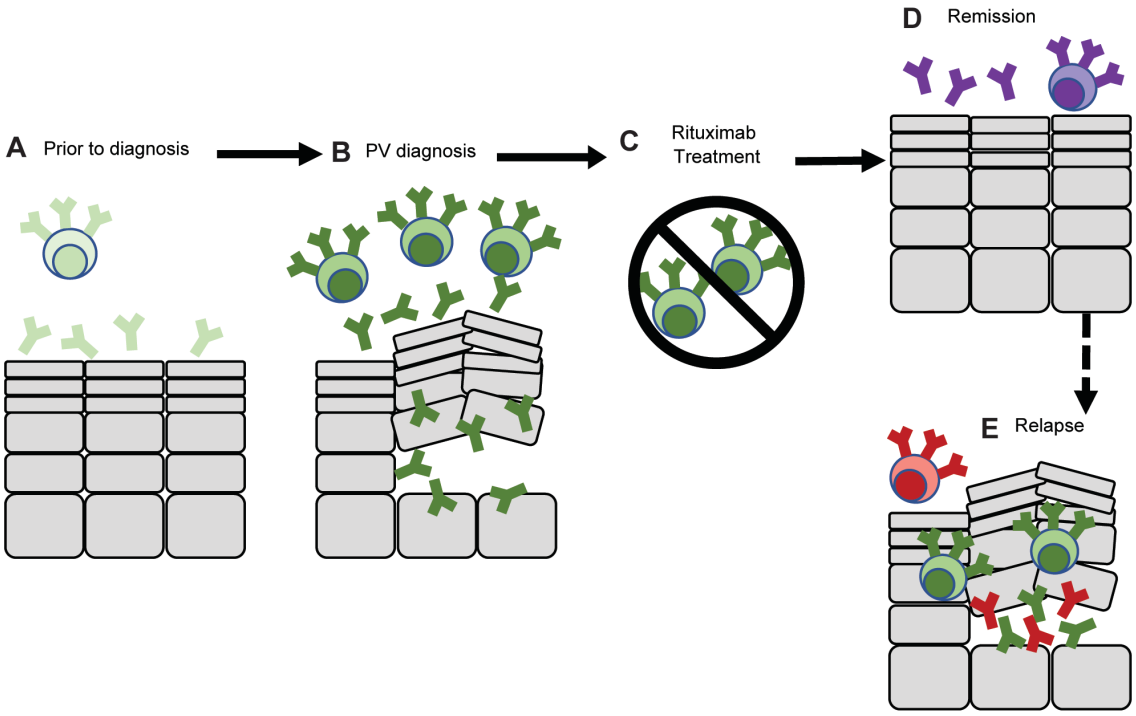

FIGURE 2. Pathogenesis and treatment of pemphigus vulgaris.

(A) Prior to development of PV disease, Dsg3-specific B cells are likely lacking from the periphery, and naïve B cells must undergo maturation to develop into PV-causing B cells. (B) At the time of PV diagnosis, Dsg3-specific antibody responses can be readily detected in PV patients. These antibodies bind to Dsg3 in the epidermis and cause loss of skin cell adhesion, also known as acantholysis, in patients, resulting in the symptomatic blistering and sores on the skin and mucosal membranes. (C) Patients can be treated with the B cell depletive agent, Rituximab, which depletes all B cells from the periphery, including Dsg3-specific B cells. (D) This causes the loss of pathogenic Dsg3-specific antibody responses and amelioration of symptoms, resulting in the patient reaching clinical remission. It is unclear if the function of reconstituted B cells is at all impacted by Rituximab therapy. (E) Relapses occur in some PV patients after the B cell compartment has returned. It remains unclear if relapse is caused by newly generated Dsg3-specific B cells, persistence of pre-existing Dsg3-specific B cells, or a combination of both.

Chapter 2: Single-cell analysis suggests that ongoing affinity maturation drives the emergence of pemphigus vulgaris autoimmune disease

Alice Cho[1,2], Amber L. Caldara[3,4], Nina A. Ran[5], Zach Menne[1,2], Robert C. Kauffman[1,2], Maurizio Affer[1,2], Alexandra Llovet[1,2], Carson Norwood[1,2], Aaron Scanlan[1,2], Grace Mantus[1,2], Bridget Bradley[4], Stephanie Zimmer[3,4], Thomas Schmidt[6], Michael Hertl[6], Aimee S. Payne[5], Ron Feldman[4], Andrew P. Kowalczyk[3,4], and Jens Wrammert*[,1,2]

[1]Department of Pediatrics, Division of Infectious Disease, Emory University School of Medicine, Atlanta, Georgia, USA; [2]Emory Vaccine Center, Emory University School of Medicine, Atlanta, Georgia, USA; [3]Department of Cell Biology, Emory University, Atlanta, Georgia, USA; [4]Department of Dermatology, Emory University School of Medicine, Atlanta, Georgia, USA; [5]Department of Dermatology, Perelman School of Medicine, University of Pennsylvania, Philadelphia, Pennsylvania, USA; [6]Department of Dermatology and Allergology, Philipps-University, Marburg, Germany

ABSTRACT

Pemphigus vulgaris (PV) is an autoantibody-mediated disease characterized by blistering sores on skin and mucosal membranes. PV autoantibodies primarily target the cellular adhesion protein, desmoglein-3 (Dsg3), making this a powerful model-system to understand the autoimmune responses induced in these patients. Dsg3-specific antibodies have been shown to be both necessary and sufficient to cause PV-like symptoms in mice. However, it remains unclear how Dsg3-specific autoantibodies develop and cause disease in humans. To address this, we performed a cross-sectional study of 32 PV patients before or after treatment to track relevant cellular responses underlying disease pathogenesis, and an in-depth single-cell analysis of 2 patients. This was done by generating a panel of mAbs from single Dsg3-specific memory B cells (MBCs) using a novel technique of antigen-baiting and detection via flow cytometry. Additionally, we analyzed a paired sample from one patient collected 15-months prior to disease diagnosis. We found that Dsg3-specific MBCs had an activated phenotype and showed signs of ongoing affinity maturation and clonal selection. Pathogenic mAbs primarily targeted the extracellular domains EC1 and EC2 of Dsg3. However, we also detected pathogenic mAbs specific for EC4. Competition analyses defined one or two epitopes in each domain, and antibodies targeting specific epitopes exhibited a restricted repertoire. Finally, combining antibodies targeting different epitopes synergistically enhanced *in vitro* pathogenicity. Overall, this study has implications for understanding how pathogenic Dsg3-specific autoantibodies develop, and the mechanism underlying how these antibodies ultimately cause disease.

INTRODUCTION

Pemphigus vulgaris (PV) is a human autoantibody-mediated disease (120, 139), in which patients experience painful blistering and sores on skin and mucosal membranes (96, 104). The primary autoantigenic target of PV is the cellular adhesion protein desmoglein-3 (Dsg3) (98, 108, 116, 120, 123, 124). This protein is a transmembrane component of the desmosome, which provides the structure necessary for epidermal keratinocytes to adhere together (111, 112). While PV patients with disease limited to mucosal tissues have IgG autoantibodies directed solely towards Dsg3, patients with the mucocutaneous variant of PV often also have autoantibodies targeting the homologous protein Dsg1 (113). Dsg3 is a calcium-dependent transmembrane glycoprotein with an extracellular component made up of 5 subdomains (EC1-5) arranged in tandem to form a linear structure (108, 154, 238). Targeting Dsg3 has been shown to be both necessary and sufficient to cause disease using *in vitro* and murine *in vivo* models of PV (98, 105, 116, 239). Unlike many autoimmune diseases that have poorly characterized or many autoantigenic targets (240, 241), identification of a well-defined autoantigenic target has made PV a unique human disease to study both B cell tolerance and autoimmune pathogenesis at an antigen-specific level. While Dsg3-specific B cells are clearly the major effector cell population in PV pathogenesis (105, 107, 108, 122, 124), it remains unclear which subset of differentiated B cells directly contribute to the polyclonal serum autoantibody response or where these cells may reside (125, 129, 179).

Dsg3-specific mAbs have been studied from PV patients using antibody phage display (APD) (141) and generation of hybridomas from memory B cells (MBCs) (142, 143, 242). These studies have been very informative to the field, and have allowed for

careful dissection of the functional qualities of Dsg3-specific human antibodies. However, while APD is a powerful tool to screen large number of recombinant antibodies, it artificially and randomly pairs heavy and light chains from large phage libraries. This may not truly represent the cognate heavy and light chain pairings of the selected repertoire present *in vivo* (151). In contrast, hybridomas generated from human MBCs does retain the natural heavy and light chain pairings, but is labor intensive and requires screening a very large number of clones. Thus, it often results in a smaller number of antigen-specific mAbs to be analyzed and may result in a suboptimal understanding of overall repertoire and function of the B cell response (243). The aforementioned studies have isolated several Dsg3-specific mAbs with varying levels of repertoire diversity and were found to have a mix of "pathogenic" and "non-pathogenic" activity (121, 141, 142). These studies have led to ongoing questions about how Dsg3-specific mAbs develop, as well as the exact mechanism by which they cause pathology. Current models suggest that epitopes crucial for Dsg3-mediated desmosomal adhesion lie in the extracellular EC1 and EC2 subdomains (153, 154), and that pathogenic autoantibodies primarily target these domains and mainly act by steric hinderance (142). Additional mechanisms of pathogenicity include engaging signaling pathways (162) and triggering endocytosis and degradation of Dsg3 (158, 160, 161, 163). Thus, it remains important to continue studying mAbs in order to better understand how they develop and contribute to the overall autoreactive response, ultimately guiding efforts to discover more effective therapies to treat PV.

Given that PV has a well-defined autoantigenic target, it represents an opportunity to address outstanding questions regarding how autoantibodies develop and eventually cause disease. Herein, we determine the dynamics of Dsg3-specific B cell responses in a

cohort of PV patients at the time of diagnosis, and after treatment with B cell depletive therapy. We show that the detection of activated Dsg3-specific MBCs correlates with presentation of disease symptoms. Despite this, circulating Dsg3-specific plasmablasts remained undetectable in all samples analyzed. Using single-cell approaches, we derived and characterized a large panel of mAbs from Dsg3-specific MBCs of two PV patients at the time of diagnosis. Additionally, we had access to a unique paired clinical sample collected 15 months prior to disease onset from one of the donors, which allowed us to show that the autoimmune cells were present over a year before disease onset. Our studies suggest that MBCs play an important role in disease pathogenesis, and that ongoing affinity maturation and clonal restriction ultimately lead to the development of highly pathogenic mAbs binding to a limited number of epitopes on Dsg3. We also found that development of PV disease symptoms correlates with an increase in the frequency of pathogenic antibodies, and that multiple pathogenic antibodies targeting distinct epitopes act in synergy to amplify overall pathogenic potency.

RESULTS

Activated Dsg3-specific memory B cells are found in PV patients presenting with active disease. In order to understand the dynamics of autoreactive B cell responses in PV patients, we performed a cross-sectional analysis of PV patients at the time of diagnosis, or at remission or relapse after treatment with the B cell depletive therapy Rituximab (Rtx) (168). Overall, 32 patients were enrolled with 9 out of 32 patients followed longitudinally throughout treatment, resulting in a total of 54 samples available for analysis. Because reconstitution of the B cell compartment typically begins around 6-9 months post-therapy (180), we only analyzed samples from remission and relapse patients who were at least 6 months post-Rituximab treatment (median 13 or 15 months, respectively) with comparable frequencies of B cells (median 8% of lymphocytes) to PV patients at diagnosis (median 8.5%) and healthy controls (median 9.5%) (Table S1).

Overall, high levels of anti-Dsg3 serum antibody titers could be detected in almost all of the PV patients at the time of diagnosis (16/17; 94%), while none of the healthy controls had detectable titers (0/17; 0%) (Figure 1A). The diagnosis patient with low anti-Dsg3 titers did have clinical data reporting titers reaching 173 U/mL during previous visits, suggesting that the low titers at this particular time point are likely driven by concomitant medications. Anti-Dsg3 titers dropped below the limit of detection after Rituximab therapy in most of the remission patients (8/10; 80%). Two patients still displayed high antibody titers despite treatment with Rituximab. Clinical data showed that in contrast to the other patients who responded to Rituximab with a massive decrease in anti-Dsg3 serum titers (Figure S1A), these patients retained high titers against Dsg3 despite efficient depletion of the B cell compartment (Figure S1B). Patients that relapsed during the study period had

detectable serum Dsg3 titers (15/17; 88%). Anti-Dsg1 serum titers were only detected in a subset of PV patients at diagnosis (7/17; 41%) and relapse (5/17; 29%) but were absent from all patients at remission (Figure S1C). Unlike serum auto-antibody titers which decrease after Rituximab treatment (Figure S1D), titers against childhood vaccines like tetanus did not significantly change in PV patients after treatment with Rituximab (Figure S1E).

We also determined if Dsg3-specific MBCs could be detected in these patients. This was done using an *in vitro* polyclonal stimulation of PBMCs with rhu-IL2 and R848 for 3 days, causing MBCs to differentiate into antibody-secreting cells (244, 245). Total and Dsg3-specific IgG-secreting cells were detected using an ELISPOT assay to determine the frequency of antigen-specific MBCs (Figure 1B). Similar to serology data, we were able to detect Dsg3-specific MBCs in almost all PV patients at the time of diagnosis (16/17; 94%) and in most of the patients at relapse (9/17; 53%), whereas these cells were completely absent in healthy controls and almost all patients during remission (8/10; 80%) (Figure 1C). It remains unclear if the presence of Dsg3-specific MBCs in relapsing patients are a result of newly generated MBCs, or the expansion of MBCs that survived Rituximab-mediated depletion (193, 245). Overall, the presence of Dsg3-specific MBCs in diagnosis patients and the re-emergence of these cells during disease relapse confirms the importance of these cells in PV pathogenesis.

We next used a fluorophore-labeled recombinant Dsg3 probe to detect antigen-specific MBCs by flow cytometry. By focusing on the two patients with the highest frequency of Dsg3-specific MBCs as measured by the ELISPOT-based assay (Figure 1C), we were able to detect Dsg3-specific MBCs by flow cytometry at a 100-fold higher

frequency than background staining in healthy controls (Figure 1D). Interestingly, the Dsg3-specific MBCs expressed the activation marker CD71, which was recently shown to be transiently expressed on HA-specific MBCs in healthy influenza vaccinees (55). Similar to that study, we found that in influenza-vaccinated healthy controls, recently activated MBCs could be detected as early as Day 7 post-vaccination, and that resting HA-specific MBCs found by Day 28 post-vaccination are CD71 negative (Figure 1D). The canonical expression of CD71 on Dsg3-specific MBCs suggest that these cells were recently activated and are partaking in ongoing immune responses, affirming their relevance to PV pathogenesis. We also enumerated Dsg3-specific plasmablasts in peripheral blood of symptomatic PV patients (Figure S2A, S2B). Strikingly, despite the presence of activated Dsg3-specific MBCs in the periphery, we were unable to detect any Dsg3-specific antibody-secreting plasmablasts using an ELISPOT assay (Figure S2C). This is similar to what has been described in a previous report from the Amagai laboratory (125). This finding is in contrast to an extensive literature describing potent peripheral blood plasmablast responses after vaccination or infection (48, 49, 55, 56, 58). These data suggest that the serum antibodies observed in PV patients are either produced by very rare plasmablasts found in circulation, or possibly in lymphoid organs or skin/mucosal tissue after local differentiation, as recently proposed (129). Overall, the data confirm that Dsg3 is an important target in PV, and that activated MBCs play an important role in disease pathogenesis.

Generation of high affinity autoreactive memory B cells via extensive affinity maturation. To further investigate the properties of Dsg3-specific MBCs, we performed

an in-depth single-cell analysis of MBCs. Using previously published primer sets (246, 247), PCR-amplicons of heavy and light immunoglobulin rearrangements from single-cell sorted Dsg3-specific MBCs were derived from patients ISD068 and ISD102. The single-cell material obtained was used for both repertoire analysis, as well as cloning and expression of mAbs (Figure 2A). Overall, we analyzed a total of 32 cells from each patient. We found that a large portion of the response was class-switched, with the IgG1 isotype most prominently used (Figure 2B). We also detected several IgG4 sequences, similar to previous reports that the IgG1 and IgG4 isotype is preferentially used by PV autoantibodies (145). Additionally, we identified a small number of Dsg3-specific MBCs that had an IgA1 isotype, as previously described (146-148). Similar isotype usage was observed in Dsg3-specific serum antibodies of these patients (Figure S3) as tested by ELISA using subclass-specific reagents confirmed to have no cross-reactivity when tested against recombinant, subclass-switched mAbs (data not shown). While previous efforts have yet to describe a significant function for the Fc-domain of Dsg3-specific antibodies (139, 155, 156), future experiments detailing the relevance of isotype usage on signaling in keratinocytes and other mechanisms will be important in establishing how these antibodies cause disease.

We observed high frequencies of clonal expansions of Dsg3-specific MBCs in both patients, with about 50% of the analyzed sequences sharing clonal origin with at least one other cell (Figure 2C). This is higher than the average frequency of clonal expansions detected in infection-induced plasmablasts, which typically averages around 20% in influenza, dengue, and cholera-infected patients (56, 57, 219). The oligoclonal Dsg3-specific MBCs showed no clear bias in V_H gene usage shared between the two patients. Analysis of the level of somatic hypermutation of these rearrangements showed that Dsg3-

specific MBCs carried high levels of mutation, comparable to levels found in infection-induced plasmablasts (Figure 2D) (57, 219, 248). Additionally, the ratio of replacement (R) versus silent (S) mutations showed a significant focus of replacement mutations within the CDRs, well above the random frequency of 2.9 (Figure 2E) (249). The high R/S ratio imply that these MBCs have undergone extensive affinity maturation in germinal center reactions. Overall, these data suggest that a small pool of clonally restricted and affinity matured MBCs dominate the autoimmune response in these patients.

To confirm that the sequences analyzed above were truly representative of Dsg3-specific immune responses, we recovered 44 mAbs generated from rearrangements observed during repertoire analysis of MBCs (ISD068 n=24; ISD 102 n=20) (Table S2). Using an ELISA assay, we found that 93% (41/44) of the mAbs bound to rDsg3 with high to moderate affinity (Figure 2F). To determine if these autoantibodies were antigen-specific and not representative of broadly cross-reactive species (90), we also tested them against a panel of other antigens such as the highly homologous protein Dsg1, the hemagglutinin antigen from the influenza virus (H1/California/2009), and cholera toxin B subunit (Figure 2F). Despite the 65% homology between Dsg3 and Dsg1 proteins (107), only two mAbs showed any binding activity above the limit of detection towards Dsg1, while no mAbs cross-reacted with the influenza or cholera proteins. To assess if any Dsg3-specific mAbs bound to quaternary epitopes that may not be present in recombinant Dsg3, we tested binding of the mAbs to native Dsg3 expressed on the cell surface of primary human keratinocytes (HK cells) by immunofluorescence staining (Figure S4A) (160, 163), as well as flow cytometry staining of an immortalized cell line of human keratinocytes (HaCaTs) (Figure S4B) (250). These assays reaffirmed the binding of mAbs against Dsg3

(Figure S4C) and confirmed that the analysis using recombinant Dsg3 did not miss any antigen-specific mAbs. Thus, single cell analysis of sorted Dsg3-specific MBCs provided a large set of exquisitely antigen-specific mAbs for further functional analyses.

Human pathogenic monoclonal antibodies bind to the EC1, EC2, or EC4 domains of Dsg3. The extracellular portion of Dsg3 consists of five cadherin domain repeats (EC1-5) (154). The EC1 domain lies at the N-term of Dsg3, while the EC5 domain is closest to the cell surface (108). To determine domain specificity of the Dsg3-specific mAbs, we used domain-switched proteins in which the extracellular domains from Dsg3 were swapped into the backbone of Dsg2, a homologous protein to which no cross-reactivity has been described (251). These constructs were incubated with the individual mAbs, followed by a pull-down assay and SDS-PAGE analysis to determine specificity (251). For mAbs that did not bind to any of the Dsg3/Dsg2 domain-swapped constructs, further testing was done using chimeric proteins in which sections of Dsg3 spanning the junction between several domains were swapped into a Dsg1 backbone (252) to determine if these mAbs bound to conformational, interdomain epitopes (Figure 3A). In order to pair the domain-specificity of each mAb with functionality, we also tested the pathogenic potential of the antibodies in an *in vitro* keratinocyte dissociation assay (Figure 3B) (239).

Overall, we found that a majority of the mAbs (30/44; 68%) bound to either the EC1 or EC2 domains. A smaller number of antibodies (6/44; 14%) bound to the EC4 domain in both patients. In addition, several antibodies (8/44; 18%) bound to interdomain epitopes found within the first 1-258 amino acids at the N-term of Dsg3 (Figure 3C). Data from the keratinocyte dissociation assay revealed that several antibodies had significantly

higher pathogenic potency than the positive control AK23, a widely used mouse mAb with pathogenic activity both *in vitro* and *in vivo* (144, 239). Interestingly, these highly pathogenic antibodies map to the EC1 domain, which contains adhesion epitopes necessary for the formation of the desmosome structure (154). It is thought that antibodies primarily target EC1 and EC2 domains and cause pathogenicity at least in part by sterically hindering adhesive interfaces found on Dsg3 (142, 253, 254). In fact, most of the pathogenic antibodies in our panel appear to target either the EC1 or EC2 domains, although interdomain-binding mAbs that also target epitopes at the N-terminus of Dsg3 appear to have low to no pathogenic activity. We also found several EC4-specific mAbs with pathogenic activity comparable to that of AK23. To our knowledge, this has not been previously described in the literature. Future research of these novel antibodies and now they cause pathogenicity will contribute to our understanding of PV pathogenesis (Figure 3D).

Interestingly, we noticed that mAbs derived from ISD102 appeared to show higher pathogenic potency than mAbs from ISD068. This observation correlates with the fact that patient ISD102 had a higher severity of disease symptoms than ISD068, as measured by the Pemphigus Disease Area Index (PDAI) score, which is used clinically to assess location, number, size, and damage of lesions (255, 256). By this measure, patient ISD102 had a score of 36, while patient ISD068 scored 8 (Table S1). Considering that both patients have similar quantities of serum Dsg3-specific antibodies, as measured by ELISA (Table S1), it appears that the functional quality of individual antibodies correlates with disease severity. Overall, we found that while EC1 and EC2 are the major targets of pathogenic autoantibodies, novel EC4-specific antibodies with pathogenic potential also exist.

Restricted V gene usage of mAbs targeting a limited number of individual epitopes on Dsg3. To characterize individual epitopes targeted by Dsg3-specific mAbs, we developed a competition assay by inhibiting binding of a biotin-labeled mAb against HaCaT cells using a 50-molar excess of unlabeled competitor antibody. The percent inhibition of binding was detected by flow cytometry. Only biotinylated-mAbs which had an MFI signal 1.5 times greater than the negative control (biotinylated-EM4C04; influenza HA-specific mAb) were used in this assay. As such, 18 antibodies were analyzed from patient ISD068 (Figure 4A), and 14 antibodies were analyzed from patient ISD102 (Figure 4B). Overall, 5 non-overlapping epitopes were described by this assay: 2 epitopes within EC1 (named EC1A and EC1B), 1 epitope within EC2 (named EC2A), and 2 epitopes within EC4 (named EC4A and EC4B). As expected, antibodies derived from the same clonal expansion had similar epitope specificity. Additionally, no specific epitope was preferentially targeted by pathogenic antibodies, although the highly pathogenic antibodies from patient ISD102 all bound the EC1A epitope. Similar epitopes were targeted in both of the donors analyzed, as antibodies that bound epitopes in EC1 and EC4 subdomains also competed between the two patients (Figure S5A, S5B). These 5 epitopes were also commonly targeted in other PV patients, as determined by competition ELISAs, where patient serum was used to block binding of a representative biotinylated-mAb specific for one of these 5 major epitopes. The EC1A epitope appeared to be most commonly targeted by serum antibodies (Figure S5C). Interestingly, competition assays revealed that none of the 5 epitopes identified appear to overlap with the AK23 antibody (Figure S5D), despite its specificity for the EC1 domain (144), suggesting that there may be a species-dependent

bias of immunodominant epitopes. Future experiments comparing human-derived versus mouse-derived Dsg3-specific mAbs will provide further insight into this observation.

We observed restricted repertoires of antibodies that targeted the individual identified epitopes. Epitope EC1A-binding mAbs primarily used V_H1-46/V_K2-24 genes (Figure 4B), while epitope EC2A-binding mAbs used V_H1-2 and V_H4-39 heavy chain genes with a limited repertoire of V_K3-11, V_K3-15, and V_K1-5 light chain gene usage (Figure 4A). Interestingly, similar V gene rearrangements have been described in previous publications. V_H1-46 antibodies, some similarly using the V_K2-24 light chain, targeting the EC1 domain have been detected in other patients (149, 257). Di Zenzo, et al. also described the presence of V_H1-2/V_K3-11 and V_H4-39/V_K3-15 antibodies that bound to the EC2 subdomain (111). The presence of similar V gene usages between various patients suggest that there may be underlying genetic factors driving autoantibodies to break tolerance and develop to cause PV pathogenesis.

Dsg3-specific B cell responses are present prior to disease onset, with extensive, ongoing affinity maturation of MBCs correlating with presentation of PV symptoms. We had access to banked PBMC and serum samples from donor ISD068 from a different previous study, conducted 15-months prior to disease onset, during which time the patient was healthy and asymptomatic (Figure 5A). This provided us with an exciting opportunity to investigate the origin of Dsg3-specific B cells and their development at a single-cell level, prior to disease onset. As previously described (Figure 1A), healthy controls do not have any anti-Dsg3 serum titers whereas PV patients at diagnosis have high titers. However, even prior to disease onset, patient ISD068 displayed elevated titers against Dsg3

(72 U/mL), with levels increasing 3-fold by the time the patient was diagnosed with PV (Figure 5B). We found similar results when tracking Dsg3-specific MBCs, which were readily detectable prior to disease onset, albeit at a lower frequency than at diagnosis (Figure 5C). Even at this early stage, Dsg3-specific MBCs displayed a CD71+ activated phenotype, suggesting that ongoing immune responses were occurring as early as 15-months prior to diagnosis.

We next performed a single-cell analysis of these Dsg3-specific MBCs to compare the development of the B cell response from pre-onset to diagnosis. This analysis included 46 single-cell derived sequences from both time points. We found that the frequency of clonal expansions increased from 22% at pre-onset to 54% at the time of diagnosis, with 8 distinct clones detected that persisted from pre-onset to PV diagnosis (Figure 5D). This suggests that disease onset is linked to clonal focusing and antigenic selection. 5 of the largest clonal expansions detected at diagnosis were derived from clones that were present at pre-onset. While the limited number of cells analyzed does not allow for a complete characterization, the presence of 8 persisting clones detected after analyzing only 46 sequences per time point suggests that the MBC responses at diagnosis largely derive from the maturation of existing clones generated prior to disease onset. Additionally, there was a significant increase in the magnitude of somatic hypermutation found in the V_H genes from Dsg3-specific MBCs at pre-onset compared to diagnosis (Figure 5E), confirming the continuous ongoing affinity maturation of MBCs overtime. There was no significant difference of the R/S ratio in the CDR regions of MBCs when comparing pre-onset to diagnosis (Figure S6A), suggesting that Dsg3-specific MBCs undergo affinity maturation as early as 15-months prior to disease onset.

To confirm the importance of affinity maturation, we generated additional antibodies to compare the functionality of mAbs derived from pre-onset to mAbs derived from disease diagnosis (n=25 for each time point) (Table S2). We determined relative affinity using a Dsg3 ELISA assay. Overall, we found that the relative affinity of the mAbs increased significantly from pre-onset to diagnosis (Figure 5F), confirming that affinity maturation occurred over time. Because 3 antibodies had binding activity below the cut-off value, determined as 3-fold signal above the EM4C04 negative control, they were removed from subsequent analysis. Additionally, we assessed the pathogenicity of these mAbs using the keratinocyte dissociation assay described in Figure 3. We found that there was a significant increase in both the pathogenic potency of the antibodies (Figure 5G), as well as the frequency of pathogenic antibodies found in the patient at diagnosis compared to pre-onset (Figure 5H). When comparing only mAbs derived from persisting clones found at both pre-onset and diagnosis, we found that these clones also showed a significant increase in affinity (Figure S6B) as well as a trend towards a significant increase when comparing pathogenicity (Figure S6C). Interestingly, we found that pathogenic mAbs had significantly higher relative affinities than non-pathogenic antibodies at diagnosis time point, but not at pre-onset (Figure 5I), suggesting that disease is driven by an active selection for affinity and pathogenic activity during affinity maturation. When using the flow-based blocking assay described in Figure 4, we also found that the overall profile of overlapping epitopes at pre-onset (Figure S7A) did not change when compared to diagnosis (Figure S7B). At both time points, about 70% of mAbs targeted the EC2A epitope, while the rest of the antibodies largely target the EC1A epitope. No EC4A or EC4B epitope-binding antibodies were detected at the pre-onset timepoint. Thus, epitope spreading does

not appear to contribute to PV pathogenesis. Interestingly, we did notice that the repertoire of antibodies targeting the EC2A epitope at pre-onset was broader than the limited V_H4-39 and V_H1-2 gene usage that was detected at diagnosis, again suggesting that a small number of MBCs are being actively selected in response to Dsg3 and driving the development of PV disease.

Dsg3-specific mAbs fail to bind the autoantigen in their V gene germline configuration. To define the origin and confirm the relevance of affinity maturation in the generation of Dsg3-specific MBCs, we selected 10 antibodies derived from both patients ISD068 and ISD102 at the time of diagnosis and reverted them to their germline form by removing all mutations detected in the V_H and V_L genes. Antibodies were selected to represent the epitope breadth described for each patient (Table S3). Overall, we found that almost all antibodies were unable to bind Dsg3 when reverted to its germline form (Figure 6A), suggesting that high-affinity Dsg3-specific B cells originated either from non-autoreactive precursors or very low-affinity naïve cells, and that SHM is an essential component of developing PV autoantibodies. Despite previous publications that suggest that V_H1-46 gene usage preferentially allows mAbs to bind Dsg3, even in germline-reverted form (149), none of our V_H1-46 antibodies retained binding after being reverted to germline (Table S3). However, we did detect a single mAb (P1E3) from patient ISD068 that was able to bind Dsg3 even when reverted to germline. This antibody uses a V_H3-33 re-arrangement. Interestingly, the mutational load of the antibody P1E3 was notably lower compared to other antibodies (Figure 6B), and did not show signs of having undergone antigenic selection, as evidenced by the low R/S ratio in the CDR region (Figure 6C).

Overall, most Dsg3-specific antibodies likely originate from non-autoreactive precursors through mechanisms such as molecular mimicry or by activation of very low-affinity naïve cells, and that somatic hypermutation and antigen selection are important to generate high-affinity Dsg3-specific antibody responses.

Pathogenic potency increases synergistically through targeting multiple domains in Dsg3. Based on our earlier observation that development of PV disease is mediated by the selection of pathogenic mAbs (Figure 5G), as well as an increase in the frequency of pathogenic mAbs (Figure 5H), we hypothesized that a mixture of pathogenic antibodies will work synergistically to enhance the overall pathogenic potency. To address this issue, we selected three pathogenic antibodies that targeted distinct epitopes on Dsg3, and tested titrated amounts of antibody to assess their individual pathogenic activity in a keratinocyte dissociation assay, compared to the pathogenicity observed when the 3 antibodies were combined in equal ratios to each other (Figure 7A). We found that the combination of the three antibodies had a considerably higher dissociation index compared to what we observed when measuring any single antibody alone. This synergy was especially clear when antibodies were combined at a limiting concentration of 0.12 μg/mL. At this point, the EC1-specific mAb still showed a robust pathogenic response, while the EC2 and EC4-specific mAbs had pathogenic activity barely above the cut-off value. However, combining the three antibodies at this concentration increased the overall pathogenic signal such that it was more than 2-fold higher than the anticipated additive value of the dissociation index numbers of the three antibodies (Figure 7B).

Overall, this suggests that multiple pathogenic antibodies can act synergistically to promote pathogenicity by targeting multiple Dsg3 epitopes.

DISCUSSION

Pemphigus vulgaris is a unique B cell-mediated autoimmune disorder caused by autoantibodies primarily against the autoantigen Dsg3. Because of this feature, PV represents a powerful model to study antigen-specific autoimmune responses and understand how pathogenic cells develop to eventually cause disease. In the current study, we have enrolled a relatively large number of PV patients sampled at disease diagnosis, as well as during remission or relapse after B cell depletive therapy. In addition to determining the dynamics of the pathogenic B cell responses observed in these patients, we have employed single-cell approaches to generate a large panel of human mAbs, providing a detailed understanding of the antibody responses induced in these patients, and their relevance to disease. We show that activated Dsg3-specific MBCs are readily detected in patients with active disease. Antibodies produced by these cells target a restricted number of unique epitopes on Dsg3, have a restricted V gene repertoire with signs of extensive affinity maturation, and can function synergistically to enhance pathogenicity. In addition, a unique sample obtained over a year before disease onset allowed us to query how the disease develops over time. In the absence of disease symptoms, activated Dsg3-specific MBCs were readily detected in this patient, and repertoire analysis showed that these cells underwent extensive affinity maturation and clonal focusing during the development of PV disease.

To understand the dynamics of B cell responses in PV patients we analyzed serum antibodies, MBCs, and plasmablast responses at the time of diagnosis and at remission or relapse after B cell depletive therapy. All the PV patients responded to Rituximab therapy with improved clinical symptoms, and the majority of patients in remission displayed the

expected rapid drop in anti-Dsg3 titers after B-cell depletion. From this, it is clear that disease is not mediated by bone marrow resident long-lived plasma cells, which do not express CD20 and are, thus, non-responsive to Rituximab (65, 178, 182). This is illustrated by the fact that while anti-Dsg3 titers drop with Rituximab treatment, we and others show that tetanus titers are unaffected by this therapy (182). This suggests that while tolerance is clearly disrupted in these patients, allowing for the formation of autoreactive B cells, there are mechanisms in place that preclude their development into long-lived plasma cells. Interestingly, while we could readily detect activated Dsg3-specific MBCs in patients with active disease, we and others were unable to detect any Dsg3-specific plasmablasts in peripheral blood (125). This is in contrast to protective immune responses against infection or vaccination, where pathogen-specific plasmablasts are readily observed (48, 49, 55, 56, 58). One interpretation of this is that the activated MBCs may be migrating to affected areas of skin/mucosae, and differentiate locally into plasmablasts. These local plasmablasts may be the source of intercellular IgG deposits found in the epidermis of PV patients (258) and directly cause lesions to form on skin and mucosal membranes. This hypothesis is supported by a recent study that showed that Dsg3-specific plasmablasts are present in skin of affected areas in PV patients (129). It might also explain the two donors in clinical remission, that still maintained high anti-Dsg3 serum titers after Rituximab treatment, despite efficient depletion of peripheral B cells. It is possible that these two donors had progressed further along the path of tolerance disruption and developed long-lived, Dsg3-specific plasma cells, resulting in persistence of high anti-Dsg3 serum titers despite B cell depletion. However, the improved clinical responses in these patients could be explained by the depletion of MBCs, resulting in reduced differentiation of plasmablasts *in situ* and

the decrease in pathogenic anti-Dsg3 antibodies in the skin. It is also possible that the maximal signal detected by the clinical anti-Dsg3 ELISA was reached by a large amount of anti-Dsg3 serum antibodies from these 2 remission patients, and that decrease in anti-Dsg3 serum titers after Rituximab treatment was undetectable due to limitations of the assay (168). While this issue remains highly speculative, additional experiments to address these questions are ongoing. Finally, the presence of activated Dsg3-specific MBCs in donors with active disease suggests that this measurement could potentially be used as a biomarker to predict patients likely to undergo future relapse.

Single-cell repertoire analysis of the Dsg3-specific MBCs derived from patients at the time of diagnosis showed that these cells were all class-switched, highly mutated, and clonally restricted. We observed that the majority of Dsg3-specific MBCs were IgG1, although IgG4 and IgA1 isotype usage was also observed. This subclass and isotype usage is similar to usage described for serum analyses of autoantibody responses in PV patients (145, 147, 148). We found no IgM producing Dsg3-specific MBCs, which aligns with previous findings that IgM likely plays no role in PV pathogenesis because pentameric IgM cannot cause pathogenicity due its bulky nature sterically preventing it from disrupting the desmosomal structure (155). Although fAbs (antibodies lacking the Fc domain) can still cause PV disease in mouse models (139), the preference for IgG1 and IgG4 isotype usage of Dsg3-specific antibodies suggest that isotype usage may directly impact antibody function. However, previous studies suggest that changing the isotype of a mAb from IgG1 to IgG4 has no impact on *in vitro* function of antibodies (156), suggesting that subclass bias may merely be a consequence of the cytokine milieu provided by Th1/Th2 Dsg3-specific T cell responses (130, 131). To our knowledge, no

studies exist on the impact of IgA isotype usage on the function of Dsg3-specific mAbs, although its function may be relevant considering that IgA1 has been associated with oral mucosal tissue (259), which can be affected in PV disease. Overall, future studies detailing how isotypes contribute to disease will be important in understanding the mechanism of Dsg3-specific antibodies.

From the single-cell derived sequences we generated a panel of 44 mAbs from the two patients. Of these antibodies, 41 mAbs showed specificity for Dsg3 by multiple binding assays. We found that these antibodies were exquisitely Dsg3-specific, with no cross-reactivity with several irrelevant antigens, such as influenza HA protein and cholera toxin B subunit. This is important, given evidence that autoreactive mAbs are often poly-reactive (90). Importantly, only one antibody showed high cross-reactive binding activity against Dsg1, which is 65% homologous to Dsg3 (108). The lack of cross-reactivity of Dsg3-specific mAbs to Dsg1 reflects the specificity of serum antibodies from both patients ISD068 and ISD102, which were exclusively specific for Dsg3, with no detectable anti-Dsg1 titers. Domain mapping experiments showed that a majority of the antibodies bound to the EC1 and EC2 domains of Dsg3. However, we also found several EC4-specific antibodies in both patients, as well as some mAbs that bound to inter-domain epitopes. The use of a novel competition assay defined only one or two sterically-distinct epitopes in each domain, with a total of 5 epitopes identified. Interestingly, several of the human EC1-specific mAbs had pathogenic potency that was up to three times higher than the archetypical pathogenic mouse monoclonal, AK23 (144). These antibodies were derived from patient ISD102, who was presenting with significantly worse disease indications than ISD068. This suggests that the pathogenic quality of individual mAbs greatly contributes

to overall severity of disease symptoms. Interestingly, competition assays showed that these antibodies all bound to the same sterically-distinct EC1A epitope which was different from the epitope targeted by the EC1-specific AK23. In fact, none of the 5 identified epitopes competed with AK23. This suggests that epitopes relevant to human disease may not be recapitulated by *in vivo* murine models, and the further study characterizing human-derived mAbs and how they may differ from well-characterized mouse mAbs (144) will be essential in better understanding PV pathogenesis.

The highly pathogenic mAbs targeting the EC1A epitope had a restricted repertoire usage of V_H1-46/V_K2-24. When observing the other epitopes, we noticed additional narrowing in repertoire usage of EC2-specific mAbs, which had a preference for V_H4-39 and V_H1-2 heavy chain, with a mix of V_K1-5 and V_K3-15 light chain usage. Although we did not detect the same rearrangements in both donors, despite similar epitopes being targeted in both patients, other laboratories have also described EC1-domain specific mAbs using similar V_H1-46/V_K2-24 (149, 242) and EC2-domain specific mAbs using a V_H1-2/V_K1-5 and V_H4-39/V_K3-15 (142). Because restricted repertoires appear to be domain/epitope dependent, this suggests that analysis of repertoire usage may provide information of which immune-dominant epitopes are targeted in patients, which may guide future efforts to provide personalized treatment options for patients. Additionally, limited repertoire usage has also been previously described in other diseases including influenza infection (219), HIV infection (260), and other autoimmune disorders like SLE (58, 261). These restricted V gene repertoires suggest that there may be underlying genetic factors driving antibody responses, such as certain V genes that may have inherent auto-reactivity to Dsg3 at germline state (149), or the existence of a consensus sequence that will elucidate

binding properties of Dsg3-specific mAbs (257). Further studies on restricted repertoire usage will contribute to our understanding of how these autoantibodies are able to break tolerance and develop to cause disease.

While most of the pathogenic antibodies were specific for the EC1 and EC2 domains, but not specific for inter-domain junctional epitopes, we also detected novel EC4-domain specific antibodies, with pathogenic activity comparable to AK23. EC1 and EC2-specific antibodies (154), including AK23 (163) are thought to cause pathogenicity by steric hindrance of Dsg3-mediated cell-cell adhesion. However, the detection of pathogenic EC4-specific mAbs suggest that additional mechanisms contribute to pathogenicity. One recent paper showed that distinct from other cadherins, Dsg3 had a prominent kink present between the EC3 and EC4 domains induced by unique calcium-binding sites (238). It is possible that this kink allows for optimal presentation of epitopes found in the EC3 or EC4 domains, and that binding to these epitopes may induce conformational changes to Dsg3, which may impact the function of Dsg3. Additionally, EC4-specific mAbs may potently engage signaling pathways and induce the endocytosis and degradation of Dsg3 (158, 160-163). Additionally, current efforts are being made to develop therapies targeting the depletion of pathogenic Dsg3-specific B cells using chimeric autoantibody receptor T cells, possibly with the use of truncated Dsg3 in a domain-specific manner (262). Although previous studies suggest that domains EC1 and EC2 are the primary targets of pathogenic antibodies (107, 142), our data show pathogenic antibodies targeting EC4 exist and that comprehensive therapies that deplete all pathogenic Dsg3-specific B cells, regardless of domain specificity, may be necessary to prevent relapse of disease. Future efforts to

determine how EC4-binding mAbs affect Dsg3 may elucidate mechanisms underlying disease pathogenesis and guide the discovery of long-lasting therapies for PV patients.

In addition to the samples collected from patients ISD068 and ISD102 at the time of diagnosis, we had access to a unique paired sample collected from patient ISD068 15-months prior to PV onset, when the patient was asymptomatic. This gave us an opportunity to study the origins and development of autoimmune responses at a single-cell, antigen-specific level. We found that both high anti-Dsg3 serum titers and the presence of activated Dsg3-specific MBCs could be readily detected 15-months prior to developing disease. Interestingly, even at pre-onset, the observed MBCs had high levels of clonality and somatic hypermutation, suggesting that these cells had already undergone antigen selection and affinity maturation. In contrast, we also found that germline-reverted antibodies were generally unable to bind Dsg3. Overall, this suggests that while disease-causing MBCs likely originate from non-autoreactive B cells precursors or naïve cells of very low affinity, antigen selection is necessary to drive the specificity and high affinity binding of MBC-derived mAbs. Despite previous publications that have shown that some germline-reverted antibodies with V_H1-46 gene usage are able to bind to Dsg3 (149), none of our V_H1-46 antibodies retained binding activity in germline form. However, we did detect one mAb that bound Dsg3 in its germline-reverted form. This antibody was distinct in its use of the V_H3-33 gene and EC4-specificity. However, it was similar to the previously described germline-reverted V_H1-46 antibodies in that our antibody also had a low number of mutations, and R/S analysis of the CDR regions showed no signs of affinity selection. Thus, this particular antibody did not need to undergo antigenic selection to bind Dsg3. Future studies of additional germline reverted antibodies that can retain binding to Dsg3 will

provide further insight into the origins of Dsg3-specific antibodies and what factors contribute to the initial induction of these autoreactive cells.

By generating additional monoclonal antibodies from the pre-onset timepoint, we could analyze changes of the Dsg3-specific MBC compartment comparing the pre-onset to diagnosis. We noticed a significant increase of both the frequency of clonally related sequences as well as the levels of somatic hypermutation, suggesting that continuous and ongoing affinity maturation and antigen-driven expansion are important for the development of PV disease. This was supported by our findings that both affinity and pathogenic potency of mAbs increased from pre-onset to diagnosis, and that pathogenic antibodies derived from the diagnosis time point had a higher affinity towards Dsg3 than non-pathogenic antibodies. In addition, there was a marked increase in the number of pathogenic antibodies found in patient ISD068 over time. Thus, it appears that affinity maturation drives the selection of pathogenic antibodies, and that accumulation of pathogenic mAbs drives development of PV disease. Previous studies of autoimmune disease such as Fogo Selvagem (263) and SLE (264) have also shown that serum autoantibodies can be detected in patients prior to disease onset. Longitudinal characterization of serum autoantibody response in these patients suggest that epitope spreading is a crucial component of disease pathogenesis. However, we did not detect similar epitope spreading of the mAbs derived from our PV patient, with overall epitope specificity similar from pre-onset to diagnosis. This is similar to previous studies which show a lack of epitope spreading in PV patients as they experience remission or relapse (251).

Based on our findings that the development of PV disease appears to be mediated by increase in pathogenic potency of individual mAbs as well as an increase in the number of pathogenic antibodies, we hypothesized that multiple pathogenic antibodies can work synergistically to increase the overall pathogenic response. By titrating either individual or combinations of mAbs in an *in vitro* keratinocyte dissociation assay, we found that pathogenic mAbs that targeted distinct epitopes did, in fact, work synergistically to increase pathogenic potency. This suggests that disease can be initiated or enhanced by engaging multiple Dsg3 epitopes. Additionally, we noted that the mAbs derived from patient ISD068 had lower pathogenic activity than those derived from patient ISD102, which appeared to correlate with patient ISD068 having a less severe presentation of disease. This suggests that individual quality of mAbs may also contribute to overall disease severity. Future experiments focused on understanding how combination of multiple antibodies drives a maximal pathogenic response and the mechanism underlying synergy will be important in understanding how this complex process works *in vivo*.

Our data suggests that PV pathogenesis appears to be mediated by a complex evolution of Dsg3-specific MBC responses. While the initial autoreactive responses appear to be generated through either molecular mimicry (150) or a very low affinity precursor, antigen selection/affinity maturation is necessary for the development of high affinity pathogenic MBCs. Pathogenic antibodies produced by these cells can work synergistically to enhance the overall pathogenic potency, and drive the initial presentation of PV symptoms. As disease progresses and antibodies continue to undergo antigen selection, individual mAbs show increase in pathogenic quality which then contributes to an increase in disease severity. Overall, these findings contribute to our current understanding of the

mechanism underlying how Dsg3-specific mAbs develop and cause PV pathogenesis, and may have important implications for improving diagnostic tools and therapeutic approaches for PV patients.

MATERIALS AND METHODS

Patients, study design, and approvals. PV patients with active disease were recruited to this study at the time of diagnosis, or were ≥6 months post-Rituximab therapy and were currently in either remission or relapse of disease. Written informed consent was obtained from all participants. This study was approved by the Emory Institutional Review Board (#IRB00054860). Demographically-matched healthy volunteers were recruited from staff and students at Emory University. Exclusion criteria included any condition that, in the opinion of the investigator, would place the subject at risk of injury from participation. An additional blood sample had been collected for patient ISD068, 15-months prior to disease diagnosis. The patient recalled participation in another research study prior to development of PV. Having had signed a consent form for this previous study (#IRB00009560), allowing for the use of banked samples for future testing, the patient agreed to pursue additional studies using the pre-clinical sample to determine if markers of autoimmune disease were present in this earlier blood draw.

PBMC and plasma isolation. Blood samples were collected in sodium citrate CPT tubes (BD Vacutainer) from PV patients or healthy controls. Plasma samples were collected and stored at -80°C. PBMCs were isolated and washed with PBS/2% FBS. Cells were used fresh or were frozen in FBS/10% DMSO. Frozen PBMCs were stored in liquid nitrogen until assayed.

ELISA assay. Anti-Dsg3 serum autoantibody titers were determined with an ELISA test (MBL International Corporation). Patient plasma diluted 1:100 were tested, and results

reported as Units/mL of sera, as determined by negative and positive calibrators according to manufacturer's instructions.

To determine specificity of patient-derived mAbs, ELISA plates (Thermo Scientific) were coated with 2 μg/mL of rDsg3 or rDsg1 (EuroImmun) diluted in PBS with 1 mM $CaCl_2$ and incubated overnight at 4°C. Plates were washed with wash buffer (PBS/0.5% Tween20/1 mM $CaCl_2$) and blocked with ELISA buffer (PBS/1% BSA/0.2% Tween20/1 mM $CaCl_2$). mAbs were added to the plates in a serial dilution series starting at 5 μg/mL. Plates were washed with wash buffer and incubated with peroxidase-conjugated goat anti-human IgG (Jackson ImmunoResearch) at room temperature for 90 minutes. Plates were washed with wash buffer, followed by a wash with PBS, and then developed using 1 mg/mL o-phenylenediamine (OPD) diluted in 0.05 M phosphate-citrate buffer, supplemented with 0.012% H_2O_2. Reactions were stopped with 1 M HCl, and absorbance was immediately measured at 490 nM. Additional ELISA assays were performed by coating plates with 1 μg/mL recombinant protein antigens CtxB (56) and the influenza HA-antigen (A/California/7/2009, eEnzyme). Minimum effective concentration was determined as the minimal concentration of mAb at which an OD signal was detectable 3-fold above the background signal measured by a negative control.

Memory B cell assay. Dsg3-specific memory B cells were measured using a polyclonal stimulation assay, essentially as previously described (244). Briefly, PBMCs were cultured at $1X10^6$ cells/mL in RPMI supplemented with penicillin/streptomycin, L-glutamine, 10% FBS, a 50 μM of beta-mercapto-ethanol (Sigma) (R10) containing R848 (1 μg/mL, Invivogen) and recombinant human-IL2 (10 μg/mL, Biolegend) for 3 days at 37°C. Total

and Dsg3-specific IgG-secreting cells were quantified by ELISPOT assay, in which a 96-well ELISPOT filter plates (Millipore) were coated overnight with either Dsg3 antigen (3 μg/mL, provided by the Hertl Lab) or polyvalent goat anti-human Ig (25 μg/mL, Rockland) in PBS/1 mM $CaCl_2$. Plates were washed and blocked by incubation with R10 at 37°C for 2 hours. PBMCs were added to the plates in a dilution series and incubated for 5 hours at 37°C. Plates were washed with PBS, followed by PBS/0.05% Tween, and incubated with biotinylated anti-human IgG antibody (Invitrogen) at room temperature for 90 minutes. After washing, plates were incubated with an avidin-D horseradish peroxidase conjugate (Vector laboratories) and developed using 3-amino-9-ethyl-carbazole substrate (Sigma). Plates were scanned and analyzed using an automated ELISPOT counter (CTL, Cellular Technologies).

Flow cytometry analysis and single-cell sorting. Immunophenotyping of circulating B cell subpopulations was performed on previously frozen PBMCs stained with the following, appropriately titrated mAbs: Live/Dead Aqua (ThermoScientific), CD3-AF700 (Biolegend, clone HIT3a), CD14-AF700 (eBioscience, clone 61D3), CD16-AF700 (eBioscience, clone CB16), CD20-V450 (BD, clone L27), CD71-FITC (Biolegend, CY1G4), IgD-PECy7 (Biolegend, clone IA6-2), CD19-PE (BD, clone HIB19), CD27-PerCPCy5.5 (Biolegend, clone O323). Antigen-specific cells were detected using His-tagged rDsg3 (5 μg/mL, provided by the Hertl lab) and a secondary anti-HisTag-APC (R&D system). Influenza HA-specific cells were detected by staining with HA antigen (A/California/7/2009, eEnzyme) which was biotinylated (EZ-Link Sulfo-NHS-Biotin, ThermoFisher) and detected with SA-APC (Life Technologies). A minimum of 1,000,000

lymphocytes were acquired on a BD LSRII flow cytometer, and analyzed using FlowJo software. Dsg3-specific MBCs were single-cell sorted into 96-well PCR plates containing hypotonic catch buffer with RNase inhibitor (Promega) supplemented with 0.2% Triton x-100 (Sigma) using a FACSAriaII, and were frozen immediately on dry ice and stored at -80°C, as previously described (49).

Generation of recombinant monoclonal antibodies. mAbs were generated from single-cell sorted MBCs by single-cell expression cloning, essentially as previously described (49, 246). In brief, single-cell cDNA was synthesized from sorted MBCs using gene-specific primers (IDT). Ig heavy chain and light chain (kappa/lambda) rearrangements were amplified by nested PCR (HotStarTaq Plus Master Mix, Qiagen) using primer cocktails specific for all V gene families and constant domains at a concentration of 200 nM per primer (247). Sense primers used in the second round of nested PCR were modified by fusing the 5' end of each primer to the M13R sequence (5'-AACAGCTATGACCATG-3') to facilitate subsequent sequencing. Next, another PCR was performed using a high-fidelity DNA polymerase (Phusion Hot Start II, NEB) and V and J gene family specific primers that incorporated Ig chain-specific restriction sites. Variable domains were directionally cloned into human mAb heavy chain (IgG1) and light chain (kappa or lambda) expression vectors (Genbank accession numbers FJ475055, FJ475056, and FJ517647). Variable domains containing internal restriction sites were amplified by a modified PCR containing 50 μM 5-methyl-dCTP (NEB) and 150 μM dCTP. This modification did not affect PCR fidelity and abrogated the truncation of variable domains after restriction digestion. Following vector construction and sequence confirmation, heavy and light chain vectors

were transiently co-transfected into Expi293F cells according manufacturer's instructions (Life Technologies). Antibodies were purified from cell culture supernatants using protein-A conjugated agarose beads (Pierce).

Repertoire analysis. Identification of antibody variable region genes were done as previously described (56, 245). V, D, and J genes were identified and analyzed using the Immunogenetics (IMGT) database as a reference. Isotype was determined by comparing the nucleotide sequence of the Fc-domain retained by nested PCR described above to the Genbank database as a reference for subclass specificity (Genbank accession numbers: IgG1 - AH007035.2; IgG2 - AJ250170.1; IgG3 - X03604.1; IgG4 - AF237586.1; IgA1 – AH007035.2; IgA2 – AH005273.2; IgM – X14940.1). To confirm IgG subclasses, a subset of MBCs was re-amplified using the first round of PCR amplification described above using a nested primer (5'-GGGCTTGTGATCTACGTTGCAG-3') that amplified nucleotide sequences to incorporate additional regions of sufficient subclass dissimilarity and compared to previously reported subclass-specific sequences (265). The number of somatic hypermutations in the V_H genes represent the total number of both replacement and silent mutations in the amplicon (FR1 through CDR3) relative to the closest germline sequence matched in the IMGT database. Members of clonal expansions were identified by sequence alignments of rearrangements with matching V and J gene usage, the same CDR3 length, and ≥80% similar junctional diversity. Germline-reverted antibodies were also generated by comparison to the IMGT database. Fragments of the germline sequence with the appropriate restriction sites were synthesized (Eurofins) and used to generate mAbs as described above.

Keratinocyte Dissociation Assay. HK cultures were seeded into 24-well dishes. 24-hours after reaching confluency, cultures were switched to low calcium media (KGM containing 50 μM $CaCl_2$) overnight to internalize all desmosomal cadherins. Cultures were switched to high calcium (550 μM $CaCl_2$) media for 3 hours, and treated with 10 μg/mL of mAbs for 6 hours. The cells were then incubated with dispase (VWR) at 37°C until monolayers were released from plate. Monolayers were transferred to Eppendorf tubes and subjected to mechanical stress by shaking on a cell shaker for one minute, and then transferred back into a 24-well plate and fixed with formaldehyde and stained with methyl blue. Fragments were imaged using an imager (CTL, Cellular Technologies), and the number of fragments was determined as the average count determined from three separate images of the same well. Dissociation index was calculated using the following equation: (1 - [(No. $fragments_{mAb}$ – No. $fragments_{negative\ control}$)/(No. $fragments_{positive\ control}$ – No. $fragments_{negative\ control}$)]) x 100, in which the negative control was the influenza-specific mAb EM4C04 (219) and the positive control was the mouse mAb AK23 (144).

Synergy of pathogenic responses detected using the above assay by treating HK cells with titrated amount of antibodies in a 3-fold dilution series starting at a concentration of 10 μg/mL. For synergy panel, 10 μg/mL of three individual antibodies were combined (final concentration 30 μg/mL) and titrated out at 3-fold dilutions.

Domain mapping. Domain mapping experiments were done using domain-swapped Dsg3-Dsg2 and Dsg3-Dsg1 molecules as previously described (251). Dsg3-Dsg2 extracellular cadherin (EC) domain-swapped constructs (generously provided by Amagai

lab, Keio University, Japan). For each construct, one extracellular domain of Dsg2 was substituted for corresponding domain in Dsg3, followed by an E-tag at the C-terminus. Plasmid constructs were transfected into 293T cells with jetPRIME (Polypus). The domain-swapped molecules were secreted into the cell culture supernatant, which was centrifuged to remove cell debris and frozen at -80°C. For antibodies not scoring in this assay, Dsg3-Dsg1 EC domain-swapped constructs (provided by Masayuki Amagai) were used for epitope mapping (252). These constructs were generated by amplifying a section of Dsg3 that span multiple junctions between several extracellular domains. These sections ($Dsg3^{1-161}$, $Dsg3^{1-258}$, and $Dsg3^{163-566}$) were swapped with the corresponding sections of Dsg1. The constructs were produced by baculovirus expression, as previously described (251), and stored at -80°C.

1 μg of mAbs was incubated overnight at 4°C with these domain-swapped constructs, followed by incubation with Protein A Agarose (Invitrogen) for 1 hour at room temperature. Pull down samples were washed with TBS/1 mM $CaCl_2$, boiled for 5 minutes at 100°C in Laemmi Sample Buffer (BioRad) and centrifuged. The immune-precipitated proteins were separated by SDS-PAGE, transferred to nitrocellulose membranes (BioRad) and visualized through incubation with HRP-conjugated goat anti-Etag antibody (Abcam) followed by exposure to Digital-ECL substrate solution (Kindle Biosciences). The chemo-luminescence signal was quantified using the *Kwik*Quant Imager (Kindle Biosciences).

HaCaT competition assay. For competition assays, mAbs were biotinylated (EZ-Link Sulfo-NHS-Biotin, ThermoFisher). Only biotinylated-mAbs that provided a signal 1.5-times brighter than the negative control, biotinylated-EM4C04, were used for this assay.

An immortalized cell line of human keratinocytes, HaCaT cells (250), was cultured to 70-80% confluency in DMEM/penicillin/streptomycin/L-glutamine/10% FBS. To collect single-cell suspensions, HaCaTs were washed with PBS, and treated with 0.25% trypsin (Lonza) before quenching reaction with culture media. Cells were washed twice and rested in 4 mL of culture media for 90 minutes at 37°C. Cells were washed with PBS, stained with Live/Dead Aqua (ThermoScientific), washed with staining buffer (PBS/2% FBS/0.05% sodium azide/1 μM CaCl2) and aliquoted into a 96-well plate. Cells were incubated with unlabeled competing antibody at 100 μg/mL for one hour at 4°C. An equal volume of buffer containing 2 μg/mL biotinylated-mAb was added, and cells were incubated for an additional 30 minutes at 4°C. Cells were then washed and incubated with appropriately diluted streptavidin-APC reagent (Invitrogen) for 30 minutes at 4°C. A minimum of 10,000 cells were acquired on a BD LSRII flow cytometer, and analyzed using FlowJo software. Percent inhibition was calculated as: $(1 - [(MFI_{sample} - MFI_{negative\ control})/(MFI_{positive\ control} - MFI_{negative\ control})]) \times 100$, in which the negative control was influenza-specific biotinylated-EM4C04 and the positive control was 1 μg/mL of biotinylated antibody without competitor.

Statistical analysis. Data was collected and graphed using GraphPad Prism software. A 1-way ANOVA Kruskal-Wallis test, Mann Whitney U-test, or Wilcoxon matched-pairs signed-rank test was used to determine statistical significance where appropriate. *P* values less than 0.05 (two-sided) were considered statistically significant.

SUPPLEMENTARY MATERIALS AND METHODS

ELISA assay. Anti-Dsg1 serum autoantibody titers were determined with an ELISA test (MBL International Corporation) using patient plasma samples. Plasma diluted 1:100 were tested according to the manufacturer's instructions. Results are reported as Units/ml of sera, as determined by negative and positive calibrators supplied by the manufacturer.

To determine serum titers against tetanus-toxoid protein, ELISA plates (ThermoScientific) were coated with 0.5 μg/mL of recombinant Tetanus toxoid (List Biological Laboratories) diluted in PBS and incubated overnight at 4°C. Plates were washed with wash buffer (PBS/0.5% Tween20) and blocked with ELISA buffer (PBS/1% BSA/0.2% Tween20). Plasma was added to the plates at a single dilution of 1:200. Plates were washed with wash buffer and incubated with peroxidase-conjugated goat anti-human IgG (Jackson ImmunoResearch) at room temperature for 90 minutes. Plates were washed with wash buffer, followed by a wash with PBS, and then developed using 1 mg/mL o-phenylenediamine (OPD) diluted in 0.05 M phosphate-citrate buffer, supplemented with 0.012% hydrogen peroxide. Plates were immediately read at an absorbance of 450 nM, with read settings set to record in 15 second intervals over the course of 300 seconds.

Flow cytometry analysis. Immunophenotyping of circulating plasmablasts B cells was performed on fresh whole blood stained with the following mAbs, appropriately titrated: CD19-FITC (BD, clone HIB19), CD24-PerCPCy5.5 (Biolegend, clone ML5), CD3-PacificBlue (BD, clone SP34-2), CD38-PE (BD, clone HIT2), CD20-PECy7 (BD, clone L27), IgD-PECy7 (Biolegend, clone IA6-2), and CD27-APC (eBiosciences, clone O323),

followed by lysis of erythrocytes (BD FACS lysis solution). 100,000 events were acquired on a BD LSRII flow cytometer, and analyzed using FlowJo software.

Plasmablast ELISPOT assay. ELISPOT was performed to enumerate Dsg3-specific plasmablasts present in PBMC samples. 96-well ELISPOT assay filter plates (Millipore) were coated overnight with recombinant Dsg3 antigen (3 μg/mL, provided by Hertl Lab) or polyvalent goat anti-human Ig (50 μg/mL, Rockland) in PBS/ 1mM $CaCl_2$. Plates were washed and blocked by incubation with R10 at 37°C for 2 hours. Freshly isolated PBMCs were added to the plates in a dilution series starting at $5x10^5$ cells and incubated overnight at 37°C. Plates were washed with PBS, followed by PBS/0.05% Tween, and then incubated with biotinylated anti-human IgG, IgA, or IgM antibody (Invitrogen) at room temperature for 90 minutes. After washing, plates were incubated with avidin D-horseradish peroxidase conjugate (Vector laboratories) and developed using 3-amino-9-ethyl-carbazole substrate (Sigma). Plates were scanned and analyzed using an automated ELISPOT counter (CTL, Cellular Technologies).

Subclass-specific ELISA. To confirm isotype specificity of serum Dsg3-specific antibody responses, ELISA plates were coated with 2 μg/mL of rDsg3. Plates were washed and blocked as previously described. Plasma samples from ISD068 and ISD102 were added to the plates in a serial dilution starting at 1:100 dilutions. After a 90-minute incubation at room temperature, plates were washed and incubated with peroxidase-conjugated mouse anti-human IgG1, IgG2, IgG3, or IgG4 subclass specific reagent (Molecular probe) or a peroxidase-conjugated goat anti-human IgG or IgA reagent (Jackson ImmunoResearch)

and incubated for an additional 90 minutes at room temperature. Plates were washed and IgG subclass signal was amplified by an additional incubation with peroxidase conjugated goat-anti mouse IgG (Kirkegaard & Perry Lab, Inc.) for 90 minutes at room temperature. Plates were then developed and analyzed as described above.

Immunofluorescence staining. Human Keratinocytes (HKs) isolated from neonatal foreskin (Emory Skin Disease and Research center) were grown in keratinocyte growth medium (Lonza). For immunofluorescence experiments these cells were cultured on glass slides (Ibidi) until confluent. Live cells were labeled with monoclonal antibodies at a concentration of 10 μg/ml for 30 minutes at 4°C. Cells were then fixed on ice using 3.7% paraformaldehyde for 10 minutes followed by permeabilization in 0.1% triton for 10 minutes at room temperature. Goat anti-human IgG cross-adsorbed secondary (Life Technologies) was then used prior to mounting with prolong gold containing Dapi (Life Technologies). Widefield images were acquired using a DMRXA2 microscope (Leica, Wetzler, Germany) equipped with a 63X/1.40 NA oil immersion objective. Images were acquired with an ORCA digital camera (Hamamatsu Photonics, Bridgewater, NJ). Analysis was preformed using Fiji ImageJ.

HaCaT binding assay. An immortalized cell line of human keratinocytes, HaCaT cells (250), was cultured to 70-80% confluency in DMEM supplemented with penicillin/streptomycin, L-glutamine, and 10% FBS. To collect single-cell suspensions, HaCaT cells were washed with PBS, and treated with 0.25% trypsin (Lonza) before quenching reaction with culture media. Cells were washed twice and rested in 4 mL of

culture media for 90 minutes at 37°C. Cells were then washed with PBS, stained with Live/Dead Aqua (ThermoScientific) and then washed with staining buffer (PBS/2% FBS/0.05% sodium azide/1 μM CaCl2) and aliquoted into a 96-well plate. Cells were incubated with 1 μg of mAb for 30 minutes at 4°C, and then washed and incubated with mouse anti-human IgG-AF488 (Life Technologies). A minimum of 10,000 cells were acquired on a BD LSRII flow cytometer, and analyzed using FlowJo software.

Blocking ELISA. To determine epitope specificity of patient sera, a blocking ELISA was performed by inhibiting the binding of a biotinylated mAb (EZ-Link Sulfo-NHS-Biotin, ThermoFisher) targeting 1 of 5 described immunodominant epitopes (from the competition assay described in Figure 4) at the half-maximal binding concentration with 1:20 diluted sera from PV patients or healthy controls to Dsg3-coated ELISA plates. To determine if the immunodominant epitopes bound to the same epitope as mouse AK23 antibody, we also used a blocking ELISA to inhibit the binding of biotinylated mAbs with a 10-fold molar excess of unlabeled AK23 to Dsg3-coated ELISA plates. Detection was done using avidin-HRP as described for the ELISA assay. The cut-off value was determined by the mean of %inhibition calculated for 9 healthy control sera plus 2 SD. Percent inhibition was calculated as follows: $(1 - [(OD_{samples} - OD_{neg\ control})/(OD_{pos\ control} - OD_{neg\ control})]) \times 100$.

Statistical analysis. Data was collected and graphed using GraphPad Prism software. A 1-way ANOVA Kruskal-Wallis test, Mann Whitney U-test, or Wilcoxon matched-pairs signed-rank test was used to determine statistical significance where appropriate. *P* values less than 0.05 (two-sided) were considered statistically significant.

AUTHOR CONTRIBUTION

Contribution: A. Cho carried out experiments, analyzed the data, and wrote the manuscript. A.C. contributed to pathogenicity assays and IF assays, and provided critical discussion of the manuscript. N.R. carried out domain-mapping experiments. Z.M. and M.A. contributed to the development and execution of competition assays. C.N. contributed to ELISA assays. R.K., A.S., and G.M. contributed to the analysis of isotype usage. A.L. contributed to the analysis of germline-reverted antibodies. B.B. contributed to analysis of data. S.Z. contributed to pathogenicity assays. T.S., and M.H. provided essential reagents and feedback on the final manuscript. A.P., A.K., and R.F. contributed to analysis, critical discussion, and editing of the manuscript. J.W. conceived the research, oversaw the experiments and data analysis, and wrote the manuscript.

Conflict-of-interest: A.P. has served as a consultant for Syntimmune, holds equity in Cabaletta Bio, and is an inventor on patents licensed by Novartis and Cabaletta Bio focused on targeted cellular therapy of autoimmunity. M.H. has received unrestricted grants from Topas Therapeuticals, Fresenius and Biotest and has served as a consultant for Argenx and Allmirall. R.F. has served as a consultant for Cabeletta, Bioverative, and Celtaxys. The other authors have declared that no conflict of interest exists.

Correspondence: Jens Wrammert, Department of Pediatrics; Division of Infection Disease; Emory Vaccine Center, School of Medicine, Emory University, 2015 Uppergate Drive, ECC Building, Room 510, Atlanta, GA 30322; email: jwramme@emory.edu.

ACKNOWLEDGEMENTS

We thank R. Karaffa at the Emory School of Medicine flow cytometry core, and A. Rae at Emory Pediatric flow cytometry core for their technical assistance with cell sorting experiments. We thank Drs. R. Ahmed and M. Slifka for providing samples used in this paper. This study was supported by grants from the National Institutes of Health (Human Immunology Pilot award under U19 AI057266) and from the International Pemphigus Pemphigoid Foundation; the Charles and Daneen Stiefel Scholar Award from the Dermatology Foundation (A.P.), the Deutsche Forschungsgemeinschaft (FOR 2497 PEGASUS, M.H. and T.S.) and the National Center for Advancing Translational Sciences of the National Institutes of Health under award number TL1TR001880 (N.R.)

FIGURES AND LEGENDS

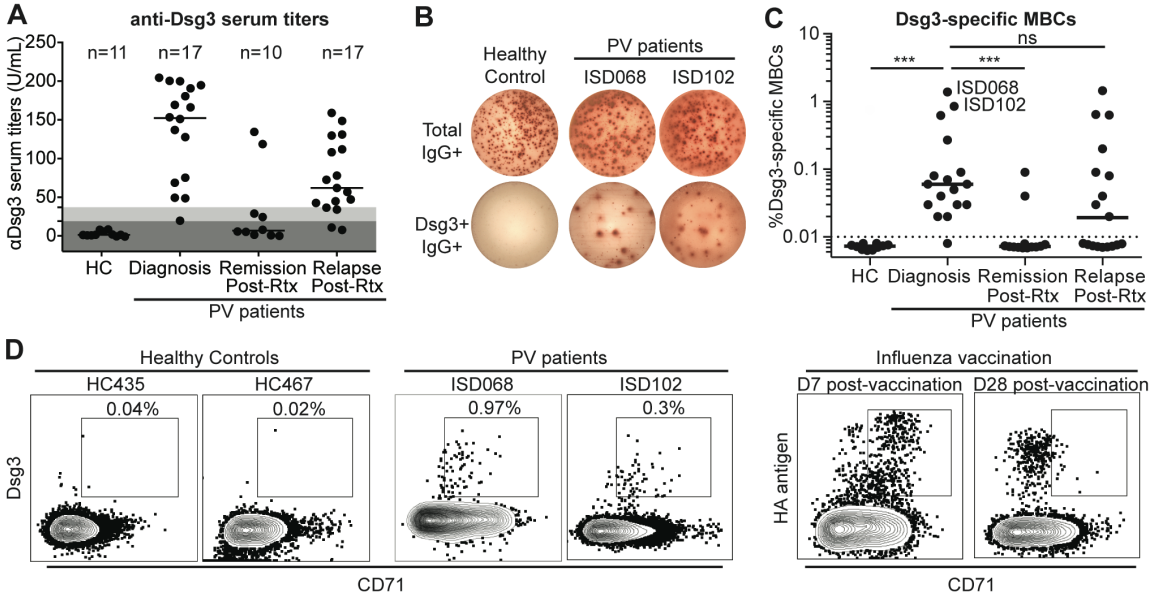

FIGURE 1. Activated Dsg3-specific memory B cells are detected exclusively in patients with active PV disease.

(A) High levels of anti-Dsg3 serum antibody titers are present in PV patients at the time of diagnosis, and when patients relapse following previous treatment with the B-cell depletive therapy Rituximab (Rtx), but not in healthy controls and patients in remission. Patients were largely sampled at a single time point, although a small subset were followed longitudinally through treatment. Cut-off values were determined based on manufacturer recommendations: dark grey = negative; light grey = indeterminate. Representative data of two individual experimental repeats is shown. (B) Representative Dsg3-specific MBC assay. $1x10^6$ PBMCs were polyclonally activated *in vitro* for 3 days, after which either total or Dsg3-specific IgG secreting cells were detected using an ELISPOT assay. (C) Significant frequencies of Dsg3+ MBCs were detected in PV patients at the time of diagnosis and after relapse, but were undetectable in healthy controls, and largely undetectable in patients in remission. Reported frequency of Dsg3-specific MBCs are averages of 3-5 replicates of a single experiment. (D) Dsg3-specific MBCs (gated on CD3-CD19+IgD-CD20+ lymphocytes) could be readily detected from two patients with high frequencies of Dsg3-specific MBCs (as shown in 1C). Dsg3-specific MBCs expressed the activation marker CD71, similar to activated HA-specific MBCs induced in response to the influenza vaccination 7 days post-vaccination. This is distinct from steady-state MBCs found later after vaccination, which are quiescent and do not express CD71 (55). Significance of comparisons of MBC frequencies was determined using one-way ANOVA. *** = $p \leq 0.001$. See also Figure S1 and S2.

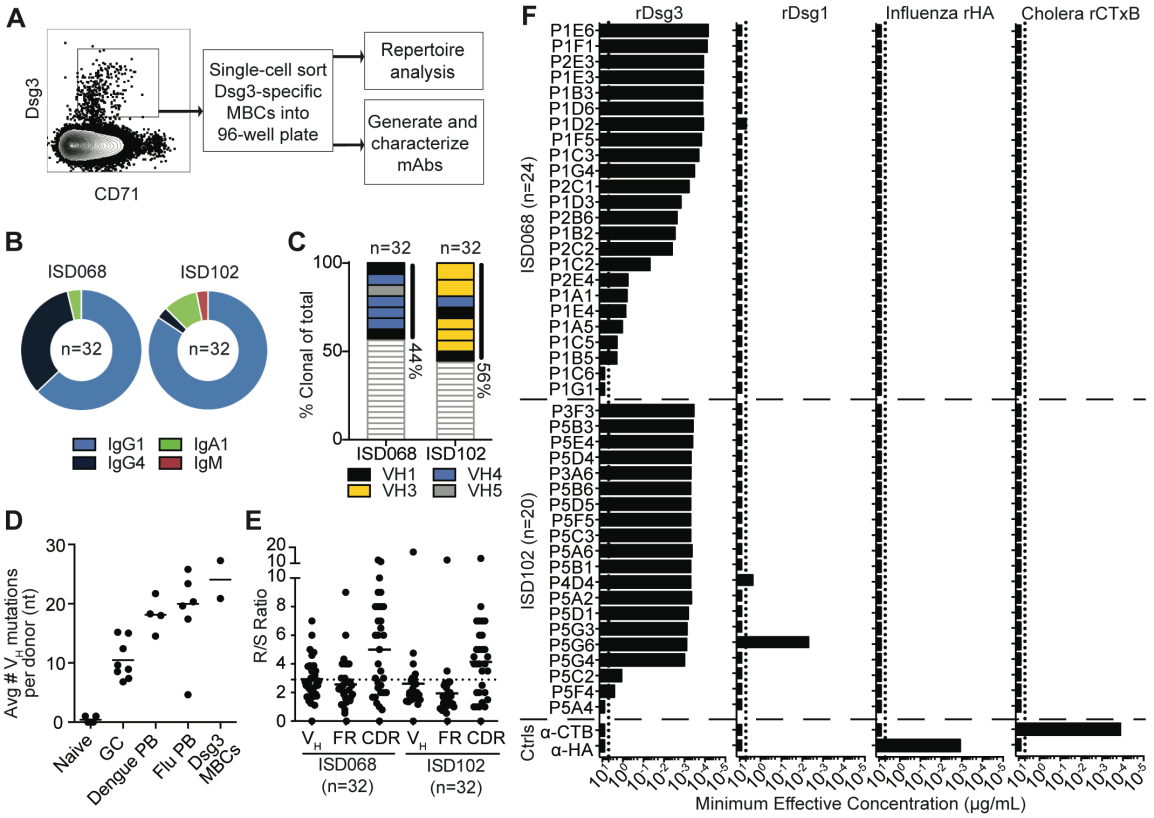
A
Dsg3
CD71
Single-cell sort Dsg3-specific MBCs into 96-well plate
Repertoire analysis
Generate and characterize mAbs
B
ISD068
ISD102
n=32
n=32
IgG1
IgG4
IgA1
IgM
C
n=32
n=32
% Clonal of total
100
50
0
44%
56%
ISD068
ISD102
VH1
VH3
VH4
VH5
D
Avg # VH mutations per donor (nt)
30
20
10
0
Naive
GC
Dengue PB
Flu PB
Dsg3 MBCs
E
R/S Ratio
20
10
10
8
6
4
2
0
VH
FR CDR
VH
FR CDR
ISD068 (n=32)
ISD102 (n=32)
F
rDsg3
rDsg1
Influenza rHA
Cholera rCTxB
ISD068 (n=24)
P1E6
P1F1
P2E3
P1E3
P1B3
P1D6
P1D2
P1F5
P1C3
P1G4
P2C1
P1D3
P2B6
P1B2
P2C2
P1C2
P2E4
P1A1
P1E4
P1A5
P1C5
P1B5
P1C6
P1G1
ISD102 (n=20)
P3F3
P5B3
P5E4
P5D4
P3A6
P5B6
P5D5
P5F5
P5C3
P5A6
P5B1
P4D4
P5A2
P5D1
P5G3
P5G6
P5G4
P5C2
P5F4
P5A4
Ctrls
α-CTB
α-HA
Minimum Effective Concentration (μg/mL)

FIGURE 2. Dsg3-specific MBCs are clonally restricted, show signs of extensive antigenic selection, and are exquisitely specific for Dsg3.

(A) Dsg3-specific MBCs were single-cell sorted and used for repertoire analysis and mAb generation, as previously described (246, 247). Dsg3-specific MBCs were (B) largely class-switched to IgG1 and (C) highly oligoclonal, with about 50% of sequences representing clonal expansions. (D) Dsg3+ MBCs display high frequencies of somatic hypermutation compared to previously analyzed B cell subsets (57, 219, 248). Each data point represents the average number of mutations of all sequences analyzed from one individual donor. (E) R/S ratio analysis of the entire V_H gene, FR, and CDR showed that Dsg3+ MBCs had an R/S ratio well above 2.9 (dotted line) in the CDRs, suggesting antigenic selection (249). (F) 44 mAbs were generated from the 2 patients. The vast majority of a mAbs displayed exquisite specificity against Dsg3 in an ELISA assay, with only two antibodies showing cross-reactivity to Dsg1. No mAbs bound irrelevant antigens, such as influenza HA (H1/California) or cholera toxin B subunit. Control mAbs against HA or CTB bound their respective antigens where appropriate. The dotted line in ELISA graph represents the highest antibody concentration tested for binding (5 μg/mL). Representative data of two individual experimental repeats is shown. See also Figure S3 and S4.

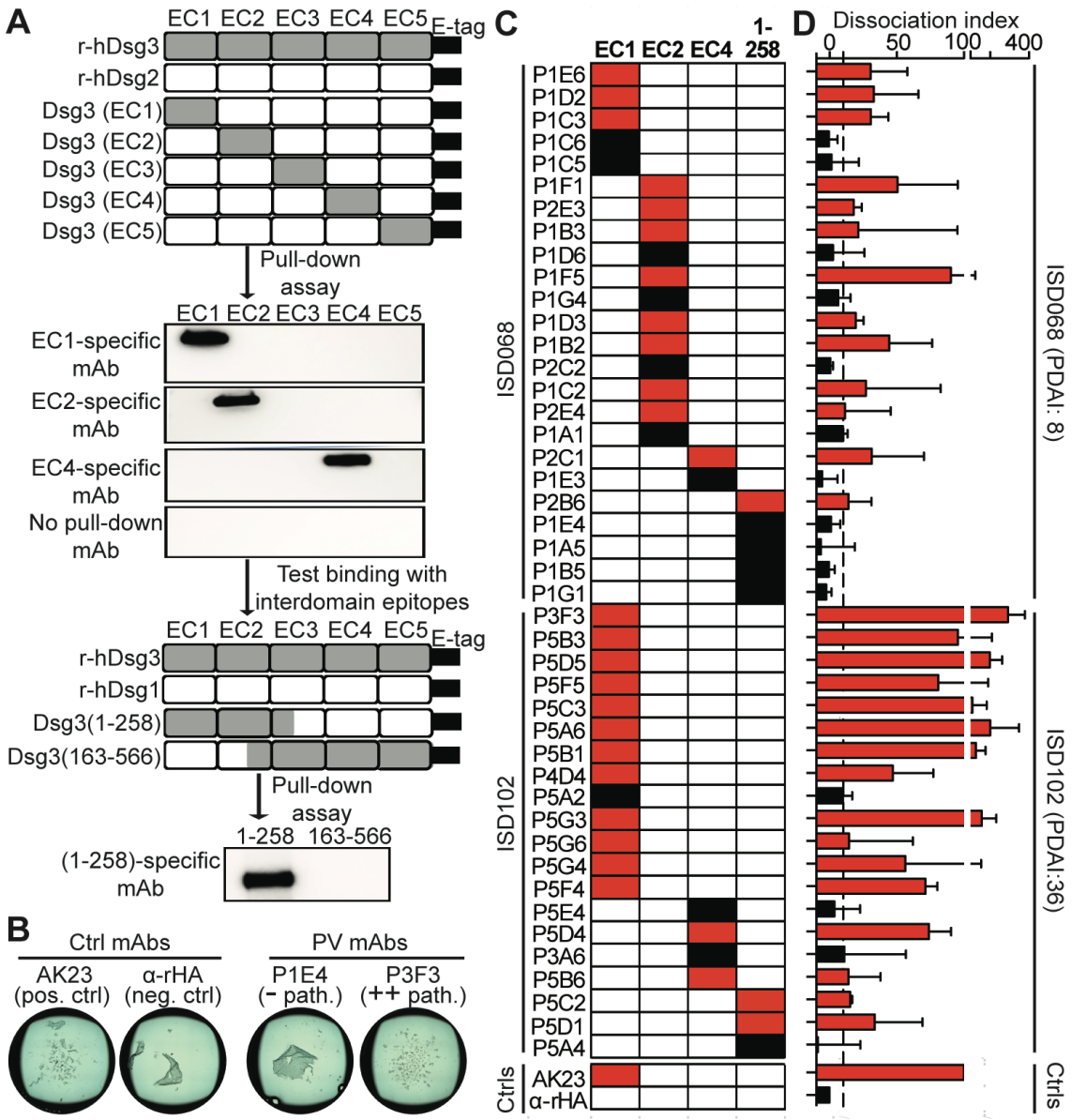
A
EC1 EC2 EC3 EC4 EC5 E-tag
r-hDsg3
r-hDsg2
Dsg3 (EC1)
Dsg3 (EC2)
Dsg3 (EC3)
Dsg3 (EC4)
Dsg3 (EC5)
Pull-down assay
EC1 EC2 EC3 EC4 EC5
EC1-specific mAb
EC2-specific mAb
EC4-specific mAb
No pull-down mAb
Test binding with interdomain epitopes
EC1 EC2 EC3 EC4 EC5 E-tag
r-hDsg3
r-hDsg1
Dsg3(1-258)
Dsg3(163-566)
Pull-down assay
1-258 163-566
(1-258)-specific mAb
B
Ctrl mAbs
PV mAbs
AK23 (pos. ctrl)
α-rHA (neg. ctrl)
P1E4 (- path.)
P3F3 (++ path.)
C
EC1 EC2 EC4 1-258
ISD068
P1E6
P1D2
P1C3
P1C6
P1C5
P1F1
P2E3
P1B3
P1D6
P1F5
P1G4
P1D3
P1B2
P2C2
P1C2
P2E4
P1A1
P2C1
P1E3
P2B6
P1E4
P1A5
P1B5
P1G1
ISD102
P3F3
P5B3
P5D5
P5F5
P5C3
P5A6
P5B1
P4D4
P5A2
P5G3
P5G6
P5G4
P5F4
P5E4
P5D4
P3A6
P5B6
P5C2
P5D1
P5A4
Ctrls
AK23
α-rHA
D
Dissociation index
0 50 100 400
ISD068 (PDAI: 8)
ISD102 (PDAI:36)
Ctrls

FIGURE 3. Pathogenic mAbs bind the EC1, EC2, or EC4 domains of Dsg3.

(A) Domain-switched chimeric proteins were generated by swapping EC domains from Dsg3 into the backbone of Dsg2, or sections of Dsg3 spanning the junction between domains into the backbone of Dsg1. Constructs were incubated with individual mAbs, followed by a pull-down assay to determine domain specificity. Representative results are shown. (B) Representative keratinocyte dissociation assay, showing the ability of mAbs to disrupt HK monolayer cultures. (C) Most mAbs were specific for the EC1 and EC2 domains, with a subset targeting either the EC4 domain, or interdomain epitopes. (D) Pathogenic mAbs (shown in red) predominantly targeted the EC1 and EC2 domain, although several pathogenic EC4-specific mAbs was also identified. Dissociation index numbers are reported at median ± interquartile range of 4 individual experimental repeats. Cut-off value (dotted line) was determined as the range of dissociation index of 6 irrelevant mAbs.

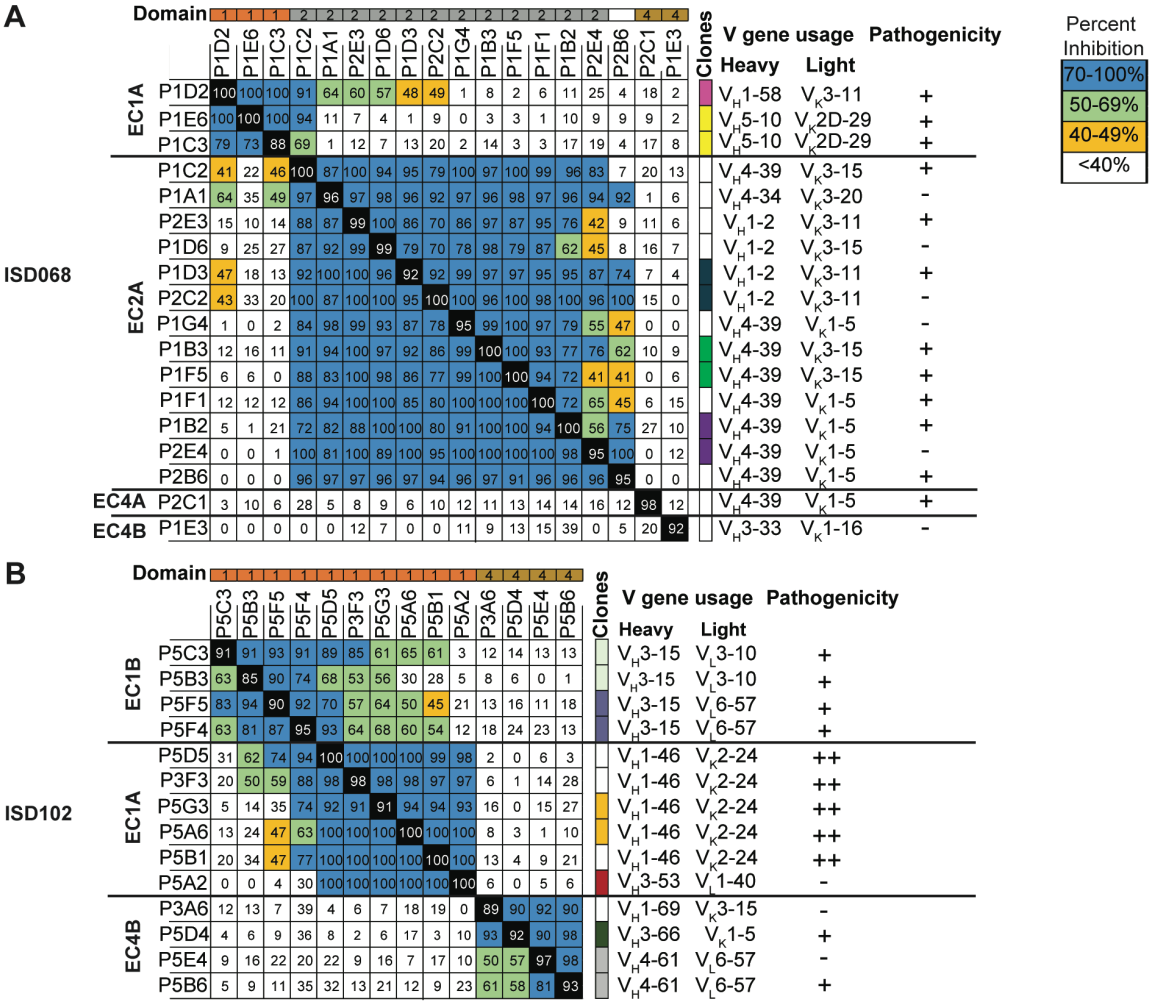
A
ISD068
Domain
Clones
V gene usage
Heavy
Light
Pathogenicity
EC1A
EC2A
EC4A
EC4B
P1D2 P1E6 P1C3 P1C2 P1A1 P2E3 P1D6 P1D3 P2C2 P1G4 P1B3 P1F5 P1F1 P1B2 P2E4 P2B6 P2C1 P1E3
P1D2 100 100 100 91 64 60 57 48 49 1 8 2 6 11 25 4 18 2 VH1-58 VK3-11 +
P1E6 100 100 100 94 11 7 4 1 9 0 3 3 1 10 9 9 9 2 VH5-10 VK2D-29 +
P1C3 79 73 88 69 1 12 7 13 20 2 14 3 3 17 19 4 17 8 VH5-10 VK2D-29 +
P1C2 41 22 46 100 87 100 94 95 79 100 97 100 99 96 83 7 20 13 VH4-39 VK3-15 +
P1A1 64 35 49 97 96 97 98 96 92 97 96 98 97 96 94 92 1 6 VH4-34 VK3-20 -
P2E3 15 10 14 88 87 99 100 86 70 86 97 87 95 76 42 9 11 6 VH1-2 VK3-11 +
P1D6 9 25 27 87 92 99 99 79 70 78 98 79 87 62 45 8 16 7 VH1-2 VK3-15 -
P1D3 47 18 13 92 100 100 96 92 92 99 97 97 95 95 87 74 7 4 VH1-2 VK3-11 +
P2C2 43 33 20 100 87 100 100 95 100 100 96 100 98 100 96 100 15 0 VH1-2 VK3-11 -
P1G4 1 0 2 84 98 99 93 87 78 95 99 100 97 79 55 47 0 0 VH4-39 VK1-5 -
P1B3 12 16 11 91 94 100 97 92 86 99 100 100 93 77 76 62 10 9 VH4-39 VK3-15 +
P1F5 6 6 0 88 83 100 98 86 77 99 100 100 94 72 41 41 0 6 VH4-39 VK3-15 +
P1F1 12 12 12 86 94 100 100 85 80 100 100 100 100 72 65 45 6 15 VH4-39 VK1-5 +
P1B2 5 1 21 72 82 88 100 100 80 91 100 100 94 100 56 75 27 10 VH4-39 VK1-5 +
P2E4 0 0 1 100 81 100 89 100 95 100 100 100 100 98 95 100 0 12 VH4-39 VK1-5 -
P2B6 0 0 0 96 97 97 96 97 94 96 97 91 96 96 96 95 0 0 VH4-39 VK1-5 +
P2C1 3 10 6 28 5 8 9 6 10 12 11 13 14 14 16 12 98 12 VH4-39 VK1-5 +
P1E3 0 0 0 0 0 12 7 0 0 11 9 13 15 39 0 5 20 92 VH3-33 VK1-16 -
Percent Inhibition
70-100%
50-69%
40-49%
<40%
B
ISD102
Domain
Clones
V gene usage
Heavy
Light
Pathogenicity
EC1B
EC1A
EC4B
P5C3 P5B3 P5F5 P5F4 P5D5 P3F3 P5G3 P5A6 P5B1 P5A2 P3A6 P5D4 P5E4 P5B6
P5C3 91 91 93 91 89 85 61 65 61 3 12 14 13 13 VH3-15 VL3-10 +
P5B3 63 85 90 74 68 53 56 30 28 5 8 6 0 1 VH3-15 VL3-10 +
P5F5 83 94 90 92 70 57 64 50 45 21 13 16 11 18 VH3-15 VL6-57 +
P5F4 63 81 87 95 93 64 68 60 54 12 18 24 23 13 VH3-15 VL6-57 +
P5D5 31 62 74 94 100 100 100 100 99 98 2 0 6 3 VH1-46 VK2-24 ++
P3F3 20 50 59 88 98 98 98 98 97 97 6 1 14 28 VH1-46 VK2-24 ++
P5G3 5 14 35 74 92 91 91 94 94 93 16 0 15 27 VH1-46 VK2-24 ++
P5A6 13 24 47 63 100 100 100 100 100 100 8 3 1 10 VH1-46 VK2-24 ++
P5B1 20 34 47 77 100 100 100 100 100 100 13 4 9 21 VH1-46 VK2-24 ++
P5A2 0 0 4 30 100 100 100 100 100 100 6 0 5 6 VH3-53 VL1-40 -
P3A6 12 13 7 39 4 6 7 18 19 0 89 90 92 90 VH1-69 VK3-15 -
P5D4 4 6 9 36 8 2 6 17 3 10 93 92 90 98 VH3-66 VK1-5 +
P5E4 9 16 22 20 22 9 16 7 17 10 50 57 97 98 VH4-61 VL6-57 -
P5B6 5 9 11 35 32 13 21 12 9 23 61 58 81 93 VH4-61 VL6-57 +

FIGURE 4. Dsg3-specific mAbs display a restricted repertoire and bind to 1 or 2 sterically-distinct epitopes in EC1, EC2 and EC4 domains of Dsg3.

A flow-based blocking assay was used to define the epitopes recognized by Dsg3-specific mAbs for patient (A) ISD068 and (B) ISD102. The figure shows the percent inhibition of binding of a biotinylated mAb when blocked with a 50-fold molar excess of an unlabeled mAb. Value shown is average percent inhibition reported from two individual experimental repeats. The suggested epitope name is located on left of chart. Colors at top of the graph represents domain specificity (Orange = EC1; Grey = EC2; Gold = EC4; White = Interdomain). Colors to the right of the graph represents mAbs in the same clonal expansion. V_H and V_L gene usage and pathogenicity are listed on the right of the panel. Pathogenicity was determined using the following cut-off values of the dissociation index number: - = DI≤10; + = DI>10; ++ = DI>100. See also Figure S5.

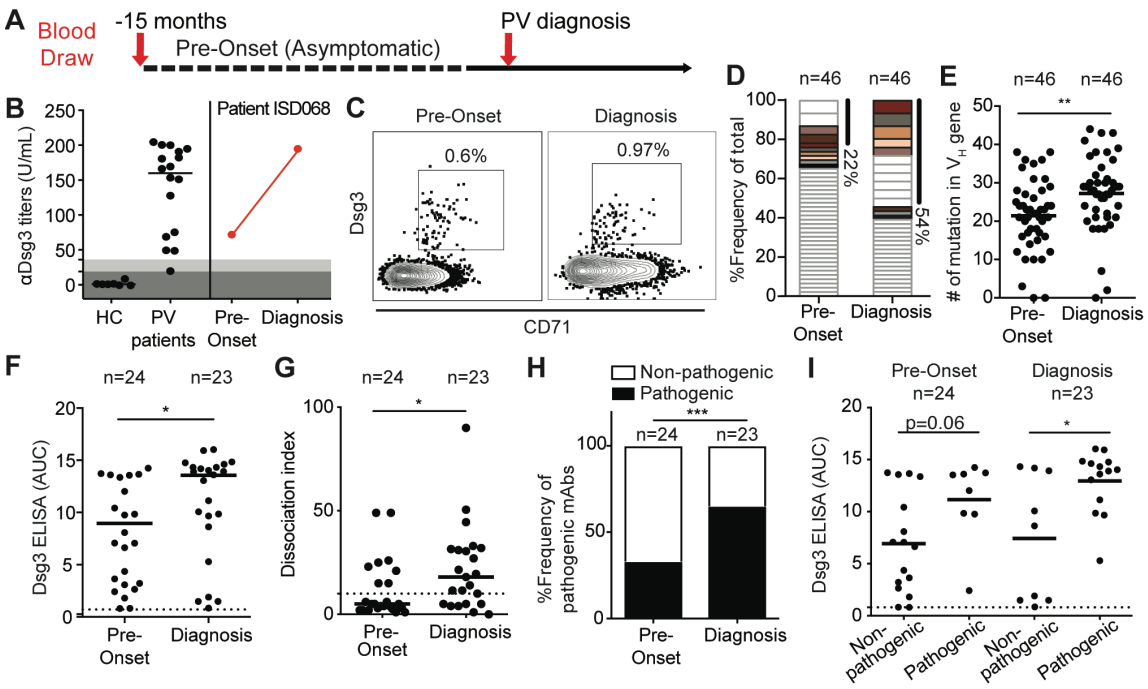
A
Blood Draw
-15 months
Pre-Onset (Asymptomatic)
PV diagnosis
B
αDsg3 titers (U/mL)
Patient ISD068
HC
PV patients
Pre-Onset
Diagnosis
C
Pre-Onset
Diagnosis
0.6%
0.97%
Dsg3
CD71
D
n=46
n=46
%Frequency of total
22%
54%
Pre-Onset
Diagnosis
E
n=46
n=46
**
# of mutation in V_H gene
Pre-Onset
Diagnosis
F
n=24
n=23
*
Dsg3 ELISA (AUC)
Pre-Onset
Diagnosis
G
n=24
n=23
*
Dissociation index
Pre-Onset
Diagnosis
H
Non-pathogenic
Pathogenic
***
n=24
n=23
%Frequency of pathogenic mAbs
Pre-Onset
Diagnosis
I
Pre-Onset
n=24
Diagnosis
n=23
p=0.06
*
Dsg3 ELISA (AUC)
Non-pathogenic
Pathogenic
Non-pathogenic
Pathogenic

FIGURE 5. Dsg3-specific MBCs are readily detected in PV patients prior to disease onset, and undergo extensive affinity maturation during disease development.

(A) A unique sample from patient ISD068 was collected 15-months prior to diagnosis, as part of a separate study. (B) Patient ISD068 had high levels of titers prior to disease onset, in contrast to healthy controls. (C) Activated CD71+ Dsg3-specific MBCs could also be readily detected before disease onset. (D) Single-cell analysis of Dsg3-specific MBCs (n=46 per time point) shows that the frequency of clonally-related cells increased 2-fold from pre-onset to diagnosis. Matching colors are representative of persisting clones detected at both time points. (E) The number of somatic hypermutations found in the V_H gene increased significantly from pre-onset to diagnosis time point. (F) Overall, 25 antibodies were derived from each time point. Relative affinity of the mAbs is reported as Area Under the Curve (AUC) of an ELISA assay. Overall, the affinity of mAbs increased significantly over time. 3 mAbs that did not bind Dsg3 were removed from subsequent analysis. Pathogenicity of mAbs were next tested in a keratinocyte dissociation assay. There was a significant increase in both (G) the pathogenic potency of the mAbs, as measured by dissociation index number, and (H) the frequency of pathogenic antibodies detected in patient ISD068, when comparing antibodies derived from pre-onset to diagnosis time point. (I) Pathogenic antibodies had significantly higher affinities than non-pathogenic mAbs at diagnosis, but not pre-onset. A Mann-Whitney U test or a Fisher exact test was used where appropriate. * = $P \leq 0.05$; ** = $P \leq 0.01$. See also Figure S6 and S7.

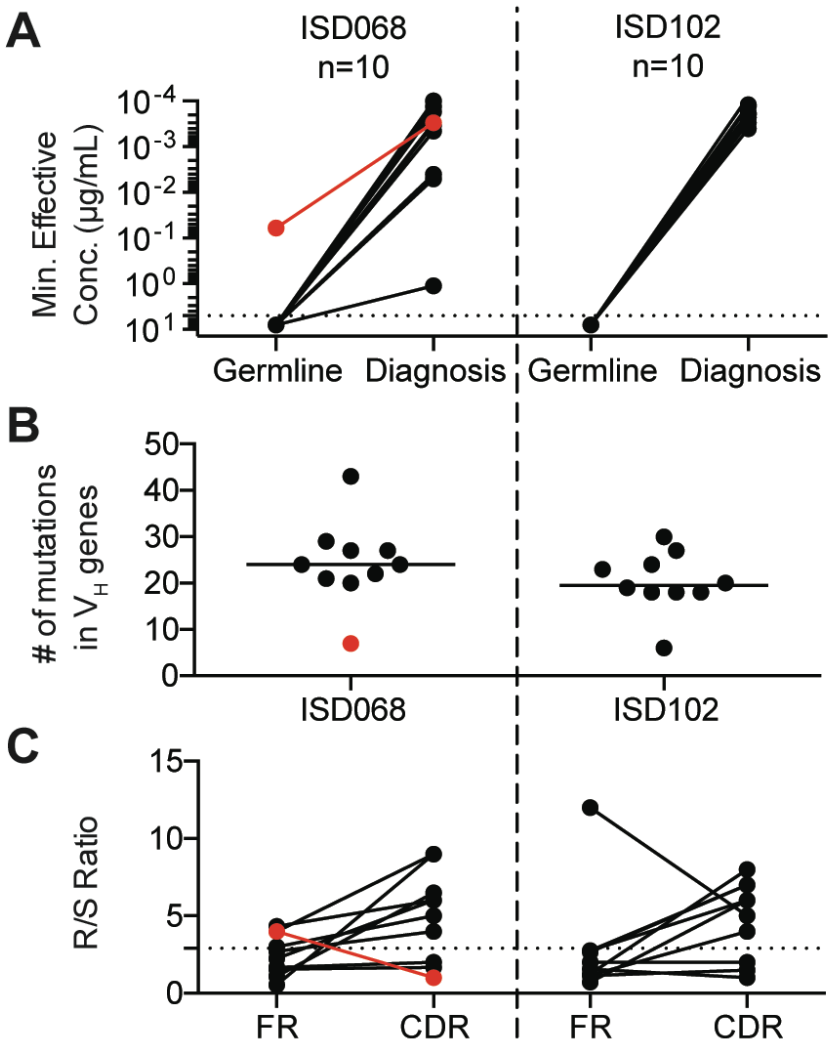

FIGURE 6. Somatic hypermutation is necessary for antibody binding of Dsg3.

(A) 10 antibodies from either patient ISD068 or ISD102 were reverted to their germline configuration. Antibodies were selected to represent the epitope breadth detected in the patient, as determined by the flow-based blocking assay (Figure 4). While the original, mutated mAbs showed high affinity binding activity towards Dsg3, only 1 germline-reverted antibody retained the ability to bind Dsg3 (red line, antibody P1E3). (B) Most mAbs had high levels of SHM in the VH gene, while P1E3 had very few mutations. (C) P1E3 showed no enrichment of amino-acid replacement mutations in the CDRs, in contrast to the other Dsg3-specific mAbs.

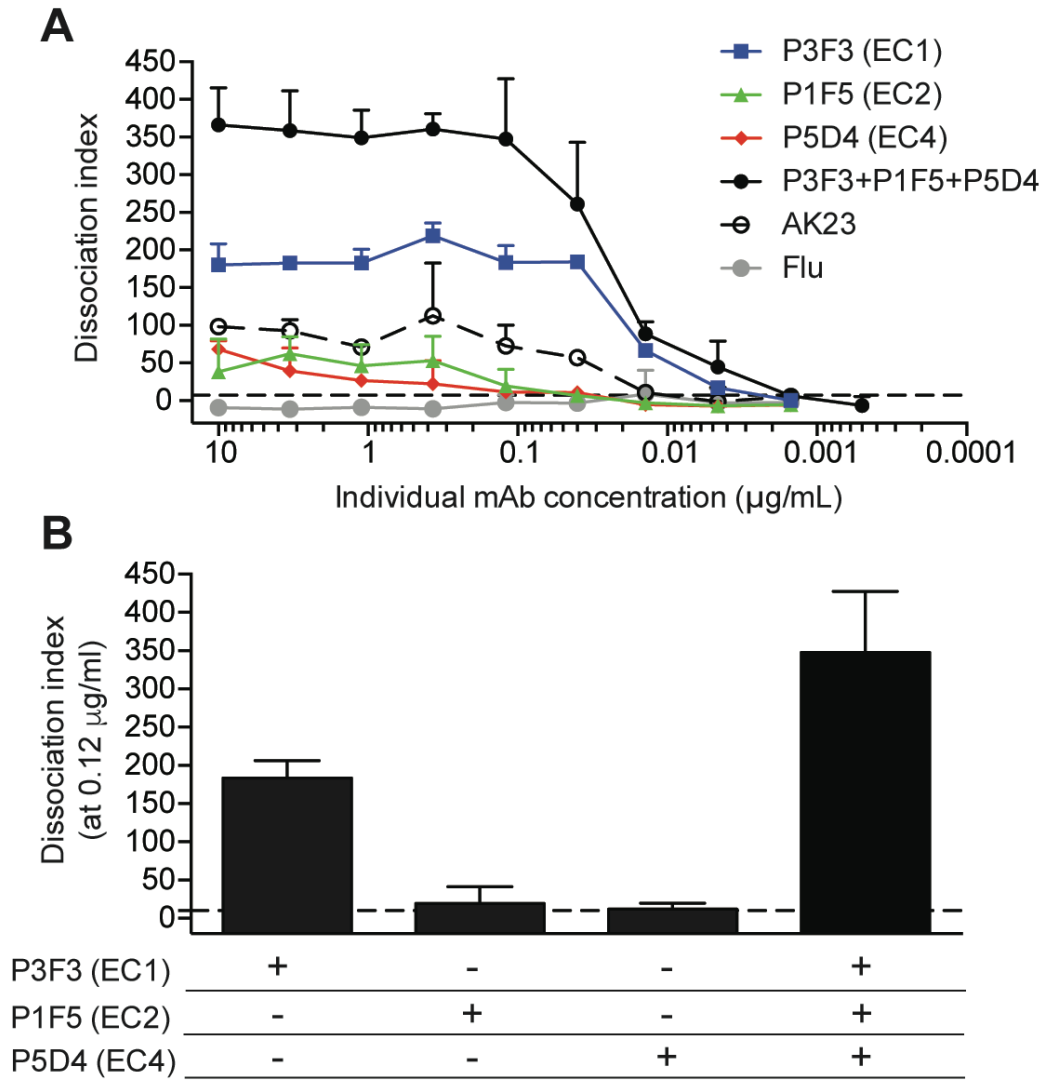

FIGURE 7. Synergistic increase of pathogenic potency by targeting multiple domains in Dsg3.

(A) Pathogenic potency was measured by a keratinocyte dissociation assay with titration of individual, or a combination of, pathogenic mAbs targeting the EC1, EC2, or EC4 domains. The combined mAbs showed clear synergy, with a higher dissociation index value than any single mAb alone. (B) Combination of the 3 antibodies at 0.12 µg/mL showed effective synergy, where the combination showed pathogenic signal two times higher than the anticipated additive signal of the single mAbs at this concentration.

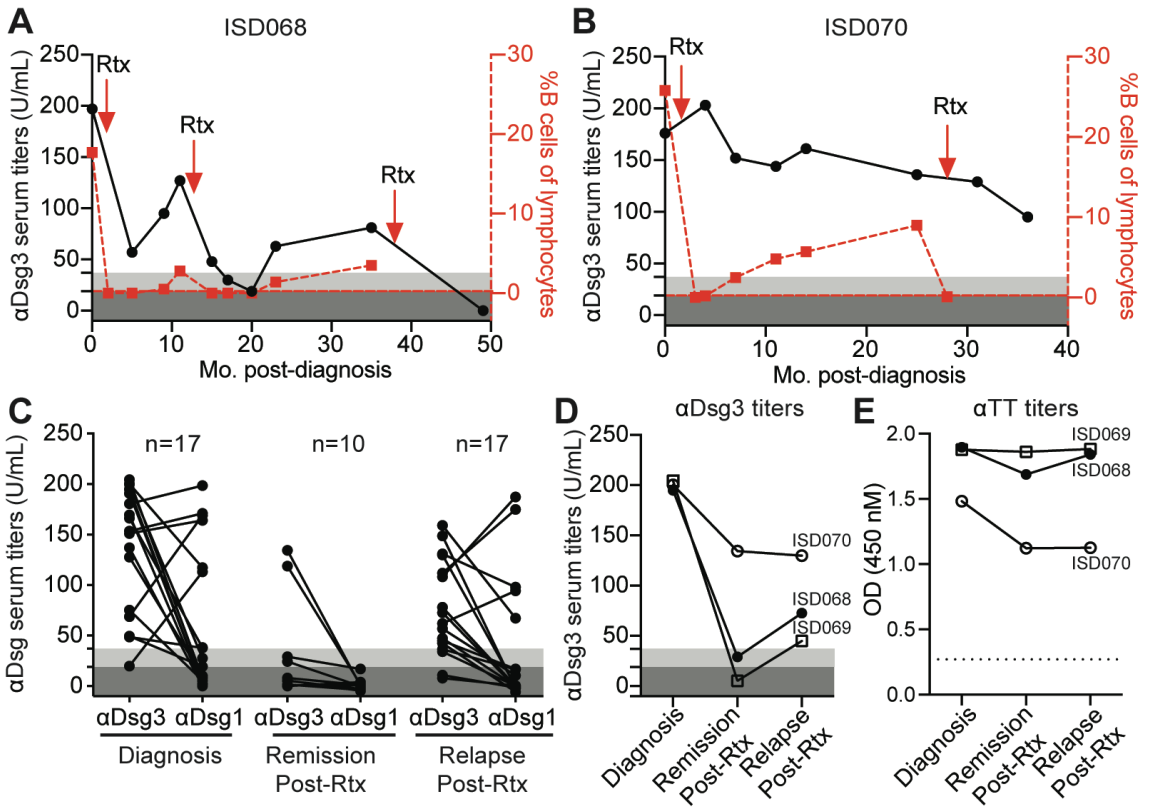
A
ISD068
Rtx
Rtx
Rtx
αDsg3 serum titers (U/mL)
%B cells of lymphocytes
Mo. post-diagnosis
B
ISD070
Rtx
Rtx
αDsg3 serum titers (U/mL)
%B cells of lymphocytes
Mo. post-diagnosis
C
αDsg serum titers (U/mL)
n=17
n=10
n=17
αDsg3 αDsg1 αDsg3 αDsg1 αDsg3 αDsg1
Diagnosis
Remission Post-Rtx
Relapse Post-Rtx
D
αDsg3 titers
αDsg3 serum titers (U/mL)
ISD070
ISD068
ISD069
Diagnosis
Remission Post-Rtx
Relapse Post-Rtx
E
αTT titers
OD (450 nM)
ISD069
ISD068
ISD070
Diagnosis
Remission Post-Rtx
Relapse Post-Rtx

FIGURE S1. Kinetics of serum antibody titers after treatment with B cell depletive therapy.

Related to Figure 1. (A) The average kinetics of anti-Dsg3 serum titers (left Y-axis, black line) and peripheral blood CD19+ B cells (right Y-axis, red line) for most PV patients after treatment with Rituximab (Rtx) therapy. Cut-off values for ELISA were determined by manufacturer's suggestion (dark grey = negative, light grey = indeterminate). Red dotted line represents limit of detection for CD19+ B cells in circulation. (B) A smaller number of patients who are in clinical remission do not have a complete decrease of anti-Dsg3 serum titers in response to Rituximab-mediated therapy, despite showing complete depletion of B cells in the periphery. (C) Anti-Dsg1 serum titers was found only in a subset of PV patients, specifically at the time of diagnosis and relapse post-Rtx, but undetectable in patients in remission. When tracking serum titers specifically in PV patients sampled longitudinally at multiple time points (D) anti-Dsg3 serum titers decreased dramatically after Rituximab-treatment while (E) anti-tetanus toxoid (TT) titers did not significantly change over time. Anti-TT titers are shown as the final OD reading of serum diluted at 1:200. Dotted-line represents the cut-off value determined by the background signal in a negative HC serum. Data is representative of two individual experimental repeats.

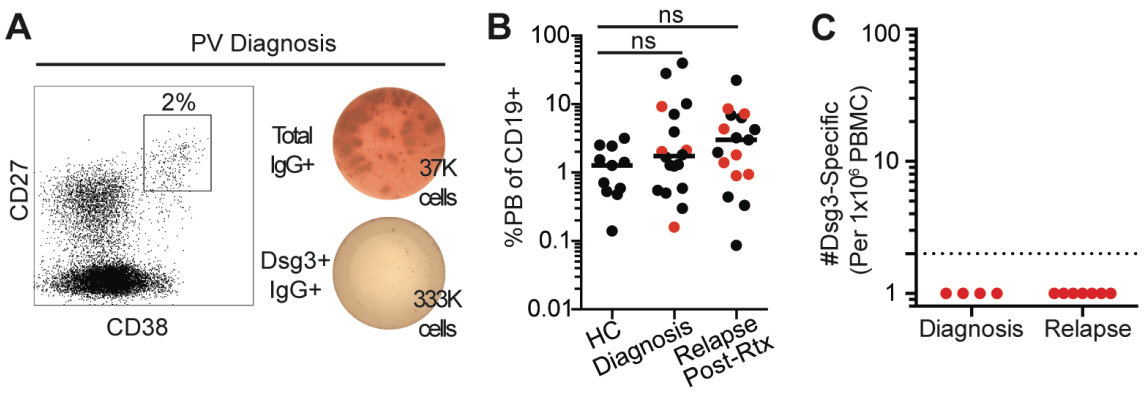

FIGURE S2. No Dsg3-specific circulating plasmablasts are detected in symptomatic PV patients.

Related to Figure 1. (A) A representative flow plot of plasmablasts detected in peripheral blood (gated on CD3-CD19+ lymphocytes) and an ELISPOT assay, showing a single dilution of titrated PBMCs probed for total IgG and Dsg3-specific IgG antibody-secreting cells from a PV patient at the time of diagnosis. (B) Frequency of plasmablasts does not differ between HC and patients at diagnosis or relapse. Red dots represent patients tested by ELISPOT for Dsg3-specific plasmablasts. (C) Absence of detectable Dsg3-specific circulating plasmablasts in patients presenting with active PV disease. Dotted line represents limit of detection for this assay at 3 antibody secreting cells per $1x10^6$ PBMCs. A one-way ANOVA was used to analyze this data.

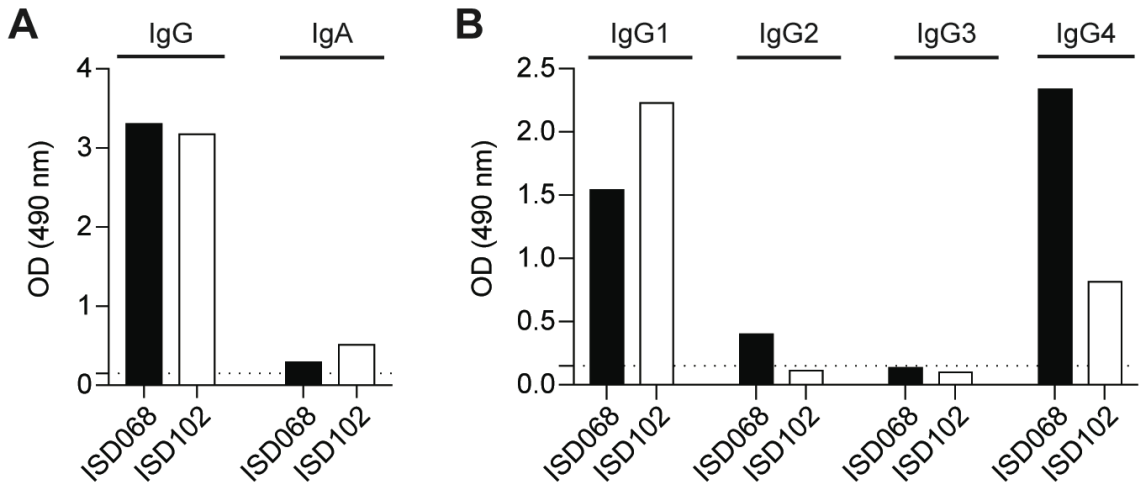

FIGURE S3. Dsg3-specific serum antibodies were primarily IgG1 and IgG4 isotype.

Related to Figure 2. An ELISA was used to determine isotype usage of Dsg3-specific serum antibodies from patients ISD068 and ISD102. Shown is the OD reading of serum diluted at 1:100. (A) Dsg3-specific serum responses are predominantly IgG, although some IgA was detected in both patients. (B) ELISA using IgG subclass reagents show that the Dsg3-specific responses are dominated by IgG1 and IgG4 subclass usage. Little to no IgG2 or IgG3 was detected in either of the patients. Dotted line represents cut-off value determined by the background signal detected in HC serum. Data is representative of two individual experimental repeats.

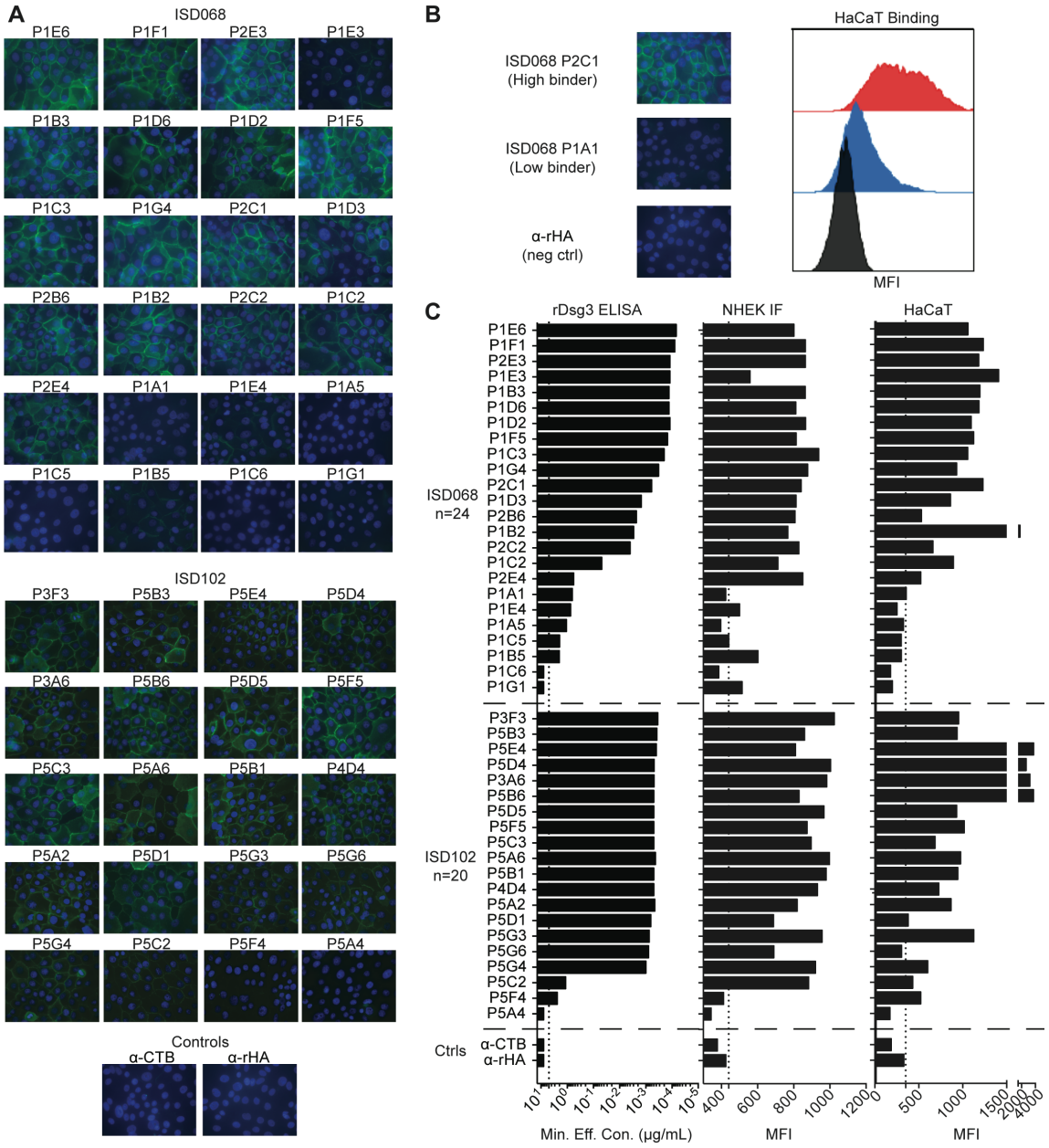
A
ISD068
P1E6 P1F1 P2E3 P1E3
P1B3 P1D6 P1D2 P1F5
P1C3 P1G4 P2C1 P1D3
P2B6 P1B2 P2C2 P1C2
P2E4 P1A1 P1E4 P1A5
P1C5 P1B5 P1C6 P1G1
ISD102
P3F3 P5B3 P5E4 P5D4
P3A6 P5B6 P5D5 P5F5
P5C3 P5A6 P5B1 P4D4
P5A2 P5D1 P5G3 P5G6
P5G4 P5C2 P5F4 P5A4
Controls
α-CTB α-rHA
B
ISD068 P2C1
(High binder)
ISD068 P1A1
(Low binder)
α-rHA
(neg ctrl)
HaCaT Binding
MFI
C
rDsg3 ELISA
NHEK IF
HaCaT
ISD068
n=24
ISD102
n=20
Ctrls
α-CTB
α-rHA
Min. Eff. Con. (μg/mL)
MFI
MFI

FIGURE S4. Assessment of mAbs binding to Dsg3 expressed on cell surface.

Related to Figure 2. Binding of mAbs to Dsg3 was determined using (A) immunofluorescent staining of HK cells (primary cells line of human keratinocytes) and (B) flow cytometry-based assay of staining HaCaT cells (immortalized cell line of human keratinocytes). (C) Summary data comparing binding measured via ELISA, IF, and flow cytometry shows that there is a range of binding activity of mAbs towards Dsg3. Representative data of two individual experimental repeats is shown. Dotted line for MFI represents cut-off value for a negative signal.

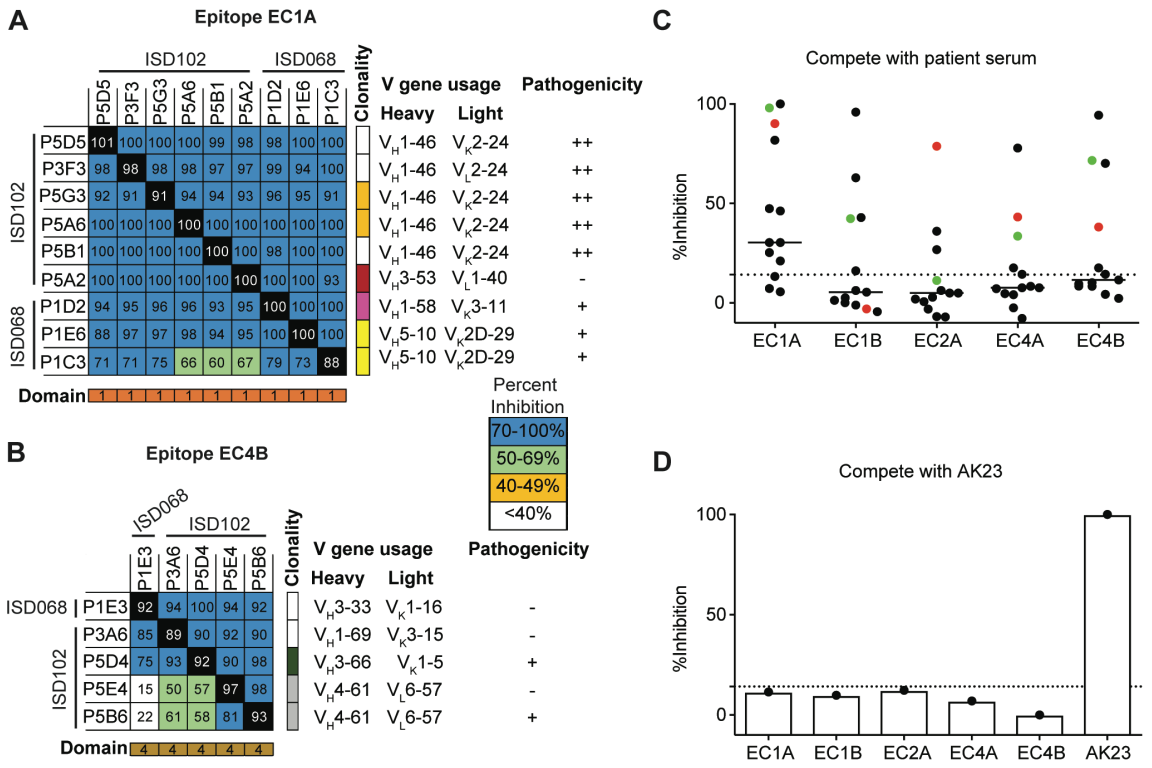
A
Epitope EC1A
ISD102
ISD068
P5D5 P3F3 P5G3 P5A6 P5B1 P5A2 P1D2 P1E6 P1C3
Clonality
V gene usage
Heavy Light
Pathogenicity
P5D5 101 100 100 100 99 98 98 100 100 VH1-46 VK2-24 ++
P3F3 98 98 98 98 97 97 99 94 100 VH1-46 VL2-24 ++
P5G3 92 91 91 94 94 93 96 95 91 VH1-46 VK2-24 ++
P5A6 100 100 100 100 100 100 100 100 100 VH1-46 VK2-24 ++
P5B1 100 100 100 100 100 100 98 100 100 VH1-46 VK2-24 ++
P5A2 100 100 100 100 100 100 100 100 93 VH3-53 VL1-40 -
P1D2 94 95 96 96 93 95 100 100 100 VH1-58 VK3-11 +
P1E6 88 97 97 98 94 95 100 100 100 VH5-10 VK2D-29 +
P1C3 71 71 75 66 60 67 79 73 88 VH5-10 VK2D-29 +
Domain 1 1 1 1 1 1 1 1 1
Percent Inhibition
70-100%
50-69%
40-49%
<40%
B
Epitope EC4B
ISD068
ISD102
P1E3 P3A6 P5D4 P5E4 P5B6
Clonality
V gene usage
Heavy Light
Pathogenicity
P1E3 92 94 100 94 92 VH3-33 VK1-16 -
P3A6 85 89 90 92 90 VH1-69 VK3-15 -
P5D4 75 93 92 90 98 VH3-66 VK1-5 +
P5E4 15 50 57 97 98 VH4-61 VL6-57 -
P5B6 22 61 58 81 93 VH4-61 VL6-57 +
Domain 4 4 4 4 4
C
Compete with patient serum
%Inhibition
100
50
0
EC1A EC1B EC2A EC4A EC4B
D
Compete with AK23
%Inhibition
100
50
0
EC1A EC1B EC2A EC4A EC4B AK23

FIGURE S5. Similar sterically-distinct epitopes detected by flow cytometry-based blocking assay were representative of other PV patients at diagnosis.

Related to Figure 4. The flow-based blocking assay was also used to define overlapping epitopes between patients ISD068 and ISD102. Antibodies targeting (A) epitope EC1A and (B) epitope EC4B could be detected in both patients. (C) A blocking ELISA was performed by using 13 PV serum from time of diagnosis to block binding of 5 different biotinylated mAbs to Dsg3, each mAb representative of the 5 detected epitopes described in Figure 4. While EC1A epitope was most commonly detected in all patients, the other 4 epitopes were targeted as well. Red dot: patient ISD068; Green dot: patient ISD102. (D) A blocking ELISA was also used to determine if the 5 detected epitopes bound to the same epitope as AK23, an EC1-specific pathogenic mouse-derived mAb (144). Interestingly, none of the 5 described epitopes targeted by the human MBC-derived mAbs bound to the same epitopes as the EC1-specific AK23, suggesting that preferred immunodominant epitopes are different for humans mAbs versus mouse mAbs. Representative data of two individual experimental repeats is shown. Dotted line represents cut-off value for positive inhibition, as determined by the mean of inhibition of 9 HC sera plus 2 SD.

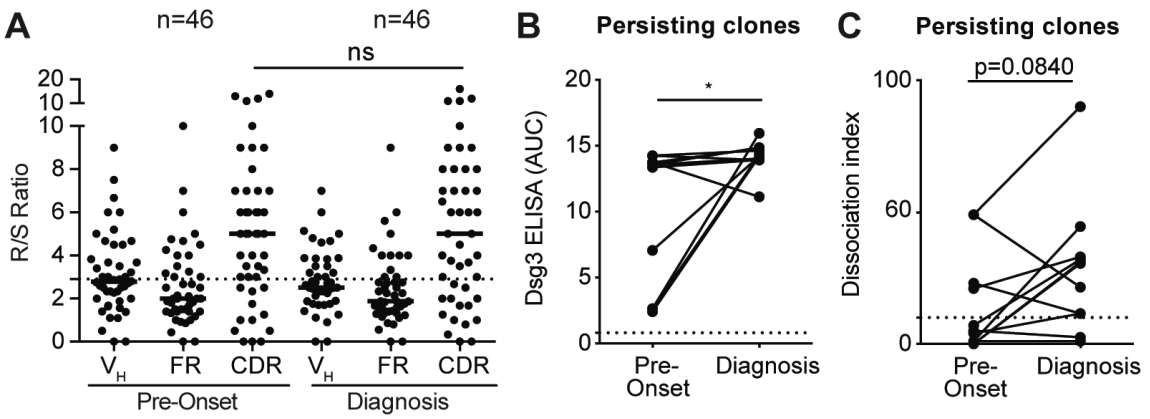

FIGURE S6. Antigen selection and ongoing affinity maturation of Dsg3-specific memory B cells.

Related to Figure 5. (A) R/S ratios were above 2.9 in the CDR at both pre-onset and diagnosis, indicating that antigenic selection is an ongoing process occurring continuously during disease development. When comparing only mAbs derived from persisting clones (MBCs from the same clonal family found at both pre-onset and diagnosis time points), (B) there was a significant increase in relative affinity of mAbs for Dsg3 and (C) a trend towards an increase in pathogenicity from pre-onset to diagnosis. A Mann-Whitney U test or Wilcoxon paired T-test was used where appropriate. * = $P \leq 0.05$

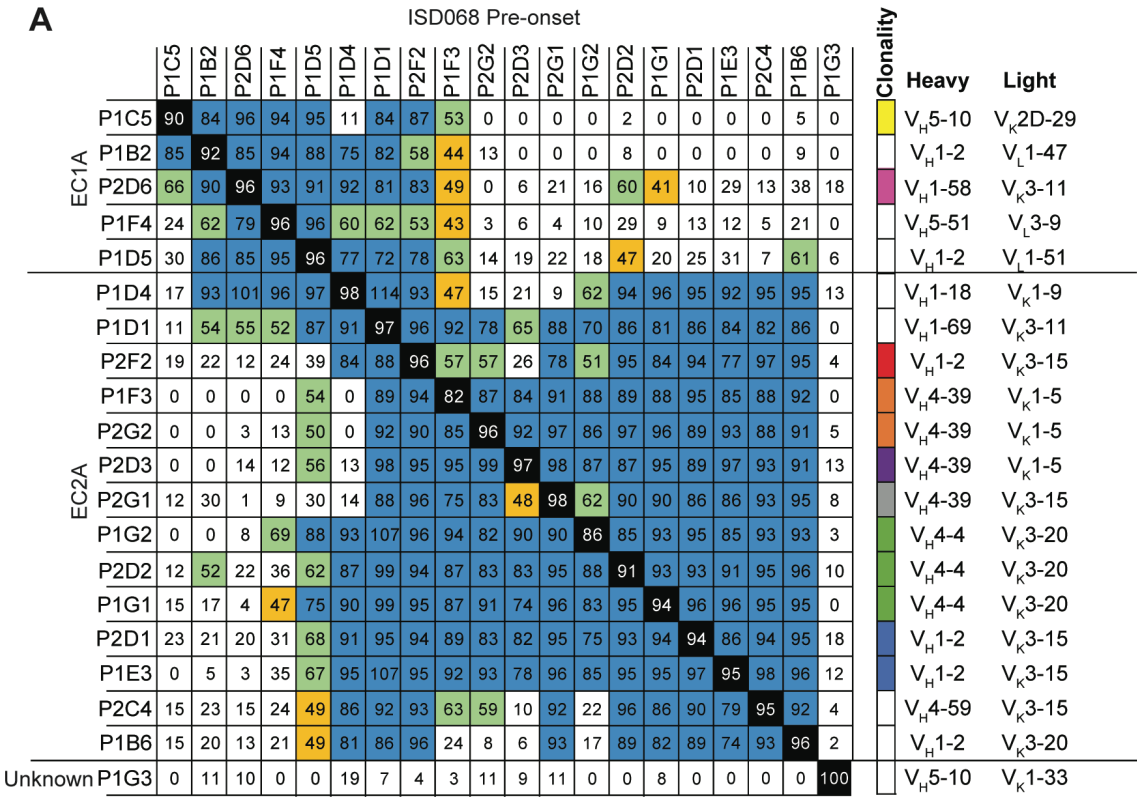
A
ISD068 Pre-onset
P1C5 P1B2 P2D6 P1F4 P1D5 P1D4 P1D1 P2F2 P1F3 P2G2 P2D3 P2G1 P1G2 P2D2 P1G1 P2D1 P1E3 P2C4 P1B6 P1G3
Clonality
Heavy
Light
EC1A
EC2A
P1C5 90 84 96 94 95 11 84 87 53 0 0 0 0 2 0 0 0 0 5 0 VH5-10 VK2D-29
P1B2 85 92 85 94 88 75 82 58 44 13 0 0 0 8 0 0 0 0 9 0 VH1-2 VL1-47
P2D6 66 90 96 93 91 92 81 83 49 0 6 21 16 60 41 10 29 13 38 18 VH1-58 VK3-11
P1F4 24 62 79 96 96 60 62 53 43 3 6 4 10 29 9 13 12 5 21 0 VH5-51 VL3-9
P1D5 30 86 85 95 96 77 72 78 63 14 19 22 18 47 20 25 31 7 61 6 VH1-2 VL1-51
P1D4 17 93 101 96 97 98 114 93 47 15 21 9 62 94 96 95 92 95 95 13 VH1-18 VK1-9
P1D1 11 54 55 52 87 91 97 96 92 78 65 88 70 86 81 86 84 82 86 0 VH1-69 VK3-11
P2F2 19 22 12 24 39 84 88 96 57 57 26 78 51 95 84 94 77 97 95 4 VH1-2 VK3-15
P1F3 0 0 0 0 54 0 89 94 82 87 84 91 88 89 88 95 85 88 92 0 VH4-39 VK1-5
P2G2 0 0 3 13 50 0 92 90 85 96 92 97 86 97 96 89 93 88 91 5 VH4-39 VK1-5
P2D3 0 0 14 12 56 13 98 95 95 99 97 98 87 87 95 89 97 93 91 13 VH4-39 VK1-5
P2G1 12 30 1 9 30 14 88 96 75 83 48 98 62 90 90 86 86 93 95 8 VH4-39 VK3-15
P1G2 0 0 8 69 88 93 107 96 94 82 90 90 86 85 93 95 85 93 93 3 VH4-4 VK3-20
P2D2 12 52 22 36 62 87 99 94 87 83 83 95 88 91 93 93 91 95 96 10 VH4-4 VK3-20
P1G1 15 17 4 47 75 90 99 95 87 91 74 96 83 95 94 96 96 95 95 0 VH4-4 VK3-20
P2D1 23 21 20 31 68 91 95 94 89 83 82 95 75 93 94 94 86 94 95 18 VH1-2 VK3-15
P1E3 0 5 3 35 67 95 107 95 92 93 78 96 85 95 95 97 95 98 96 12 VH1-2 VK3-15
P2C4 15 23 15 24 49 86 92 93 63 59 10 92 22 96 86 90 79 95 92 4 VH4-59 VK3-15
P1B6 15 20 13 21 49 81 86 96 24 8 6 93 17 89 82 89 74 93 96 2 VH1-2 VK3-20
Unknown P1G3 0 11 10 0 0 19 7 4 3 11 9 11 0 0 8 0 0 0 0 100 VH5-10 VK1-33

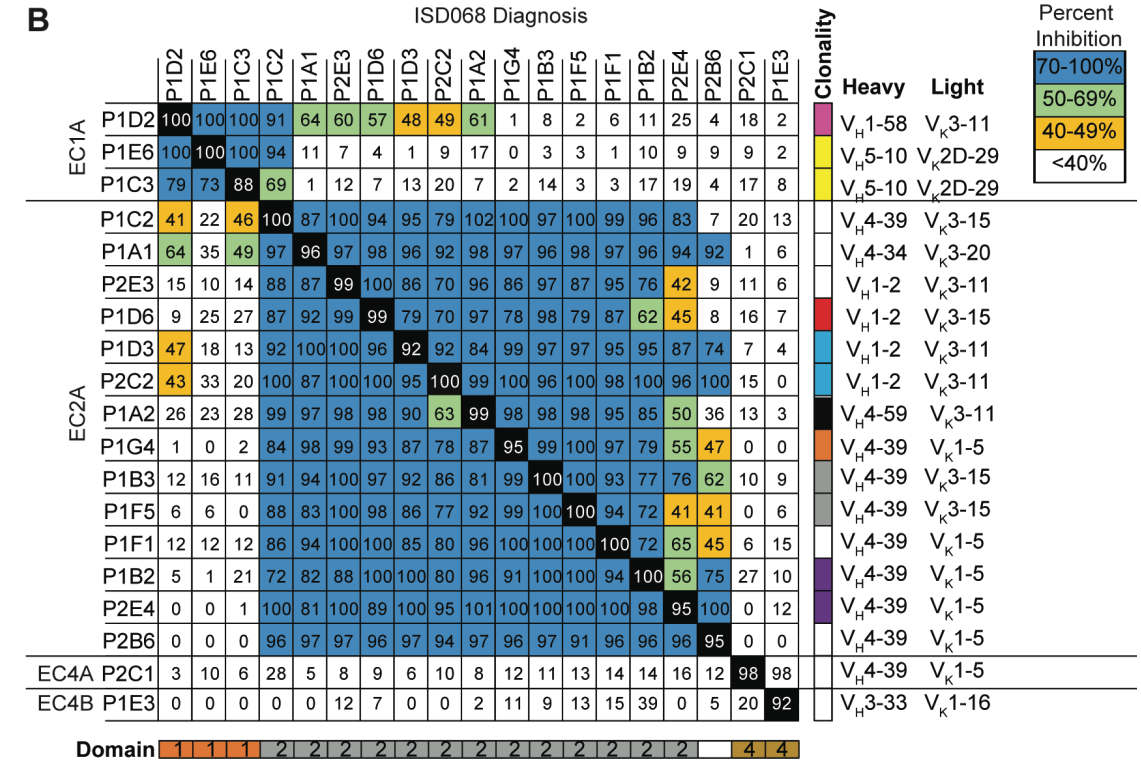
B
ISD068 Diagnosis
P1D2 P1E6 P1C3 P1C2 P1A1 P2E3 P1D6 P1D3 P2C2 P1A2 P1G4 P1B3 P1F5 P1F1 P1B2 P2E4 P2B6 P2C1 P1E3
Clonality
Heavy
Light
Percent Inhibition
70-100%
50-69%
40-49%
<40%
EC1A
EC2A
EC4A
EC4B
P1D2 100 100 100 91 64 60 57 48 49 61 1 8 2 6 11 25 4 18 2 VH1-58 VK3-11
P1E6 100 100 100 94 11 7 4 1 9 17 0 3 3 1 10 9 9 9 2 VH5-10 VK2D-29
P1C3 79 73 88 69 1 12 7 13 20 7 2 14 3 3 17 19 4 17 8 VH5-10 VK2D-29
P1C2 41 22 46 100 87 100 94 95 79 102 100 97 100 99 96 83 7 20 13 VH4-39 VK3-15
P1A1 64 35 49 97 96 97 98 96 92 98 97 96 98 97 96 94 92 1 6 VH4-34 VK3-20
P2E3 15 10 14 88 87 99 100 86 70 96 86 97 87 95 76 42 9 11 6 VH1-2 VK3-11
P1D6 9 25 27 87 92 99 99 79 70 97 78 98 79 87 62 45 8 16 7 VH1-2 VK3-15
P1D3 47 18 13 92 100 100 96 92 92 84 99 97 97 95 95 87 74 7 4 VH1-2 VK3-11
P2C2 43 33 20 100 87 100 100 95 100 99 100 96 100 98 100 96 100 15 0 VH1-2 VK3-11
P1A2 26 23 28 99 97 98 98 90 63 99 98 98 98 95 85 50 36 13 3 VH4-59 VK3-11
P1G4 1 0 2 84 98 99 93 87 78 87 95 99 100 97 79 55 47 0 0 VH4-39 VK1-5
P1B3 12 16 11 91 94 100 97 92 86 81 99 100 100 93 77 76 62 10 9 VH4-39 VK3-15
P1F5 6 6 0 88 83 100 98 86 77 92 99 100 100 94 72 41 41 0 6 VH4-39 VK3-15
P1F1 12 12 12 86 94 100 100 85 80 96 100 100 100 100 72 65 45 6 15 VH4-39 VK1-5
P1B2 5 1 21 72 82 88 100 100 80 96 91 100 100 94 100 56 75 27 10 VH4-39 VK1-5
P2E4 0 0 1 100 81 100 89 100 95 101 100 100 100 100 98 95 100 0 12 VH4-39 VK1-5
P2B6 0 0 0 96 97 97 96 97 94 97 96 97 91 96 96 96 95 0 0 VH4-39 VK1-5
EC4A P2C1 3 10 6 28 5 8 9 6 10 8 12 11 13 14 14 16 12 98 98 VH4-39 VK1-5
EC4B P1E3 0 0 0 0 0 12 7 0 0 2 11 9 13 15 39 0 5 20 92 VH3-33 VK1-16
Domain 1 1 1 2 2 2 2 2 2 2 2 2 2 2 2 2 4 4

FIGURE S7. Similar sterically-distinct epitopes are detected at pre-onset and diagnosis time points.

Related to Figure 5. A flow-based blocking assay was used to detect sterically-distinct epitopes of antibodies from patient ISD068 derived from (A) pre-onset and (B) diagnosis time points. Similar frequencies of EC1A and EC2A epitopes could be detected at pre-diagnosis, as well as diagnosis time point, suggesting that no epitope spreading has occurred between the two time points. Designated name of the epitope bound by antibodies is specified on the left of the chart where appropriate. Domain-specificity of mAbs derived from the diagnosis time point is illustrated at the bottom of the chart (Orange: EC1; Grey: EC2; Gold: EC4; White: Interdomain). mAbs in the same clonal family are represented on the right of the chart. Heavy and light chain usage is also detailed on the right.

TABLES

TABLE S1. Characteristics of subjects at time of enrollment.

GROUP	Patient ID	Gender	Age	Disease	% B cells of lymphocytes	Medications (mg/d)	Mo. Post recent Rtx	# Previous Rtx	PDAI[1]	Dsg3 Titer	Dsg1 titer
PV patients DIAGNOSIS (n=17)	ISD001	M	48	mucocutaneous	10.9	Prednisone (30)			12	20	133
	ISD003	M	26	mucosal	8.2	Prednisone (20)			11	137	0
	ISD020	M	48	mucocutaneous	6.3	Prednisone (60)			15	69	169
	ISD058	F	43	mucosal	15.8	Prednisone (30)			15	50	19
	ISD061	F	54	mucosal	8.8	Prednisone (60)			6	191	2
	ISD066	M	52	mucocutaneous	1.8	Prednisone (30)			36	181	199
	ISD068	M	60	mucocutaneous	4.3	Prednisone (40)			8	195	2
	ISD069	M	38	mucocutaneous	13.7	Prednisone (30)			55	204	8
	ISD070	M	48	mucocutaneous	11.8	None			0	200	117
	ISD082	M	54	mucocutaneous	9.4	Prednisone (80)			5	49	38
	ISD086	F	31	mucocutaneous	10.0	Prednisone (60)			4	128	10
	ISD091	F	45	mucocutaneous	5.7	Prednisone (60)			64	153	171
	ISD100	M	60	mucocutaneous	10.1	Prednisone (20)			20	169	0
	ISD102	F	45	mucocutaneous	6.5	Prednisone (10)			36	200	28
	ISD106	F	51	mucocutaneous	11.5	Prednisone (20)			4	75	6
	ISD109	F	48	mucocutaneous	6.8	Prednisone (80)			20	166	38
	ISD112	M	42	mucosal	7.5	Data unavailable			30*	151	164
PV patients REMISSION[2] (post-Rtx) (n=10)	R15	F	45	mucosal	10.8	None	20	0	1	8	1
	R15-06	M	41	mucosal	8.8	Cellcept (500)	19	2	0	120	2
	ISD002	F	48	mucosal	2.3	None	6	1	0	2	0
	ISD025	M	58	mucosal	7.8	Prednisone (2.5)	22	0	0	0	4
	ISD060	F	47	mucosal	13.2	None	17	0	2	24	0
	ISD068	M	63	mucocutaneous	3.2	None	11	2	0	29	17
	ISD069	M	39	mucocutaneous	7.6	None	13	0	3	5	0
	ISD070	M	51	mucocutaneous	8.2	None	29	0	1	135	0
	ISD072	F	51	mucocutaneous	8.9	None	12	0	0	6	0
	ISD082	M	55	mucocutaneous	5.5	None	13	0	0	1	1

PV patients RELAPSE[2] (post-Rtx) (n=17)	ISD005	M	64	mucocutaneous	3.2	Prednisone (40)	77	0	12	131	98
	ISD031	M	77	mucocutaneous	5.4	None	27	1	1	11	0
	ISD038	M	66	mucocutaneous	5.6	None	13	0	15	112	175
	ISD060	F	48	mucosal	11.9	None	22	0	5	43	0
	ISD061	F	55	mucosal	5.5	None	11	0	0	34	0
	ISD063	F	61	mucocutaneous	10.6	None	8	0	12	149	0
	ISD068	M	62	mucocutaneous	3.1	None	13	1	2	73	0
	ISD069	M	41	mucocutaneous	16	None	20	1	2	45	17
	ISD070	M	51	mucocutaneous	7.1	None	36	0	7	130	0
	ISD072	F	52	mucocutaneous	13.1	None	21	1	0	108	187
	ISD074	M	49	mucocutaneous	9.6	None	12	3	15	62	94
	ISD084	F	50	mucocutaneous	4.3	None	9	0	3	8	1
	ISD086	F	32	mucocutaneous	9.3	None	17	0	3	159	67
	ISD104	F	50	mucosal	37.2	None	10	0	22	57	10
	ISD106	F	51	mucocutaneous	7.33	None	8	0	4	47	0
	ISD110	M	37	mucocutaneous	14.4	None	20	0	2	37	17
	ISD122	M	63	mucocutaneous	3.7	None	45	4	25	78	0
Healthy controls (n=11)	HC01	F	48		11.3						
	HC02	F	53		12.3						
	HC08	F	57		8.7						
	HC13	M	40		4.1						
	HC15	F	31		11.5						
	H15-08	F	45		4.9						
	H15-11	F	45		6.6						
	H15-13	F	46		14.9						
	HC421	F	25		5.6						
	HC435	F	27		9.5						
	HC467	M	37		10.0						

* PDAI score calculated from photos

[1]Pemphigus Disease Activity Index (According to: Rosenbach M, et al. Reliability and convergent validity of two outcome instruments for pemphigus. *The Journal of investigative dermatology.* 2009;129(10):2404-10.

[2]According to Rosenbach M, et al. Reliability and convergent validity of two outcome instruments for pemphigus. *The Journal of investigative dermatology.* 2009;129(10):2404-10.

TABLE S2. Repertoire analysis of Dsg3-specific mAbs isolated from two PV patients.

Patient	mAb±	Isotype	Heavy Chain		CDR3 length (nt)	# Mutations (R/S ratio)	Light Chain			CDR3 length (nt)	# Mutations (R/S ratio)
			V gene	J gene			K/L	V gene	J gene		
ISD102 Diagnosis (n=20)	P3F3	IgG1	V_H1-46	J_H3	54	23 (19/4)	Kappa	V_K2-24	J_K5	27	8 (7/1)
	P5D5	IgG1	V_H1-46	J_H2	27	25 (20/5)	Kappa	V_K2-24	J_K2	27	14 (10/4)
	P5F5^{+}	IgA1	V_H3-15	J_H4	54	18 (11/7)	Lambda	V_L6-57	J_L3	30	18 (15/3)
	P5F4^{+}	IgA1	V_H3-15	J_H4	54	22 (14/8)	Lambda	V_L6-57	J_L3	30	19 (16/3)
	P5B3$^{\sim}$	IgG1	V_H3-15	J_H4	54	20 (13/7)	Lambda	V_L3-10	J_L3	33	17 (12/5)
	P5C3$^{\sim}$	IgG1	V_H3-15	J_H4	54	26 (15/11)	Lambda	V_L3-10	J_L3	33	20 (15/5)
	P5A6$^{\delta}$	IgG1	V_H1-46	J_H3	45	14 (9/5)	Kappa	V_K2-24	J_K5	27	13 (8/5)
	P5G3$^{\delta}$	IgG1	V_H1-46	J_H3	45	18 (13/5)	Kappa	V_K2-24	J_K5	27	12 (9/3)
	P5B1	IgG1	V_H1-46	J_H6	54	24 (14/10)	Kappa	V_K2-24	J_K1	27	7 (4/3)
	P4D4$^{\beta}$	IgG1	V_H3-23	J_H1	57	19 (14/5)	Lambda	V_L3-21	J_L3	33	21 (15/7)
	P5G4$^{\beta}$	IgG1	V_H3-23	J_H1	57	15 (10/5)	Lambda	V_L3-21	J_L3	33	16 (15/1)
	P5D1$^{\beta}$	IgG1	V_H3-23	J_H1	57	17 (11/6)	Lambda	V_L3-21	J_L3	33	21 (17/4)
	P5A2	IgG1	V_H3-53	J_H4	45	6 (4/2)	Lambda	V_L1-40	J_L3	33	12 (10/2)
	P5G6	IgG1	V_H1-2	J_H4	42	27 (20/7)	Lambda	V_L3-21	J_L2	36	12 (11/1)
	P5E4$^{\Omega}$	IgG1	V_H4-61	J_H4	36	19 (11/8)	Lambda	V_L6-57	J_L3	30	14 (11/3)
	P5B6$^{\Omega}$	IgG1	V_H4-61	J_H4	36	15 (9/6)	Lambda	V_L6-57	J_L3	30	12 (9/3)
	P5D4	IgG1	V_H3-66	J_H4	33	18 (17/1)	Kappa	V_K1-5	J_K2	27	5 (4/1)
	P3A6	IgG1	V_H1-69	J_H3	54	30 (23/7)	Kappa	V_K3-15	J_K2	30	11 (9/2)
	P5C2	IgG1	V_H4-4	J_H4	42	17 (11/6)	Kappa	V_K3-11	J_K4	27	2 (2/0)
	P5A4	IgM	V_H1-2	J_H4	57	0	Kappa	V_K3-20	J_K1	27	0
ISD068 Diagnosis (n=25)	P1E6*	IgG4	V_H5-10	J_H4	48	18 (14/4)	Kappa	V_K2D-29	J_K4	27	14 (9/5)
	P1C3*	IgG4	V_H5-10	J_H4	48	24 (21/3)	Kappa	V_K2D-29	J_K4	27	19 (9/10)
	P1D2$^{\pm}$	IgG1	V_H1-58	J_H3	33	24 (20/4)	Kappa	V_K3-11	J_K2	30	12 (9/3)
	P1A1	IgG4	V_H4-34	J_H4	69	27 (25/12)	Kappa	V_K3-20	J_K2	27	13 (11/2)
	P1C5	IgG1	V_H4-59	J_H4	60	39 (31/8)	Kappa	V_K3-15	J_K1	30	11 (8/3)
	P1C6	IgG1	V_H3-23	J_H3	63	26 (19/7)	Kappa	V_K4-1	J_K5	27	16 (10/6)
	P1F1	IgG1	V_H4-39	J_H2	42	29 (21/8)	Kappa	V_K1-5	J_K1	27	26 (19/7)
	P1B3$^{\#}$	IgG4	V_H4-39	J_H2	84	43 (28/15)	Kappa	V_K3-15	J_K2	33	18 (10/8)
	P1F5$^{\#}$	IgG1	V_H4-39	J_H2	33	29 (17/12)	Kappa	V_K3-15	J_K2	33	20 (16/4)
	P1D6†	IgG4	V_H1-2	J_H1	30	22 (14/8)	Kappa	V_K3-15	J_K1	33	16 (12/4)
	P2E3	IgG4	V_H1-2	J_H4	30	20 (15/5)	Kappa	V_K3-11	J_K2	33	15 (11/4)
	P1G4	IgG1	V_H4-39	J_H2	42	30 (21/9)	Kappa	V_K1-5	J_K1	27	20 (14/6)
	P1D3$^{\wedge}$	IgG1	V_H1-2	J_H4	72	29 (24/5)	Kappa	V_K3-11	J_K2	33	16 (11/5)
	P2C2$^{\wedge}$	IgG1	V_H1-2	J_H4	72	28 (24/4)	Kappa	V_K3-11	J_K2	33	21 (17/4)
	P1B2$^{\%}$	IgG1	V_H4-39	J_H2	42	21 (16/5)	Kappa	V_K1-5	J_K1	27	20 (14/6)

	P2E4[%]	IgG1	V_H4-39	J_H2	42	21 (15/6)	Kappa	V_K1-5	J_K1	27	20 (12/8)
	P1C2	IgG4	V_H4-39	J_H5	39	30 (19/11)	Kappa	V_K3-15	J_K2	33	15 (13/2)
	P1A2[‡]	IgG1	V_H4-59	J_H2	54	29 (20/9)	Kappa	V_K3-11	J_K2	18	15 (11/4)
	P2C1	IgG1	V_H4-39	J_H4	48	27 (17/10)	Kappa	V_K1-5	J_K1	21	13 (9/4)
	P2B6	IgG1	V_H4-39	J_H4	42	27 (19/8)	Kappa	V_K1-5	J_K1	27	20 (14/6)
	P1E4[&]	IgG1	V_H4-4	J_H5	45	28 (23/5)	Kappa	V_K3-15	J_K3	30	15 (9/6)
	P1B5[&]	IgG1	V_H4-4	J_H5	45	36 (28/8)	Kappa	V_K3-15	J_K3	30	12 (7/5)
	P1A5	IgG1	V_H3-23	J_H4	39	0	Lambda	V_L1-47	J_L2	33	0
	P1G1	IgA1	V_H3-74	J_H3	51	19 (14/5)	Kappa	V_K3-15	J_K3	27	11 (10/1)
	P1E3	IgG4	V_H3-33	J_H3	60	7 (5/2)	Kappa	V_K1-16	J_K4	27	6 (3/3)
ISD068 Pre-Diagnosis (n=25)	P1D4	IgG4	V_H1-18	J_H4	42	16 (11/5)	Kappa	V_K1-9	J_K4	27	8 (7/1)
	P2F2[†]	IgG4	V_H1-2	J_H1	30	25 (18/7)	Kappa	V_K3-15	J_K1	33	17 (13/4)
	P1D5	IgG4	V_H1-2	J_H3	48	23 (14/9)	Lambda	V_L1-51	J_L3	36	8 (5/3)
	P1D6	IgG1	V_H1-2	J_H3	27	31 (18/13)	Kappa	V_K3-11	J_K5	33	13 (8/5)
	P1B2	IgG1	V_H1-2	J_H4	42	36 (25/11)	Lambda	V_L1-47	J_L1	33	21 (10/11)
	P1B6	IgG4	V_H1-2	J_H4	24	16 (10/6)	Kappa	V_K3-20	J_K4	27	12 (10/2)
	P2D1[^]	IgG1	V_H1-2	J_H4	39	22 (17/5)	Kappa	V_K3-15	J_K4	33	15 (12/3)
	P1E3[^]	IgG4	V_H1-2	J_H4	39	17 (15/2)	Kappa	V_K3-15	J_K4	33	12 (10/2)
	P1G5[^]	IgG4	V_H1-2	J_H4	39	24 (14/10)	Kappa	V_K3-15	J_K4	33	12 (10/2)
	P2D6[±]	IgG4	V_H1-58	J_H3	33	10 (9/1)	Kappa	V_K3-11	J_K2	30	8 (6/2)
	P1D1	IgG1	V_H1-69	J_H5	54	28 (22/6)	Kappa	V_K3-11	J_K4	30	5 (4/1)
	P1C4	IgM	V_H3-23	J_H1	54	3 (1/2)	Lambda	V_L3-25	J_L2	33	10 (7/3)
	P2F4	IgG4	V_H3-53	J_H6	42	31 (26/5)	Kappa	V_K1-5	J_K1	27	15 (10/5)
	P1G1[§]	IgG1	V_H4-4	J_H2	72	35 (26/9)	Kappa	V_K3-20	J_K4	30	18 (14/4)
	P1G2[§]	IgG1	V_H4-4	J_H2	72	36 (27/9)	Kappa	V_K3-20	J_K4	30	14 (12/2)
	P2D2[§]	IgG1	V_H4-4	J_H2	72	38 (28/10)	Kappa	V_K3-20	J_K4	30	16 (13/3)
	P2D3[%]	IgA1	V_H4-39	J_H2	42	15 (11/4)	27	V_K1-5	J_K1	27	11 (10/1)
	P2G2[α]	IgG1	V_H4-39	J_H2	42	21 (11/10)	Kappa	V_K1-5	J_K1	27	17 (11/6)
	P1F3[α]	IgG1	V_H4-39	J_H2	42	20 (14/6)	Kappa	V_K1-5	J_K1	27	15 (10/5)
	P2G1[#]	IgG1	V_H4-39	J_H2	51	23 (15/8)	Kappa	V_K3-15	J_K2	33	14 (12/2)
	P2C4	IgG1	V_H4-59	J_H4	60	34 (28/6)	Kappa	V_K3-15	J_K1	30	9 (6/3)
	P1D2[‡]	IgG1	V_H4-59	J_H2	48	27 (20/7)	Kappa	V_K3-11	J_K2	18	16 (11/5)
	P1C5*	IgG4	V_H5-10	J_H4	48	14 (10/4)	Kappa	V_K2D-29	J_K4	27	11 (5/6)
	P1G3	IgG1	V_H5-10	J_H3	51	21 (18/3)	Kappa	V_K1-33	J_K2	27	19 (15/4)
	P1F4	IgG4	V_H5-51	J_H5	75	23 (20/3)	Lambda	V_L3-9	J_L3	30	18 (9/9)

[⊢] Matching symbols indicate mAbs that are part of the same clonal expansion.

TABLE S3. Characteristics of antibodies selected for germline reversion.

Patient	mAb	Isotype	Heavy Chain		CDR3 length (nt)	R/S Ratio			# unique clones	Epitope	Pathogenicity*
			V gene	J gene		VH	FR	CDR			
ISD068 (n=10)	P1C3	IgG2	VH5-10	JH4	48	7	4	9	2	EC1A	+
		Kappa	VK2D-29	JK4	27						
	P1D2	IgG1	VH1-58	JH3	33	5	4.33	6	2	EC1A	+
		Kappa	VK3-11	JK2	30						
	P1A1	IgG2	VH4-34	JH4	69	1.25	1.56	1.67	1	EC2A	-
		Kappa	VK3-20	JK2	27						
	P1B2	IgG1	VH4-39	JH2	42	3.2	3	5	3	EC2A	+
		Kappa	VK1-5	JK1	27						
	P1B3	IgG2	VH4-39	JH2	84	1.87	1.1	6.5	2	EC2A	+
		Kappa	VK3-14	JK2	33						
	P1D6	IgG2	VH1-2	JH1	30	1.75	1.67	2	1	EC2A	-
		Kappa	VK3-15	JK1	33						
	P1F1	IgG1	VH4-39	JH2	42	2.63	2.71	4	3	EC2A	+
		Kappa	VK1-5	JK1	27						
	P2E3	IgG2	VH1-2	JH4	30	3	2.25	6	1	EC2A	+
		Kappa	VK3-11	JK2	33						
	P2C1	IgG1	VH4-39	JH4	48	1.7	0.55	9	1	EC4A	+
		Kappa	VK1-5	JK1	21						
	P1E3	IgG2	VH3-33	JH3	60	2.5	4	1	1	EC4B	-
		Kappa	VK1-16	JK4	27						
ISD102 (n=10)	P3F3	IgG1	VH1-46	JH3	54	4.75	2.75	7	1	EC1A	++
		Kappa	VK2-24	JK5	27						
	P5A2	IgG1	VH3-53	JH4	45	2	2	2	2	EC1A	-
		Lambda	VL1-40	JL3	33						
	P5B1	IgG1	VH1-46	JH6	54	1.86	1.57	1	1	EC1A	++
		Kappa	VK2-24	JK4	27						
	P5G3	IgG1	VH1-46	JH3	45	2.60	2.75	6	2	EC1A	++
		Kappa	VK2-24	JK5	27						
	P5G6	IgG1	VH1-2	JH4	42	2.86	1.25	8	1	EC1 domain	-
		Lambda	VL3-21	JL2	36						
	P5B3	IgG1	VH3-15	JH4	54	1.86	0.71	6	3	EC1B	+
		Lambda	VL3-10	JL3	33						
	P5F5	IgA1	VH3-15	JH4	54	1.57	1.17	4	3	EC1B	+
		Lambda	VL6-57	JL3	30						
	P3A6	IgG1	VH1-69	JH3	54	3.29	2.67	7	1	EC4B	-
		Kappa	VK3-15	JK2	30						
	P5D4	IgG1	VH3-66	JH4	33	17	12	5	2	EC4B	+
		Kappa	VK1-5	JK2	27						
	P5E4	IgG1	VH4-61	JH4	36	1.38	1.14	1.5	2	EC4B	-
		Lambda	VL6-57	JL3	30						

*Pathogenicity was determined using the following cut-off values for the dissociation index number: - = DI≤10; + = DI>10; ++ = DI>100.

Chapter 3:

Robust memory responses against influenza vaccination in previously Rituximab-treated pemphigus patients

Alice Cho[1,2], Bridget Bradley[3], Robert Kauffman[1,2], Lalita Priyamvada[1,2], Yevgeniy Kovalenkov[1,2], Ron Feldman[3], and Jens Wrammert[1,2]

[1]Department of Pediatrics, Division of Infectious Disease, Emory University School of Medicine, Atlanta, Georgia, USA; [2]Emory Vaccine Center, Emory University School of Medicine, Atlanta, Georgia, USA; [3]Department of Dermatology, Emory University School of Medicine, Atlanta, Georgia, USA

Chapter adapted from:

Cho, A., Bradley, B., Kauffman, R., Priyamvada, L., Kovalenkov, Y., Feldman, R., & Wrammert, J. (2017). Robust memory responses against influenza vaccination in pemphigus patients previously treated with rituximab. *JCI Insight*, *2*(12). PMID: 28614800; PMCID: PMC5470882l; doi: 10.1172/jci.insight.93222

Available at: https://insight.jci.org/articles/view/93222

ABSTRACT

Rituximab is a therapeutic anti-CD20 monoclonal antibody widely used to treat B cell lymphoma and autoimmune diseases such as rheumatic arthritis, systemic lupus erythematosus, and autoimmune blistering skin diseases (AIBD). While Rituximab fully deplete peripheral blood B cells, it remains unclear if some pre-existing B cell memory to pathogens or vaccines may survive depletion, especially in lymphoid tissues, and if they can undergo homeostatic expansion du8ring recovery from depletion. The limited data available on vaccine efficacy in this setting have been performed on Rituximab-treated patients receiving concomitant chemotherapy or other potent immunosuppressants. Here, we present an in-depth analysis of seasonal influenza vaccine responses in AIBD patients previously treated with Rituximab, but that were generally not receiving additional therapeutic interventions. We found that despite a lack of influenza-specific memory B cells in the blood, patients mount robust recall responses to vaccination, comparable to healthy controls, both at a cellular and serological level. Repertoire analyses of plasmablast responses suggest that they likely derive from a diverse pool of tissue-resident memory cells, refractory to depletion. Overall, these data have important implications for establishing an effective vaccine schedule for AIBD patients, the clinical care of Rituximab-treated patients in general, and contribute to our basic understanding of maintenance of normal and pathogenic human B cell memory.

INTRODUCTION

Influenza infection is a leading cause of morbidity and mortality worldwide (201, 202), especially in young children, the elderly, and immune-compromised individuals (266). Influenza vaccination is often recommended to these target populations as an effective preventative measure, although vaccine responses in these patient populations is relatively poor compared to healthy vaccinees (266, 267). Since serum antibodies are a correlate of protection for vaccine efficacy in humans (268) it is clinically important to study vaccine responses in patients who are receiving medication, or who have a disease, that modulates B cell responses.

Rituximab is a B cell depleting anti-CD20 monoclonal antibody developed to treat B cell lymphoma (171). It is FDA-approved to treat rheumatoid arthritis (RA) and anti-neutrophil cytoplasmic autoantibody vasculitis (173). There is increasing off-label use for B cell-mediated autoimmune disorders such as systemic lupus erythematosus (80) and autoimmune blistering skin diseases (AIBD) (175, 269). Rituximab targets all B cells, except early precursor pro-B cells and long-lived plasma cells that do not express CD20 (65, 178). Thus, it has little impact on pre-existing serum antibody titers produced by long-lived plasma cells, such as antibodies against childhood vaccines including tetanus or meningitis (171, 178), but completely eliminates peripheral B cell memory. Depletion of peripheral B cells typically lasts for 6-9 months, with numbers recovering after one year (180). Despite recovery of total B cell numbers, the repopulated B cell compartment consists largely of naïve cells, and total memory B cells (MBCs) remain almost absent in peripheral blood, even five years post-treatment (183). It is unknown whether the very small number of MBCs that are detected represent cells that escaped depletion, or are newly

generated memory cells. It is also unclear if antigen-specific MBCs can avoid depletion in lymphoid organs (270) and/or possibly expand through homeostatic mechanisms, as is the case for T cells (271).

AIBD are a group of potentially fatal B cell-mediated autoimmune disorders affecting skin and/or mucous membranes, including pemphigus and pemphigoid (94-96). Pemphigus results in severe erosions caused by autoantibodies directed against intercellular proteins in the epidermis called desmogleins-1 and 3 (98, 99). Pemphigoid causes blistering due to autoantibodies specific for proteins in the basement membrane zone between the epidermis and dermis, including collagen XVII (272, 273). Historically, AIBD patients have been treated with systemic corticosteroids or adjuvant immunosuppressants (166), but recently, treatment with Rituximab has gained popularity (106, 165, 169, 170, 274, 275). To our knowledge, there are no reports describing vaccine efficacy in Rituximab-treated AIBD patients. Previous studies have reported severely impaired immune responses to influenza vaccination in other types of Rituximab-treated patients, primarily RA or lymphoma patients (225-229). A major caveat to these earlier studies was that patients were treated with concomitant immunosuppressive drugs or chemotherapy, making it difficult to determine the impact of the individual drugs on vaccine responses. In contrast, AIBD patients are often weaned off additional immunosuppressive drugs after Rituximab depletion, making it possible to study vaccine responses in Rituximab-treated patients that are not currently prescribed additional immunosuppressive therapies. It is also possible that underlying autoimmune disease may differentially affect vaccine responses, with AIBD patients reacting differently from RA or lymphoma patients. Thus, it is important to study the impact of Rituximab on vaccine

responses in the context of various diseases.

Here, we measured influenza vaccine responses in AIBD patients that received Rituximab therapy 5-24 months earlier, and compared them to a matched cohort of healthy control subjects. Surprisingly, we found that despite the absence of detectable pre-existing influenza-specific MBCs in peripheral blood, patients mounted a robust humoral immune response to the vaccine, of comparable magnitude, quality and repertoire breadth to those observed in healthy vaccinees. Interestingly, these responses had all the hallmarks of a memory recall response. This suggests that significant numbers of MBCs can survive Rituximab depletion, presumably in lymphoid tissues, and act as a source for protective recall responses. These findings have important implications for the clinical care of AIBD patients, and our understanding of memory B cell homeostasis and its role in autoimmune disease etiology, as well as vaccine responses in the context of B cell ablative therapies in humans.

RESULTS

Reconstitution of the B cell compartment in Rituximab-treated AIBD patients. We enrolled 23 AIBD patients and 28 healthy controls that received the influenza vaccine during the 2014/15 or 2015/16 influenza season. Recruited patients had received Rituximab therapy within the last 24 months (median 11 months) and importantly, at the time of vaccination, the majority were not receiving other immunosuppressive therapies. Healthy controls were demographically-matched with similar influenza vaccination histories (Table 1).

Numerical reconstitution of the B cell compartment after Rituximab treatment typically begins around 6-9 months, with total B cell numbers returning to a normal range after one year (179, 180, 182) (Figure 1A). During this time, enrolled patients showed improved clinical symptoms, and a general decrease in serum autoantibody titers (Figure S1). We focused our study on patients who were within 5-24 months of receiving Rituximab therapy, when patients exhibited disease remission and the B cell compartment was numerically reconstituted, either partially or fully (Figure 1A). Based on pharmacokinetic data for Rituximab (180), we expect little Rituximab to remain in circulation at this point, which would be important for interpretation. Overall, the frequency of peripheral B cells, defined as $CD3^{-}CD19^{+}$ lymphocytes (Figure 1B), did not significantly differ between patients and healthy controls (4.1% versus 7.2%, respectively; P=0.16). Additionally, there was no significant difference when comparing total number of B cells between patients and healthy controls. However, there were seven patients recruited during early numerical reconstitution, with B cell frequencies less than 1% (Figure 1C). It was previously reported that a large wave of $CD24^{hi}CD38^{hi}$ transitional B

cells, recently emigrated from the bone marrow, dominate the B cell compartment during initial reconstitution (182, 276). Accordingly, the Rituximab-treated AIBD patients had a higher frequency of transitional B cells compared to healthy controls (10.3% versus 5%, respectively; $P \leq 0.001$), with similar differences observed when comparing absolute counts of transitional B cells (Figure 1D). Notably, the patients recruited during early reconstitution, with low total B cell frequencies, were generally the ones with higher frequencies of transitional cells.

Lack of peripheral influenza-specific memory B cells in patients previously treated with Rituximab. Little information is available on the survival or potential homeostatic recovery of antigen-specific memory cells after B cell depletion in humans (270). However, it is clear that the overall MBC population remains low for long periods of time after depletion (277) (Figure 2A). Accordingly, the frequency of $CD27^+$ MBCs of total B cells was significantly lower in patients than in healthy controls (4% versus 25.5%, respectively; $P \leq 0.0001$). This was also true when comparing absolute numbers of $CD27^+$ MBC (Figure 2B). We next used an ELISPOT-based assay to detect stimulated antigen-specific MBCs present in both patients and healthy controls prior to vaccination (278). Importantly, we could not detect influenza-specific MBCs in almost all of the patients, with only 3 patients showing measurable numbers of influenza-specific MBCs. In contrast, these cells were detectable in all but one healthy control prior to vaccination (median 0.4%), similar to previous reports (49, 279) (Figure 2C). It remains unclear if the low number of MBCs in patients represent newly generated memory cells, or are pre-existing memory cells that survived depletion. Overall, although total B cell numbers return to normal over

time, Rituximab has a profound and long-lasting impact on the memory B cell compartment in blood.

Potent plasmablast responses after vaccination despite the lack of circulating influenza-specific memory B cells. Previous studies have shown that the magnitude of plasmablast responses correlate with the serological outcome of vaccination, and can be used as a predictor of influenza vaccination efficacy (51, 52). In healthy controls, these responses are primarily of IgG isotype, peak about 7 days post-vaccination, and are thought to predominantly originate from memory B cells (49, 51). These rapid and potent anamnestic responses are transient in peripheral blood, with some plasmablasts likely taking up residence in survival niches within the bone marrow (60) or possibly other lymphoid organs. Surprisingly, we found that despite the lack of detectable influenza-specific MBCs in peripheral blood, patients mounted potent plasmablast responses after vaccination, of comparable magnitude and kinetics to those observed in healthy controls. This was shown by flow cytometric analysis, measuring plasmablast frequency (Figure 3A), as well as ELISPOT assay, measuring influenza-specific antibody-secreting cells (ASCs) (Figure 3B). The average numbers of influenza-specific ASCs per million PBMCs at day 7 was similar between healthy controls and patients comparing IgG (820 versus 730, respectively), IgA (330 versus 240, respectively), and IgM (83 versus 22, respectively) isotypes. These responses were clearly dominated by class-switched antibodies in both healthy controls and patients, suggesting that these responses were of memory origin (Figure 3C). Interestingly, patients who had received multiple Rituximab treatments in the past did have a significantly smaller IgG and IgA plasmablast responses compared to

patients who had only received a single cycle of Rituximab, with one patient who had previously received 2 rounds of Rituximab treatment failing to produce any detectable plasmablast response. While there was no significant difference when comparing IgM responses, we believe this is likely due to low IgM plasmablast responses in both patient cohorts (Figure 3D). This suggests that multiple rounds of Rituximab may increase the level of depletion of memory B cells in patients.

The magnitude of the plasmablast response does not seem to depend on the amount of time after receiving Rituximab (Figure S2A). Additionally, there was no difference in the magnitude of the plasmablast response when comparing patients who were not receiving additional immunosuppressants at time of vaccination versus those who were (Figure S2B), although this may be due to the low dose of immunosuppressants typically prescribed to AIBD patients. Finally, different types of AIBD (Figure S2C) and relapse within 2 years of vaccination (Figure S2D) did not have a significant impact on the plasmablast response. From these data, we conclude that after peripheral B cell reconstitution has begun, patients can mount a robust plasmablast response likely originating from memory cells, despite low or undetectable numbers of memory B cells in peripheral blood.

Protective serum antibody responses to vaccination in patients and healthy controls. In addition to comparable plasmablast responses, both patients and healthy controls mounted robust serological responses to the vaccine. After vaccination during the 2014/15 influenza season, HAI geometric mean titers (GMT) increased significantly ($P \leq 0.05$) against the H1 strain for both patients (22 to 61) and healthy controls (31 to 145), as well

as the H3 strain for patients (31 to 123) and healthy controls (119 to 215). Similar results were observed in vaccinees enrolled during the 2015/16 influenza season, with GMTs increasing in the H1 strain in patients (14 to 46) and healthy controls (26 to 98), as well as the H3 strain in patients (12 to 40) and healthy controls (11 to 44) (Figure 4A). Additionally, the frequency of seroprotection in patients and healthy controls post-vaccination were comparable, suggesting that vaccination provided similar protective immunity in both cohorts (Figure S3A).

MN assays showed similar results. During the 2014/15 influenza seasons, significant increases in MN GMT ($P<0.05$) was observed against the H1 strain in patients (16 to 40) and healthy controls (34 to 125), as well as for the H3 strain in patients (29 to 136) and healthy controls (226 to 371). These increases were also observed during the 2015/16 influenza seasons against the H1 strain in patients (64 to 905) and healthy controls (290 to 6890), as well as for the H3 strain in patients (86 to 260) and healthy controls (38 to 138) (Figure 4B). The frequency of seroprotection as determined by MN assay was comparable between patients and healthy controls, which confirmed the robustness of the vaccine responses in both cohorts (Figure S3B). Overall, these serological analyses demonstrated that both the quantity and quality of the vaccine-induced immune response were similar for healthy controls and patients.

Rituximab does not impair the generation of antigen-specific memory B cells. To evaluate if previous Rituximab had any impact on the generation of new MBCs, we determined the frequency of influenza-specific MBCs post-vaccination. To this end, we used a six-day polyclonal *in vitro* stimulation of PBMCs, causing MBCs to differentiate

into ASCs. This was followed by ELISPOT measures of both total and influenza-specific IgG-secreting cells, with responses reported as the frequency of antigen-specificity per total IgG secreting cells (278) (Figure 5A).

As mentioned previously (Figure 2C), only 3 patients had detectable influenza-specific MBCs prior to vaccination, whereas these cells were present in 23 out of 24 healthy controls pre-vaccination. This shows that Rituximab efficiently depletes peripheral antigen-specific MBCs. Strikingly, we observed a robust increase in the frequency of influenza-specific IgG+ MBCs from day 0 to day 28 post-vaccination in both healthy controls (0.4% to 1.8%, $P \leq 0.001$) and patients (0.0% to 4.2%, $P \leq 0.001$) alike, such that a difference in the frequency at day 28 between healthy controls and patients was no longer observed (Figure 5B). This suggests that the generation of new peripheral MBCs is not impaired in these patients. Further studies on the longevity of these cells will elucidate if previous Rituximab therapy has any impact on the long-term maintenance of these newly generated memory cells.

We were unable to obtain data for 10 of the patients using our standard memory B cell assay. Although total MBCs were detectable by flow cytometry, B cells failed to expand *in vitro*, presumably due to the low frequency of memory cells in the PBMC preparation (Figure S4A). To recover some of these data points, we evaluated an alternative polyclonal stimulation method, using R848 and huIL-2 (244). This approach provided almost identical data compared to the classical method at high levels of MBCs, but was much more efficient in stimulating samples with low frequencies of MBCs (Figure S4B and C). We were able to obtain antigen-specific MBC frequencies from an additional 6 patients using this optimized methodology. Data from these patients confirmed the findings

shown in Figure 5B. All but one patient had undetectable influenza-specific MBCs prior to vaccination, with robust increases in antigen-specific memory cells from day 0 to day 28 post-vaccination in all patients (median 0.0% to 1.0%). In contrast, all healthy controls re-tested with the alternative mitogen cocktail had detectable influenza-specific MBCs prior to vaccination (median 0.23%) that expanded post-vaccination (median 2.2%) (Figure S4D). Overall, these results show that although Rituximab successfully depletes MBCs in the periphery, patients can still develop new peripheral antigen-specific memory B cells in response to an antigenic challenge.

Repertoire of vaccine-induced plasmablasts is similar between patients and healthy controls. To determine if the plasmablast responses derived from an expansion of a small number of precursor MBCs or a more diverse pool of memory cells, we analyzed the antibody repertoire breadth of plasmablasts from a subset of patients and healthy controls. Using previously published primer sets (246, 247), we amplified the V_H gene from single-cell sorted plasmablasts using multiplex PCR, and analyzed the sequences of class-switched heavy chains. Overall, we analyzed 172 sequences from 5 healthy controls and 286 sequences from 8 patients, with a range of 22-46 sequences per vaccinee (Table S1). Comparing patients and healthy controls, we observed no difference between the average number of somatic hypermutations observed in the V_H gene (21 to 20, respectively; P=0.49). The high level of mutation further confirms the memory origin of the plasmablast response in both cohorts (Figure 6A). Additionally, there was no difference between patients and healthy controls when measuring the average CDR3 length (15.6 to 16.4, respectively; P=0.22) (Figure 6B) as well as the average frequency of clonal expansions

(22.6% to 23.4%, respectively; *P*=0.93) (Figure 6C). Both the number of unique clonal families, as well as the number of variants per family, were not significantly different between patients and healthy controls, further confirming that there was no difference in the repertoire breadth of plasmablast responses between the two cohorts (data not shown). Since the plasmablast responses were not clonally restricted in patients, but as diverse as that observed in healthy controls, we conclude that this likely means that the plasmablast response originated from a diverse pool of MBCs rather than from the small number of MBCs present in peripheral blood. This suggests that tissue-resident memory B cells are able to survive Rituximab-mediated depletion, likely in lymphoid organs (270), despite circulating memory cells being fully depleted.

Because pemphigus has been associated with a bias towards serum IgG1 and IgG4 (145), we also characterized the isotype usage in the plasmablast responses. Overall, there was a similar distribution of isotypes comparing patients and healthy controls, with no IgG4 detected in either cohort (Figure 6D). Although the distribution of V_H gene was similar between healthy controls and patients (Figure 6E), patients had a bias of V_H1 gene usage in clonally expanded populations that was not observed in healthy controls (Figure 6F). Overall, sequence analysis shows that plasmablasts likely originate from a diverse pool of memory cells in both patients and healthy controls, and suggests that there is little impact of Rituximab or autoimmune disease on the quality and repertoire of the plasmablast response.

DISCUSSION

In this study, we observed robust influenza vaccine responses in Rituximab-treated AIBD patients, comparable to those mounted in healthy controls. To our knowledge, this is the first study to assess these responses in Rituximab-treated AIBD patients. AIBD patients are typically given Rituximab with a tapering course of low-dose systemic corticosteroids, which gives us an opportunity to study vaccine responses in patients that received B cell ablative therapy, but are not taking additional immunosuppressants at the time of vaccination. This is different from other Rituximab-treated patient populations, who are typically prescribed immunosuppressants or chemotherapy both during and after Rituximab treatment. Additionally, underlying autoimmune disease may differentially impact vaccine responses after Rituximab treatment. For example, AIBD has well-defined antigenic targets confined to the skin, which is different from the complexity of other systemic B-cell mediated diseases such as RA (240), or lymphoma (280). These differences may explain the robust vaccine responses observed in this study, which differs from previous reports suggesting that Rituximab impairs influenza vaccine responses (225-229).

The majority of patients enrolled in this study had a repopulated B cell compartment, with normal total B cell numbers in peripheral blood. However, patients had significantly less peripheral MBCs than healthy controls. Moreover, while almost all healthy controls had influenza-specific MBCs prior to vaccination, these cells were undetectable in all but 3 of the Rituximab-treated patients. Because these 3 patients had not been vaccinated within the last 3 years, it is likely that these cells are a result of a recent infection, or MBCs that survived depletion. Surprisingly, despite the impaired memory

compartment, patients retained their ability to mount a recall response to the influenza vaccine. This was evident by potent plasmablast responses of comparable magnitude, kinetics, and immunoglobulin isotype to those observed in healthy controls, as well as normal expansion of influenza-specific MBCs after vaccination. Additionally, patients mounted serological responses similar in magnitude and quality to healthy controls. Importantly, the patients that had received multiple cycles of Rituximab, displayed reduced responses (Figure 3), suggesting that multiple cycles might provide a more complete depletion of memory B cells in tissues. One patient failed to mount a plasmablast response altogether, despite having a normal number of peripheral B cells at 16 months post-Rituximab and not taking any additional immunosuppressants. Interestingly, this patient had previously received 2 previous rounds of Rituximab. This finding is supported by a previous study in which patients who had previously received maintenance Rituximab monotherapy to treat neuromyelitis optica appeared to have blunted vaccine responses (227), suggesting that repeat dosages or Rituximab may be associated with poor influenza vaccine efficacy. It is possible that the repeat treatments affected a more complete depletion, specifically in lymphoid tissues, which could explain the lack of plasmablast response. Additional studies of the effect of multiple depletions on tissue-resident MBCs and subsequent vaccine responses may be warranted in order to better optimize Rituximab dosages and schedules for patients, to further determine the optimal therapy to treat autoimmune disorders.

Repertoire analysis of plasmablast responses in both patients and healthy controls revealed highly mutated immunoglobulin sequences, further confirming the memory origins of these responses. Additionally, patients and healthy controls had similar

frequencies of clonal expansions in their plasmablast responses, which suggests that these cells originated from a diverse pool of memory cells, rather than from a rapid expansion of the small number of peripheral blood MBCs. Based on a previous observation in splenectomized immune thrombocytopenia patients that revealed the presence of persisting antigen-specific MBCs in the spleen (44, 270), we believe it is likely that this diverse pool of cells survives in tissues. Additionally, a recent study showed that tissue-resident MBCs in a mouse model are enriched for broadly-neutralizing influenza-specific antibodies compared to those in circulation (46). If influenza vaccine responses in patients are originating from a diverse pool of tissue-resident MBCs, this mouse study could potentially explain how patients are able to mount a protective response to vaccination despite the low number of MBCs.

Despite previous observations that both autoimmune disease pathogenesis (145, 281) and Rituximab therapy (197) may impact the overall immunoglobulin diversity, we observed no unique mutation frequency, CDR3 length, or isotype frequency in the plasmablast population of AIBD patients compared to healthy controls. Although there was no difference in overall V_H gene usage between patients and healthy controls, patients did have a bias in V_H1 gene usage in clonal expansions. This may be an interesting finding considering recent reports which have observed a bias of V_H1-69 gene usage in broadly neutralizing antibodies (219), as well as a potential role for V_H1-46 gene usage in pemphigus pathogenesis (150). Future experiments with monoclonal antibodies selected from these clonal expansions may reveal subtle differences in the quality of antibody responses comparing healthy controls and Rituximab-treated AIBD patients.

Previous observations have suggested that some B cells survive depletion after Rituximab-therapy within secondary lymphoid organs (185, 186, 231, 277, 282-284). However, there are very few studies of this in humans, and it is often difficult to interpret the data from these studies due to low sample numbers and patient-to-patient variability. To our knowledge, there is only one report of human antigen-specific MBCs surviving in the spleen after Rituximab depletion (270). Several mechanisms underlying the persistence of B cells in tissues have been proposed, including resistance of activated B cells to Rituximab-mediated depletion (231, 285), impact of Fc glycosylation on Rituximab and its resulting interaction with Fc receptors on accessory cells (286), inflammatory or cytokine milieu allowing for B cells to survive (287, 288), or possibly the inability of Rituximab to fully access tissues to deplete B cells (187). It is also possible that CD20 expression is downregulated in B cells residing in tissues. Although a large number of studies have shown that memory B cells in the spleen (287), bone marrow (284), human blood and lymph node (289) general co-express CD19 and CD20 at high levels, we cannot out rule the possibility that a small number of memory B cells downregulate CD20, similar to plasma cells (65). It is also possible that a combination of several of the proposed mechanisms work in concert to impact B cell depletion in tissues. Consistent with these findings, our data suggests that tissue-resident MBCs survive Rituximab-mediated depletion and maintain the ability to initiate recall responses upon antigenic challenge. While this may be beneficial for vaccine responses, it is possible that surviving MBCs may also paradoxically act as a source for pathogenic responses, causing relapse in autoimmune disease. In fact, previous reports have detected persisting clones of autoimmune memory B cells after Rituximab treatment, both in pemphigus and anti-MAG neuropathy (193,

197). Given that almost all diseases currently treated with Rituximab depletion have a tendency to relapse, including other autoimmune diseases such as RA and SLE, as well as B cell lymphomas, it is critically important to understand how tissue-resident MBCs survive depletion and their role in both protective and pathogenic recall responses. These findings indicate that future analyses of immunological memory and the development of new generations of antibody-based B cell depletion strategies should focus on ways to optimize the depletion of MBCs in tissues as a way to minimize relapsing disease. These new strategies may include improving the current Rituximab therapy by modulating its Fc domain to improve its effector function (290), or the use of CD19 as a target for depletion of B cells (291)

Overall, these data show that although the patients lacked pre-existing, antigen-specific MBCs in circulation prior to vaccination, they were uniformly able to respond to vaccination, with a response of similar magnitude, quality and repertoire breadth as that found in healthy controls. This suggests that a significant pool of non-circulating MBCs remain present in lymphoid tissues after depletion, and can serve to seed these responses. These findings have important implications for vaccination strategies for AIBD patients and other Rituximab-treated patients, and contribute to our understanding of memory B cell homeostasis and survival.

MATERIALS AND METHODS

Study design. Subjects received a single dose of commercially available trivalent, inactivated influenza vaccine administered intramuscularly. For the 2014/15 influenza season, vaccine (Flucelvax, Novartis) contained influenza strains: A/Brisbane/10/2010 (H1N1, A/California/7/2009-like virus), NYMC X-223A (H3N2, A/Victoria/361/2011-like virus), and B/Massachusetts/2/2012. During the 2015/16 influenza season, vaccine (Fluvirin, Novartis) contained influenza strains: A/Christchurch/16/2010, NIB-74 (H1N1, A/California/7/2009 pdm09-like virus), NIB-88 (H3N2, A/Switzerland/9715293/2013-like virus), and B/Phuket/3073/2013. Blood sample were collected in sodium citrate CPT tubes (BD Vacutainer) at baseline, Day 7 (± 1 day), and Day 28 (± 5 days) post-vaccination. Plasma samples were collected and stored at -80°C. PBMCs were isolated and washed with phosphate-buffered saline (PBS)/2% fetal bovine serum (FBS). Cells were used fresh or were frozen in FBS/10% dimethyl sulfoxide. Frozen PBMCs were stored in liquid nitrogen until assayed.

Flow cytometry analysis and single-cell sorting. Immunophenotyping of circulating B cell subpopulations was performed on fresh whole blood stained with the following mAbs, appropriately titrated: CD19-FITC (BD, clone HIB19), CD24-PerCPCy5.5 (Biolegend, clone ML5), CD3-PacificBlue (BD, clone SP34-2), CD38-PE (BD, clone HIT2), CD20-PECy7 (BD, L27), IgD-PECy7 (Biolegend, clone IA6-2), and CD27-APC (eBiosciences, clone O323), followed by lysis of erythrocytes (BD FACS lysis solution). 100,000 events were acquired on a BD FACSCantoII flow cytometer, and analyzed using FlowJo software. Plasmablasts were single-cell sorted into 96-well PCR plates containing hypotonic catch

buffer with RNase inhibitor (Promega) using a FACSAriaII, and were frozen immediately on dry ice, as previously described (49). Additional cells were bulk-sorted into RPMI supplemented with penicillin/streptomycin, L-glutamine, and 10% FBS (R10).

Total B cell counts. Total lymphocyte counts for patient enrolled in 2014/15 were determined by Complete Blood Counts routinely done during their visit to the clinic. Total lymphocyte counts for 2014/15 healthy controls were estimated using the average number of peripheral lymphocytes, as reported by the Mayo Clinic (292). TruCount tubes (BD) were used during the 2015/16 influenza season to count B cells. 50 μL of blood was added to TruCount tubes and incubated for 20 minutes with CD45-PE (Biolegend, clone HI30) and CD3-Pacific Blue (BD). 450 μL of FACs lysis solution (BD) was added and mixture was incubated for 20 minutes before running sample on a BD FACSCantoII, and analyzed using FlowJo software.

ELISPOT assay. ELISPOT was performed to enumerate influenza-specific plasmablasts present in both PBMC samples and bulk-sorted plasmablasts. 96-well ELISPOT assay filter plates (Millipore) were coated overnight with either influenza vaccine (1:20, Novartis) or polyvalent goat anti-human Ig (10 μg/mL, Jackson ImmunoResearch) in PBS. Plates were washed and blocked by incubation with R10 at 37°C for 2 hours. Freshly isolated PBMCs were added to the plates in a dilution series starting at $5x10^5$ cells and incubated overnight at 37°C. Plates were washed with PBS, followed by PBS/0.05% Tween, and then incubated with biotinylated anti-human IgG, IgA, or IgM antibody (Invitrogen) at room temperature for 90 minutes. After washing, plates were incubated with

avidin D-horseradish peroxidase conjugate (Vector laboratories) and developed using 3-amino-9-ethyl-carbazole substrate (Sigma). Plates were scanned and analyzed using an automated ELISPOT counter (CTL, Cellular Technologies).

Memory B cell assay. Antigen-specific memory B cells were detected essentially as previously described (278). In brief, PBMCs were cultured at $1x10^6$ cells per mL of R10 supplemented with 50 μM of beta-mercaptoethanol (Sigma) and polyclonally stimulated with pokeweed mitogen extract (1 μg/mL, Sigma), phosphothiolated CpG ODN-2006 (6 μg/mL, Invivogen), and *Staphylococcus aureus* Cowan (1:10,000, Sigma) for 6 days. After *in vitro* stimulation, total and influenza -specific IgG secreting cells were quantified by ELISPOT assay, as described above.

Hemagglutination inhibition (HAI) assay. HAI assay was done as per World Health Organization criteria (293). Briefly, plasma samples were treated with receptor destroying enzyme (Denka Seiken) and heat inactivated. Samples were serially diluted in PBS in a 96-well v-bottom plate with 8 HAU of live, egg-grown virus added to the well. Viruses were generously provided by A. Ellebedy (Emory University, Atlanta), A. Lowen (Emory University, Atlanta), and S. Gangappa (CDC, Atlanta). After a 30-minute incubation at room temperature, 50 μL of 0.5% turkey RBCs (Lampire) suspended in PBS was added to each well. After a 30-minute incubation at room temperature, HAI titers were determined based on the final dilution for which agglutination inhibition was observed.

Microneutralization (MN) assay. MN assays were performed as previously described by the WHO (294). Briefly, plasma was heat-inactivated and serially diluted in DMEM with 10% BSA, 2% HEPES, and penicillin/streptomycin. Virus diluted at 100x TCID50 per 50 μL, as determined by the Reed-Muench method, was added and the mixture was incubated at 37°C for 1 hour. MDCK cells (ATCC), diluted at $1.5x10^5$ cells/mL, were added to the plate and incubated for another 20 hours at 37°C. Plate was washed with PBS and fixed with cold 80% acetone in PBS. Plates were washed with PBS/Tween20 and incubated with anti-influenza NP monoclonal antibody (Millipore), diluted 1:1000 in 5% milk, for 1 hour at room temperature. After washing, HRP-conjugated goat anti-mouse IgG (Kirkegaard and Perry Laboratories) diluted at 1:2000 in milk was added, and incubated for another hour at room temperature. After wash, plates were developed for 8-12 minutes using OPD tablets (Sigma #P8787) diluted in citrate buffer (Sigma #P4560). Absorbance readings were measured at OD490 on a microplate reader. Microneutralization titers were reported as the serum dilution corresponding to 50% neutralization.

Repertoire analysis. Identification of antibody variable region genes were done essentially as previously described (49, 246). In brief, single-cell cDNA was synthesized from sorted plasmablasts using random hexamers (Sensiscript, Qiagen). Ig heavy chain rearrangements were then amplified by nested PCR (HotStarTaq Plus Master Mix, Qiagen) using primer cocktails specific for all V gene families and constant domains at a concentration of 200 nM per primer (247). Sense primers used in the second round of nested PCR were modified by fusing the 5' end of each primer to the M13R sequence (5'-AACAGCTATGACCATG-3') to facilitate subsequent sequencing. V, D, and J genes were

identified and analyzed using the ImMunoGeneTics (IMGT) database as a reference. Somatic hypermutation levels in the V_H genes represent the number of mutations in the amplicon (FR1 through CDR3) relative to the closest germline sequence matched in the IMGT database. Clonal expansions were determined by sequence alignments of rearrangements with matching V and J gene usage, where cells with identical junctional diversity were grouped as part of the same clonal expansion.

Statistical analysis. Data was collected and graphed using GraphPad Prism software. A Mann-Whitney *U* test, Wilcoxon matched-pairs test, or 1-way ANOVA Kruskal-Wallis test was used to determine statistical significance where appropriate. Seroprotection was analyzed using a Fisher exact test. *P* values less than 0.05 (two-sided) were considered statistically significant.

Study approval. Patient volunteers were informed of the study during routine clinical visits at the Department of Dermatology and enrolled based on interest in receiving seasonal influenza vaccination during the 2014/15 or 2015/16 influenza seasons. Patient inclusion criteria included age ≥18 years old and treatment with Rituximab for AIBD within the last 24 months. Demographically-matched healthy volunteers were recruited from staff and students receiving the influenza vaccination at Emory University. Written informed consent was obtained from all participants. Exclusion criteria included prior vaccination within the current season as well as any condition that, in the opinion of the investigator, would place the subject at risk of injury from participation. This study was approved by the Emory Institutional Review Board (IRB#00069980).

SUPPLEMENTARY MATERIALS AND METHODS

Memory B cell assay. An alternative mitogen cocktail was used essentially as previously described (244). Briefly, PBMCs were cultured at $1X10^6$ cells per mL of R10 supplemented with 50 μM of beta-mercaptomethanol (Sigma) containing R848 (1 μg/mL, Invivogen) and human-IL2 (10 μg/mL, Biolegend) for 3 days. Total and influenza vaccine-specific IgG secreting cells were quantified by ELISPOT assay.

Desmoglein-specific ELISA. Anti-Dsg1 and anti-Dsg3 serum autoantibody titers were determined with an ELISA test (MESACUP DSG1 & DSG3 ELISA test system, MBL International Corporation) using patient sera sampled during routine clinical visits. 1:100 diluted sera samples were tested according to manufacturer's instructions. Results are reported as Units/mL of sera, as determined by negative and positive calibrators supplied by the manufacturer.

Statistical analysis. Seroprotection was analyzed using a Fisher exact test. *P* values less than 0.05 were considered statistically significant.

AUTHOR CONTRIBUTION

Contribution: A.C. carried out experiments, analyzed the data, and wrote the manuscript. B.B. provided clinical support of the study. R.K., L.P., and Y.K. contributed to sample collection and analysis, critical discussion, and editing of this manuscript. R.F. and J.W. conceived the research, oversaw the experiments and data analysis, and wrote and approved the final manuscript.

Conflict-of-interest: The authors have declared that no conflict of interest exists.

Correspondence: Jens Wrammert, Department of Pediatrics; Division of Infection Disease; Emory Vaccine Center, School of Medicine, Emory University, 1760 Haygood Drive, HSRB Building E480, Atlanta, GA 30322; email: jwramme@emory.edu.

ACKNOWLEDGEMENTS

We thank R. Karaffa and S. Durham at the Emory School of Medicine flow cytometry core, and A. Rae at Emory Pediatric's flow cytometry core for their technical assistance with cell sorting experiments. We would also like to thank A. Ellebedy, A. Lowen, and S. Gangappa for providing the influenza virus strains for our experiment. We also thank the Dermatology Foundation for support of our work through a Career Development Award to R.F. This study was supported by the National Institutes of Health (U19 AI057266) and Centers of Excellence of Influenza Research and Surveillance (HHSN 255200700006Z).

FIGURES AND LEGENDS

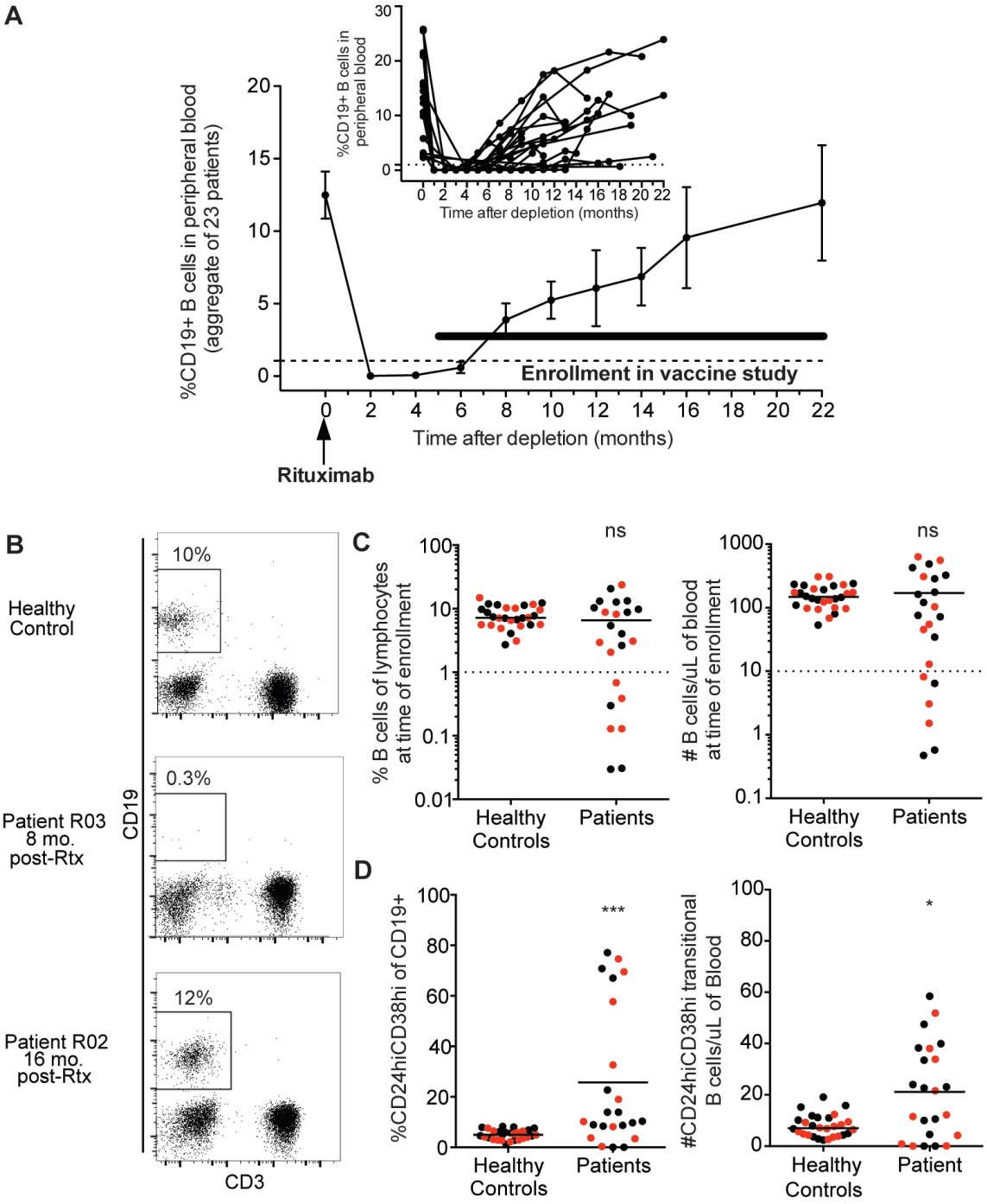

FIGURE 1. Reconstitution of the B cell compartment after Rituximab treatment.

(A) Average kinetics of peripheral blood CD19+ B cells after Rituximab therapy. Dotted line represents depletion at 1% B cells of total lymphocytes. Graph in the upper left part of the panel depicts B cell depletion kinetics for each individual patient. (B) Representative flow plots of CD3-CD19+ peripheral B cells, gated on lymphocytes, at time of enrollment. (C) Overall, median frequency and total counts of B cells was comparable between healthy controls and patients. (D) Median frequency and total number of transitional B cells, defined as CD24hiCD38hi, were significantly higher in patients than in healthy controls. Mann-Whitney U test was used to analyze data. * = $P \leq 0.05$; *** = $P \leq 0.001$. Black circles represent data from 2014/15 influenza season; red circles represent data from 2015/16 influenza season.

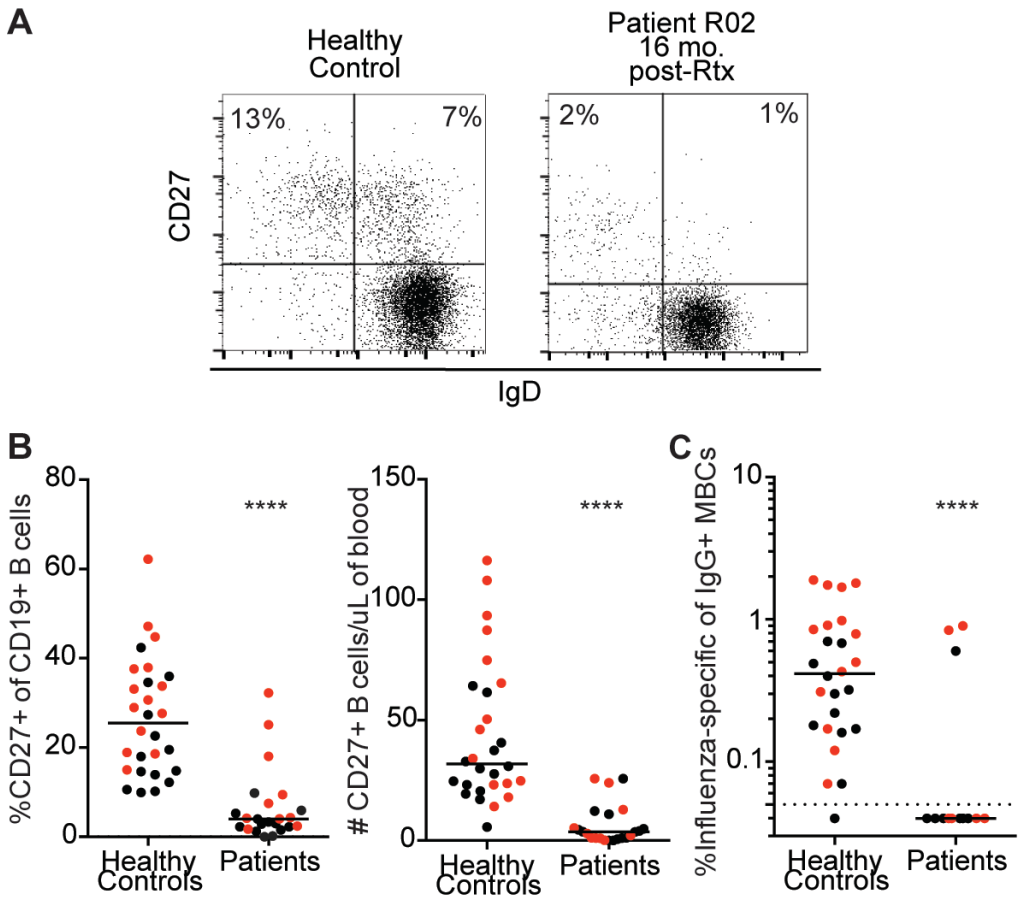

FIGURE 2. Lack of memory B cells (MBCs) in peripheral blood in Rituximab-treated patients.

(A) Representative flow cytometry plots showing CD27+ MBCs, gated on CD19+ lymphocytes, at time of enrollment in a healthy control and a patient. (B) Median frequency and total number of MBCs were significantly lower in patients than in healthy controls. (C) Antigen-specific MBCs were stimulated in vitro and detected using an ELISPOT-based assay, as previously described (39, 41). Median frequency of influenza-specific IgG+ MBCs was significantly lower in patients than in healthy controls prior to vaccination. Mann-Whitney U test was used to analyze data. **** = P≤0.0001. Black circles represent data from 2014/15 influenza season; red circles represent data from 2015/16 influenza season.

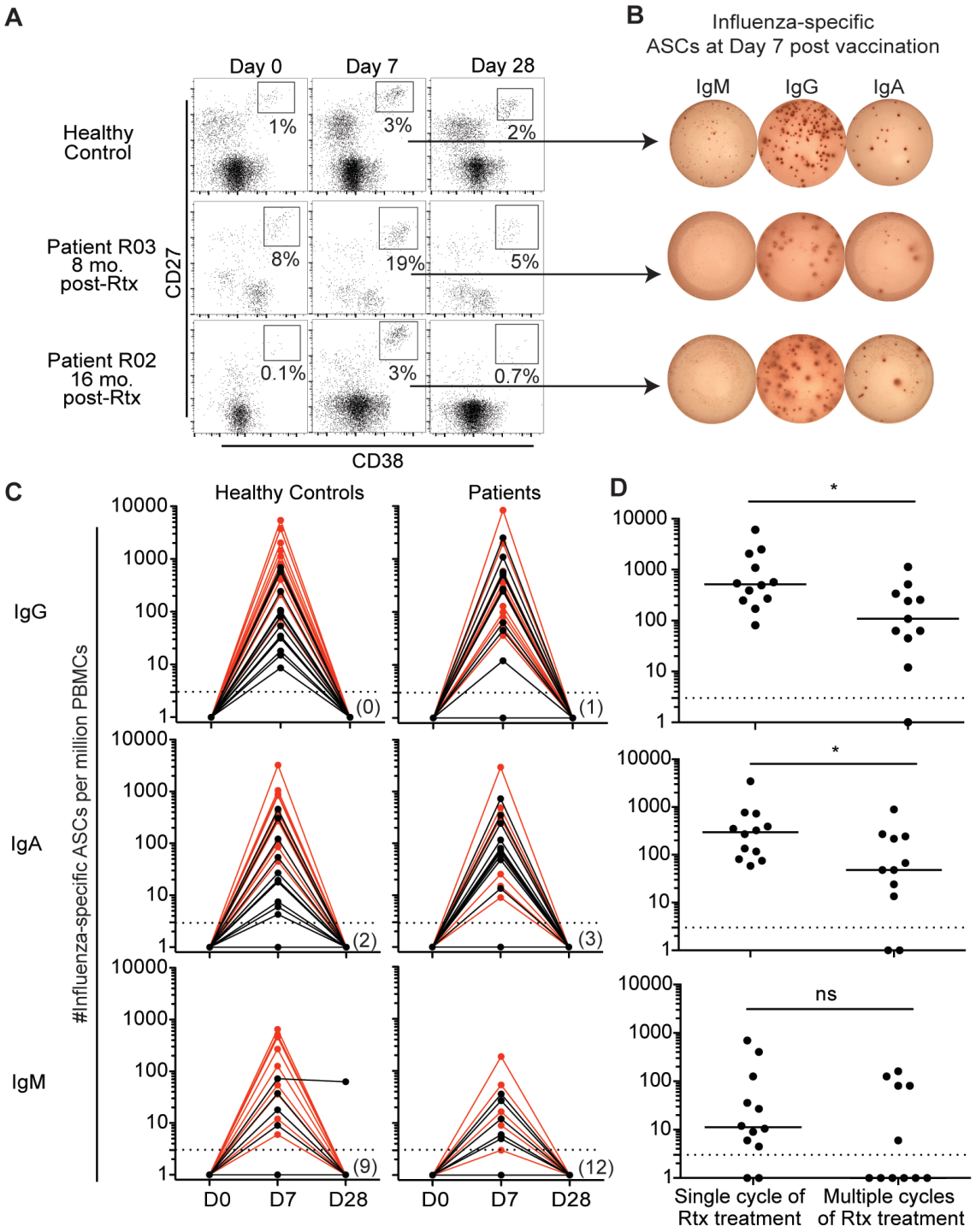
A
Day 0
Day 7
Day 28
Healthy Control
Patient R03 8 mo. post-Rtx
Patient R02 16 mo. post-Rtx
1%
3%
2%
8%
19%
5%
0.1%
3%
0.7%
CD27
CD38
B
Influenza-specific ASCs at Day 7 post vaccination
IgM
IgG
IgA
C
Healthy Controls
Patients
IgG
IgA
IgM
#Influenza-specific ASCs per million PBMCs
10000
1000
100
10
1
(0)
(1)
(2)
(3)
(9)
(12)
D0
D7
D28
D
*
*
ns
Single cycle of Rtx treatment
Multiple cycles of Rtx treatment

FIGURE 3. Robust vaccine-induced plasmablast responses likely originating from memory recall responses.

(A) Representative flow cytometry plots showing transient expansion of CD27hiCD38hi plasmablasts, gated on CD19+ B cells, induced at Day 7 post-vaccination. (B) Representative ELISPOT of influenza-specific plasmablasts at Day 7 post-vaccination. (C) Influenza-specific antibody secreting cells (ASCs) were measured by ELISPOT at Day 0, 7, and 28 after vaccination. Average number of influenza-specific ASCs per million PBMCs were plotted by IgG, IgA, and IgM isotypes. Dotted line represents limit of detection of ELISPOT assay. Number in parentheses represents the number of vaccinees that did not have a detectable influenza-specific plasmablast response. (D) Patients who had no history of Rituximab treatment prior to enrollment had a significantly higher IgG and IgA plasmablast response to vaccination compared to patients who had received multiple cycles of Rituximab (range: 2-4). Black lines represent data from 2014/15 influenza season; red lines represent data from 2015/16 influenza season. Mann-Whitney U test was used to analyze data. * = $P \leq 0.05$.

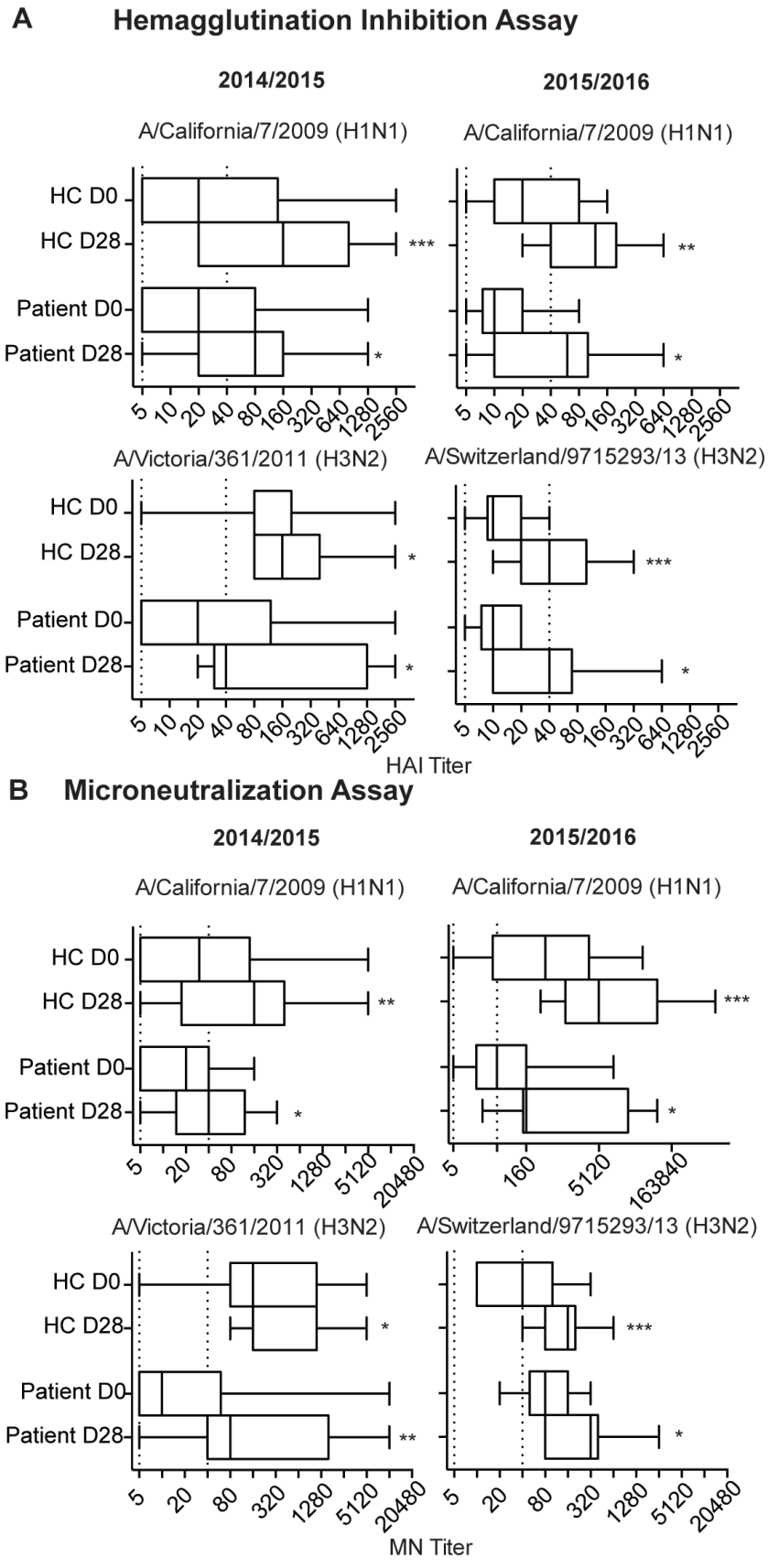
A
Hemagglutination Inhibition Assay
2014/2015
2015/2016
A/California/7/2009 (H1N1)
A/California/7/2009 (H1N1)
HC D0
HC D28
Patient D0
Patient D28
***
**
*
5 10 20 40 80 160 320 640 1280 2560
A/Victoria/361/2011 (H3N2)
A/Switzerland/9715293/13 (H3N2)
HAI Titer
B
Microneutralization Assay
2014/2015
2015/2016
A/California/7/2009 (H1N1)
A/California/7/2009 (H1N1)
5 20 80 320 1280 5120 20480
5 160 5120 163840
A/Victoria/361/2011 (H3N2)
A/Switzerland/9715293/13 (H3N2)
MN Titer

FIGURE 4. Comparable serological responses to vaccination in patients and healthy controls.

(A) Influenza-specific serum antibody titers determined by HAI. HAI titers were plotted, comparing serum samples from Day 0 to Day 28 post-vaccination. Dotted line represents limit of detection of assay at an HAI titer of 5, and seroprotection at an HAI titer of 40. (B) Influenza-neutralizing serum antibody titers determined by microneutralization assay. Titers graphed as a box and whisker plot. Horizontal line within the box indicates median, while width of the box shows interquartile range. Whiskers show highest and lowest titer values measured. The experiments were performed in duplicate and reproduced twice. One representative experiment in shown. Wilcoxon paired T-test was used to compare Day 0 to Day 28 post-vaccination within cohorts. *** = $P \leq 0.005$; ** = $P \leq 0.01$; * = $P \leq 0.05$.

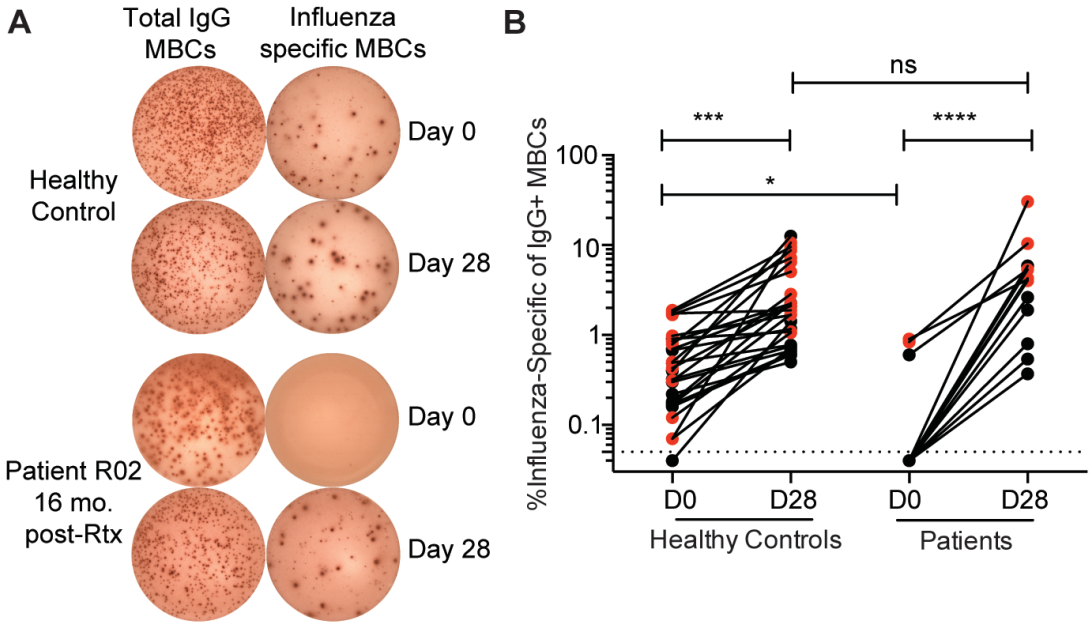

FIGURE 5. Previous Rituximab depletion has no impact on the generation of new influenza-specific memory B cells.

Frequency of influenza-vaccine specific MBCs were measured at baseline and Day 28 post-vaccination. (A) Representative memory B cell assay. PBMCs were stimulated with a mitogen cocktail, and frequency of antigen-specific IgG+ MBCs of total IgG+ MBCs were determined by ELISPOT. (B) Frequency of influenza-specific IgG+ MBCs at Day 0 and Day 28 post-vaccination. Only vaccinees that responded to the polyclonal stimulation were included. One-way ANOVA was used to analyze data. *** = P≤0.001; * = P≤0.05. Black circles represent data from 2014/15 influenza season; red circles represent data from 2015/16 influenza season.

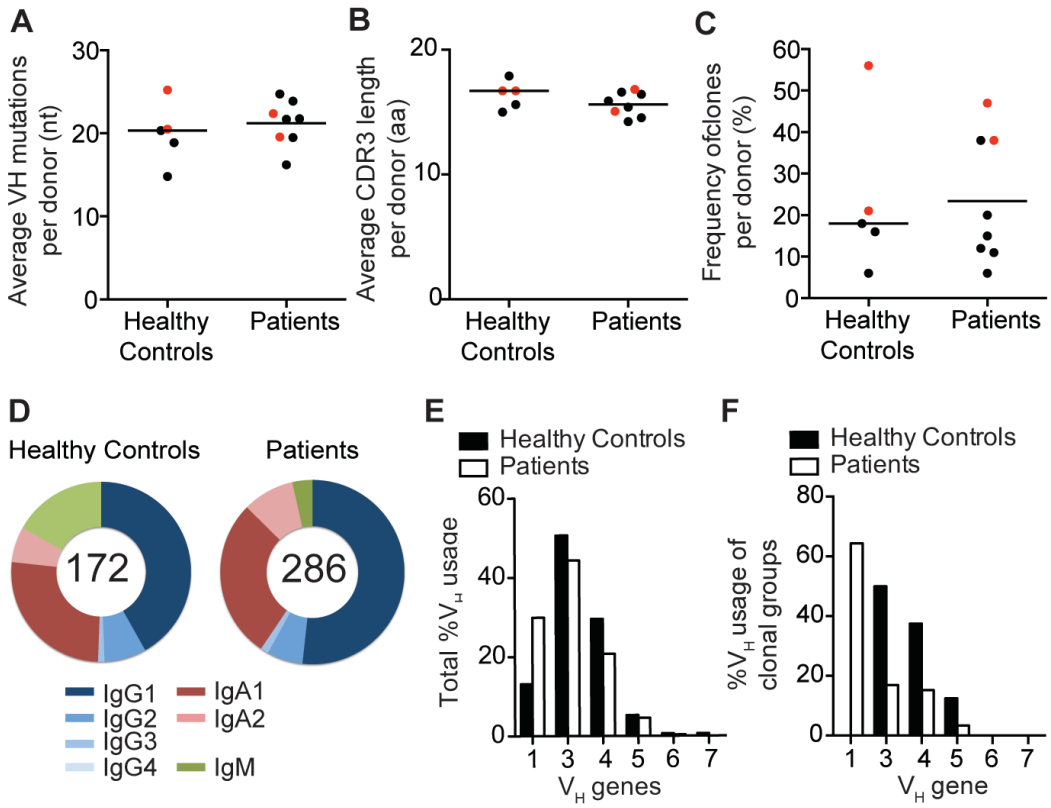

FIGURE 6. Vaccine-induced plasmablasts display comparable repertoire breadth in patients and healthy controls.

Variable genes from plasmablasts induced by the seasonal influenza vaccine were amplified by single-cell PCR and analyzed for (A) number of somatic mutations, (B) CDR3 length, and (C) clonality (shared identical VH gene, JH gene, and CDR3 junction) of class-switched sequences. Each dot represents one individual donor, averaged from 22-46 sequences. (D) Frequency of isotypes in patients and healthy controls. A total of 172 sequences were analyzed from 5 healthy controls, and 286 sequences from 8 patients. (E) Overall VH gene usage of class-switched sequences, reported as a frequency of total sequences analyzed from each cohort. (F) VH gene usage of antibodies in clonal groups reported as a frequency of total number of antibodies involved in clonal groups identified. Black circles represent data from 2014/15 influenza season; red circles represent data from 2015/16 influenza season.

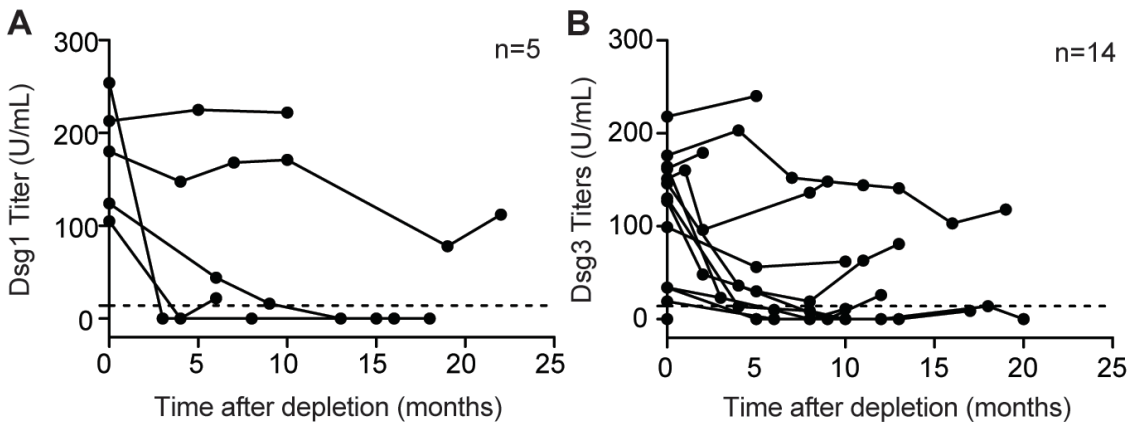

FIGURES S1. Anti-desmoglein autoantibody titers decrease after Rituximab treatment.

(A) Anti-desmoglein-1 antibody titers (major target in PF) in 5 PF patients and (B) anti-desmoglein-3 antibody titers (major target in PV) in 14 PV patients were determined by ELISA. Dotted lines represent the value at which titers were considered to be positive, as recommended by the manufacturer (Dsg1 = 18 U/mL, Dsg3 = 19 U/mL). Samples were tested during routine clinical visits. Generally, serum titers decreased after Rituximab treatment, although several patients sustained high levels of serum autoantibody titers. However, all patients showed improved clinical symptoms in response to Rituximab treatment.

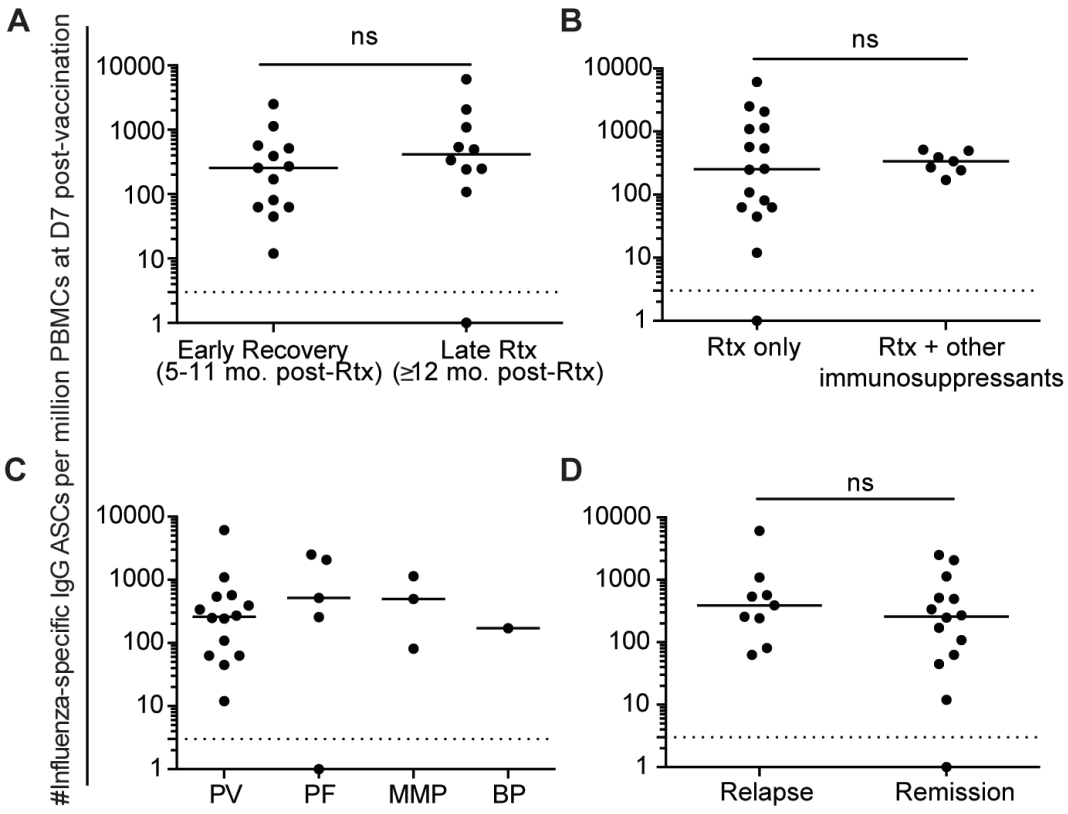

FIGURE S2. Impact of AIBD disease and treatment on plasmablast responses to influenza vaccine.

(A) There was no difference in magnitudes of plasmablast responses to influenza comparing patients who were early in recovery from Rituximab treatment (5-11 months post-Rtx) to patients late in recovery (≥12 months post-Rtx (B) No significant difference was observed when comparing patients who received the vaccine while treated with Rituximab as a stand-alone therapy compared to patients who were prescribed additional immunosuppressants. (C) There appears to be no major differences in plasmablast responses based on various types of AIBD disease. (D) Responses were also compared between patients who experienced disease and patients who stayed in remission (follow-up time: 1-2 years). No significant different was observed. Mann-Whitney U test was used to compare patients where appropriate.

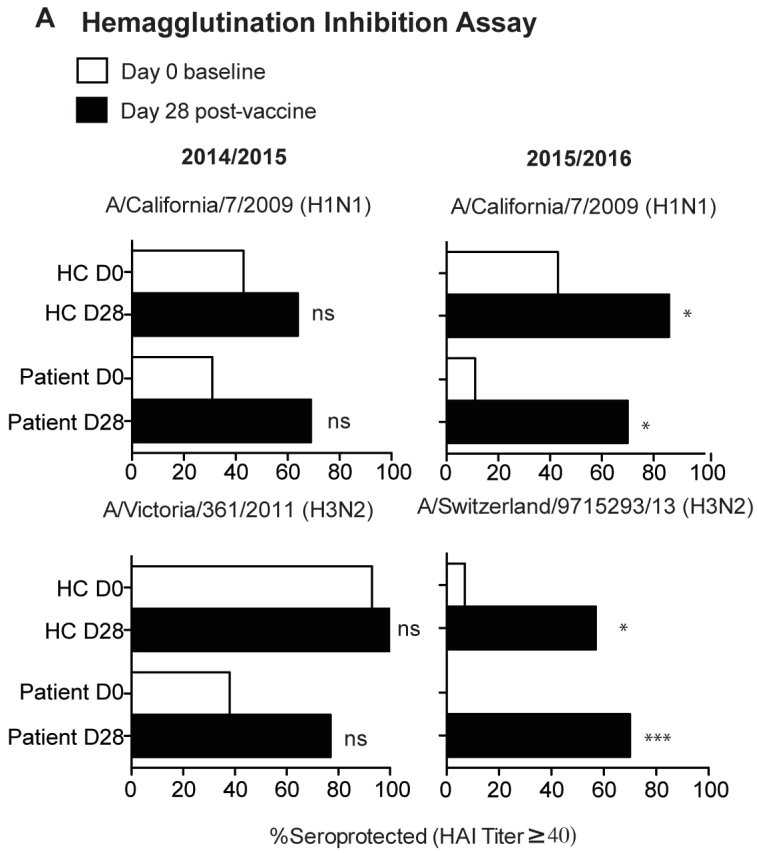
A Hemagglutination Inhibition Assay
Day 0 baseline
Day 28 post-vaccine
2014/2015
2015/2016
A/California/7/2009 (H1N1)
A/California/7/2009 (H1N1)
HC D0
HC D28
Patient D0
Patient D28
ns
*
ns
*
0 20 40 60 80 100
A/Victoria/361/2011 (H3N2)
A/Switzerland/9715293/13 (H3N2)
HC D0
HC D28
Patient D0
Patient D28
ns
*
ns
***
0 20 40 60 80 100
%Seroprotected (HAI Titer ≥40)

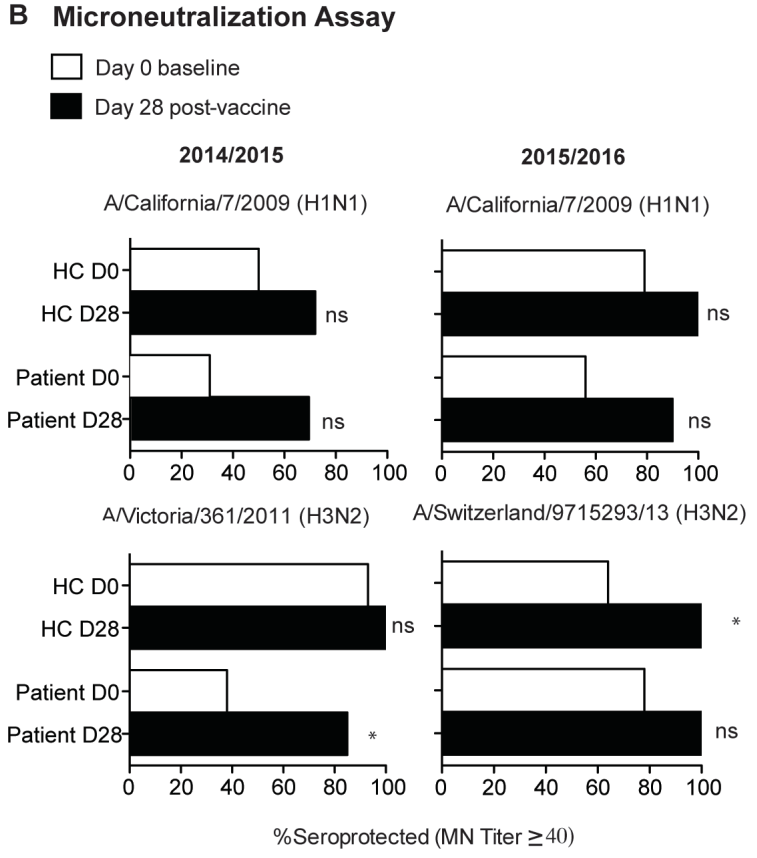
B Microneutralization Assay
Day 0 baseline
Day 28 post-vaccine
2014/2015
2015/2016
A/California/7/2009 (H1N1)
A/California/7/2009 (H1N1)
HC D0
HC D28
Patient D0
Patient D28
ns
ns
ns
ns
0 20 40 60 80 100
A/Victoria/361/2011 (H3N2)
A/Switzerland/9715293/13 (H3N2)
HC D0
HC D28
Patient D0
Patient D28
ns
*
*
ns
0 20 40 60 80 100
%Seroprotected (MN Titer ≥40)

FIGURE S3. Comparable frequencies of seroprotection in patients and healthy controls.

(A) Percentage of seroprotected individuals, as determined by HAI titers ≥40, after one dose of vaccination. (B) Percentage of seroprotected individuals, as determined by MN titers ≥40. A Fisher exact test was used to compare seroprotection at Day 0 to Day 28 post-vaccination. *** = $P<0.005$; * = $P\leq0.05$; ns = not significant.

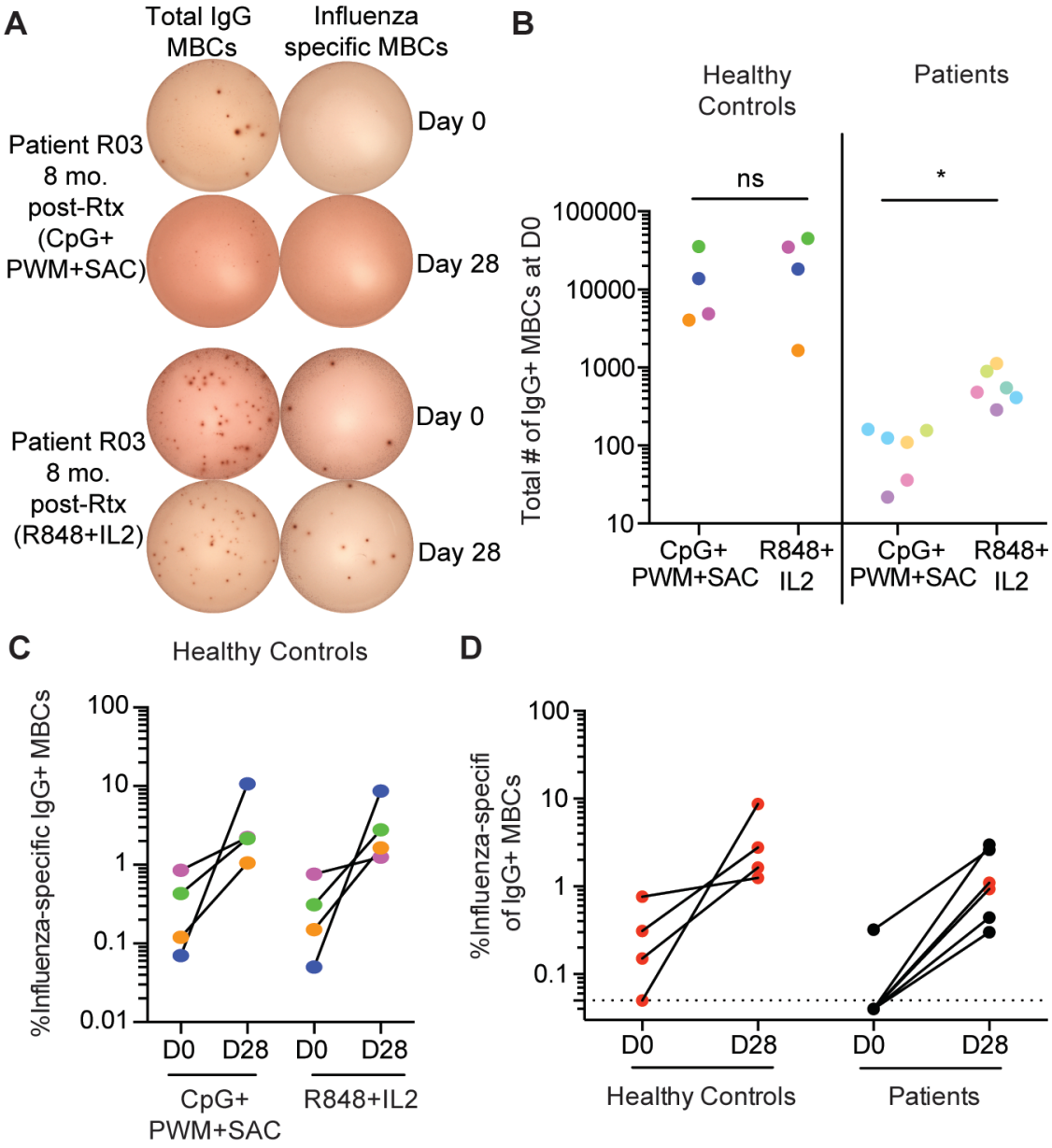
A
Total IgG MBCs
Influenza specific MBCs
Patient R03 8 mo. post-Rtx (CpG+ PWM+SAC)
Day 0
Day 28
Patient R03 8 mo. post-Rtx (R848+IL2)
Day 0
Day 28
B
Healthy Controls
Patients
ns
*
Total # of IgG+ MBCs at D0
100000
10000
1000
100
10
CpG+ PWM+SAC
R848+ IL2
CpG+ PWM+SAC
R848+ IL2
C
Healthy Controls
%Influenza-specific IgG+ MBCs
100
10
1
0.1
0.01
D0
D28
D0
D28
CpG+ PWM+SAC
R848+IL2
D
%Influenza-specifi of IgG+ MBCs
100
10
1
0.1
D0
D28
D0
D28
Healthy Controls
Patients

FIGURE S4. R848+IL2 mitogen cocktail is an effective alternative to assess antigen-specific memory B cells.

(A) Representative ELISPOT data of a patient who failed stimulation using a mitogen cocktail composed of CpG, PWM, and SAC, but responded sufficiently to R848 with IL2. (B) Total numbers of IgG+ memory B cells detected at Day 0 using the different mitogen cocktails. Healthy controls, with high numbers of memory B cells, showed comparable levels of stimulation regardless of mitogens used. However, patients with low number of memory B cells who failed stimulation with CpG/PWM/SAC had significantly increased stimulation with R848/IL2 mitogens. Each color circle represents one individual vaccinee. Wilcoxon-paired T-test was used to compare groups. * = $P \leq 0.05$. (C) The frequency of antigen-specific MBCs measured in healthy controls did not differ when using either method of stimulation. (D) Frequency of vaccine-specific IgG memory B cells at day 0 and day 28 post-vaccination from vaccinees stimulated using the R848/IL2 mitogen cocktail. Black circles represent data from 2014/15 influenza season; red circles represent data from 2015/16 influenza season.

TABLES

TABLE 1. Characteristics of subjects at time of enrollment.

	Patients *n*=23	Healthy controls *n*=28
Gender (M/F)	8/15	9/19
Age in years, median (range)	51 (28-73)	45 (22-70)
Ethnicity		
Caucasian	14	15
African American	7	12
Other	2	1
Received influenza vaccination during 2011-2013	16*	20
Enrollment		
2014/15 flu season	13	14
2015/16 flu season	10	14
Time since Rituximab dose in months, median (range)	11 (5-24)	
5-11 months post-Rituximab (early)	13	
At least 12 months post-Rituximab (late)	10	
No. of previous Rituximab cycles		
0	12	
1	7	
2	2	
4	2	
Other medications at time of vaccination		
None	16	
Cellcept	3	
Azathioprine	2	
Prednisone	1	
Prednisone + Cellcept	1	
Disease type		
Pemphigus Vulgaris (PV)	14	
Pemphigus Foliaceus (115)	5	
Mucous Membrane Pemphigoid (MMP)	3	
Bullous Pemphigoid (BP)	1	

*Four patients were unable to recall vaccination history

TABLE SI. Characteristics of subjects used for plasmablast repertoire analysis

	Patients *n*=8	Healthy controls *n*=5
Gender (M/F)	3/5	2/3
Age in years, median (range)	54 (28-74)	42 (26-67)
Ethnicity		
Caucasian	2	4
African American	5	1
Other	1	0
Received influenza vaccination during 2011-2013	4*	2
Enrollment		
2014/15 flu season	6	3
2015/16 flu season	2	2
Time since Rituximab dose in months, median (range)	12 (5-19)	
5-11 months post-Rituximab (early)	5	
At least 12 months post-Rituximab (late)	3	
No. of previous Rituximab cycles		
0	6	
1	2	
Other medications at time of vaccination		
None	5	
Cellcept	2	
Azathioprine	1	

*One patient was unable to recall vaccination history

Chapter 4: Discussion

SUMMARY

Pemphigus vulgaris is a potentially lethal human B cell-mediated autoimmune disease characterized by blisters and sores on the skin and mucosal membranes. It is caused by the production of autoantibodies targeting the protein Dsg3. Its well-characterized autoantigenic target and topical disease symptoms makes PV an ideal model system to understand how human B cell mediated autoimmune disorders develop. The work presented in this dissertation suggest that memory B cells are important effector cells that drive the initial presentation of the autoimmune disease pemphigus vulgaris, and that memory B cells can provide robust recall responses to vaccination after treatment with the B cell ablative therapy, Rituximab.

As described in Chapter 2, the detection of autoimmune Dsg3-specific MBCs correlates with presentation of disease symptoms. Their evolution from their predicted germline naïve precursor to a pathogenic memory B cell suggest that ongoing and continuous germinal center reactions are essential for driving pathogenic responses. In-depth characterization of memory B cell-derived Dsg3-specific monoclonal antibodies have provided novel insight into how these antibodies may mechanistically drive disease pathogenesis in PV patients. Additionally, we show in Chapter 3 that while the B cell ablative therapy Rituximab completely depletes B cells from the periphery, a small number of non-circulating memory B cells are likely able to survive Rituximab treatment, and provide a robust protective recall response towards foreign antigens such as influenza vaccination. Overall, these findings provide novel insight into the development and maintenance of autoimmune and protective memory B cell responses.

This dissertation suggests that memory B cells are a crucial component of driving autoimmune responses in PV patients. Because MBCs express CD20, it is likely that they are highly impacted by Rituximab therapy, and that the ablation of Dsg3-specific MBCs by Rituximab contributes to amelioration of disease symptoms. Memory B cells are efficiently depleted from the periphery, as seen by the lack of both influenza-specific and Dsg3-specific memory B cells in Rituximab-treated patients. We showed that normal MBC responses towards influenza vaccination can persist after the B cell compartment has recovered after Rituximab treatment, suggesting that it is also possible that pathogenic autoimmune MBCs may also persist and function normally, which may be the mechanism underlying relapse in PV patients. Additionally, antigen-specific memory B cells are able to return back into the periphery in normal frequencies after antigenic challenge although total number of MBCs remains, either after vaccination or during relapse in PV disease. Thus, while we provide evidence that these returning memory B cells are likely persisting memory B cells that may reside in tissues, it is possible that they may also be newly formed memory B cells. Ongoing experiments proposed herein will help answer these essential questions, provide insight into where pathogenic autoimmune memory B cells may reside, and the mechanism of action of how autoantibodies cause disease symptoms.

FUTURE CONSIDERATIONS

B cells in PV patients who relapse after Rituximab treatment

Relapse in PV disease after treatment with Rituximab remains a major clinical problem, with over 40% of patients relapsing within 2 years of treatment (169). However, some PV patients have been observed to stay in remission for up to 10 years after treatment with multiple infusions of Rituximab in combination with intravenous immunoglobulin (295), suggesting that permanent amelioration of PV symptoms may be possible. It remains unclear which patients are prone to relapse and which ones will remain in remission, making it increasingly more important to understand the mechanism underlying relapse and provide biomarkers to better predict patients prone to relapse after Rituximab. Additionally, ongoing studies to determine if remission actually persists for the lifetime of the patient, and if remission can be attributed to the complete depletion of the B cell compartment will provide insight into how treatment options can be improved for PV patients.

It is unknown if relapse in autoimmune disease after treatment with Rituximab is driven by the autoreactive B cells that somehow survive depletion and re-expand to cause disease, ongoing emergence of novel autoimmune B cells, or a combination of both outcomes. This is an important question to consider, because if relapse is caused by a persisting reservoir of autoimmune B cells, then long-term remission could be possible if the B cell compartment is completely depleted. However, if disease is caused by ongoing, *de novo* B cell responses, then this suggests that it is just a matter of time until all autoimmune patients eventually relapse in disease after sufficient expansion of these new, autoreactive cells. Several studies have suggested that persisting B cells can cause relapse

in disease, including evidence that a small subsets of B cells can survive Rituximab-mediated depletion by residing in secondary lymphoid organs (186, 231, 277, 283) or even in inflamed tissue (185), as well as the fact that the early return of memory B cells is thought to be a biomarker in rheumatoid arthritis patients to predict which patients may eventually relapse after treatment with Rituximab (189).

Our own studies suggest that Dsg3-specific memory B cells can be found only in patients presenting disease symptoms, and that memory B cells can likely survive Rituximab therapy and provide normal protective immune responses. However, it remains unclear how memory B cells respond during secondary pathogenic autoimmune recall responses in relapsing patients. These results are further supported by earlier immunoscope analyses that suggest that Rituximab treatment of PV patients often have a loss of clonal or oligoclonal expansions in their peripheral B cell compartment, and that reemergence of the same clones was at least partially responsible for driving relapse in PV disease (179, 182). Additionally, antibody phage display and targeted PCR analysis showed that specific sequences could be found to persist prior to and after relapse post-Rituximab treatment in PV patients, and that sequences detected prior to treatment remain undetected in patients in long-term remission after treatment (193). Thus, it is possible that successful depletion of pathogenic clones may provide long-term treatment for PV patients.

However, there are many caveats to these previous studies. Primarily, they use whole PBMCs to detect clones, and make it impossible to determine the subset of B cells responsible for these clonal expansions. This is particularly problematic for the immunoscope studies, which uses total RNA isolated from PBMC samples as a template to determine clonal expansions (182). Antibody secreting cells are disproportionately

enriched for immunoglobulin mRNA (55, 296) and are inherently clonal in nature when detected in circulation (49). Thus, it is possible that clonal expansions detected by immunoscope may be an overrepresentation of the plasmablast compartment detected in PBMCs, and that a loss of clonality may be attributed to decreased frequencies of plasmablasts. Additionally, while evidence from targeted PCR analysis compellingly suggests that pathogenic sequences detected at time of diagnosis cannot be amplified from PBMCs derived from that same PV patient in remission, it is impossible to determine if PCR is simply not sensitive enough to detect sequences that may be present at very low levels in remission patients. Thus, ongoing analysis of the B cell compartment after Rituximab and how it may be impacted by treatment will be important in understanding the mechanism underlying relapse in these patients. We propose using our method of antigen-baiting and detection by flow cytometry in order to provide single-cell analysis of Dsg3-specific B cells found in relapsing patients in order to better characterize the origin of these cells.

As described previously in Chapter 2 of this thesis, we are able to detect both serum titers and memory B cells specific for Dsg3 in patients at diagnosis, as well as in relapse after Rituximab treatment. Tracking these responses longitudinally in a patient over the course of diagnosis and treatment with Rituximab show that the presence of Dsg3-specific serum antibodies and MBCs correlate nicely with presentation of disease symptoms (Figure 1A). Similar to what we described for patients at diagnosis, we saw that when detecting Dsg3-specific MBCs by flow cytometry in relapsing patients, these cells were highly activated, as shown by the upregulation of CD71. Interestingly, in Rituximab-treated patients, CD71 seemed to be upregulated in almost the entire memory B cell

compartment and not just the Dsg3-specific ones (Figure 1B), suggesting that there may be underlying dysfunction of reconstituted B cells after Rituximab that has yet to be described.

In a preliminary analysis of the repertoire of these Dsg3-specific MBCs, we were unable to detect any persisting sequences detected at relapse that was also present at diagnosis. However, we did notice that there was a substantial preference of the VH4 gene usage of these MBCs at both diagnosis and relapse time points (Figure 1C). It is possible that naïve B cells expressing the germline sequence of VH4 gene usage may have higher reactivity towards Dsg3 than other V gene usages, which would argue that ongoing development of naïve B cells may drive relapse in disease. Analysis of germline-reverted antibodies using these specific VH4 genes, and determining their binding profile against Dsg3 will determine if these naïve B cells may play a role in PV disease pathogenesis. Additionally, further analysis of a larger number of Dsg3-specific memory B cells derived from the relapse timepoint may eventually yield detection of persisting clones found at both time points. Next-generation sequencing of bulk B cells pre and post-Rituximab may also reveal if there are any larger shifts in repertoire of the total B cell compartment in terms of V gene usage, frequency of clonality, or somatic hypermutation, which may also reveal additional dysfunction to B cells induced by Rituximab.

In a preliminary panel of Dsg3-specific antibodies derived from memory B cells detected at relapse, we were able to identify not only high affinity IgG antibodies, as described in patients at diagnosis (see Chapter 2), but also we found high affinity, unmutated antibodies using the IgM isotype. This supports the idea that relapse may be mediated by a combination of *de novo* immune response derived from naïve B cells, as

well as the persistence of highly mutated, class-switched MBCs that resist Rituximab-mediated depletion. Future studies detailing how these IgM antibodies contribute to disease pathogenesis, and if they change over time and undergo germinal center reactions will provide better insight into why PV patients may relapse in disease, and how these mAbs contribute to disease pathogenesis. Additionally, ongoing identification and analysis of naïve B cells with germline immunoglobulin genes which bind Dsg3 will provide deeper understanding into how autoreactive B cells in PV disease develop over time.

Overall, there clearly exists interesting, ongoing disruptions to the B cell compartment after recovery from Rituximab-mediated depletion. While total B cells return, there is a long-term decrease in the frequency of memory B cells found in Rituximab-treated patients, with low frequencies persisting even 5 years after post-therapy (183, 245). Additionally, we have observed that a large frequency of the memory B cell compartment upregulates CD71 when compared to healthy controls and pemphigus patients who have never received Rituximab. However, it remains unclear if CD71 upregulation has any impact on the functionality of these memory B cells, such as if these cells have increased proliferative capacity. Future studies detailing how Rituximab effects the overall B cell compartment, specifically memory B cells, may provide better insight on how to improve therapy options by increasing the efficiency of B cell depletive agents, and how autoimmune immune responses may be affected in Rituximab-treated patients. These finding will have implications in understanding how to clinically treat both PV patients and patients with other B cell mediated autoimmune disorders such that they reach long-term remission.

Skin-resident B cells

While we have clearly implicated memory B cells as important effector cells for driving disease pathogenesis at time of diagnosis, there appears to be a disconnect between the limited repertoire of Dsg3-specific B cell in the periphery versus the diverse repertoire of Dsg3-specific antibodies found in the serum of PV patients, with only 20% of sequences in serum represented by those detected from PBMCs (128). This suggests that non-circulating B cell responses may be partially response for overall pathogenic serum Dsg3-specific responses. Additionally, we proposed in Chapter 3 of this dissertation that some B cells may survive Rituximab-mediated depletion, presumably by residing in tissues. This may be an underlying factor causing relapse in patients. Based on the finding that tissue-resident B cells survive Rituximab-mediated depletion (186, 231, 277, 283), especially in inflamed tissue (185), it is possible that B cells found at perilesional sites on the skin and mucosal membranes may provide a unique survival niche for Dsg3-specific B cells and allow them to resist Rituximab treatment to eventually cause relapse in patients.

Studies of skin-homing B cells from human PBMC samples have been difficult due to the allusive nature of identify clear skin homing markers for lymphocytes in the blood. Cutaneous Lymphocyte Antigen (CLA) has been described to be upregulated on T cells that home specifically to normal and inflamed skin (297-299). However, CLA expression is found only on a low frequency of circulating B cells, and it remains unclear if expression has any role on B cells homing to skin (300). Additionally, it appears that B cells are rarely found in the skin during normal homeostasis (301), although more recent studies suggest that B cells may be present in the skin at higher frequencies during inflammatory conditions (302-304).

A recent paper compellingly suggests that both memory B cells and antibody secreting cells specific for Dsg3 can reside at perilesional sites in the skin of PV patients. These B cells are often found in close contact to T cells in the skin, suggesting that structures reminiscent of tertiary lymphoid organs may form in the skin. Thus, Dsg3-specific B cells may actually differentiate and go through affinity maturation at the site of disease presentation (129). However, it remains unclear how these locally producing B cells may contribute to disease pathogenesis.

Future experiments trying to isolate these skin-resident Dsg3-specific B cells, and cloning antibodies from them may provide novel insight into the role of pathogenic monoclonal antibodies in driving disease pathogenesis, and if these cells at all differ from those described in circulation. Additional analysis using single-cell RNA-sequencing may also reveal if these cells are genetically distinct from those in the periphery, such as if any prominent homing markers drive the migration of B cells to site of disease. This could provide novel therapeutic approaches including inhibiting B cells from homing to the skin and preventing development and differentiation at the site of disease, or potentially describing novel markers for B cells specifically found in the skin that may make them specifically targetable for depletion.

Pathogenic mechanism of human-derived Dsg3-specific antibodies

The exact mechanism underlying how Dsg3-specific antibodies cause pathogenicity is currently unclear, although it is likely that a combination of both steric hindrance of desmosome formation (107, 142) and engaging signaling pathways (162, 163) can contribute to the overall pathogenicity of mAbs (254). Additionally, an active area of

research on pathogenic Dsg3-specific antibodies is trying to understand the relevance of mixtures of monoclonal antibodies to reflect the nature of polyclonal serum antibodies which clearly play an important role in driving disease pathogenesis (128).

Initial studies on the synergy of monoclonal antibodies used mouse-derived Dsg3-specific antibodies to show that when multiple antibodies were combined, including some nonpathogenic antibodies, synergy could be observed when tested in an *in vitro* keratinocyte dissociation assay as well as an *in vivo* ascites formation assay (164). However, the results are difficult to interpret because it remains unclear if any of the combinations tested used antibodies that may sterically hinder binding of the other antibodies in the mixture. Additionally, it remains unclear if these antibodies are merely working additively or if there is a true synergistic effect of combining antibodies.

Additional studies also observed the impact of polyclonal mixtures versus monoclonal antibodies on engaging signaling pathways involved in pathogenicity. Polyclonal human PV patient IgG purified from serum was compared to the mouse-derived monoclonal antibody AK23, both of which have been shown to have comparable pathogenic potential when measured *in vitro* in the keratinocyte dissociation assay. However, when either PV IgG or AK23 was used to treat *in vitro* cultures of human keratinocytes, only the polyclonal PV IgG caused extensive alteration in the cellular trafficking of Dsg3, with clustering and endocytosis of cell surface Dsg3 of the keratinocytes. Furthermore, pathogenic activity of polyclonal PV IgG can be attributed to p38 MAPK-dependent clustering and endocytosis of Dsg3, while the pathogenic mouse monoclonal antibody AK23 is functionally independent of this pathway (163). Overall, this

has led to the hypothesis that the synergy of a polyclonal antibody response is crucial in driving disease pathogenesis.

We have shown in our own data that pathogenic Dsg3-specific monoclonal antibodies can work synergistically to enhance the overall pathogenic response detected in an *in vitro* keratinocyte dissociation assay (Chapter 2), and suggest that the accumulation of pathogenic antibodies work in synergy to cause the initial presentation of disease. The synergy experiment from Chapter 2 showed that combining monoclonal antibodies which are at functionally irrelevant concentrations had no synergistic effect, suggesting that some pathogenic effect must by present to actually enhance the signal. There are still ongoing questions about which combination of antibodies may provide the optimal synergistic pathogenic response, including if nonpathogenic antibodies actually have any impact on enhancing overall pathogenicity.

Preliminary studies of our human derived monoclonal antibodies described in Chapter 2 of this dissertation showed that when 10 μg/mL of non-pathogenic antibodies was used to treat *in vitro* cultures of HK cells for 6 hours, no disruption of the border between two keratinocytes could be observed. Surprisingly, treatment of HK cells with 10 μg/mL of the pathogenic monoclonal antibody P3F3 caused clustering and endocytosis of Dsg3 from the cell surface (Figure 2A), distinct from previous reports that the pathogenic mouse-derived monoclonal antibody AK23 did not engage in these signaling pathways (163). It is possible that we are observing differences in the ability of mAbs in engaging signaling pathways because of species-dependent differences between the two antibodies, with the human-derived P3F3 being more relevant than mouse-derived AK23 to understanding which mechanisms can be engaged by pathogenic antibodies. Our earlier

findings showed that P3F3 bound to a distinct, non-overlapping epitope on the EC1 domain of Dsg3, different from AK23, which may also indicate that epitope-specific binding of antibodies to Dsg3 is necessary to engage signaling pathways. P3F3 was also significantly more pathogenic than the mouse-derived AK23. Thus, it is also possible that the other pathogenic EC1-specific human-derived antibodies with either comparable or lower pathogenic activity than AK23 may not engage the same signaling pathways as P3F3. Lastly, we described novel EC4-specific pathogenic monoclonal antibodies, which, to our knowledge, has never been reported. Because binding to the EC4 domain has no impact on sterically hindering adhesive binding sites of Dsg3, it would also be interesting to see if these non-EC1 pathogenic antibodies engage any signaling pathways that may elucidate how they act functionally. Overall, future studies on testing out the full panel of the human-derived mAbs on the endocytosis of Dsg3 will provide better insight into understanding how Dsg3-specific monoclonal antibodies cause pathogenicity in PV patients.

In order to understand how these monoclonal antibodies may act as a polyclonal mixture, HK cells were treated for 6 hours with a mixture of 6 non-pathogenic, high affinity antibodies at a total of 60 μg/mL of antibody, each targeting a distinct non-overlapping epitope on Dsg3. Even at this high concentration, the polyclonal mixture failed to engage any changes to Dsg3 expression on the surface of keratinocytes. However, when the pathogenic antibody P3F3 was added at just 1 μg/mL to the nonpathogenic mixture, the clustering and endocytosis of Dsg3 could once again be detected (Figure 2B). These observations align with our earlier synergy assays, which show that low pathogenic activity needs to be present in order to observe any synergistic effect of combining several antibodies. While it is possible that the linear arrays observed when combining the

nonpathogenic antibodies with the small amount of P3F3 is caused solely by the pathogenic activity of 1 μg/mL of P3F3, further efforts of titrating out signals will be valuable in understanding which signals are actually engaging these pathways. Additionally, while it is now clear that polyclonal mixtures of nonpathogenic antibodies have no impact on causing the endocytosis of Dsg3, there are still ongoing questions about which combinations of antibodies are relevant to engaging signaling pathways. Using both this endocytosis assays in tandem with the *in vitro* keratinocyte dissociation assays to test out multiple combinations of antibodies will be valuable in better describing the impact of polyclonal serum antibodies in driving PV pathogenesis and provide better insight into the development of novel therapies for patients with this devastating disease.

CONCLUSION

Although the identification of desmoglein-3 as the major autoantigenic target of pemphigus vulgaris has now been identified over 20 years ago, there are still many questions that linger concerning disease pathogenesis and treatment of PV. There exist ongoing questions about how these autoantibodies develop and become pathogenic, and if there are other potential autoantigenic targets driving disease pathogenesis. Additionally, a deeper understanding of how these antibodies drive disease will allow for improved treatment of PV patients, including the development and introduction of novel therapies to target pathogenic autoantibodies and autoimmune B cells.

Overall, PV and its well-characterized autoantigen make it an ideal human disease to study as a model to better understand human B cell mediated autoimmune disorders. Ongoing studies on this devastating disease will yield not only insight into how to improve the clinical care of patients with PV, but will also contribute to our understanding of basic immunology by addressing questions about how tolerance is broken and cause the development of autoimmunity in an antigen-specific manner.

FIGURES AND LEGENDS

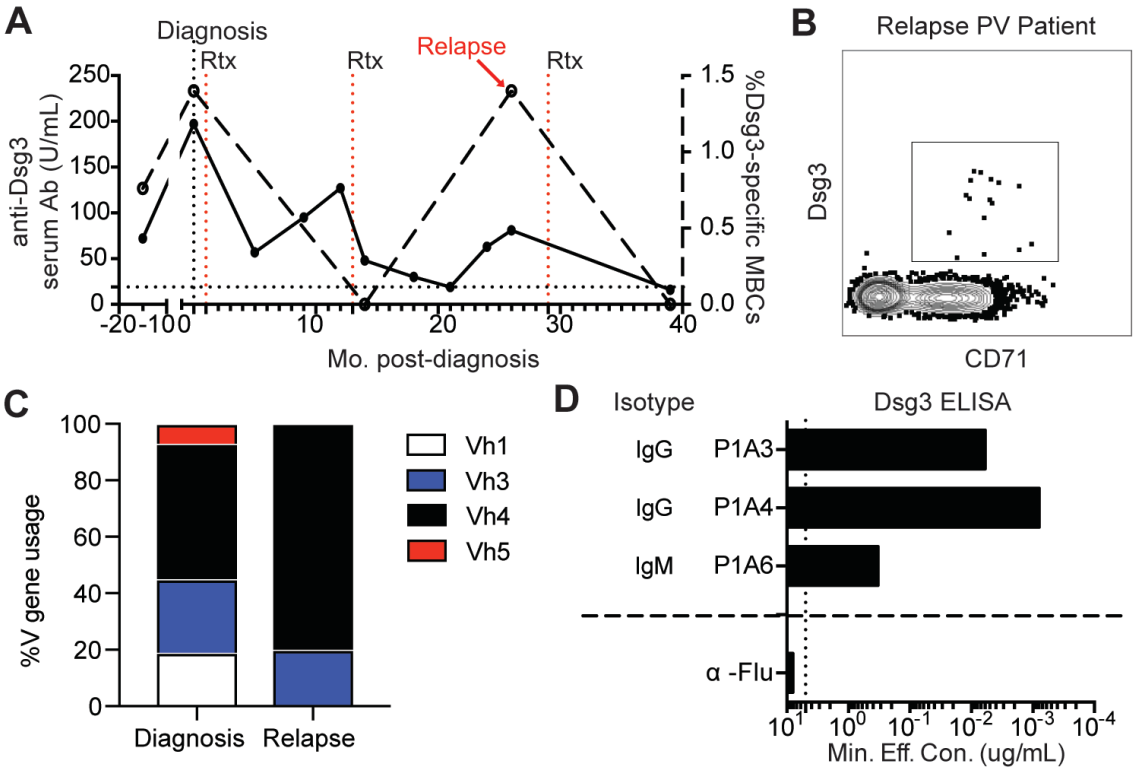

FIGURE 1. Presence of Dsg3-specific memory B cells correlate with relapse in disease after treatment with Rituximab.

(A) A longitudinal sampling of Dsg3-specific serum and memory B cell responses from patient ISD068 (described in Chapter 2) showed that Dsg3-specific B cell responses can be found when patient is presenting disease symptom. (B) When the patient is undergoing disease relapse (collected at red arrow show in Figure 1A), a high frequency of activated Dsg3-specific MBCs (gated on CD3-CD19+IgD-CD20+ lymphocytes) can be detected by flow cytometry. Additional, total MBCs appear to upregulate CD71, including the Dsg3-specific MBCs. (C) Repertoire analysis showed that there was a clear bias in VH4 gene usage of Dsg3-specific antibodies derived from both diagnosis and relapse timepoints. (D) A preliminary panel of Dsg3-specific mAbs derived from the MBC from the relapse sample shows the presence of both IgM and IgG antibodies with high affinity towards Dsg3.

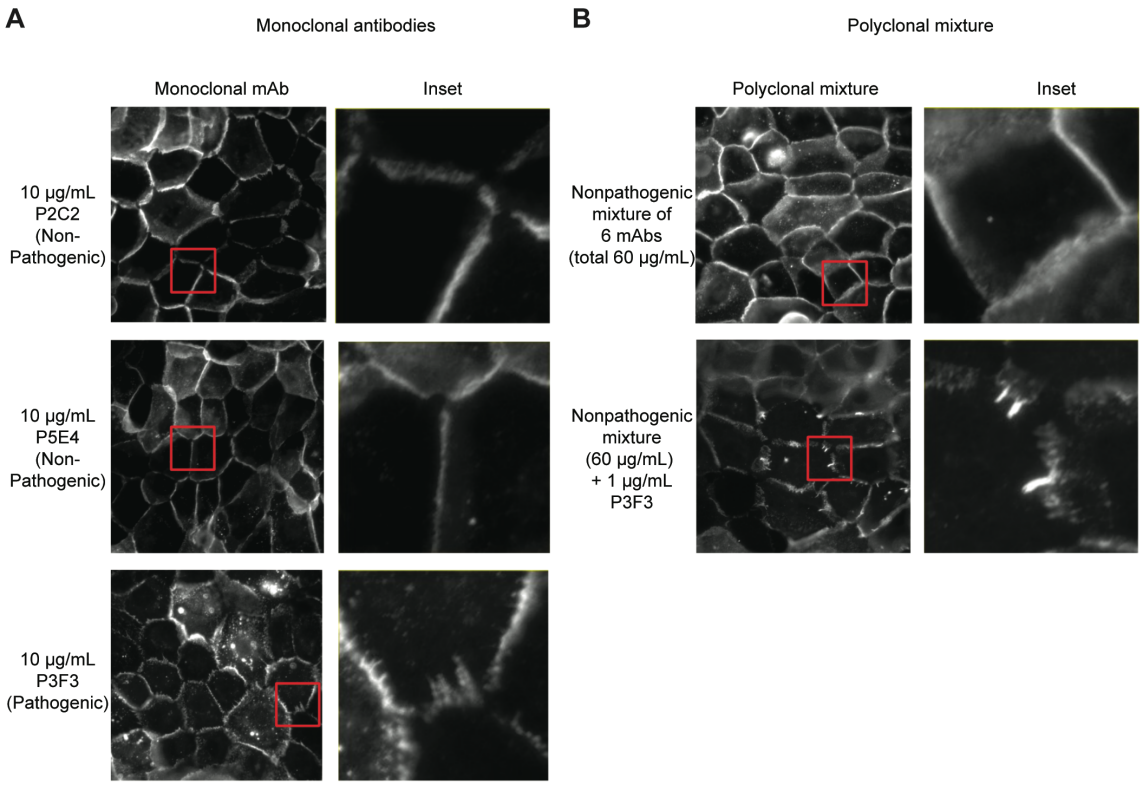

FIGURE 2. Human-derived pathogenic monoclonal antibodies can engage endocytosis and degradation of Dsg3 from the surface of keratinocytes.

(A) 10 µg/mL of non-pathogenic antibodies (P2C2, P5E4) or 10 µg/mL of a pathogenic antibody (P3F3) were used to treat HK cells for 6 hours to observe their ability to disrupt the border between two keratinocytes. While non-pathogenic mAbs had no impact on the HK cells, the pathogenic P3F3 mAb caused Dsg3 clustering and disruption of desmosomal structure. (B) When combining 6 different non-pathogenic mAbs, each at 10 µg/mL for a total of 60 µg/mL mixture of antibodies, there was still no impact on the border between two cells despite this high concentration of antibody treatment. However, when 1 µg/mL of pathogenic P3F3 mAb was added to the mixture, disruption to the cell border could be observed.

References

1. von Behring E, Kitasato S. [The mechanism of diphtheria immunity and tetanus immunity in animals. 1890]. Mol Immunol. 1991;28(12):1317, 9-20. Epub 1991/12/01. PubMed PMID: 1749380.

2. Chase MW. The cellular transfer of cutaneous hypersensitivity. J Bacteriol. 1946;51:643. Epub 1946/05/01. PubMed PMID: 20987083.

3. Lawrence HS. The cellular transfer of cutaneous hypersensitivity to tuberculin in man. Proc Soc Exp Biol Med. 1949;71(4):516-22. Epub 1949/08/01. PubMed PMID: 18139800.

4. Cooper MD, Raymond DA, Peterson RD, South MA, Good RA. The functions of the thymus system and the bursa system in the chicken. The Journal of experimental medicine. 1966;123(1):75-102. PubMed PMID: 5323079; PMCID: PMC2138128.

5. Osmond DG, Nossal GJ. Differentiation of lymphocytes in mouse bone marrow. II. Kinetics of maturation and renewal of antiglobulin-binding cells studied by double labeling. Cell Immunol. 1974;13(1):132-45. PubMed PMID: 4141645.

6. Ryser JE, Vassalli P. Mouse bone marrow lymphocytes and their differentiation. Journal of immunology. 1974;113(3):719-28. PubMed PMID: 4213258.

7. Hardy RR, Hayakawa K. B cell development pathways. Annu Rev Immunol. 2001;19:595-621. doi: 10.1146/annurev.immunol.19.1.595. PubMed PMID: 11244048.

8. Hozumi N, Tonegawa S. Evidence for somatic rearrangement of immunoglobulin genes coding for variable and constant regions. Proceedings of the

National Academy of Sciences of the United States of America. 1976;73(10):3628-32. PubMed PMID: 824647; PMCID: PMC431171.

9. Schatz DG, Oettinger MA, Baltimore D. The V(D)J recombination activating gene, RAG-1. Cell. 1989;59(6):1035-48. Epub 1989/12/22. PubMed PMID: 2598259.

10. Nemazee D. Mechanisms of central tolerance for B cells. Nat Rev Immunol. 2017;17(5):281-94. Epub 2017/04/04. doi: 10.1038/nri.2017.19. PubMed PMID: 28368006; PMCID: PMC5623591.

11. Mond JJ, Lees A, Snapper CM. T cell-independent antigens type 2. Annual review of immunology. 1995;13:655-92. Epub 1995/01/01. doi: 10.1146/annurev.iy.13.040195.003255. PubMed PMID: 7612238.

12. Sharon R, McMaster PR, Kask AM, Owens JD, Paul WE. DNP-Lys-ficoll: a T-independent antigen which elicits both IgM and IgG anti-DNP antibody-secreting cells. Journal of immunology. 1975;114(5):1585-9. Epub 1975/05/01. PubMed PMID: 1091706.

13. Mosier DE, Mond JJ, Goldings EA. The ontogeny of thymic independent antibody responses in vitro in normal mice and mice with an X-linked B cell defect. Journal of immunology. 1977;119(6):1874-8. Epub 1977/12/01. PubMed PMID: 334975.

14. Mongini PK, Stein KE, Paul WE. T cell regulation of IgG subclass antibody production in response to T-independent antigens. The Journal of experimental medicine. 1981;153(1):1-12. Epub 1981/01/01. PubMed PMID: 6969777; PMCID: PMC2186053.

15. Bortnick A, Allman D. What is and what should always have been: long-lived plasma cells induced by T cell-independent antigens. Journal of immunology. 2013;190(12):5913-8. Epub 2013/06/12. doi: 10.4049/jimmunol.1300161. PubMed PMID: 23749966; PMCID: PMC4234153.

16. Foote JB, Mahmoud TI, Vale AM, Kearney JF. Long-term maintenance of polysaccharide-specific antibodies by IgM-secreting cells. Journal of immunology. 2012;188(1):57-67. Epub 2011/11/26. doi: 10.4049/jimmunol.1100783. PubMed PMID: 22116821; PMCID: PMC3244511.

17. Taillardet M, Haffar G, Mondiere P, Asensio MJ, Gheit H, Burdin N, Defrance T, Genestier L. The thymus-independent immunity conferred by a pneumococcal polysaccharide is mediated by long-lived plasma cells. Blood. 2009;114(20):4432-40. Epub 2009/09/22. doi: 10.1182/blood-2009-01-200014. PubMed PMID: 19767510.

18. De Silva NS, Klein U. Dynamics of B cells in germinal centres. Nat Rev Immunol. 2015;15(3):137-48. doi: 10.1038/nri3804. PubMed PMID: 25656706; PMCID: PMC4399774.

19. Victora GD, Nussenzweig MC. Germinal centers. Annual review of immunology. 2012;30:429-57. doi: 10.1146/annurev-immunol-020711-075032. PubMed PMID: 22224772.

20. Marrack P, Kappler JW. The role of H-2-linked genes in helper T cell function. VII. Expression of I region and immune response genes by B cells in bystander help assays. The Journal of experimental medicine. 1980;152(5):1274-88. Epub 1980/11/01. PubMed PMID: 6159447; PMCID: PMC2185988.

21. Berek C, Berger A, Apel M. Maturation of the immune response in germinal centers. Cell. 1991;67(6):1121-9. PubMed PMID: 1760840.

22. Gitlin AD, Shulman Z, Nussenzweig MC. Clonal selection in the germinal centre by regulated proliferation and hypermutation. Nature. 2014;509(7502):637-40. Epub 2014/05/09. doi: 10.1038/nature13300. PubMed PMID: 24805232; PMCID: PMC4271732.

23. McKean D, Huppi K, Bell M, Staudt L, Gerhard W, Weigert M. Generation of antibody diversity in the immune response of BALB/c mice to influenza virus hemagglutinin. Proceedings of the National Academy of Sciences of the United States of America. 1984;81(10):3180-4. Epub 1984/05/01. PubMed PMID: 6203114; PMCID: PMC345245.

24. Chaudhuri J, Tian M, Khuong C, Chua K, Pinaud E, Alt FW. Transcription-targeted DNA deamination by the AID antibody diversification enzyme. Nature. 2003;422(6933):726-30. doi: 10.1038/nature01574. PubMed PMID: 12692563.

25. Stewart I, Radtke D, Phillips B, McGowan SJ, Bannard O. Germinal Center B Cells Replace Their Antigen Receptors in Dark Zones and Fail Light Zone Entry when Immunoglobulin Gene Mutations are Damaging. Immunity. 2018;49(3):477-89 e7. Epub 2018/09/21. doi: 10.1016/j.immuni.2018.08.025. PubMed PMID: 30231983; PMCID: PMC6162340.

26. Shih TA, Meffre E, Roederer M, Nussenzweig MC. Role of BCR affinity in T cell dependent antibody responses in vivo. Nature immunology. 2002;3(6):570-5. Epub 2002/05/22. doi: 10.1038/ni803. PubMed PMID: 12021782.

27. Heesters BA, Chatterjee P, Kim YA, Gonzalez SF, Kuligowski MP, Kirchhausen T, Carroll MC. Endocytosis and recycling of immune complexes by follicular dendritic cells enhances B cell antigen binding and activation. Immunity. 2013;38(6):1164-75. doi: 10.1016/j.immuni.2013.02.023. PubMed PMID: 23770227; PMCID: PMC3773956.

28. Heesters BA, Myers RC, Carroll MC. Follicular dendritic cells: dynamic antigen libraries. Nat Rev Immunol. 2014;14(7):495-504. doi: 10.1038/nri3689. PubMed PMID: 24948364.

29. Allen CD, Okada T, Tang HL, Cyster JG. Imaging of germinal center selection events during affinity maturation. Science. 2007;315(5811):528-31. Epub 2006/12/23. doi: 10.1126/science.1136736. PubMed PMID: 17185562.

30. Shulman Z, Gitlin AD, Weinstein JS, Lainez B, Esplugues E, Flavell RA, Craft JE, Nussenzweig MC. Dynamic signaling by T follicular helper cells during germinal center B cell selection. Science. 2014;345(6200):1058-62. Epub 2014/08/30. doi: 10.1126/science.1257861. PubMed PMID: 25170154; PMCID: PMC4519234.

31. Liu YJ, Malisan F, de Bouteiller O, Guret C, Lebecque S, Banchereau J, Mills FC, Max EE, Martinez-Valdez H. Within germinal centers, isotype switching of immunoglobulin genes occurs after the onset of somatic mutation. Immunity. 1996;4(3):241-50. Epub 1996/03/01. PubMed PMID: 8624814.

32. Schroeder HW, Jr., Cavacini L. Structure and function of immunoglobulins. J Allergy Clin Immunol. 2010;125(2 Suppl 2):S41-52. Epub 2010/03/05. doi: 10.1016/j.jaci.2009.09.046. PubMed PMID: 20176268; PMCID: PMC3670108.

33. Muramatsu M, Kinoshita K, Fagarasan S, Yamada S, Shinkai Y, Honjo T. Class switch recombination and hypermutation require activation-induced cytidine deaminase (AID), a potential RNA editing enzyme. Cell. 2000;102(5):553-63. Epub 2000/09/28. PubMed PMID: 11007474.

34. Victora GD, Schwickert TA, Fooksman DR, Kamphorst AO, Meyer-Hermann M, Dustin ML, Nussenzweig MC. Germinal center dynamics revealed by multiphoton microscopy with a photoactivatable fluorescent reporter. Cell. 2010;143(4):592-605. Epub 2010/11/16. doi: 10.1016/j.cell.2010.10.032. PubMed PMID: 21074050; PMCID: PMC3035939.

35. Crotty S. T follicular helper cell differentiation, function, and roles in disease. Immunity. 2014;41(4):529-42. doi: 10.1016/j.immuni.2014.10.004. PubMed PMID: 25367570; PMCID: PMC4223692.

36. Taylor JJ, Pape KA, Steach HR, Jenkins MK. Humoral immunity. Apoptosis and antigen affinity limit effector cell differentiation of a single naive B cell. Science. 2015;347(6223):784-7. Epub 2015/02/01. doi: 10.1126/science.aaa1342. PubMed PMID: 25636798; PMCID: PMC4412594.

37. Gitlin AD, von Boehmer L, Gazumyan A, Shulman Z, Oliveira TY, Nussenzweig MC. Independent Roles of Switching and Hypermutation in the Development and Persistence of B Lymphocyte Memory. Immunity. 2016;44(4):769-81. Epub 2016/03/06. doi: 10.1016/j.immuni.2016.01.011. PubMed PMID: 26944202; PMCID: PMC4838502.

38. Tarlinton D, Good-Jacobson K. Diversity among memory B cells: origin, consequences, and utility. Science. 2013;341(6151):1205-11. doi: 10.1126/science.1241146. PubMed PMID: 24031013.

39. Crotty S, Felgner P, Davies H, Glidewell J, Villarreal L, Ahmed R. Cutting edge: long-term B cell memory in humans after smallpox vaccination. Journal of immunology. 2003;171(10):4969-73. PubMed PMID: 14607890.

40. McHeyzer-Williams LJ, McHeyzer-Williams MG. Antigen-specific memory B cell development. Annual review of immunology. 2005;23:487-513. doi: 10.1146/annurev.immunol.23.021704.115732. PubMed PMID: 15771579.

41. McHeyzer-Williams LJ, Milpied PJ, Okitsu SL, McHeyzer-Williams MG. Class-switched memory B cells remodel BCRs within secondary germinal centers. Nature immunology. 2015;16(3):296-305. doi: 10.1038/ni.3095. PubMed PMID: 25642821; PMCID: PMC4333102.

42. Frolich D, Giesecke C, Mei HE, Reiter K, Daridon C, Lipsky PE, Dorner T. Secondary immunization generates clonally related antigen-specific plasma cells and memory B cells. Journal of immunology. 2010;185(5):3103-10. doi: 10.4049/jimmunol.1000911. PubMed PMID: 20693426.

43. Franz B, May KF, Jr., Dranoff G, Wucherpfennig K. Ex vivo characterization and isolation of rare memory B cells with antigen tetramers. Blood. 2011;118(2):348-57. doi: 10.1182/blood-2011-03-341917. PubMed PMID: 21551230; PMCID: PMC3138687.

44. Giesecke C, Frolich D, Reiter K, Mei HE, Wirries I, Kuhly R, Killig M, Glatzer T, Stolzel K, Perka C, Lipsky PE, Dorner T. Tissue distribution and dependence of

responsiveness of human antigen-specific memory B cells. Journal of immunology. 2014;192(7):3091-100. doi: 10.4049/jimmunol.1302783. PubMed PMID: 24567530.

45. Pichyangkul S, Yongvanitchit K, Limsalakpetch A, Kum-Arb U, Im-Erbsin R, Boonnak K, Thitithayanont A, Jongkaewwattana A, Wiboon-Ut S, Mongkolsirichaikul D, Mahanonda R, Spring M, Chuang I, Mason CJ, Saunders DL. Tissue Distribution of Memory T and B Cells in Rhesus Monkeys following Influenza A Infection. Journal of immunology. 2015;195(9):4378-86. doi: 10.4049/jimmunol.1501702. PubMed PMID: 26408671; PMCID: PMC4642841.

46. Adachi Y, Onodera T, Yamada Y, Daio R, Tsuiji M, Inoue T, Kobayashi K, Kurosaki T, Ato M, Takahashi Y. Distinct germinal center selection at local sites shapes memory B cell response to viral escape. The Journal of experimental medicine. 2015;212(10):1709-23. doi: 10.1084/jem.20142284. PubMed PMID: 26324444; PMCID: PMC4577849.

47. Allie SR, Bradley JE, Mudunuru U, Schultz MD, Graf BA, Lund FE, Randall TD. The establishment of resident memory B cells in the lung requires local antigen encounter. Nature immunology. 2019;20(1):97-108. Epub 2018/12/05. doi: 10.1038/s41590-018-0260-6. PubMed PMID: 30510223; PMCID: PMC6392030.

48. Wrammert J, Onlamoon N, Akondy RS, Perng GC, Polsrila K, Chandele A, Kwissa M, Pulendran B, Wilson PC, Wittawatmongkol O, Yoksan S, Angkasekwinai N, Pattanapanyasat K, Chokephaibulkit K, Ahmed R. Rapid and massive virus-specific plasmablast responses during acute dengue virus infection in humans. J Virol.

2012;86(6):2911-8. doi: 10.1128/JVI.06075-11. PubMed PMID: 22238318; PMCID: PMC3302324.

49. Wrammert J, Smith K, Miller J, Langley WA, Kokko K, Larsen C, Zheng NY, Mays I, Garman L, Helms C, James J, Air GM, Capra JD, Ahmed R, Wilson PC. Rapid cloning of high-affinity human monoclonal antibodies against influenza virus. Nature. 2008;453(7195):667-71. doi: 10.1038/nature06890. PubMed PMID: 18449194; PMCID: 2515609.

50. Odendahl M, Mei H, Hoyer BF, Jacobi AM, Hansen A, Muehlinghaus G, Berek C, Hiepe F, Manz R, Radbruch A, Dorner T. Generation of migratory antigen-specific plasma blasts and mobilization of resident plasma cells in a secondary immune response. Blood. 2005;105(4):1614-21. Epub 2004/10/28. doi: 10.1182/blood-2004-07-2507. PubMed PMID: 15507523.

51. Li GM, Chiu C, Wrammert J, McCausland M, Andrews SF, Zheng NY, Lee JH, Huang M, Qu X, Edupuganti S, Mulligan M, Das SR, Yewdell JW, Mehta AK, Wilson PC, Ahmed R. Pandemic H1N1 influenza vaccine induces a recall response in humans that favors broadly cross-reactive memory B cells. Proceedings of the National Academy of Sciences of the United States of America. 2012;109(23):9047-52. doi: 10.1073/pnas.1118979109. PubMed PMID: 22615367; PMCID: PMC3384143.

52. Nakaya HI, Wrammert J, Lee EK, Racioppi L, Marie-Kunze S, Haining WN, Means AR, Kasturi SP, Khan N, Li GM, McCausland M, Kanchan V, Kokko KE, Li S, Elbein R, Mehta AK, Aderem A, Subbarao K, Ahmed R, Pulendran B. Systems biology of vaccination for seasonal influenza in humans. Nature immunology.

2011;12(8):786-95. doi: 10.1038/ni.2067. PubMed PMID: 21743478; PMCID: PMC3140559.

53. Magnani DM, Silveira CGT, Ricciardi MJ, Gonzalez-Nieto L, Pedreno-Lopez N, Bailey VK, Gutman MJ, Maxwell HS, Domingues A, Costa PR, Ferrari L, Goulart R, Martins MA, Martinez-Navio JM, Fuchs SP, Kalil J, Timenetsky MDC, Wrammert J, Whitehead SS, Burton DR, Desrosiers RC, Kallas EG, Watkins DI. Potent Plasmablast-Derived Antibodies Elicited by the National Institutes of Health Dengue Vaccine. J Virol. 2017;91(22). Epub 2017/09/08. doi: 10.1128/JVI.00867-17. PubMed PMID: 28878078; PMCID: PMC5660501.

54. Rahman A, Rashu R, Bhuiyan TR, Chowdhury F, Khan AI, Islam K, LaRocque RC, Ryan ET, Wrammert J, Calderwood SB, Qadri F, Harris JB. Antibody-secreting cell responses after Vibrio cholerae O1 infection and oral cholera vaccination in adults in Bangladesh. Clin Vaccine Immunol. 2013;20(10):1592-8. Epub 2013/08/16. doi: 10.1128/CVI.00347-13. PubMed PMID: 23945156; PMCID: PMC3807192.

55. Ellebedy AH, Jackson KJ, Kissick HT, Nakaya HI, Davis CW, Roskin KM, McElroy AK, Oshansky CM, Elbein R, Thomas S, Lyon GM, Spiropoulou CF, Mehta AK, Thomas PG, Boyd SD, Ahmed R. Defining antigen-specific plasmablast and memory B cell subsets in human blood after viral infection or vaccination. Nature immunology. 2016;17(10):1226-34. Epub 2016/08/16. doi: 10.1038/ni.3533. PubMed PMID: 27525369; PMCID: PMC5054979.

56. Kauffman RC, Bhuiyan TR, Nakajima R, Mayo-Smith LM, Rashu R, Hoq MR, Chowdhury F, Khan AI, Rahman A, Bhaumik SK, Harris L, O'Neal JT, Trost JF, Alam NH, Jasinskas A, Dotsey E, Kelly M, Charles RC, Xu P, Kovac P, Calderwood SB, Ryan

ET, Felgner PL, Qadri F, Wrammert J, Harris JB. Single-Cell Analysis of the Plasmablast Response to Vibrio cholerae Demonstrates Expansion of Cross-Reactive Memory B Cells. MBio. 2016;7(6). doi: 10.1128/mBio.02021-16. PubMed PMID: 27999163; PMCID: PMC5181778.

57. Priyamvada L, Cho A, Onlamoon N, Zheng NY, Huang M, Kovalenkov Y, Chokephaibulkit K, Angkasekwinai N, Pattanapanyasat K, Ahmed R, Wilson PC, Wrammert J. B Cell Responses during Secondary Dengue Virus Infection Are Dominated by Highly Cross-Reactive, Memory-Derived Plasmablasts. J Virol. 2016;90(12):5574-85. doi: 10.1128/JVI.03203-15. PubMed PMID: 27030262; PMCID: PMC4886779.

58. Tipton CM, Fucile CF, Darce J, Chida A, Ichikawa T, Gregoretti I, Schieferl S, Hom J, Jenks S, Feldman RJ, Mehr R, Wei C, Lee FE, Cheung WC, Rosenberg AF, Sanz I. Diversity, cellular origin and autoreactivity of antibody-secreting cell population expansions in acute systemic lupus erythematosus. Nature immunology. 2015;16(7):755-65. doi: 10.1038/ni.3175. PubMed PMID: 26006014.

59. Blanchard-Rohner G, Pulickal AS, Jol-van der Zijde CM, Snape MD, Pollard AJ. Appearance of peripheral blood plasma cells and memory B cells in a primary and secondary immune response in humans. Blood. 2009;114(24):4998-5002. Epub 2009/10/22. doi: 10.1182/blood-2009-03-211052. PubMed PMID: 19843885; PMCID: PMC2788974.

60. Nutt SL, Hodgkin PD, Tarlinton DM, Corcoran LM. The generation of antibody-secreting plasma cells. Nat Rev Immunol. 2015;15(3):160-71. doi: 10.1038/nri3795. PubMed PMID: 25698678.

61. Magri G, Comerma L, Pybus M, Sintes J, Llige D, Segura-Garzon D, Bascones S, Yeste A, Grasset EK, Gutzeit C, Uzzan M, Ramanujam M, van Zelm MC, Albero-Gonzalez R, Vazquez I, Iglesias M, Serrano S, Marquez L, Mercade E, Mehandru S, Cerutti A. Human Secretory IgM Emerges from Plasma Cells Clonally Related to Gut Memory B Cells and Targets Highly Diverse Commensals. Immunity. 2017;47(1):118-34 e8. Epub 2017/07/16. doi: 10.1016/j.immuni.2017.06.013. PubMed PMID: 28709802; PMCID: PMC5519504.

62. Slifka MK, Antia R, Whitmire JK, Ahmed R. Humoral immunity due to long-lived plasma cells. Immunity. 1998;8(3):363-72. PubMed PMID: 9529153.

63. Amanna IJ, Carlson NE, Slifka MK. Duration of humoral immunity to common viral and vaccine antigens. The New England journal of medicine. 2007;357(19):1903-15. Epub 2007/11/09. doi: 10.1056/NEJMoa066092. PubMed PMID: 17989383.

64. Mankarious S, Lee M, Fischer S, Pyun KH, Ochs HD, Oxelius VA, Wedgwood RJ. The half-lives of IgG subclasses and specific antibodies in patients with primary immunodeficiency who are receiving intravenously administered immunoglobulin. J Lab Clin Med. 1988;112(5):634-40. Epub 1988/11/01. PubMed PMID: 3183495.

65. Halliley JL, Tipton CM, Liesveld J, Rosenberg AF, Darce J, Gregoretti IV, Popova L, Kaminiski D, Fucile CF, Albizua I, Kyu S, Chiang KY, Bradley KT, Burack R, Slifka M, Hammarlund E, Wu H, Zhao L, Walsh EE, Falsey AR, Randall TD, Cheung WC, Sanz I, Lee FE. Long-Lived Plasma Cells Are Contained within the CD19(-)CD38(hi)CD138(+) Subset in Human Bone Marrow. Immunity. 2015;43(1):132-45.

doi: 10.1016/j.immuni.2015.06.016. PubMed PMID: 26187412; PMCID: PMC4680845.

66. Nguyen DC, Garimalla S, Xiao H, Kyu S, Albizua I, Galipeau J, Chiang KY, Waller EK, Wu R, Gibson G, Roberson J, Lund FE, Randall TD, Sanz I, Lee FE. Factors of the bone marrow microniche that support human plasma cell survival and immunoglobulin secretion. Nat Commun. 2018;9(1):3698. Epub 2018/09/14. doi: 10.1038/s41467-018-05853-7. PubMed PMID: 30209264; PMCID: PMC6135805.

67. Yurasov S, Wardemann H, Hammersen J, Tsuiji M, Meffre E, Pascual V, Nussenzweig MC. Defective B cell tolerance checkpoints in systemic lupus erythematosus. The Journal of experimental medicine. 2005;201(5):703-11. doi: 10.1084/jem.20042251. PubMed PMID: 15738055; PMCID: 2212839.

68. Tsuiji M, Yurasov S, Velinzon K, Thomas S, Nussenzweig MC, Wardemann H. A checkpoint for autoreactivity in human IgM+ memory B cell development. The Journal of experimental medicine. 2006;203(2):393-400. doi: 10.1084/jem.20052033. PubMed PMID: 16446381; PMCID: PMC2118214.

69. Goodnow CC. Balancing immunity and tolerance: deleting and tuning lymphocyte repertoires. Proceedings of the National Academy of Sciences of the United States of America. 1996;93(6):2264-71. PubMed PMID: 8637861; PMCID: PMC39784.

70. Nemazee DA, Burki K. Clonal deletion of B lymphocytes in a transgenic mouse bearing anti-MHC class I antibody genes. Nature. 1989;337(6207):562-6. doi: 10.1038/337562a0. PubMed PMID: 2783762.

71. Nemazee D, Buerki K. Clonal deletion of autoreactive B lymphocytes in bone marrow chimeras. Proceedings of the National Academy of Sciences of the United States of America. 1989;86(20):8039-43. PubMed PMID: 2682636; PMCID: PMC298209.

72. Russell DM, Dembic Z, Morahan G, Miller JF, Burki K, Nemazee D. Peripheral deletion of self-reactive B cells. Nature. 1991;354(6351):308-11. doi: 10.1038/354308a0. PubMed PMID: 1956380; PMCID: PMC3787863.

73. Pulendran B, Kannourakis G, Nouri S, Smith KG, Nossal GJ. Soluble antigen can cause enhanced apoptosis of germinal-centre B cells. Nature. 1995;375(6529):331-4. doi: 10.1038/375331a0. PubMed PMID: 7753199.

74. Gay D, Saunders T, Camper S, Weigert M. Receptor editing: an approach by autoreactive B cells to escape tolerance. The Journal of experimental medicine. 1993;177(4):999-1008. PubMed PMID: 8459227; PMCID: PMC2190958.

75. Goodnow CC, Crosbie J, Jorgensen H, Brink RA, Basten A. Induction of self-tolerance in mature peripheral B lymphocytes. Nature. 1989;342(6248):385-91. doi: 10.1038/342385a0. PubMed PMID: 2586609.

76. Hartley SB, Crosbie J, Brink R, Kantor AB, Basten A, Goodnow CC. Elimination from peripheral lymphoid tissues of self-reactive B lymphocytes recognizing membrane-bound antigens. Nature. 1991;353(6346):765-9. doi: 10.1038/353765a0. PubMed PMID: 1944535.

77. Lang J, Jackson M, Teyton L, Brunmark A, Kane K, Nemazee D. B cells are exquisitely sensitive to central tolerance and receptor editing induced by ultralow

affinity, membrane-bound antigen. The Journal of experimental medicine. 1996;184(5):1685-97. PubMed PMID: 8920858; PMCID: PMC2192881.

78. Duty JA, Szodoray P, Zheng NY, Koelsch KA, Zhang Q, Swiatkowski M, Mathias M, Garman L, Helms C, Nakken B, Smith K, Farris AD, Wilson PC. Functional anergy in a subpopulation of naive B cells from healthy humans that express autoreactive immunoglobulin receptors. The Journal of experimental medicine. 2009;206(1):139-51. doi: 10.1084/jem.20080611. PubMed PMID: 19103878; PMCID: PMC2626668.

79. Goenka R, Scholz JL, Sindhava VJ, Cancro MP. New roles for the BLyS/BAFF family in antigen-experienced B cell niches. Cytokine Growth Factor Rev. 2014;25(2):107-13. doi: 10.1016/j.cytogfr.2014.01.001. PubMed PMID: 24507939; PMCID: PMC3999179.

80. Lesley R, Xu Y, Kalled SL, Hess DM, Schwab SR, Shu HB, Cyster JG. Reduced competitiveness of autoantigen-engaged B cells due to increased dependence on BAFF. Immunity. 2004;20(4):441-53. Epub 2004/04/16. PubMed PMID: 15084273.

81. Thien M, Phan TG, Gardam S, Amesbury M, Basten A, Mackay F, Brink R. Excess BAFF rescues self-reactive B cells from peripheral deletion and allows them to enter forbidden follicular and marginal zone niches. Immunity. 2004;20(6):785-98. Epub 2004/06/11. doi: 10.1016/j.immuni.2004.05.010. PubMed PMID: 15189742.

82. Liu XG, Hou M. Immune thrombocytopenia and B-cell-activating factor/a proliferation-inducing ligand. Semin Hematol. 2013;50 Suppl 1:S89-99. doi: 10.1053/j.seminhematol.2013.03.021. PubMed PMID: 23664525.

83. Vincent FB, Morand EF, Schneider P, Mackay F. The BAFF/APRIL system in SLE pathogenesis. Nat Rev Rheumatol. 2014;10(6):365-73. doi: 10.1038/nrrheum.2014.33. PubMed PMID: 24614588.

84. Vincent FB, Saulep-Easton D, Figgett WA, Fairfax KA, Mackay F. The BAFF/APRIL system: emerging functions beyond B cell biology and autoimmunity. Cytokine Growth Factor Rev. 2013;24(3):203-15. doi: 10.1016/j.cytogfr.2013.04.003. PubMed PMID: 23684423.

85. Mauri C, Bosma A. Immune regulatory function of B cells. Annual review of immunology. 2012;30:221-41. doi: 10.1146/annurev-immunol-020711-074934. PubMed PMID: 22224776.

86. Matsumoto M, Baba A, Yokota T, Nishikawa H, Ohkawa Y, Kayama H, Kallies A, Nutt SL, Sakaguchi S, Takeda K, Kurosaki T, Baba Y. Interleukin-10-producing plasmablasts exert regulatory function in autoimmune inflammation. Immunity. 2014;41(6):1040-51. doi: 10.1016/j.immuni.2014.10.016. PubMed PMID: 25484301.

87. Blair PA, Norena LY, Flores-Borja F, Rawlings DJ, Isenberg DA, Ehrenstein MR, Mauri C. CD19(+)CD24(hi)CD38(hi) B cells exhibit regulatory capacity in healthy individuals but are functionally impaired in systemic Lupus Erythematosus patients. Immunity. 2010;32(1):129-40. doi: 10.1016/j.immuni.2009.11.009. PubMed PMID: 20079667.

88. Flores-Borja F, Bosma A, Ng D, Reddy V, Ehrenstein MR, Isenberg DA, Mauri C. CD19+CD24hiCD38hi B cells maintain regulatory T cells while limiting TH1 and

TH17 differentiation. Science translational medicine. 2013;5(173):173ra23. doi: 10.1126/scitranslmed.3005407. PubMed PMID: 23427243.

89. Wardemann H, Yurasov S, Schaefer A, Young JW, Meffre E, Nussenzweig MC. Predominant autoantibody production by early human B cell precursors. Science. 2003;301(5638):1374-7. doi: 10.1126/science.1086907. PubMed PMID: 12920303.

90. Tiller T, Tsuiji M, Yurasov S, Velinzon K, Nussenzweig MC, Wardemann H. Autoreactivity in human IgG+ memory B cells. Immunity. 2007;26(2):205-13. doi: 10.1016/j.immuni.2007.01.009. PubMed PMID: 17306569; PMCID: PMC1839941.

91. Kaur K, Zheng NY, Smith K, Huang M, Li L, Pauli NT, Henry Dunand CJ, Lee JH, Morrissey M, Wu Y, Joachims ML, Munroe ME, Lau D, Qu X, Krammer F, Wrammert J, Palese P, Ahmed R, James JA, Wilson PC. High Affinity Antibodies against Influenza Characterize the Plasmablast Response in SLE Patients After Vaccination. PLoS One. 2015;10(5):e0125618. doi: 10.1371/journal.pone.0125618. PubMed PMID: 25951191; PMCID: PMC4423960.

92. Yurasov S, Tiller T, Tsuiji M, Velinzon K, Pascual V, Wardemann H, Nussenzweig MC. Persistent expression of autoantibodies in SLE patients in remission. The Journal of experimental medicine. 2006;203(10):2255-61. doi: 10.1084/jem.20061446. PubMed PMID: 16966430; PMCID: PMC2118096.

93. Browning JL. B cells move to centre stage: novel opportunities for autoimmune disease treatment. Nat Rev Drug Discov. 2006;5(7):564-76. doi: 10.1038/nrd2085. PubMed PMID: 16816838.

94. Baum S, Sakka N, Artsi O, Trau H, Barzilai A. Diagnosis and classification of autoimmune blistering diseases. Autoimmun Rev. 2014;13(4-5):482-9. doi: 10.1016/j.autrev.2014.01.047. PubMed PMID: 24434358.

95. Bhol K, Natarajan K, Nagarwalla N, Mohimen A, Aoki V, Ahmed AR. Correlation of peptide specificity and IgG subclass with pathogenic and nonpathogenic autoantibodies in pemphigus vulgaris: a model for autoimmunity. Proceedings of the National Academy of Sciences of the United States of America. 1995;92(11):5239-43. PubMed PMID: 7761479; PMCID: 41884.

96. Cirillo N, Al-Jandan BA. Desmosomal adhesion and pemphigus vulgaris: the first half of the story. Cell communication & adhesion. 2013;20(1-2):1-10. doi: 10.3109/15419061.2013.763799. PubMed PMID: 23368972.

97. Furue M, Kadono T. Bullous pemphigoid: What's ahead? J Dermatol. 2015. doi: 10.1111/1346-8138.13207. PubMed PMID: 26603373.

98. Amagai M, Koch PJ, Nishikawa T, Stanley JR. Pemphigus vulgaris antigen (desmoglein 3) is localized in the lower epidermis, the site of blister formation in patients. The Journal of investigative dermatology. 1996;106(2):351-5. PubMed PMID: 8601740.

99. Amagai M, Stanley JR. Desmoglein as a target in skin disease and beyond. The Journal of investigative dermatology. 2012;132(3 Pt 2):776-84. doi: 10.1038/jid.2011.390. PubMed PMID: 22189787; PMCID: 3279627.

100. Stanley JR, Klaus-Kovtun V, Sampaio SA. Antigenic specificity of fogo selvagem autoantibodies is similar to North American pemphigus foliaceus and

distinct from pemphigus vulgaris autoantibodies. The Journal of investigative dermatology. 1986;87(2):197-201. Epub 1986/08/01. PubMed PMID: 3525686.

101. Korman N. Pemphigus. Journal of the American Academy of Dermatology. 1988;18(6):1219-38. PubMed PMID: 3290286.

102. Ettlin DA. Pemphigus. Dent Clin North Am. 2005;49(1):107-25, viii-ix. doi: 10.1016/j.cden.2004.08.002. PubMed PMID: 15567364.

103. Geller S, Gat A, Zeeli T, Hafner A, Eming R, Hertl M, Sprecher E. The expanding spectrum of IgA pemphigus: a case report and review of the literature. The British journal of dermatology. 2014;171(3):650-6. doi: 10.1111/bjd.12940. PubMed PMID: 24601812.

104. Singer KH, Hashimoto K, Jensen PJ, Morioka S, Lazarus GS. Pathogenesis of autoimmunity in pemphigus. Annual review of immunology. 1985;3:87-108. doi: 10.1146/annurev.iy.03.040185.000511. PubMed PMID: 3904774.

105. Amagai M, Hashimoto T, Shimizu N, Nishikawa T. Absorption of pathogenic autoantibodies by the extracellular domain of pemphigus vulgaris antigen (Dsg3) produced by baculovirus. The Journal of clinical investigation. 1994;94(1):59-67. doi: 10.1172/JCI117349. PubMed PMID: 8040292; PMCID: 296282.

106. Feldman RJ, Ahmed AR. Relevance of rituximab therapy in pemphigus vulgaris: analysis of current data and the immunologic basis for its observed responses. Expert review of clinical immunology. 2011;7(4):529-41. doi: 10.1586/eci.11.22. PubMed PMID: 21790294.

107. Amagai M, Karpati S, Prussick R, Klaus-Kovtun V, Stanley JR. Autoantibodies against the amino-terminal cadherin-like binding domain of pemphigus vulgaris

antigen are pathogenic. The Journal of clinical investigation. 1992;90(3):919-26. doi: 10.1172/JCI115968. PubMed PMID: 1522242; PMCID: 329947.

108. Amagai M, Klaus-Kovtun V, Stanley JR. Autoantibodies against a novel epithelial cadherin in pemphigus vulgaris, a disease of cell adhesion. Cell. 1991;67(5):869-77. PubMed PMID: 1720352.

109. Pokutta S, Herrenknecht K, Kemler R, Engel J. Conformational changes of the recombinant extracellular domain of E-cadherin upon calcium binding. Eur J Biochem. 1994;223(3):1019-26. Epub 1994/08/01. PubMed PMID: 8055942.

110. Beutner EH, Jordon RE. Demonstration of Skin Antibodies in Sera of Pemphigus Vulgaris Patients by Indirect Immunofluorescent Staining. Proc Soc Exp Biol Med. 1964;117:505-10. Epub 1964/11/01. PubMed PMID: 14233481.

111. Delva E, Tucker DK, Kowalczyk AP. The desmosome. Cold Spring Harb Perspect Biol. 2009;1(2):a002543. Epub 2010/01/13. doi: 10.1101/cshperspect.a002543. PubMed PMID: 20066089; PMCID: PMC2742091.

112. Kowalczyk AP, Green KJ. Structure, function, and regulation of desmosomes. Prog Mol Biol Transl Sci. 2013;116:95-118. Epub 2013/03/14. doi: 10.1016/B978-0-12-394311-8.00005-4. PubMed PMID: 23481192; PMCID: PMC4336551.

113. Ding X, Aoki V, Mascaro JM, Jr., Lopez-Swiderski A, Diaz LA, Fairley JA. Mucosal and mucocutaneous (generalized) pemphigus vulgaris show distinct autoantibody profiles. The Journal of investigative dermatology. 1997;109(4):592-6. Epub 1997/10/27 20:25. PubMed PMID: 9326396.

114. Mahoney MG, Wang Z, Rothenberger K, Koch PJ, Amagai M, Stanley JR. Explanations for the clinical and microscopic localization of lesions in pemphigus

foliaceus and vulgaris. The Journal of clinical investigation. 1999;103(4):461-8. Epub 1999/02/18. doi: 10.1172/JCI5252. PubMed PMID: 10021453; PMCID: PMC408100.

115. Czech W, Schaller J, Schopf E, Kapp A. Granulocyte activation in bullous diseases: release of granular proteins in bullous pemphigoid and pemphigus vulgaris. Journal of the American Academy of Dermatology. 1993;29(2 Pt 1):210-5. PubMed PMID: 8393016.

116. Koch PJ, Mahoney MG, Ishikawa H, Pulkkinen L, Uitto J, Shultz L, Murphy GF, Whitaker-Menezes D, Stanley JR. Targeted disruption of the pemphigus vulgaris antigen (desmoglein 3) gene in mice causes loss of keratinocyte cell adhesion with a phenotype similar to pemphigus vulgaris. J Cell Biol. 1997;137(5):1091-102. PubMed PMID: 9166409; PMCID: PMC2136216.

117. Ahmed AR, Carrozzo M, Caux F, Cirillo N, Dmochowski M, Alonso AE, Gniadecki R, Hertl M, Lopez-Zabalza MJ, Lotti R, Pincelli C, Pittelkow M, Schmidt E, Sinha AA, Sprecher E, Grando SA. Monopathogenic vs multipathogenic explanations of pemphigus pathophysiology. Exp Dermatol. 2016;25(11):839-46. Epub 2016/10/30. doi: 10.1111/exd.13106. PubMed PMID: 27305362.

118. Kalantari-Dehaghi M, Anhalt GJ, Camilleri MJ, Chernyavsky AI, Chun S, Felgner PL, Jasinskas A, Leiferman KM, Liang L, Marchenko S, Nakajima-Sasaki R, Pittelkow MR, Zone JJ, Grando SA. Pemphigus vulgaris autoantibody profiling by proteomic technique. PLoS One. 2013;8(3):e57587. doi: 10.1371/journal.pone.0057587. PubMed PMID: 23505434; PMCID: PMC3591405.

119. Mao X, Nagler AR, Farber SA, Choi EJ, Jackson LH, Leiferman KM, Ishii N, Hashimoto T, Amagai M, Zone JJ, Payne AS. Autoimmunity to desmocollin 3 in pemphigus vulgaris. The American journal of pathology. 2010;177(6):2724-30. doi: 10.2353/ajpath.2010.100483. PubMed PMID: 20952584; PMCID: 2993297.

120. Ishii K, Amagai M, Hall RP, Hashimoto T, Takayanagi A, Gamou S, Shimizu N, Nishikawa T. Characterization of autoantibodies in pemphigus using antigen-specific enzyme-linked immunosorbent assays with baculovirus-expressed recombinant desmogleins. Journal of immunology. 1997;159(4):2010-7. PubMed PMID: 9257868.

121. Sharma PM, Choi EJ, Kuroda K, Hachiya T, Ishii K, Payne AS. Pathogenic anti-desmoglein MAbs show variable ELISA activity because of preferential binding of mature versus proprotein isoforms of desmoglein 3. The Journal of investigative dermatology. 2009;129(9):2309-12. doi: 10.1038/jid.2009.41. PubMed PMID: 19282843; PMCID: PMC2841796.

122. Anhalt GJ, Labib RS, Voorhees JJ, Beals TF, Diaz LA. Induction of pemphigus in neonatal mice by passive transfer of IgG from patients with the disease. The New England journal of medicine. 1982;306(20):1189-96. doi: 10.1056/NEJM198205203062001. PubMed PMID: 7040962.

123. Ohyama M, Amagai M, Tsunoda K, Ota T, Koyasu S, Hata J, Umezawa A, Nishikawa T. Immunologic and histopathologic characterization of an active disease mouse model for pemphigus vulgaris. The Journal of investigative dermatology. 2002;118(1):199-204. doi: 10.1046/j.0022-202x.2001.01643.x. PubMed PMID: 11851895.

124. Amagai M, Tsunoda K, Suzuki H, Nishifuji K, Koyasu S, Nishikawa T. Use of autoantigen-knockout mice in developing an active autoimmune disease model for pemphigus. The Journal of clinical investigation. 2000;105(5):625-31. doi: 10.1172/JCI8748. PubMed PMID: 10712434; PMCID: PMC292455.

125. Nishifuji K, Amagai M, Kuwana M, Iwasaki T, Nishikawa T. Detection of antigen-specific B cells in patients with pemphigus vulgaris by enzyme-linked immunospot assay: requirement of T cell collaboration for autoantibody production. The Journal of investigative dermatology. 2000;114(1):88-94. doi: 10.1046/j.1523-1747.2000.00840.x. PubMed PMID: 10620121.

126. Panko J, Florell SR, Hadley J, Zone J, Leiferman K, Vanderhooft S. Neonatal pemphigus in an infant born to a mother with serologic evidence of both pemphigus vulgaris and gestational pemphigoid. Journal of the American Academy of Dermatology. 2009;60(6):1057-62. doi: 10.1016/j.jaad.2008.10.025. PubMed PMID: 19467379.

127. Cheng SW, Kobayashi M, Kinoshita-Kuroda K, Tanikawa A, Amagai M, Nishikawa T. Monitoring disease activity in pemphigus with enzyme-linked immunosorbent assay using recombinant desmogleins 1 and 3. The British journal of dermatology. 2002;147(2):261-5. PubMed PMID: 12174096.

128. Chen J, Zheng Q, Hammers CM, Ellebrecht CT, Mukherjee EM, Tang HY, Lin C, Yuan H, Pan M, Langenhan J, Komorowski L, Siegel DL, Payne AS, Stanley JR. Proteomic Analysis of Pemphigus Autoantibodies Indicates a Larger, More Diverse, and More Dynamic Repertoire than Determined by B Cell Genetics. Cell Rep.

2017;18(1):237-47. Epub 2017/01/05. doi: 10.1016/j.celrep.2016.12.013. PubMed PMID: 28052253; PMCID: PMC5221611.

129. Yuan H, Zhou S, Liu Z, Cong W, Fei X, Zeng W, Zhu H, Xu R, Wang Y, Zheng J, Pan M. Pivotal Role of Lesional and Perilesional T/B Lymphocytes in Pemphigus Pathogenesis. The Journal of investigative dermatology. 2017;137(11):2362-70. Epub 2017/06/26. doi: 10.1016/j.jid.2017.05.032. PubMed PMID: 28647348.

130. Eming R, Hennerici T, Backlund J, Feliciani C, Visconti KC, Willenborg S, Wohde J, Holmdahl R, Sonderstrup G, Hertl M. Pathogenic IgG antibodies against desmoglein 3 in pemphigus vulgaris are regulated by HLA-DRB1*04:02-restricted T cells. Journal of immunology. 2014;193(9):4391-9. Epub 2014/09/26. doi: 10.4049/jimmunol.1401081. PubMed PMID: 25252957.

131. Veldman C, Stauber A, Wassmuth R, Uter W, Schuler G, Hertl M. Dichotomy of autoreactive Th1 and Th2 cell responses to desmoglein 3 in patients with pemphigus vulgaris (PV) and healthy carriers of PV-associated HLA class II alleles. Journal of immunology. 2003;170(1):635-42. PubMed PMID: 12496453.

132. Rizzo C, Fotino M, Zhang Y, Chow S, Spizuoco A, Sinha AA. Direct characterization of human T cells in pemphigus vulgaris reveals elevated autoantigen-specific Th2 activity in association with active disease. Clinical and experimental dermatology. 2005;30(5):535-40. doi: 10.1111/j.1365-2230.2005.01836.x. PubMed PMID: 16045688.

133. Zhu H, Chen Y, Zhou Y, Wang Y, Zheng J, Pan M. Cognate Th2-B cell interaction is essential for the autoantibody production in pemphigus vulgaris.

Journal of clinical immunology. 2012;32(1):114-23. doi: 10.1007/s10875-011-9597-4. PubMed PMID: 22009001.

134. Takahashi H, Kuwana M, Amagai M. A single helper T cell clone is sufficient to commit polyclonal naive B cells to produce pathogenic IgG in experimental pemphigus vulgaris. Journal of immunology. 2009;182(3):1740-5. PubMed PMID: 19155523.

135. Veldman C, Eming R, Wolff-Franke S, Sonderstrup G, Kwok WW, Hertl M. Detection of low avidity desmoglein 3-reactive T cells in pemphigus vulgaris using HLA-DR beta 1*0402 tetramers. Clin Immunol. 2007;122(3):330-7. doi: 10.1016/j.clim.2006.09.014. PubMed PMID: 17113829.

136. Hennerici T, Pollmann R, Schmidt T, Seipelt M, Tackenberg B, Mobs C, Ghoreschi K, Hertl M, Eming R. Increased Frequency of T Follicular Helper Cells and Elevated Interleukin-27 Plasma Levels in Patients with Pemphigus. PLoS One. 2016;11(2):e0148919. Epub 2016/02/13. doi: 10.1371/journal.pone.0148919. PubMed PMID: 26872212; PMCID: PMC4752242.

137. Wada N, Nishifuji K, Yamada T, Kudoh J, Shimizu N, Matsumoto M, Peltonen L, Nagafuchi S, Amagai M. Aire-dependent thymic expression of desmoglein 3, the autoantigen in pemphigus vulgaris, and its role in T-cell tolerance. The Journal of investigative dermatology. 2011;131(2):410-7. doi: 10.1038/jid.2010.330. PubMed PMID: 21048786.

138. Kawana S, Geoghegan WD, Jordon RE, Nishiyama S. Deposition of the membrane attack complex of complement in pemphigus vulgaris and pemphigus

foliaceus skin. The Journal of investigative dermatology. 1989;92(4):588-92. PubMed PMID: 2703726.

139. Mascaro JM, Jr., Espana A, Liu Z, Ding X, Swartz SJ, Fairley JA, Diaz LA. Mechanisms of acantholysis in pemphigus vulgaris: role of IgG valence. Clin Immunol Immunopathol. 1997;85(1):90-6. Epub 1997/11/05. PubMed PMID: 9325074.

140. Anhalt GJ, Till GO, Diaz LA, Labib RS, Patel HP, Eaglstein NF. Defining the role of complement in experimental pemphigus vulgaris in mice. Journal of immunology. 1986;137(9):2835-40. PubMed PMID: 3760574.

141. Payne AS, Ishii K, Kacir S, Lin C, Li H, Hanakawa Y, Tsunoda K, Amagai M, Stanley JR, Siegel DL. Genetic and functional characterization of human pemphigus vulgaris monoclonal autoantibodies isolated by phage display. The Journal of clinical investigation. 2005;115(4):888-99. doi: 10.1172/JCI24185. PubMed PMID: 15841178; PMCID: 1070425.

142. Di Zenzo G, Di Lullo G, Corti D, Calabresi V, Sinistro A, Vanzetta F, Didona B, Cianchini G, Hertl M, Eming R, Amagai M, Ohyama B, Hashimoto T, Sloostra J, Sallusto F, Zambruno G, Lanzavecchia A. Pemphigus autoantibodies generated through somatic mutations target the desmoglein-3 cis-interface. The Journal of clinical investigation. 2012;122(10):3781-90. doi: 10.1172/JCI64413. PubMed PMID: 22996451; PMCID: 3461925.

143. Qian Y, Diaz LA, Ye J, Clarke SH. Dissecting the anti-desmoglein autoreactive B cell repertoire in pemphigus vulgaris patients. Journal of immunology. 2007;178(9):5982-90. PubMed PMID: 17442983.

144. Tsunoda K, Ota T, Aoki M, Yamada T, Nagai T, Nakagawa T, Koyasu S, Nishikawa T, Amagai M. Induction of pemphigus phenotype by a mouse monoclonal antibody against the amino-terminal adhesive interface of desmoglein 3. Journal of immunology. 2003;170(4):2170-8. PubMed PMID: 12574390.

145. Futei Y, Amagai M, Ishii K, Kuroda-Kinoshita K, Ohya K, Nishikawa T. Predominant IgG4 subclass in autoantibodies of pemphigus vulgaris and foliaceus. J Dermatol Sci. 2001;26(1):55-61. PubMed PMID: 11323221.

146. Ellebrecht CT, Mukherjee EM, Zheng Q, Choi EJ, Reddy SG, Mao X, Payne AS. Autoreactive IgG and IgA B Cells Evolve through Distinct Subclass Switch Pathways in the Autoimmune Disease Pemphigus Vulgaris. Cell Rep. 2018;24(9):2370-80. Epub 2018/08/30. doi: 10.1016/j.celrep.2018.07.093. PubMed PMID: 30157430; PMCID: PMC6156788.

147. Mentink LF, de Jong MC, Kloosterhuis GJ, Zuiderveen J, Jonkman MF, Pas HH. Coexistence of IgA antibodies to desmogleins 1 and 3 in pemphigus vulgaris, pemphigus foliaceus and paraneoplastic pemphigus. The British journal of dermatology. 2007;156(4):635-41. Epub 2007/02/01. doi: 10.1111/j.1365-2133.2006.07717.x. PubMed PMID: 17263817.

148. Spaeth S, Riechers R, Borradori L, Zillikens D, Budinger L, Hertl M. IgG, IgA and IgE autoantibodies against the ectodomain of desmoglein 3 in active pemphigus vulgaris. The British journal of dermatology. 2001;144(6):1183-8. Epub 2001/06/26. PubMed PMID: 11422039.

149. Cho MJ, Lo ASY, Mao XM, Nagler AR, Ellebrecht CT, Mukherjee EM, Hammers CM, Choi EJ, Sharma PM, Uduman M, Li H, Rux AH, Farber SA, Rubin CB, Kleinstein

SH, Sachais BS, Posner MR, Cavacini LA, Payne AS. Shared VH1-46 gene usage by pemphigus vulgaris autoantibodies indicates common humoral immune responses among patients. Nat Commun. 2014;5. doi: ARTN 4167 10.1038/ncomms5167. PubMed PMID: WOS:000338838500023.

150. Cho MJ, Ellebrecht CT, Hammers CM, Mukherjee EM, Sapparapu G, Boudreaux CE, McDonald SM, Crowe JE, Jr., Payne AS. Determinants of VH1-46 Cross-Reactivity to Pemphigus Vulgaris Autoantigen Desmoglein 3 and Rotavirus Antigen VP6. Journal of immunology. 2016;197(4):1065-73. doi: 10.4049/jimmunol.1600567. PubMed PMID: 27402694; PMCID: PMC4976025.

151. Hammers CM, Stanley JR. Antibody phage display: technique and applications. The Journal of investigative dermatology. 2014;134(2):1-5. Epub 2014/01/16. doi: 10.1038/jid.2013.521. PubMed PMID: 24424458; PMCID: PMC3951127.

152. Traggiai E, Becker S, Subbarao K, Kolesnikova L, Uematsu Y, Gismondo MR, Murphy BR, Rappuoli R, Lanzavecchia A. An efficient method to make human monoclonal antibodies from memory B cells: potent neutralization of SARS coronavirus. Nat Med. 2004;10(8):871-5. Epub 2004/07/13. doi: 10.1038/nm1080. PubMed PMID: 15247913.

153. Boggon TJ, Murray J, Chappuis-Flament S, Wong E, Gumbiner BM, Shapiro L. C-cadherin ectodomain structure and implications for cell adhesion mechanisms. Science. 2002;296(5571):1308-13. Epub 2002/04/20. doi: 10.1126/science.1071559. PubMed PMID: 11964443.

154. Wu Y, Jin X, Harrison O, Shapiro L, Honig BH, Ben-Shaul A. Cooperativity between trans and cis interactions in cadherin-mediated junction formation. Proceedings of the National Academy of Sciences of the United States of America. 2010;107(41):17592-7. Epub 2010/09/30. doi: 10.1073/pnas.1011247107. PubMed PMID: 20876147; PMCID: PMC2955114.

155. Tsunoda K, Ota T, Saito M, Hata T, Shimizu A, Ishiko A, Yamada T, Nakagawa T, Kowalczyk AP, Amagai M. Pathogenic relevance of IgG and IgM antibodies against desmoglein 3 in blister formation in pemphigus vulgaris. The American journal of pathology. 2011;179(2):795-806. Epub 2011/07/02. doi: 10.1016/j.ajpath.2011.04.015. PubMed PMID: 21718682; PMCID: PMC3157249.

156. Lo AS, Mao X, Mukherjee EM, Ellebrecht CT, Yu X, Posner MR, Payne AS, Cavacini LA. Pathogenicity and Epitope Characteristics Do Not Differ in IgG Subclass-Switched Anti-Desmoglein 3 IgG1 and IgG4 Autoantibodies in Pemphigus Vulgaris. PLoS One. 2016;11(6):e0156800. doi: 10.1371/journal.pone.0156800. PubMed PMID: 27304671; PMCID: PMC4909199.

157. Shimizu A, Ishiko A, Ota T, Tsunoda K, Amagai M, Nishikawa T. IgG binds to desmoglein 3 in desmosomes and causes a desmosomal split without keratin retraction in a pemphigus mouse model. The Journal of investigative dermatology. 2004;122(5):1145-53. doi: 10.1111/j.0022-202X.2004.22426.x. PubMed PMID: 15140217.

158. Calkins CC, Setzer SV, Jennings JM, Summers S, Tsunoda K, Amagai M, Kowalczyk AP. Desmoglein endocytosis and desmosome disassembly are coordinated responses to pemphigus autoantibodies. The Journal of biological

chemistry. 2006;281(11):7623-34. Epub 2005/12/27. doi: 10.1074/jbc.M512447200. PubMed PMID: 16377623.

159. Jennings JM, Tucker DK, Kottke MD, Saito M, Delva E, Hanakawa Y, Amagai M, Kowalczyk AP. Desmosome disassembly in response to pemphigus vulgaris IgG occurs in distinct phases and can be reversed by expression of exogenous Dsg3. The Journal of investigative dermatology. 2011;131(3):706-18. doi: 10.1038/jid.2010.389. PubMed PMID: 21160493; PMCID: PMC3235416.

160. Stahley SN, Saito M, Faundez V, Koval M, Mattheyses AL, Kowalczyk AP. Desmosome assembly and disassembly are membrane raft-dependent. PLoS One. 2014;9(1):e87809. Epub 2014/02/06. doi: 10.1371/journal.pone.0087809. PubMed PMID: 24498201; PMCID: PMC3907498.

161. Stahley SN, Warren MF, Feldman RJ, Swerlick RA, Mattheyses AL, Kowalczyk AP. Super-Resolution Microscopy Reveals Altered Desmosomal Protein Organization in Tissue from Patients with Pemphigus Vulgaris. The Journal of investigative dermatology. 2016;136(1):59-66. doi: 10.1038/JID.2015.353. PubMed PMID: 26763424; PMCID: PMC4730957.

162. Mao X, Sano Y, Park JM, Payne AS. p38 MAPK activation is downstream of the loss of intercellular adhesion in pemphigus vulgaris. The Journal of biological chemistry. 2011;286(2):1283-91. Epub 2010/11/17. doi: 10.1074/jbc.M110.172874. PubMed PMID: 21078676; PMCID: PMC3020736.

163. Saito M, Stahley SN, Caughman CY, Mao X, Tucker DK, Payne AS, Amagai M, Kowalczyk AP. Signaling dependent and independent mechanisms in pemphigus

vulgaris blister formation. PLoS One. 2012;7(12):e50696. doi: 10.1371/journal.pone.0050696. PubMed PMID: 23226536; PMCID: PMC3513318.

164. Kawasaki H, Tsunoda K, Hata T, Ishii K, Yamada T, Amagai M. Synergistic pathogenic effects of combined mouse monoclonal anti-desmoglein 3 IgG antibodies on pemphigus vulgaris blister formation. The Journal of investigative dermatology. 2006;126(12):2621-30. Epub 2006/07/15. doi: 10.1038/sj.jid.5700450. PubMed PMID: 16841036.

165. Cianchini G, Lupi F, Masini C, Corona R, Puddu P, De Pita O. Therapy with rituximab for autoimmune pemphigus: results from a single-center observational study on 42 cases with long-term follow-up. Journal of the American Academy of Dermatology. 2012;67(4):617-22. doi: 10.1016/j.jaad.2011.11.007. PubMed PMID: 22243765.

166. Almugairen N, Hospital V, Bedane C, Duvert-Lehembre S, Picard D, Tronquoy AF, Houivet E, D'Incan M, Joly P. Assessment of the rate of long-term complete remission off therapy in patients with pemphigus treated with different regimens including medium- and high-dose corticosteroids. Journal of the American Academy of Dermatology. 2013;69(4):583-8. doi: 10.1016/j.jaad.2013.05.016. PubMed PMID: 23850258.

167. Bystryn JC, Steinman NM. The adjuvant therapy of pemphigus. An update. Archives of dermatology. 1996;132(2):203-12. PubMed PMID: 8629830.

168. Joly P, Maho-Vaillant M, Prost-Squarcioni C, Hebert V, Houivet E, Calbo S, Caillot F, Golinski ML, Labeille B, Picard-Dahan C, Paul C, Richard MA, Bouaziz JD, Duvert-Lehembre S, Bernard P, Caux F, Alexandre M, Ingen-Housz-Oro S, Vabres P,

Delaporte E, Quereux G, Dupuy A, Debarbieux S, Avenel-Audran M, D'Incan M, Bedane C, Beneton N, Jullien D, Dupin N, Misery L, Machet L, Beylot-Barry M, Dereure O, Sassolas B, Vermeulin T, Benichou J, Musette P, French study group on autoimmune bullous skin d. First-line rituximab combined with short-term prednisone versus prednisone alone for the treatment of pemphigus (Ritux 3): a prospective, multicentre, parallel-group, open-label randomised trial. Lancet. 2017;389(10083):2031-40. Epub 2017/03/28. doi: 10.1016/S0140-6736(17)30070-3. PubMed PMID: 28342637.

169. Joly P, Mouquet H, Roujeau JC, D'Incan M, Gilbert D, Jacquot S, Gougeon ML, Bedane C, Muller R, Dreno B, Doutre MS, Delaporte E, Pauwels C, Franck N, Caux F, Picard C, Tancrede-Bohin E, Bernard P, Tron F, Hertl M, Musette P. A single cycle of rituximab for the treatment of severe pemphigus. The New England journal of medicine. 2007;357(6):545-52. doi: 10.1056/NEJMoa067752. PubMed PMID: 17687130.

170. Schmidt E, Goebeler M, Zillikens D. Rituximab in severe pemphigus. Annals of the New York Academy of Sciences. 2009;1173:683-91. doi: 10.1111/j.1749-6632.2009.04744.x. PubMed PMID: 19758216.

171. Du J, Wang H, Zhong C, Peng B, Zhang M, Li B, Huo S, Guo Y, Ding J. Structural basis for recognition of CD20 by therapeutic antibody Rituximab. The Journal of biological chemistry. 2007;282(20):15073-80. doi: 10.1074/jbc.M701654200. PubMed PMID: 17395584.

172. Uchida J, Hamaguchi Y, Oliver JA, Ravetch JV, Poe JC, Haas KM, Tedder TF. The innate mononuclear phagocyte network depletes B lymphocytes through Fc

receptor-dependent mechanisms during anti-CD20 antibody immunotherapy. The Journal of experimental medicine. 2004;199(12):1659-69. doi: 10.1084/jem.20040119. PubMed PMID: 15210744; PMCID: 2212805.

173. UFaD A. Rituximab Information 2015 [updated Updated July, 2015; cited 2015 Accessed August]. Available from: http://www.fda.gov/Drugs/DrugSafety/PostmarketDrugSafetyInformationforPatientsandProviders/ucm109106.htm.

174. Genentech. FDA Grants Breakthrough Therapy Designation for Rituxan® (Rituximab) in Pemphigus Vulgaris 2017 [updated Thursday, March 23, 2017; cited 2017]. Available from: https://www.gene.com/media/press-releases/14656/2017-03-23/fda-grants-breakthrough-therapy-designat.

175. Nagel A, Hertl M, Eming R. B-cell-directed therapy for inflammatory skin diseases. The Journal of investigative dermatology. 2009;129(2):289-301. doi: 10.1038/jid.2008.192. PubMed PMID: 19148218.

176. Fleischmann RM. Safety of biologic therapy in rheumatoid arthritis and other autoimmune diseases: focus on rituximab. Seminars in arthritis and rheumatism. 2009;38(4):265-80. doi: 10.1016/j.semarthrit.2008.01.001. PubMed PMID: 18336874.

177. Sehn LH, Donaldson J, Chhanabhai M, Fitzgerald C, Gill K, Klasa R, MacPherson N, O'Reilly S, Spinelli JJ, Sutherland J, Wilson KS, Gascoyne RD, Connors JM. Introduction of combined CHOP plus rituximab therapy dramatically improved outcome of diffuse large B-cell lymphoma in British Columbia. J Clin Oncol. 2005;23(22):5027-33. doi: 10.1200/JCO.2005.09.137. PubMed PMID: 15955905.

178. Hoyer BF, Manz RA, Radbruch A, Hiepe F. Long-lived plasma cells and their contribution to autoimmunity. Annals of the New York Academy of Sciences. 2005;1050:124-33. doi: 10.1196/annals.1313.014. PubMed PMID: 16014527.

179. Colliou N, Picard D, Caillot F, Calbo S, Le Corre S, Lim A, Lemercier B, Le Mauff B, Maho-Vaillant M, Jacquot S, Bedane C, Bernard P, Caux F, Prost C, Delaporte E, Doutre MS, Dreno B, Franck N, Ingen-Housz-Oro S, Chosidow O, Pauwels C, Picard C, Roujeau JC, Sigal M, Tancrede-Bohin E, Templier I, Eming R, Hertl M, D'Incan M, Joly P, Musette P. Long-term remissions of severe pemphigus after rituximab therapy are associated with prolonged failure of desmoglein B cell response. Science translational medicine. 2013;5(175):175ra30. doi: 10.1126/scitranslmed.3005166. PubMed PMID: 23467561.

180. Breedveld F, Agarwal S, Yin M, Ren S, Li NF, Shaw TM, Davies BE. Rituximab pharmacokinetics in patients with rheumatoid arthritis: B-cell levels do not correlate with clinical response. J Clin Pharmacol. 2007;47(9):1119-28. doi: 10.1177/0091270007305297. PubMed PMID: 17766699.

181. Kamburova EG, Koenen HJ, Boon L, Hilbrands LB, Joosten I. In vitro effects of rituximab on the proliferation, activation and differentiation of human B cells. American journal of transplantation : official journal of the American Society of Transplantation and the American Society of Transplant Surgeons. 2012;12(2):341-50. doi: 10.1111/j.1600-6143.2011.03833.x. PubMed PMID: 22070501.

182. Mouquet H, Musette P, Gougeon ML, Jacquot S, Lemercier B, Lim A, Gilbert D, Dutot I, Roujeau JC, D'Incan M, Bedane C, Tron F, Joly P. B-cell depletion immunotherapy in pemphigus: effects on cellular and humoral immune responses.

The Journal of investigative dermatology. 2008;128(12):2859-69. doi: 10.1038/jid.2008.178. PubMed PMID: 18563177.

183. Sutter JA, Kwan-Morley J, Dunham J, Du YZ, Kamoun M, Albert D, Eisenberg RA, Luning Prak ET. A longitudinal analysis of SLE patients treated with rituximab (anti-CD20): factors associated with B lymphocyte recovery. Clin Immunol. 2008;126(3):282-90. doi: 10.1016/j.clim.2007.11.012. PubMed PMID: 18226586.

184. Eming R, Nagel A, Wolff-Franke S, Podstawa E, Debus D, Hertl M. Rituximab exerts a dual effect in pemphigus vulgaris. The Journal of investigative dermatology. 2008;128(12):2850-8. doi: 10.1038/jid.2008.172. PubMed PMID: 18563178.

185. Doorenspleet ME, Klarenbeek PL, de Hair MJ, van Schaik BD, Esveldt RE, van Kampen AH, Gerlag DM, Musters A, Baas F, Tak PP, de Vries N. Rheumatoid arthritis synovial tissue harbours dominant B-cell and plasma-cell clones associated with autoreactivity. Annals of the rheumatic diseases. 2014;73(4):756-62. doi: 10.1136/annrheumdis-2012-202861. PubMed PMID: 23606709.

186. Schroder C, Azimzadeh AM, Wu G, Price JO, Atkinson JB, Pierson RN. Anti-CD20 treatment depletes B-cells in blood and lymphatic tissue of cynomolgus monkeys. Transplant immunology. 2003;12(1):19-28. doi: 10.1016/S0966-3274(03)00059-5. PubMed PMID: 14551029.

187. Vos K, Thurlings RM, Wijbrandts CA, van Schaardenburg D, Gerlag DM, Tak PP. Early effects of rituximab on the synovial cell infiltrate in patients with rheumatoid arthritis. Arthritis and rheumatism. 2007;56(3):772-8. doi: 10.1002/art.22400. PubMed PMID: 17328049.

188. Vital EM, Dass S, Buch MH, Henshaw K, Pease CT, Martin MF, Ponchel F, Rawstron AC, Emery P. B cell biomarkers of rituximab responses in systemic lupus erythematosus. Arthritis and rheumatism. 2011;63(10):3038-47. doi: 10.1002/art.30466. PubMed PMID: 21618204.

189. Roll P, Dorner T, Tony HP. Anti-CD20 therapy in patients with rheumatoid arthritis: predictors of response and B cell subset regeneration after repeated treatment. Arthritis and rheumatism. 2008;58(6):1566-75. doi: 10.1002/art.23473. PubMed PMID: 18512772.

190. Albers LN, Liu Y, Bo N, Swerlick RA, Feldman RJ. Developing biomarkers for predicting clinical relapse in pemphigus patients treated with rituximab. Journal of the American Academy of Dermatology. 2017;77(6):1074-82. Epub 2017/09/21. doi: 10.1016/j.jaad.2017.07.012. PubMed PMID: 28927663.

191. Feldman RJ, Christen WG, Ahmed AR. Comparison of immunological parameters in patients with pemphigus vulgaris following rituximab and IVIG therapy. The British journal of dermatology. 2012;166(3):511-7. Epub 2011/10/05. doi: 10.1111/j.1365-2133.2011.10658.x. PubMed PMID: 21967407.

192. Boes M. Role of natural and immune IgM antibodies in immune responses. Mol Immunol. 2000;37(18):1141-9. Epub 2001/07/14. PubMed PMID: 11451419.

193. Hammers CM, Chen J, Lin C, Kacir S, Siegel DL, Payne AS, Stanley JR. Persistence of anti-desmoglein 3 IgG(+) B-cell clones in pemphigus patients over years. The Journal of investigative dermatology. 2015;135(3):742-9. doi: 10.1038/jid.2014.291. PubMed PMID: 25142730; PMCID: 4294994.

194. Nagel A, Podstawa E, Eickmann M, Muller HH, Hertl M, Eming R. Rituximab mediates a strong elevation of B-cell-activating factor associated with increased pathogen-specific IgG but not autoantibodies in pemphigus vulgaris. The Journal of investigative dermatology. 2009;129(9):2202-10. doi: 10.1038/jid.2009.27. PubMed PMID: 19282839.

195. Chamberlain N, Massad C, Oe T, Cantaert T, Herold KC, Meffre E. Rituximab does not reset defective early B cell tolerance checkpoints. The Journal of clinical investigation. 2015. doi: 10.1172/JCI83840. PubMed PMID: 26642366.

196. Sellam J, Rouanet S, Hendel-Chavez H, Abbed K, Sibilia J, Tebib J, Le Loet X, Combe B, Dougados M, Mariette X, Taoufik Y. Blood memory B cells are disturbed and predict the response to rituximab in patients with rheumatoid arthritis. Arthritis and rheumatism. 2011;63(12):3692-701. doi: 10.1002/art.30599. PubMed PMID: 22127692.

197. Maurer MA, Rakocevic G, Leung CS, Quast I, Lukacisin M, Goebels N, Munz C, Wardemann H, Dalakas M, Lunemann JD. Rituximab induces sustained reduction of pathogenic B cells in patients with peripheral nervous system autoimmunity. The Journal of clinical investigation. 2012;122(4):1393-402. doi: 10.1172/JCI58743. PubMed PMID: 22426210; PMCID: PMC3314454.

198. Huang H, Benoist C, Mathis D. Rituximab specifically depletes short-lived autoreactive plasma cells in a mouse model of inflammatory arthritis. Proceedings of the National Academy of Sciences of the United States of America. 2010;107(10):4658-63. doi: 10.1073/pnas.1001074107. PubMed PMID: 20176942; PMCID: PMC2842072.

199. Pescovitz MD, Torgerson TR, Ochs HD, Ocheltree E, McGee P, Krause-Steinrauf H, Lachin JM, Canniff J, Greenbaum C, Herold KC, Skyler JS, Weinberg A, Type 1 Diabetes TrialNet Study G. Effect of rituximab on human in vivo antibody immune responses. J Allergy Clin Immunol. 2011;128(6):1295-302 e5. doi: 10.1016/j.jaci.2011.08.008. PubMed PMID: 21908031; PMCID: PMC3659395.

200. Muhammad K, Roll P, Einsele H, Dorner T, Tony HP. Delayed acquisition of somatic hypermutations in repopulated IGD+CD27+ memory B cell receptors after rituximab treatment. Arthritis and rheumatism. 2009;60(8):2284-93. doi: 10.1002/art.24722. PubMed PMID: 19644860.

201. Thompson WW, Shay DK, Weintraub E, Brammer L, Bridges CB, Cox NJ, Fukuda K. Influenza-associated hospitalizations in the United States. JAMA. 2004;292(11):1333-40. doi: 10.1001/jama.292.11.1333. PubMed PMID: 15367555.

202. Thompson WW, Shay DK, Weintraub E, Brammer L, Cox N, Anderson LJ, Fukuda K. Mortality associated with influenza and respiratory syncytial virus in the United States. JAMA. 2003;289(2):179-86. PubMed PMID: 12517228.

203. Writing Committee of the WHOCoCAoPI, Bautista E, Chotpitayasunondh T, Gao Z, Harper SA, Shaw M, Uyeki TM, Zaki SR, Hayden FG, Hui DS, Kettner JD, Kumar A, Lim M, Shindo N, Penn C, Nicholson KG. Clinical aspects of pandemic 2009 influenza A (H1N1) virus infection. The New England journal of medicine. 2010;362(18):1708-19. doi: 10.1056/NEJMra1000449. PubMed PMID: 20445182.

204. Bouvier NM, Palese P. The biology of influenza viruses. Vaccine. 2008;26 Suppl 4:D49-53. PubMed PMID: 19230160; PMCID: PMC3074182.

205. Parrish CR, Kawaoka Y. The origins of new pandemic viruses: the acquisition of new host ranges by canine parvovirus and influenza A viruses. Annu Rev Microbiol. 2005;59:553-86. doi: 10.1146/annurev.micro.59.030804.121059. PubMed PMID: 16153179.

206. Gerdil C. The annual production cycle for influenza vaccine. Vaccine. 2003;21(16):1776-9. PubMed PMID: 12686093.

207. Clements ML, Murphy BR. Development and persistence of local and systemic antibody responses in adults given live attenuated or inactivated influenza A virus vaccine. J Clin Microbiol. 1986;23(1):66-72. PubMed PMID: 3700610; PMCID: PMC268574.

208. Mohn KG, Bredholt G, Brokstad KA, Pathirana RD, Aarstad HJ, Tondel C, Cox RJ. Longevity of B-cell and T-cell responses after live attenuated influenza vaccination in children. J Infect Dis. 2015;211(10):1541-9. doi: 10.1093/infdis/jiu654. PubMed PMID: 25425696; PMCID: PMC4407761.

209. Chambers BS, Parkhouse K, Ross TM, Alby K, Hensley SE. Identification of Hemagglutinin Residues Responsible for H3N2 Antigenic Drift during the 2014-2015 Influenza Season. Cell Rep. 2015;12(1):1-6. doi: 10.1016/j.celrep.2015.06.005. PubMed PMID: 26119736; PMCID: PMC4487778.

210. Wiley DC, Wilson IA, Skehel JJ. Structural identification of the antibody-binding sites of Hong Kong influenza haemagglutinin and their involvement in antigenic variation. Nature. 1981;289(5796):373-8. PubMed PMID: 6162101.

211. Air GM. Influenza virus antigenicity and broadly neutralizing epitopes. Curr Opin Virol. 2015;11:113-21. doi: 10.1016/j.coviro.2015.03.006. PubMed PMID: 25846699; PMCID: PMC4456283.

212. Chiu C, Wrammert J, Li GM, McCausland M, Wilson PC, Ahmed R. Cross-reactive humoral responses to influenza and their implications for a universal vaccine. Annals of the New York Academy of Sciences. 2013;1283:13-21. doi: 10.1111/nyas.12012. PubMed PMID: 23405860.

213. Ekiert DC, Wilson IA. Broadly neutralizing antibodies against influenza virus and prospects for universal therapies. Curr Opin Virol. 2012;2(2):134-41. doi: 10.1016/j.coviro.2012.02.005. PubMed PMID: 22482710; PMCID: PMC3368890.

214. Lee PS, Wilson IA. Structural characterization of viral epitopes recognized by broadly cross-reactive antibodies. Curr Top Microbiol Immunol. 2015;386:323-41. doi: 10.1007/82_2014_413. PubMed PMID: 25037260; PMCID: PMC4358778.

215. Andrews SF, Huang Y, Kaur K, Popova LI, Ho IY, Pauli NT, Henry Dunand CJ, Taylor WM, Lim S, Huang M, Qu X, Lee JH, Salgado-Ferrer M, Krammer F, Palese P, Wrammert J, Ahmed R, Wilson PC. Immune history profoundly affects broadly protective B cell responses to influenza. Science translational medicine. 2015;7(316):316ra192. Epub 2015/12/04. doi: 10.1126/scitranslmed.aad0522. PubMed PMID: 26631631; PMCID: PMC4770855.

216. McCarthy KR, Watanabe A, Kuraoka M, Do KT, McGee CE, Sempowski GD, Kepler TB, Schmidt AG, Kelsoe G, Harrison SC. Memory B Cells that Cross-React with Group 1 and Group 2 Influenza A Viruses Are Abundant in Adult Human

Repertoires. Immunity. 2018;48(1):174-84 e9. Epub 2018/01/19. doi: 10.1016/j.immuni.2017.12.009. PubMed PMID: 29343437; PMCID: PMC5810956.

217. Ellebedy AH, Krammer F, Li GM, Miller MS, Chiu C, Wrammert J, Chang CY, Davis CW, McCausland M, Elbein R, Edupuganti S, Spearman P, Andrews SF, Wilson PC, Garcia-Sastre A, Mulligan MJ, Mehta AK, Palese P, Ahmed R. Induction of broadly cross-reactive antibody responses to the influenza HA stem region following H5N1 vaccination in humans. Proceedings of the National Academy of Sciences of the United States of America. 2014;111(36):13133-8. Epub 2014/08/27. doi: 10.1073/pnas.1414070111. PubMed PMID: 25157133; PMCID: PMC4246941.

218. Joyce MG, Wheatley AK, Thomas PV, Chuang GY, Soto C, Bailer RT, Druz A, Georgiev IS, Gillespie RA, Kanekiyo M, Kong WP, Leung K, Narpala SN, Prabhakaran MS, Yang ES, Zhang B, Zhang Y, Asokan M, Boyington JC, Bylund T, Darko S, Lees CR, Ransier A, Shen CH, Wang L, Whittle JR, Wu X, Yassine HM, Santos C, Matsuoka Y, Tsybovsky Y, Baxa U, Program NCS, Mullikin JC, Subbarao K, Douek DC, Graham BS, Koup RA, Ledgerwood JE, Roederer M, Shapiro L, Kwong PD, Mascola JR, McDermott AB. Vaccine-Induced Antibodies that Neutralize Group 1 and Group 2 Influenza A Viruses. Cell. 2016;166(3):609-23. Epub 2016/07/28. doi: 10.1016/j.cell.2016.06.043. PubMed PMID: 27453470; PMCID: PMC4978566.

219. Wrammert J, Koutsonanos D, Li GM, Edupuganti S, Sui J, Morrissey M, McCausland M, Skountzou I, Hornig M, Lipkin WI, Mehta A, Razavi B, Del Rio C, Zheng NY, Lee JH, Huang M, Ali Z, Kaur K, Andrews S, Amara RR, Wang Y, Das SR, O'Donnell CD, Yewdell JW, Subbarao K, Marasco WA, Mulligan MJ, Compans R, Ahmed R, Wilson PC. Broadly cross-reactive antibodies dominate the human B cell

response against 2009 pandemic H1N1 influenza virus infection. The Journal of experimental medicine. 2011;208(1):181-93. doi: 10.1084/jem.20101352. PubMed PMID: 21220454; PMCID: PMC3023136.

220. Pica N, Hai R, Krammer F, Wang TT, Maamary J, Eggink D, Tan GS, Krause JC, Moran T, Stein CR, Banach D, Wrammert J, Belshe RB, Garcia-Sastre A, Palese P. Hemagglutinin stalk antibodies elicited by the 2009 pandemic influenza virus as a mechanism for the extinction of seasonal H1N1 viruses. Proceedings of the National Academy of Sciences of the United States of America. 2012;109(7):2573-8. doi: 10.1073/pnas.1200039109. PubMed PMID: 22308500; PMCID: PMC3289326.

221. Li Y, Myers JL, Bostick DL, Sullivan CB, Madara J, Linderman SL, Liu Q, Carter DM, Wrammert J, Esposito S, Principi N, Plotkin JB, Ross TM, Ahmed R, Wilson PC, Hensley SE. Immune history shapes specificity of pandemic H1N1 influenza antibody responses. The Journal of experimental medicine. 2013;210(8):1493-500. doi: 10.1084/jem.20130212. PubMed PMID: 23857983; PMCID: PMC3727314.

222. Miller MS, Gardner TJ, Krammer F, Aguado LC, Tortorella D, Basler CF, Palese P. Neutralizing antibodies against previously encountered influenza virus strains increase over time: a longitudinal analysis. Science translational medicine. 2013;5(198):198ra07. doi: 10.1126/scitranslmed.3006637. PubMed PMID: 23946196; PMCID: PMC4091683.

223. Adachi Y, Onodera T, Yamada Y, Daio R, Tsuiji M, Inoue T, Kobayashi K, Kurosaki T, Ato M, Takahashi Y. Distinct germinal center selection at local sites shapes memory B cell response to viral escape. The Journal of experimental medicine. 2015. doi: 10.1084/jem.20142284. PubMed PMID: 26324444.

224. Bingham CO, 3rd, Looney RJ, Deodhar A, Halsey N, Greenwald M, Codding C, Trzaskoma B, Martin F, Agarwal S, Kelman A. Immunization responses in rheumatoid arthritis patients treated with rituximab: results from a controlled clinical trial. Arthritis and rheumatism. 2010;62(1):64-74. doi: 10.1002/art.25034. PubMed PMID: 20039397.

225. Bedognetti D, Zoppoli G, Massucco C, Zanardi E, Zupo S, Bruzzone A, Sertoli MR, Balleari E, Racchi O, Messina M, Caltabiano G, Icardi G, Durando P, Marincola FM, Boccardo F, Ferrarini M, Ansaldi F, De Maria A. Impaired response to influenza vaccine associated with persistent memory B cell depletion in non-Hodgkin's lymphoma patients treated with rituximab-containing regimens. Journal of immunology. 2011;186(10):6044-55. doi: 10.4049/jimmunol.1004095. PubMed PMID: 21498665; PMCID: 3530046.

226. Eisenberg RA, Jawad AF, Boyer J, Maurer K, McDonald K, Prak ET, Sullivan KE. Rituximab-treated patients have a poor response to influenza vaccination. Journal of clinical immunology. 2013;33(2):388-96. doi: 10.1007/s10875-012-9813-x. PubMed PMID: 23064976; PMCID: 3565069.

227. Kim W, Kim SH, Huh SY, Kong SY, Choi YJ, Cheong HJ, Kim HJ. Reduced antibody formation after influenza vaccination in patients with neuromyelitis optica spectrum disorder treated with rituximab. European journal of neurology : the official journal of the European Federation of Neurological Societies. 2013;20(6):975-80. doi: 10.1111/ene.12132. PubMed PMID: 23521577.

228. Oren S, Mandelboim M, Braun-Moscovici Y, Paran D, Ablin J, Litinsky I, Comaneshter D, Levartovsky D, Mendelson E, Azar R, Wigler I, Balbir-Gurman A,

Caspi D, Elkayam O. Vaccination against influenza in patients with rheumatoid arthritis: the effect of rituximab on the humoral response. Annals of the rheumatic diseases. 2008;67(7):937-41. doi: 10.1136/ard.2007.077461. PubMed PMID: 17981914.

229. van Assen S, Holvast A, Benne CA, Posthumus MD, van Leeuwen MA, Voskuyl AE, Blom M, Risselada AP, de Haan A, Westra J, Kallenberg CG, Bijl M. Humoral responses after influenza vaccination are severely reduced in patients with rheumatoid arthritis treated with rituximab. Arthritis and rheumatism. 2010;62(1):75-81. doi: 10.1002/art.25033. PubMed PMID: 20039396.

230. Nazi I, Kelton JG, Larche M, Snider DP, Heddle NM, Crowther MA, Cook RJ, Tinmouth AT, Mangel J, Arnold DM. The effect of rituximab on vaccine responses in patients with immune thrombocytopenia. Blood. 2013;122(11):1946-53. doi: 10.1182/blood-2013-04-494096. PubMed PMID: 23851398; PMCID: PMC3773242.

231. Nakou M, Katsikas G, Sidiropoulos P, Bertsias G, Papadimitraki E, Raptopoulou A, Koutala H, Papadaki HA, Kritikos H, Boumpas DT. Rituximab therapy reduces activated B cells in both the peripheral blood and bone marrow of patients with rheumatoid arthritis: depletion of memory B cells correlates with clinical response. Arthritis Res Ther. 2009;11(4):R131. doi: 10.1186/ar2798. PubMed PMID: 19715572; PMCID: PMC2745815.

232. Misumi I, Whitmire JK. B cell depletion curtails CD4+ T cell memory and reduces protection against disseminating virus infection. Journal of immunology. 2014;192(4):1597-608. doi: 10.4049/jimmunol.1302661. PubMed PMID: 24453250; PMCID: PMC3925510.

233. Lykken JM, DiLillo DJ, Weimer ET, Roser-Page S, Heise MT, Grayson JM, Weitzmann MN, Tedder TF. Acute and chronic B cell depletion disrupts CD4+ and CD8+ T cell homeostasis and expansion during acute viral infection in mice. Journal of immunology. 2014;193(2):746-56. doi: 10.4049/jimmunol.1302848. PubMed PMID: 24928986; PMCID: PMC4290158.

234. Arad U, Tzadok S, Amir S, Mandelboim M, Mendelson E, Wigler I, Sarbagil-Maman H, Paran D, Caspi D, Elkayam O. The cellular immune response to influenza vaccination is preserved in rheumatoid arthritis patients treated with rituximab. Vaccine. 2011;29(8):1643-8. doi: 10.1016/j.vaccine.2010.12.072. PubMed PMID: 21211590.

235. Bentebibel SE, Jacquemin C, Schmitt N, Ueno H. Analysis of human blood memory T follicular helper subsets. Methods in molecular biology. 2015;1291:187-97. doi: 10.1007/978-1-4939-2498-1_16. PubMed PMID: 25836312.

236. Bentebibel SE, Lopez S, Obermoser G, Schmitt N, Mueller C, Harrod C, Flano E, Mejias A, Albrecht RA, Blankenship D, Xu H, Pascual V, Banchereau J, Garcia-Sastre A, Palucka AK, Ramilo O, Ueno H. Induction of ICOS+CXCR3+CXCR5+ TH cells correlates with antibody responses to influenza vaccination. Science translational medicine. 2013;5(176):176ra32. doi: 10.1126/scitranslmed.3005191. PubMed PMID: 23486778; PMCID: 3621097.

237. Xu X, Shi Y, Cai Y, Zhang Q, Yang F, Chen H, Gu Y, Zhang M, Yu L, Yang T. Inhibition of increased circulating Tfh cell by anti-CD20 monoclonal antibody in patients with type 1 diabetes. PLoS One. 2013;8(11):e79858. doi: 10.1371/journal.pone.0079858. PubMed PMID: 24278195; PMCID: PMC3835920.

238. Harrison OJ, Brasch J, Lasso G, Katsamba PS, Ahlsen G, Honig B, Shapiro L. Structural basis of adhesive binding by desmocollins and desmogleins. Proceedings of the National Academy of Sciences of the United States of America. 2016;113(26):7160-5. Epub 2016/06/15. doi: 10.1073/pnas.1606272113. PubMed PMID: 27298358; PMCID: PMC4932976.

239. Ishii K, Harada R, Matsuo I, Shirakata Y, Hashimoto K, Amagai M. In vitro keratinocyte dissociation assay for evaluation of the pathogenicity of anti-desmoglein 3 IgG autoantibodies in pemphigus vulgaris. The Journal of investigative dermatology. 2005;124(5):939-46. doi: 10.1111/j.0022-202X.2005.23714.x. PubMed PMID: 15854034.

240. Robert-Pachot M, Desbos A, Moreira A, Becchi M, Tebib J, Bonnin M, Aitsiselmi T, Bienvenu J, Fabien N. A new target for autoantibodies in patients with rheumatoid arthritis. Annals of the New York Academy of Sciences. 2007;1108:382-91. PubMed PMID: 17894001.

241. Sherer Y, Gorstein A, Fritzler MJ, Shoenfeld Y. Autoantibody explosion in systemic lupus erythematosus: more than 100 different antibodies found in SLE patients. Seminars in arthritis and rheumatism. 2004;34(2):501-37. PubMed PMID: 15505768.

242. Yeh SW, Cavacini LA, Bhol KC, Lin MS, Kumar M, Duval M, Posner MR, Ahmed AR. Pathogenic human monoclonal antibody against desmoglein 3. Clin Immunol. 2006;120(1):68-75. Epub 2006/04/26. doi: 10.1016/j.clim.2006.03.006. PubMed PMID: 16635589.

243. Corti D, Lanzavecchia A. Efficient Methods To Isolate Human Monoclonal Antibodies from Memory B Cells and Plasma Cells. Microbiol Spectr. 2014;2(5). Epub 2015/06/25. doi: 10.1128/microbiolspec.AID-0018-2014. PubMed PMID: 26104354.

244. Pinna D, Corti D, Jarrossay D, Sallusto F, Lanzavecchia A. Clonal dissection of the human memory B-cell repertoire following infection and vaccination. Eur J Immunol. 2009;39(5):1260-70. doi: 10.1002/eji.200839129. PubMed PMID: 19404981; PMCID: PMC3864550.

245. Cho A, Bradley B, Kauffman R, Priyamvada L, Kovalenkov Y, Feldman R, Wrammert J. Robust memory responses against influenza vaccination in pemphigus patients previously treated with rituximab. JCI Insight. 2017;2(12). Epub 2017/06/15. doi: 10.1172/jci.insight.93222. PubMed PMID: 28614800; PMCID: PMC5470882.

246. Smith K, Garman L, Wrammert J, Zheng NY, Capra JD, Ahmed R, Wilson PC. Rapid generation of fully human monoclonal antibodies specific to a vaccinating antigen. Nature protocols. 2009;4(3):372-84. doi: 10.1038/nprot.2009.3. PubMed PMID: 19247287; PMCID: 2750034.

247. Tiller T, Meffre E, Yurasov S, Tsuiji M, Nussenzweig MC, Wardemann H. Efficient generation of monoclonal antibodies from single human B cells by single cell RT-PCR and expression vector cloning. J Immunol Methods. 2008;329(1-2):112-24. doi: 10.1016/j.jim.2007.09.017. PubMed PMID: 17996249; PMCID: PMC2243222.

248. Pauli NT, Kim HK, Falugi F, Huang M, Dulac J, Henry Dunand C, Zheng NY, Kaur K, Andrews SF, Huang Y, DeDent A, Frank KM, Charnot-Katsikas A, Schneewind O, Wilson PC. Staphylococcus aureus infection induces protein A-mediated immune evasion in humans. The Journal of experimental medicine. 2014;211(12):2331-9. Epub 2014/10/29. doi: 10.1084/jem.20141404. PubMed PMID: 25348152; PMCID: PMC4235641.

249. Dorner T, Brezinschek HP, Brezinschek RI, Foster SJ, Domiati-Saad R, Lipsky PE. Analysis of the frequency and pattern of somatic mutations within nonproductively rearranged human variable heavy chain genes. Journal of immunology. 1997;158(6):2779-89. Epub 1997/03/15. PubMed PMID: 9058813.

250. Denning MF, Guy SG, Ellerbroek SM, Norvell SM, Kowalczyk AP, Green KJ. The expression of desmoglein isoforms in cultured human keratinocytes is regulated by calcium, serum, and protein kinase C. Exp Cell Res. 1998;239(1):50-9. Epub 1998/03/25. doi: 10.1006/excr.1997.3890. PubMed PMID: 9511724.

251. Ohyama B, Nishifuji K, Chan PT, Kawaguchi A, Yamashita T, Ishii N, Hamada T, Dainichi T, Koga H, Tsuruta D, Amagai M, Hashimoto T. Epitope spreading is rarely found in pemphigus vulgaris by large-scale longitudinal study using desmoglein 2-based swapped molecules. The Journal of investigative dermatology. 2012;132(4):1158-68. doi: 10.1038/jid.2011.448. PubMed PMID: 22277941.

252. Futei Y, Amagai M, Sekiguchi M, Nishifuji K, Fujii Y, Nishikawa T. Use of domain-swapped molecules for conformational epitope mapping of desmoglein 3 in pemphigus vulgaris. The Journal of investigative dermatology. 2000;115(5):829-34.

Epub 2000/11/09. doi: 10.1046/j.1523-1747.2000.00137.x. PubMed PMID: 11069620.

253. Pollmann R, Schmidt T, Eming R, Hertl M. Pemphigus: a Comprehensive Review on Pathogenesis, Clinical Presentation and Novel Therapeutic Approaches. Clin Rev Allergy Immunol. 2018;54(1):1-25. Epub 2018/01/10. doi: 10.1007/s12016-017-8662-z. PubMed PMID: 29313220.

254. Spindler V, Eming R, Schmidt E, Amagai M, Grando S, Jonkman MF, Kowalczyk AP, Muller EJ, Payne AS, Pincelli C, Sinha AA, Sprecher E, Zillikens D, Hertl M, Waschke J. Mechanisms Causing Loss of Keratinocyte Cohesion in Pemphigus. The Journal of investigative dermatology. 2018;138(1):32-7. Epub 2017/10/19. doi: 10.1016/j.jid.2017.06.022. PubMed PMID: 29037765.

255. Daniel BS, Hertl M, Werth VP, Eming R, Murrell DF. Severity score indexes for blistering diseases. Clin Dermatol. 2012;30(1):108-13. Epub 2011/12/06. doi: 10.1016/j.clindermatol.2011.03.017. PubMed PMID: 22137234; PMCID: PMC3928011.

256. Grover S. Scoring systems in pemphigus. Indian J Dermatol. 2011;56(2):145-9. Epub 2011/07/01. doi: 10.4103/0019-5154.80403. PubMed PMID: 21716537; PMCID: PMC3108511.

257. Yamagami J, Payne AS, Kacir S, Ishii K, Siegel DL, Stanley JR. Homologous regions of autoantibody heavy chain complementarity-determining region 3 (H-CDR3) in patients with pemphigus cause pathogenicity. The Journal of clinical investigation. 2010;120(11):4111-7. Epub 2010/10/28. doi: 10.1172/JCI44425. PubMed PMID: 20978359; PMCID: PMC2964997.

258. Witte M, Zillikens D, Schmidt E. Diagnosis of Autoimmune Blistering Diseases. Front Med (Lausanne). 2018;5:296. Epub 2018/11/20. doi: 10.3389/fmed.2018.00296. PubMed PMID: 30450358; PMCID: PMC6224342.

259. Korsrud FR, Brandtzaeg P. Quantitative immunohistochemistry of immunoglobulin- and J-chain-producing cells in human parotid and submandibular salivary glands. Immunology. 1980;39(2):129-40. Epub 1980/02/01. PubMed PMID: 6769784; PMCID: PMC1457971.

260. Bonsignori M, Zhou T, Sheng Z, Chen L, Gao F, Joyce MG, Ozorowski G, Chuang GY, Schramm CA, Wiehe K, Alam SM, Bradley T, Gladden MA, Hwang KK, Iyengar S, Kumar A, Lu X, Luo K, Mangiapani MC, Parks RJ, Song H, Acharya P, Bailer RT, Cao A, Druz A, Georgiev IS, Kwon YD, Louder MK, Zhang B, Zheng A, Hill BJ, Kong R, Soto C, Program NCS, Mullikin JC, Douek DC, Montefiori DC, Moody MA, Shaw GM, Hahn BH, Kelsoe G, Hraber PT, Korber BT, Boyd SD, Fire AZ, Kepler TB, Shapiro L, Ward AB, Mascola JR, Liao HX, Kwong PD, Haynes BF. Maturation Pathway from Germline to Broad HIV-1 Neutralizer of a CD4-Mimic Antibody. Cell. 2016;165(2):449-63. Epub 2016/03/08. doi: 10.1016/j.cell.2016.02.022. PubMed PMID: 26949186; PMCID: PMC4826291.

261. Pugh-Bernard AE, Silverman GJ, Cappione AJ, Villano ME, Ryan DH, Insel RA, Sanz I. Regulation of inherently autoreactive VH4-34 B cells in the maintenance of human B cell tolerance. The Journal of clinical investigation. 2001;108(7):1061-70. Epub 2001/10/03. doi: 10.1172/JCI12462. PubMed PMID: 11581307; PMCID: PMC200949.

262. Ellebrecht CT, Bhoj VG, Nace A, Choi EJ, Mao X, Cho MJ, Di Zenzo G, Lanzavecchia A, Seykora JT, Cotsarelis G, Milone MC, Payne AS. Reengineering chimeric antigen receptor T cells for targeted therapy of autoimmune disease. Science. 2016;353(6295):179-84. doi: 10.1126/science.aaf6756. PubMed PMID: 27365313.

263. Li N, Aoki V, Hans-Filho G, Rivitti EA, Diaz LA. The role of intramolecular epitope spreading in the pathogenesis of endemic pemphigus foliaceus (fogo selvagem). The Journal of experimental medicine. 2003;197(11):1501-10. Epub 2003/05/29. doi: 10.1084/jem.20022031. PubMed PMID: 12771179; PMCID: PMC2193910.

264. Arbuckle MR, McClain MT, Rubertone MV, Scofield RH, Dennis GJ, James JA, Harley JB. Development of autoantibodies before the clinical onset of systemic lupus erythematosus. The New England journal of medicine. 2003;349(16):1526-33. Epub 2003/10/17. doi: 10.1056/NEJMoa021933. PubMed PMID: 14561795.

265. Vidarsson G, Dekkers G, Rispens T. IgG subclasses and allotypes: from structure to effector functions. Front Immunol. 2014;5:520. Epub 2014/11/05. doi: 10.3389/fimmu.2014.00520. PubMed PMID: 25368619; PMCID: PMC4202688.

266. Kunisaki KM, Janoff EN. Influenza in immunosuppressed populations: a review of infection frequency, morbidity, mortality, and vaccine responses. Lancet Infect Dis. 2009;9(8):493-504. doi: 10.1016/S1473-3099(09)70175-6. PubMed PMID: 19628174; PMCID: PMC2775097.

267. Govaert TM, Thijs CT, Masurel N, Sprenger MJ, Dinant GJ, Knottnerus JA. The efficacy of influenza vaccination in elderly individuals. A randomized double-blind placebo-controlled trial. JAMA. 1994;272(21):1661-5. PubMed PMID: 7966893.

268. Potter CW, Oxford JS. Determinants of immunity to influenza infection in man. Br Med Bull. 1979;35(1):69-75. PubMed PMID: 367490.

269. Gurcan HM, Keskin DB, Stern JN, Nitzberg MA, Shekhani H, Ahmed AR. A review of the current use of rituximab in autoimmune diseases. Int Immunopharmacol. 2009;9(1):10-25. doi: 10.1016/j.intimp.2008.10.004. PubMed PMID: 19000786.

270. Mamani-Matsuda M, Cosma A, Weller S, Faili A, Staib C, Garcon L, Hermine O, Beyne-Rauzy O, Fieschi C, Pers JO, Arakelyan N, Varet B, Sauvanet A, Berger A, Paye F, Andrieu JM, Michel M, Godeau B, Buffet P, Reynaud CA, Weill JC. The human spleen is a major reservoir for long-lived vaccinia virus-specific memory B cells. Blood. 2008;111(9):4653-9. doi: 10.1182/blood-2007-11-123844. PubMed PMID: 18316630.

271. King C, Ilic A, Koelsch K, Sarvetnick N. Homeostatic expansion of T cells during immune insufficiency generates autoimmunity. Cell. 2004;117(2):265-77. PubMed PMID: 15084263.

272. Giudice GJ, Emery DJ, Diaz LA. Cloning and primary structural analysis of the bullous pemphigoid autoantigen BP180. The Journal of investigative dermatology. 1992;99(3):243-50. PubMed PMID: 1324962.

273. Stanley JR, Hawley-Nelson P, Yuspa SH, Shevach EM, Katz SI. Characterization of bullous pemphigoid antigen: a unique basement membrane protein of stratified squamous epithelia. Cell. 1981;24(3):897-903. PubMed PMID: 7018697.

274. Ahmed AR, Spigelman Z, Cavacini LA, Posner MR. Treatment of pemphigus vulgaris with rituximab and intravenous immune globulin. The New England journal of medicine. 2006;355(17):1772-9. doi: 10.1056/NEJMoa062930. PubMed PMID: 17065638.

275. Cianchini G, Corona R, Frezzolini A, Ruffelli M, Didona B, Puddu P. Treatment of severe pemphigus with rituximab: report of 12 cases and a review of the literature. Archives of dermatology. 2007;143(8):1033-8. doi: 10.1001/archderm.143.8.1033. PubMed PMID: 17709662.

276. Palanichamy A, Barnard J, Zheng B, Owen T, Quach T, Wei C, Looney RJ, Sanz I, Anolik JH. Novel human transitional B cell populations revealed by B cell depletion therapy. Journal of immunology. 2009;182(10):5982-93. doi: 10.4049/jimmunol.0801859. PubMed PMID: 19414749; PMCID: PMC2746373.

277. Anolik JH, Barnard J, Owen T, Zheng B, Kemshetti S, Looney RJ, Sanz I. Delayed memory B cell recovery in peripheral blood and lymphoid tissue in systemic lupus erythematosus after B cell depletion therapy. Arthritis and rheumatism. 2007;56(9):3044-56. doi: 10.1002/art.22810. PubMed PMID: 17763423.

278. Crotty S, Aubert RD, Glidewell J, Ahmed R. Tracking human antigen-specific memory B cells: a sensitive and generalized ELISPOT system. J Immunol Methods. 2004;286(1-2):111-22. doi: 10.1016/j.jim.2003.12.015. PubMed PMID: 15087226.

279. Sasaki S, Jaimes MC, Holmes TH, Dekker CL, Mahmood K, Kemble GW, Arvin AM, Greenberg HB. Comparison of the influenza virus-specific effector and memory B-cell responses to immunization of children and adults with live attenuated or inactivated influenza virus vaccines. J Virol. 2007;81(1):215-28. doi: 10.1128/JVI.01957-06. PubMed PMID: 17050593; PMCID: PMC1797237.

280. Shankland KR, Armitage JO, Hancock BW. Non-Hodgkin lymphoma. Lancet. 2012;380(9844):848-57. doi: 10.1016/S0140-6736(12)60605-9. PubMed PMID: 22835603.

281. Sanz I. Multiple mechanisms participate in the generation of diversity of human H chain CDR3 regions. Journal of immunology. 1991;147(5):1720-9. PubMed PMID: 1908883.

282. Audia S, Samson M, Guy J, Janikashvili N, Fraszczak J, Trad M, Ciudad M, Leguy V, Berthier S, Petrella T, Aho-Glele S, Martin L, Maynadie M, Lorcerie B, Rat P, Cheynel N, Katsanis E, Larmonier N, Bonnotte B. Immunologic effects of rituximab on the human spleen in immune thrombocytopenia. Blood. 2011;118(16):4394-400. doi: 10.1182/blood-2011-03-344051. PubMed PMID: 21876120; PMCID: PMC3204911.

283. Leandro MJ, Cooper N, Cambridge G, Ehrenstein MR, Edwards JC. Bone marrow B-lineage cells in patients with rheumatoid arthritis following rituximab therapy. Rheumatology (Oxford). 2007;46(1):29-36. doi: 10.1093/rheumatology/kel148. PubMed PMID: 16735454.

284. Teng YK, Levarht EW, Hashemi M, Bajema IM, Toes RE, Huizinga TW, van Laar JM. Immunohistochemical analysis as a means to predict responsiveness to

rituximab treatment. Arthritis and rheumatism. 2007;56(12):3909-18. doi: 10.1002/art.22967. PubMed PMID: 18050222.

285. Adlowitz DG, Barnard J, Biear JN, Cistrone C, Owen T, Wang W, Palanichamy A, Ezealah E, Campbell D, Wei C, Looney RJ, Sanz I, Anolik JH. Expansion of Activated Peripheral Blood Memory B Cells in Rheumatoid Arthritis, Impact of B Cell Depletion Therapy, and Biomarkers of Response. PLoS One. 2015;10(6):e0128269. doi: 10.1371/journal.pone.0128269. PubMed PMID: 26047509; PMCID: PMC4457888.

286. Anolik JH, Campbell D, Felgar RE, Young F, Sanz I, Rosenblatt J, Looney RJ. The relationship of FcgammaRIIIa genotype to degree of B cell depletion by rituximab in the treatment of systemic lupus erythematosus. Arthritis and rheumatism. 2003;48(2):455-9. doi: 10.1002/art.10764. PubMed PMID: 12571855.

287. Mahevas M, Patin P, Huetz F, Descatoire M, Cagnard N, Bole-Feysot C, Le Gallou S, Khellaf M, Fain O, Boutboul D, Galicier L, Ebbo M, Lambotte O, Hamidou M, Bierling P, Godeau B, Michel M, Weill JC, Reynaud CA. B cell depletion in immune thrombocytopenia reveals splenic long-lived plasma cells. The Journal of clinical investigation. 2013;123(1):432-42. doi: 10.1172/JCI65689. PubMed PMID: 23241960; PMCID: PMC3533302.

288. Wieland A, Shashidharamurthy R, Kamphorst AO, Han JH, Aubert RD, Choudhury BP, Stowell SR, Lee J, Punkosdy GA, Shlomchik MJ, Selvaraj P, Ahmed R. Antibody effector functions mediated by Fcgamma-receptors are compromised during persistent viral infection. Immunity. 2015;42(2):367-78. doi: 10.1016/j.immuni.2015.01.009. PubMed PMID: 25680276; PMCID: PMC4339104.

289. Colovai AI, Giatzikis C, Ho EK, Farooqi M, Suciu-Foca N, Cattoretti G, Orazi A. Flow cytometric analysis of normal and reactive spleen. Mod Pathol. 2004;17(8):918-27. doi: 10.1038/modpathol.3800141. PubMed PMID: 15263909.

290. Teeling JL, Mackus WJ, Wiegman LJ, van den Brakel JH, Beers SA, French RR, van Meerten T, Ebeling S, Vink T, Slootstra JW, Parren PW, Glennie MJ, van de Winkel JG. The biological activity of human CD20 monoclonal antibodies is linked to unique epitopes on CD20. Journal of immunology. 2006;177(1):362-71. PubMed PMID: 16785532.

291. Hammer O. CD19 as an attractive target for antibody-based therapy. MAbs. 2012;4(5):571-7. doi: 10.4161/mabs.21338. PubMed PMID: 22820352; PMCID: PMC3499297.

292. Clinic M. CBC with Differential, Blood 2015 [cited 2015 Accessed August]. Available from: http://www.mayomedicallaboratories.com/test-catalog/Clinical+and+Interpretive/9109.

293. R Webster NC, K Stohr. World Health Organization Manual on Animal Influenza Diagnosis and Surveillance Geneva: WHO; 2002 [updated Updated May, 2002; cited 2015 Accessed March]. Available from: http://www.who.int/csr/resources/publications/influenza/whocdscsrncs20025rev.pdf.

294. Organization WH. Serological diagnosis of influenza by microneutralization assay 2010 [updated Updated December, 2010; cited 2015 Accessed March]. Available from:

http://www.who.int/influenza/gisrs_laboratory/2010_12_06_serological_diagnosis_of_influenza_by_microneutralization_assay.pdf.

295. Ahmed AR, Kaveri S, Spigelman Z. Long-Term Remissions in Recalcitrant Pemphigus Vulgaris. The New England journal of medicine. 2015;373(27):2693-4. Epub 2015/12/31. doi: 10.1056/NEJMc1508234. PubMed PMID: 26716930.

296. Shaffer AL, Shapiro-Shelef M, Iwakoshi NN, Lee AH, Qian SB, Zhao H, Yu X, Yang L, Tan BK, Rosenwald A, Hurt EM, Petroulakis E, Sonenberg N, Yewdell JW, Calame K, Glimcher LH, Staudt LM. XBP1, downstream of Blimp-1, expands the secretory apparatus and other organelles, and increases protein synthesis in plasma cell differentiation. Immunity. 2004;21(1):81-93. Epub 2004/09/04. doi: 10.1016/j.immuni.2004.06.010. PubMed PMID: 15345222.

297. Clark RA, Chong B, Mirchandani N, Brinster NK, Yamanaka K, Dowgiert RK, Kupper TS. The vast majority of CLA+ T cells are resident in normal skin. Journal of immunology. 2006;176(7):4431-9. Epub 2006/03/21. PubMed PMID: 16547281.

298. Ni Z, Campbell JJ, Niehans G, Walcheck B. The monoclonal antibody CHO-131 identifies a subset of cutaneous lymphocyte-associated antigen T cells enriched in P-selectin-binding cells. Journal of immunology. 2006;177(7):4742-8. Epub 2006/09/20. PubMed PMID: 16982914.

299. Ni Z, Walcheck B. Cutaneous lymphocyte-associated antigen (CLA) T cells up-regulate P-selectin ligand expression upon their activation. Clin Immunol. 2009;133(2):257-64. Epub 2009/08/12. doi: 10.1016/j.clim.2009.07.010. PubMed PMID: 19665434; PMCID: PMC2760600.

300. Yoshino T, Okano M, Chen HL, Tsuchiyama J, Kondo E, Nishiuchi R, Teramoto N, Nishizaki K, Akagi T. Cutaneous lymphocyte antigen is expressed on memory/effector B cells in the peripheral blood and monocytoid B cells in the lymphoid tissues. Cell Immunol. 1999;197(1):39-45. Epub 1999/11/11. doi: 10.1006/cimm.1999.1552. PubMed PMID: 10555994.

301. Olszewski WL, Grzelak I, Ziolkowska A, Engeset A. Immune cell traffic from blood through the normal human skin to lymphatics. Clin Dermatol. 1995;13(5):473-83. Epub 1995/09/01. PubMed PMID: 8665458.

302. Egbuniwe IU, Karagiannis SN, Nestle FO, Lacy KE. Revisiting the role of B cells in skin immune surveillance. Trends Immunol. 2015;36(2):102-11. Epub 2015/01/27. doi: 10.1016/j.it.2014.12.006. PubMed PMID: 25616715.

303. Geherin SA, Fintushel SR, Lee MH, Wilson RP, Patel RT, Alt C, Young AJ, Hay JB, Debes GF. The skin, a novel niche for recirculating B cells. Journal of immunology. 2012;188(12):6027-35. Epub 2012/05/09. doi: 10.4049/jimmunol.1102639. PubMed PMID: 22561151; PMCID: PMC3370056.

304. Geherin SA, Gomez D, Glabman RA, Ruthel G, Hamann A, Debes GF. IL-10+ Innate-like B Cells Are Part of the Skin Immune System and Require alpha4beta1 Integrin To Migrate between the Peritoneum and Inflamed Skin. Journal of immunology. 2016;196(6):2514-25. Epub 2016/02/07. doi: 10.4049/jimmunol.1403246. PubMed PMID: 26851219; PMCID: PMC4779667.